

POST GRADUATE DEGREE PROGRAMME (CBCS) IN

MATHEMATICS

SEMESTER IV

SELF LEARNING MATERIAL

PAPER : DSE 4.3
(Applied Stream)

Mathematical Biology



Directorate of Open and Distance Learning
University of Kalyani
Kalyani, Nadia
West Bengal, India

Content Writers

DSE 4.3 Mathematical Biology	Dr. Priti Kumar Roy Professor Department of Mathematics Jadavpur University
---------------------------------	--

April, 2024

Directorate of Open and Distance Learning, University of Kalyani

Published by the Directorate of Open and Distance Learning

University of Kalyani, 741235, West Bengal

All rights reserved. No part of this work should be reproduced in any form without the permission in writing from the Directorate of Open and Distance Learning, University of Kalyani.

Director's Message

Satisfying the varied needs of distance learners, overcoming the obstacle of Distance and reaching the un-reached students are the three fold functions catered by Open and Distance Learning (ODL) systems. The onus lies on writers, editors, production professionals and other personnel involved in the process to overcome the challenges inherent to curriculum design and production of relevant Self Learning Materials (SLMs). At the University of Kalyani a dedicated team under the able guidance of the Hon'ble Vice-Chancellor has invested its best efforts, professionally and in keeping with the demands of Post Graduate CBCS Programmes in Distance Mode to devise a self-sufficient curriculum for each course offered by the Directorate of Open and Distance Learning (DODL), University of Kalyani.

Development of printed SLMs for students admitted to the DODL within a limited time to cater to the academic requirements of the Course as per standards set by Distance Education Bureau of the University Grants Commission, New Delhi, India under Open and Distance Mode UGC Regulations, 2020 had been our endeavor. We are happy to have achieved our goal.

Utmost care and precision have been ensured in the development of the SLMs, making them useful to the learners, besides avoiding errors as far as practicable. Further suggestions from the stakeholders in this would be welcome.

During the production-process of the SLMs, the team continuously received positive stimulations and feedback from Professor **(Dr.) Amalendu Bhunia, Hon'ble Vice-Chancellor, University of Kalyani**, who kindly accorded directions, encouragements and suggestions, offered constructive criticism to develop it with in proper requirements. We gracefully, acknowledge his inspiration and guidance.

Sincere gratitude is due to the respective chairpersons as well as each and every member of PGBOS (DODL), University of Kalyani. Heartfelt thanks are also due to the Course Writers-faculty members at the DODL, subject-experts serving at University Post Graduate departments and also to the authors and academicians whose academic contributions have enriched the SLMs. We humbly acknowledge their valuable academic contributions. I would especially like to convey gratitude to all other University dignitaries and personnel involved either at the conceptual or operational level of the DODL of University of Kalyani.

Their persistent and coordinated efforts have resulted in the compilation of comprehensive, learner-friendly, flexible texts that meet the curriculum requirements of the Post Graduate Programme through Distance Mode.

Self Learning Materials (SLMs) have been published by the Directorate of Open and Distance Learning, University of Kalyani, Kalyani-741235, West Bengal and all the copyrights reserved for University of Kalyani. No part of this work should be reproduced in any form without permission in writing from the appropriate authority of the University of Kalyani.

All the Self Learning Materials are self written and collected from e-book, journals and websites.

Director

Directorate of Open and Distance Learning

University of Kalyani

Post Graduate Board of Studies
Department of Mathematics
Directorate of Open and Distance Learning
University of Kalyani

Sl No.	Name & Designation	Role
1	Dr. Samares Pal, Professor & Head Department of Mathematics, University of Kalyani	Chairperson
2	Dr. Pulak Sahoo, Professor Department of Mathematics, University of Kalyani	Member
3	Dr. Sahidul Islam, Associate Professor Department of Mathematics, University of Kalyani	Member
4	Dr. Sushanta Kumar Mohanta, Professor Department of Mathematics, West Bengal State University	External Nominated Member
5	Ms. Audrija Choudhury, Assistant Professor Department of Mathematics Directorate of Open and Distance Learning University of Kalyani	Member
6	Director Directorate of Open and Distance Learning University of Kalyani	Convener

Discipline Specific Elective Paper

DSE 4.3

Marks : 100 (SEE : 80; IA : 20)

Mathematical Biology (Applied Stream)

Syllabus

• Unit 1 •

Epidemic models: Simple epidemic; SIS epidemic model; SIS epidemic model with specific rate of infection, SIS epidemic model with constant number of carriers.

• Unit 2 •

General epidemic model; Approximate solution, Recurring epidemic model.

• Unit 3 •

Stochastic epidemic models without removal, Basic system of equations and its solution.

• Unit 4 •

Stochastic epidemic models: with multiple infections; Removal; Carriers; Infectives, immigration and emigration.

• Unit 5 •

Basic model for inheritance of genetic characteristics, Hardy-Wienberg law.

• Unit 6 •

Correlation between genetic composition of siblings, Bayes theorem and its applications in genetics

• Unit 7 •

Extension of basic model for inheritance of genetic characteristics, Models for genetic improvement

• Unit 8 •

Genetic Improvement through elimination of Recessives, Selection and Mutation, Alternative Discussion of selection.

• Unit 9 •

Some basic concepts of fluid dynamics, Hagen-Poiseuille Flow, Reynolds number Flow, Non-Newtonian Fluids

• Unit 10 •

Basic concepts about blood, Cardiovascular system, Special Characteristics of Blood flow, Structure and mechanical properties of blood vessels

• Unit 11 •

Non-Newtonian Flow in Circular Tubes, Power-Law, Herschel-Bulkley and Casson fluid flow in circular tubes.

• Unit 12 •

Fahraeus-Lindqvist Effect, Pulsatile Flow in Circular Rigid Tube, Blood Flow through Artery with Mild Stenosis.

• Unit 13 •

Peristaltic Motion in a Channel and Tube, Long-wavelength approximation.

• Unit 14 •

Two-dimensional Flow in Renal Tubule, Function of Renal Tubule, Basic Equations and Boundary Conditions, Solution under approximations.

• Unit 15 •

Diffusion and Diffusion-Reaction Models, Fick's Law of Diffusion, Solutions of One and Two-dimensional Diffusion Equation.

• Unit 16 •

Diffusivity of Population Models, Diffusion on Stability of Single Species, Two Species and Prey-Predator Model.

• Unit 17 •

Stochastic Model exploring Disease Dynamics, Formation of Kolmogorov's Forward equation, Expected Time to extinction.

• Unit 18 •

Leslie-Gower Prey-Predator Model, Functional Responses, Effect of Nutrients on Autotroph-Herbivore Interaction, Phytoplankton-Zooplankton Systems, Bio-Control in Plankton Models with Nutrient Recycling, Stability of Food Chain models.

• Unit 19 •

Integer-Ordered Model and the CF Fractionalized Micobacterial Model, Iterative Scheme, Existence and Uniqueness of Solutions, Stability Analysis.

• Unit 20 •

Predator Prey Model in Presence of Infection, Viral Infections on Phytoplankton-Zooplankton System, Mathematical Stability Analysis and Interpretations.

Contents

Director's Message

1	Conjugate Space	1
1.1	Introduction	1
1.2	Simple Epidemic Model	2
1.3	SIS Epidemic Model	4
1.3.1	SIS Model with Specific Rate of Infection as a Function of t	5
1.3.2	SIS Model with Constant Number of Carriers	5
1.4	Simple Epidemic Model with Carriers	6
1.5	SEIR Epidemic Model	6
1.5.1	Detailed Description of SEIR Mathematical Model	7
1.5.2	Equilibrium Points	8
1.5.3	Stability Analysis	8
1.5.4	Conclusion	8
1.6	SEIRS Mathematical Model	8
1.6.1	Model Description	8
1.6.2	Equilibrium Points	9
1.6.3	Linearization	9
1.6.4	Eigenvalues	10
1.6.5	Conclusion	10
2		11
2.1	General Epidemic Model	11
2.2	Approximate Solution	13
2.3	Recurring epidemic	16
2.4	Behaviour of Seasonal Dynamics in Recurrent Epidemics	17
2.4.1	Classical Forced SIR Model	20
3		23
3.1	Discrete Mathematical Modelling	23
3.1.1	Model Formulation with Suitable Assumptions	24
3.1.2	Equilibria and Stability Analysis	24
3.1.3	Stability of the Disease-free Equilibrium	25
3.1.4	Stability Analysis of the Interior Equilibrium	26
3.1.5	Bifurcation Analysis	26
3.2	Stochastic Epidemic Model Without Removal	29
3.3	Essence in Mathematics	29
3.4	Basic System of Equation	30

3.4.1	Solution of the System of Equation	31
4		35
4.1	Other Stochastic Epidemic Models	35
4.1.1	Epidemics with Multiple Infections	36
4.1.2	Stochastic Epidemic Model with Removal	36
5		43
5.1	Introduction	43
5.2	Basic Model for Inheritance	43
5.3	Hardy-Weinberg Law	47
5.3.1	Assumptions	47
5.3.2	Equations	48
5.3.3	Genotype Frequency Equation	48
5.3.4	Applications	48
5.3.5	Conclusion	49
6		55
6.1	Correlation between Genetic Composition of Siblings	55
6.2	Bayes Theorem and Its Applications in Genetics	56
7		63
7.1	Further Discussion of Basic Model for Inheritance of Genetic Characteristics	63
7.1.1	Phenotype Ratios	63
7.2	Multiple Alleles and Application to Blood Groups	64
7.3	Models for Genetic Improvement: Selection and Mutation	68
7.3.1	Genetic Improvement through Cross Breeding	69
8		75
8.1	Genetic Improvement through Elimination Recessives	75
8.2	Selection and Mutation	78
8.3	An Alternative Discussion of Selection	80
9		83
9.1	Introduction	83
9.2	Navier-Stokes Equations for the Flow of a Viscous Incompressible Fluid	83
9.3	Hagen-Poiseuille Flow	87
9.4	Inlet Length Flow	90
9.5	Reynolds Number of Flows	90
9.6	Non-Newtonian Fluids	92
10		95
10.1	Basic Concepts about Blood, Cardiovascular System and Blood Flow	95
10.1.1	Constitution of Blood	95
10.1.2	Viscosity of Blood	97
10.1.3	Cardiovascular System	99
10.1.4	Special Characteristics of Blood Flow	99
10.1.5	Structure and function of Blood Vessels	101
10.1.6	Principal of Blood Vessels	101

CONTENTS

10.1.7	Mechanical Properties of Blood Vessels	103
11		107
11.1	Steady Non-Newtonian Fluid Flow in Circular Tubes	107
11.1.1	Basic Equations for Fluid Flow	107
11.2	Flow of Power-Law Fluid in Circular Tube	110
11.3	Flow of Herschel-Bulkley Fluid in Circular Tube	112
11.4	Flow of Casson Fluid in Circular Tube	114
12		119
12.1	Newtonian Fluid Models	119
12.1.1	Fahraeus-Lindqvist Effect	119
12.2	Blood Flow through Artery with Mild Stenosis	123
12.2.1	Effect of Stenosis	123
12.2.2	Analysis of Mild Stenosis	124
13		127
13.1	Peristaltic Flows in Tubes and Channel	127
13.1.1	Peristaltic Flows in Biomechanics	128
14		135
14.1	Two Dimensional Flow in Renal Tubule	135
14.1.1	Function of Renal Tubule	136
14.1.2	Basic Equations and Boundary Conditions	136
14.1.3	Solution When Radial Velocity at Wall Decreases Linearly with z	137
15		143
15.1	The Diffusion Equation	143
15.1.1	Fick's Laws of Diffusion	143
15.1.2	Some Solution of the One-dimensional Diffusion Equation	145
15.1.3	Some Solutions of the Two-dimensional Diffusion Equation	148
16		151
16.1	Application of Diffusion and Diffusion-Reaction Models in Population Biology	151
16.2	Absence of Diffusive Instability for Single Species	152
16.3	Possibility of Diffusive Instability for Two Species	153
16.4	Influence of Diffusion on the Stability of Prey-Predator Models	155
17		159
17.1	Stochastic Model Exploring Fundamentals of a Disease Dynamics	159
17.2	The Deterministic Model	160
17.3	Analysis of the Stochastic Model	161
17.3.1	Formulation of the Kolmogorov's Forward Equation	162
17.3.2	The Quasi-Stationary distribution	163
17.3.3	Distribution of the Time to Extinction	164
17.3.4	Diffusion approximation and approximation of Quasi-Stationary distribution	165
17.3.5	The expected time to extinction	167
17.4	Numerical Illustrations	167
17.5	Summary	168

18	171
18.1 Leslie-Gower Predator-prey model with different functional responses	171
18.1.1 Characteristics, Classifications and Features	172
18.2 Effect of Nutrients on Autotroph-Herbivore Interaction	175
18.3 Phytoplankton-zooplankton System and its Stability Analysis	176
18.4 Bio-Control in Plankton Models with Nutrient Recycling	178
18.5 Stability of food Chain Models	179
19	183
19.1 Preliminaries	183
19.2 The Basic Integer-Order Model and the CF Fractionalized Model	184
19.2.1 The Iterative Scheme	185
19.2.2 Stability Analysis	186
19.2.3 Existence of the Solutions	189
19.2.4 Uniqueness of the Solutions	192
19.3 Equilibria and Stability	193
20	195
20.1 Predator Prey Model in Presence of Infection	195
20.1.1 Jacobian, Characteristic Polynomial and Stability Analysis of Steady States	196
20.2 Viral Infections on Phytoplankton and Zooplankton System	199
20.2.1 Mathematical Model on Viral Infection of phytoplankton-zooplankton system	199
References	203

Unit 1

Conjugate Space

Course Structure

- Terminologies related to epidemic
 - Simple epidemic
 - SIS Epidemic Model
 - SIS Epidemic Model with Specific Rate of Infection as a Function of time
 - SIS Model with Constant Number of Carriers
 - Simple Epidemic Model with Carriers
 - SEIR Epidemic model
 - SEIRS Mathematical Model
-

1.1 Introduction

The study of mathematical theory of epidemic can be look upon as a continuation of our previous study in the sense that here also our concern is about the population sizes when effected by epidemics. In fact, we will draw our attention in modelling of problems of epidemics in mathematical terms. Sometimes such study is also called the study of mathematical epidemiology.

In order to pose a problem of epidemic, let us think of a small group of individuals who can carry a communicable infection to a large group of individuals, who can therefore be consider to be capable of the conducting the disease. Our immediate problem is to investigate how the disease is develop. In order to have a mathematical model of such situation we need some assumption regarding the characteristic of the disease as well as the mixing of the population. For this we need to consider the basic definition.

- **Susceptible Individuals:** An individual who is capable of conducting the disease directly or indirectly from another infected individual and is thereby become an infectious.
- **Infective Individuals:** An individual who is capable of transmitting the disease to others.
- **Removed Individuals:** An individual who had the disease and has recover or is death and is permanently immune or is latent (existing but not developed) until recovering an permanent immunity occurs.
- **Latent Period:** This it the period during which a disease is developed within a newly infected individual in purely internal way.
- **Infections Period:** This is the period during which the infected is liable to communicate infectious material to susceptible.
- **Incubation Period:** This is the interval between the exposer to disease and the appearance of symptoms.
- **Genial Period:** This is the time interval between the appearance of symptoms in one case and the appearance of symptoms in another case infected from the first.

- Remark 1.1.1.**
- The disease under consideration confers permanent immunity upon any individuals who has completely recovers from it and has a negligible short incubation period.
 - An individuals who conduct the disease becomes infective immediately.
 - The population is obviously divided into three classes, viz. susceptible class, infective class and removed class.

We next consider some simple cases depending on the nature of the epidemic. We consider three types of epidemic, viz. *simple*, *general* and *recurring* epidemic.

1.2 Simple Epidemic Model

This is the simplest type of epidemic in which a disease may spread among a group of susceptible but there is removal by death or by recovering or by isolation. In reality this may be taken as the reasonable approximation to the early stages of the upper respiratory infection. Over a long time may elapse before an infective is removed.

Let there n susceptible (S) and let us introduce an simple infective (I) into this group at time $t = 0$, so that we have a group of $(n + 1)$ individuals. Let $S(t)$ and $I(t)$ be the respective number of susceptible and infective at time t so that

$$S(t) + I(t) = n + 1 \quad (1.2.1)$$

We now assume that the disease spread in such a way that the average number of new cases of the disease in an interval Δt is proportional to both the number of susceptible and the infective.

Let $\gamma > 0$ be the constant rate between the members at time Δt so that

$$\Delta S = -\gamma SI \Delta t \quad (1.2.2)$$

Proceeding to the limit $\Delta t \rightarrow 0$, we have

$$\frac{dS}{dt} = -\gamma SI \quad (1.2.3)$$

which can also be written as

$$\begin{aligned} \frac{dS}{d\tau} &= -SI \quad \text{where } \tau = \gamma t \\ \Rightarrow \frac{dS}{d\tau} &= -S[n+1-S] \quad [\text{using Eq. (1.2.1)}] \end{aligned} \quad (1.2.4)$$

The solution of Eq. (1.2.4) subject to the initial conditions $S = n$ at $\tau = 0$ is given by

$$S = \frac{n(n+1)}{n + e^{(n+1)\tau}} \quad (1.2.5)$$

Therefore the rate which new cases occur is given by

$$-\frac{dS}{d\tau} = S[n+1-S] = \frac{n(n+1)^2 e^{(n+1)\tau}}{\{n + e^{(n+1)\tau}\}^2} \quad (1.2.6)$$

The rate $\frac{dS}{d\tau} < 0$ because it represents change in S , and S , the number of susceptible is decreasing as the epidemic develop.

Fig. 1.1 is known as epidemic curve and has a maximum at $\tau = \frac{\ln(n)}{n+1}$. We therefore, conclude that the rate appearance of the new cases increases rapidly to begin with rises to a maximum and there after falls to zero.

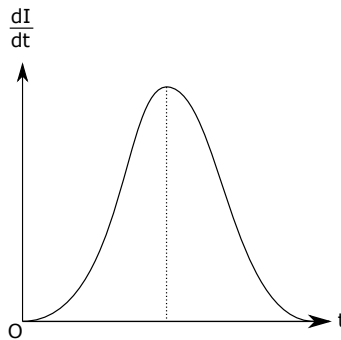


Figure 1.1: Epidemic Curve

Remark 1.2.1. The above analysis does not less tell us the rate at which the infection is spreading. To do this we take the basic equation

$$S + I = N \quad (1.2.7)$$

$$\frac{dS}{dt} = -\gamma SI \quad (1.2.8)$$

where N is size of total population. Therefore we have,

$$\begin{aligned} \frac{d}{dt}(N - I) &= -\gamma(N - I)I \\ \Rightarrow \frac{dI}{dt} &= \gamma(N - I)I \quad [\because N \text{ is time independent}] \end{aligned} \quad (1.2.9)$$

On integration of the Eq. (1.2.9), with the condition $I(0) = 1$, we have

$$I(t) = \frac{N}{(N-1)e^{-\gamma Nt} + 1} \quad (1.2.10)$$

Since γ is positive, $I(t)$ goes to N as $t \rightarrow \infty$ one can conclude that every individual in the population will eventually contact the disease. Thus one can calculate $S(t)$ using Eq. (1.2.7) in the form

$$S(t) = \frac{N(N-1)e^{-\gamma Nt}}{1 + (N-1)e^{-\gamma Nt}} \quad (1.2.11)$$

The rate at which the infection takes place is given by

$$\frac{dI}{dt} = \frac{N^2(N-1)\gamma e^{-\gamma Nt}}{[1 + (N-1)e^{-\gamma Nt}]^2} \quad (1.2.12)$$

The curve representing $\frac{dI}{dt}$ vs t is known as the epidemic curve. Now to investigate the maximum value, the rate at which the infections takes place let us compute

$$\frac{d^2I}{dt^2} = \left[\frac{(N-1)N^3\gamma^2 e^{-\gamma Nt}}{1 + (N-1)e^{-\gamma Nt}} \right] [(N-1)e^{-\gamma Nt} - 1] \quad (1.2.13)$$

Now the factor inside the first bracket is positive for all values of t . Thus the sign of $\frac{d^2I}{dt^2}$ only depends on the other factor namely $[(N-1)e^{-\gamma Nt} - 1]$. At $t = 0$, this factor is positive and becomes negative when $t \rightarrow \infty$, so there exist an extreme value when $(N-1)e^{-\gamma Nt} - 1 = 0$. So the rate has a maximum at

$$t = \frac{\ln(N-1)}{\gamma N} = t_{max} \quad (1.2.14)$$

Then $\left(\frac{dI}{dt}\right)_{max} = \frac{N^2\gamma}{4}$ and $I_{max} = \frac{N}{2}$.

Note:

1. One can note from the expression of t_{max} that if γ is small t_{max} tends to the large, i.e., smaller the γ longer it take to reach the peak value. Also the epidemic will be complete in a much shorter time for a dense population than for a sparse one.

2. A serious limitation of this epidemic model is that everyone in the population will contact the disease as many susceptible still remain in the population.

1.3 SIS Epidemic Model

In this model, a susceptible person can become infected at a rate proportional to SI and an infected person can recover and become susceptible again at a rate γI so that we get the model

$$\frac{dS}{dt} = -\beta SI + \gamma I, \quad (1.3.1)$$

$$\frac{dI}{dt} = \beta SI - \gamma I \quad (1.3.2)$$

which gives

$$S(t) + I(t) = N = S(0) + I(0) = S_0 + I_0 \quad (I_0 \neq 0). \quad (1.3.3)$$

From (1.3.1)-(1.3.3),

$$\frac{dI}{dt} = (\beta N - \gamma)I - \beta I^2 = kI - \beta I^2. \quad (1.3.4)$$

Integrating (1.3.4), we obtain

$$I(t) = \begin{cases} \frac{\exp(kt)}{\beta[\exp(kt) - 1]/k + I_0^{-1}} & (k \neq 0) \\ \frac{1}{\beta t + I_0^{-1}} & (k = 0) \end{cases} \quad (1.3.5)$$

As $t \rightarrow \infty$,

$$I(t) \rightarrow \begin{cases} N - \rho & \text{if } N > \rho = \gamma/\beta \\ 0 & \text{if } N \leq \rho = \gamma/\beta \end{cases} \quad (1.3.6)$$

1.3.1 SIS Model with Specific Rate of Infection as a Function of t

In this case, (1.3.4) becomes

$$\frac{dI}{dt} = [\beta(t)N - \gamma]I - \beta(t)I^2 \quad (1.3.7)$$

or

$$\frac{dJ}{dt} + [\beta(t)N - \gamma]J = \beta(t), \quad (1.3.8)$$

where

$$J(t) = [I(t)]^{-1}. \quad (1.3.9)$$

Integrating (1.3.8), we get

$$J(t) \left[\exp \left\{ \int_0^t [\beta(t)N - \gamma] dt \right\} \right] = \int_0^t \beta(t) \left[\exp \left\{ \int_0^t [\beta(t)N - \gamma] dt \right\} \right] dt + J_0. \quad (1.3.10)$$

Simplifying this equation and using (1.3.9)

$$I(t) = \frac{\exp \left[N \int_0^t \beta(u) du - \gamma t \right]}{\int_0^t \beta(v) \exp \left[N \int_0^v \beta(u) du - \gamma v \right] dv + I_0^{-1}}. \quad (1.3.11)$$

1.3.2 SIS Model with Constant Number of Carriers

In this model, infection is spread both by infectives and a constant number C of carriers so that (1.3.1) and (1.3.2) becomes

$$\frac{dI}{dt} = \beta(I + C)S - \gamma I = \beta CN + \beta(N - C - \rho)I - \beta I^2. \quad (1.3.12)$$

Integrating, we get

$$I(t) = \frac{\alpha_1(I_0 - \alpha_2)e^{\beta\alpha_1 t} + \alpha_2(\alpha_1 - I_0)e^{\beta\alpha_2 t}}{(I_0 - \alpha_2)e^{\beta\alpha_1 t} + (\alpha_1 - I_0)e^{\beta\alpha_2 t}} \quad (1.3.13)$$

where

$$\alpha_1, \alpha_2 = \frac{1}{2} \left[(N - C - \rho) \pm \{(N - C - \rho)^2 + 4CN\}^{1/2} \right]; \quad (1.3.14)$$

α_1, α_2 correspond to the positive and negative roots respectively of the equations $I^2 - (N - C - \rho)I - NC = 0$. Now, as $t \rightarrow \infty$,

$$I(t) \rightarrow \alpha_1 \quad (1.3.15)$$

so that $I(t)$ is asymptotic to a positive constant for all values of N and ρ . Thus, with a constant number of carriers, $I(t)$ does not tend to zero.

1.4 Simple Epidemic Model with Carriers

In this model, only carriers spread the disease and their number decreases exponentially with time as they are identified and eliminated. Here, if $S(t)$, $I(t)$ and $C(t)$ respectively represent the number of susceptibles, infectives, and carriers at time t , we have

$$\begin{aligned} \frac{dS}{dt} &= -\beta C(t)S(t) + \gamma I(t), \\ \frac{dI}{dt} &= \beta C(t)S(t) - \gamma I(t), \\ \frac{dC}{dt} &= -\alpha C \end{aligned} \quad (1.4.1)$$

so that

$$S(t) + I(t) = S_0 + I_0 = N, \quad C(t) = C_0 \exp[-\alpha t],$$

$$\frac{dI}{dt} = \beta C_0 N \exp(-\alpha t) - [\beta C_0 \exp(-\alpha t) + \gamma] I \quad (1.4.2)$$

whose solution is

$$I(t) = \frac{\beta C_0 N \int_0^t \exp[-\alpha v - \beta C_0 \exp(-\alpha v)/\alpha + \gamma v] dv + I_0 \exp(-\beta C_0/\alpha)}{\exp[-(\beta C_0/\alpha) \exp(-\alpha t) + \gamma t]} \quad (1.4.3)$$

It can be now shown that

$$\lim_{t \rightarrow \infty} I(t) = 0. \quad (1.4.4)$$

1.5 SEIR Epidemic Model

The Susceptible-Exposed-Infectious-Recovered (SEIR) epidemic model is a mathematical framework used to study the spread of infectious diseases within a population. In this model, individuals can transition through four states: susceptible (S), exposed (E), infectious (I), and recovered (R). Exposed individuals are infected but not yet infectious, and recovered individuals are assumed to be immune to further infection.

1.5.1 Detailed Description of SEIR Mathematical Model

Let $S(t)$, $E(t)$, $I(t)$, and $R(t)$ denote the number of individuals in each state at time t . The dynamics of the SEIR epidemic model can be described by the following system of ordinary differential equations (ODEs):

$$\begin{aligned}\frac{dS}{dt} &= -\beta \frac{SI}{N} \\ \frac{dE}{dt} &= \beta \frac{SI}{N} - \sigma E \\ \frac{dI}{dt} &= \sigma E - \gamma I \\ \frac{dR}{dt} &= \gamma I\end{aligned}\tag{1.5.1}$$

where:

- β is the transmission rate (rate of infection).
- σ is the rate at which exposed individuals become infectious.
- γ is the recovery rate (rate of recovery or transition from infectious to recovered).
- N is the total population size.

This system variant of the SIR model of Kermack and McKendrick. Here, we neglect the birth and death rates, i.e., we consider a model without vital dynamics. The average incubation period is $\frac{1}{\alpha}$, the parameter β is the product of the average number of contacts per person and per unit time by the probability of disease transmission in a contact between a susceptible and an infectious individual, γ is a transition rate so that $\frac{1}{\gamma}$ measures the duration of the infection of an individual and N is the total population size. In the Covid-19 pandemic, the average incubation period is of several days and this is why an SEIR model has to be preferred to a simple SIR model. Many qualitative features are the same in the two models but the compartment E of exposed individuals makes the analysis significantly more delicate and realistic. Unreported cases or asymptomatic individuals are not taken into account here: this is an important aspect of the Covid-19 epidemic, with important consequences on the epidemic size, but probably not so much on the qualitative issues. Other factors, like delays for the transmission of the information studied, certainly also play a pivotal role in the current outbreak.

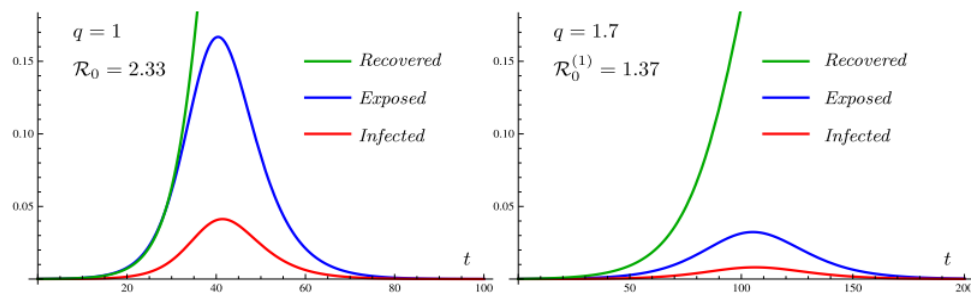


Figure 1.2: The peak of the outbreak in the SEIR model. The time t is counted in days. The vertical axis represents the fraction of the population. The basic reproduction ratio is either $R_0 = 2.33$ (left) or 1.37 (right) corresponding to a reduction of social interactions by a factor $q = 1.7$. This illustrates the flattening of the curves.

1.5.2 Equilibrium Points

The equilibrium points of the SEIR epidemic model can be found by setting the rates of change of all compartments to zero. Solving the resulting system of equations yields the equilibrium points.

For the SEIR model, the equilibrium points are:

$$\begin{aligned} S^* &= \frac{\gamma}{\beta} \\ E^* &= 0 \\ I^* &= \frac{\sigma}{\gamma} \left(1 - \frac{\gamma}{\beta}\right) \\ R^* &= N - S^* - I^* \end{aligned}$$

where N is the total population size.

1.5.3 Stability Analysis

Similar to the SIS model, stability analysis of the SEIR model involves linearizing the system of ODEs around the equilibrium points and examining the eigenvalues of the resulting Jacobian matrix.

1.5.4 Conclusion

The SEIR epidemic model provides a more detailed understanding of disease dynamics by incorporating an exposed compartment, representing individuals who have been infected but are not yet infectious. By studying the behavior of the model and analyzing its equilibrium points and stability, researchers can gain insights into the spread and control of infectious diseases within populations.

1.6 SEIRS Mathematical Model

The Susceptible-Exposed-Infectious-Recovered-Susceptible (SEIRS) epidemic model is a mathematical framework used to study the spread of infectious diseases within a population. This model extends the SEIR model by incorporating a temporary immunity period, allowing recovered individuals to become susceptible again after a certain period.

1.6.1 Model Description

Let $S(t)$, $E(t)$, $I(t)$, $R(t)$, and $S_{\text{new}}(t)$ denote the number of individuals in each state at time t . The dynamics of the SEIRS epidemic model can be described by the following system of ordinary differential equations (ODEs):

$$\begin{aligned} \frac{dS}{dt} &= -\beta \frac{SI}{N} + \xi S_{\text{new}} \\ \frac{dE}{dt} &= \beta \frac{SI}{N} - \sigma E \\ \frac{dI}{dt} &= \sigma E - \gamma I \\ \frac{dR}{dt} &= \gamma I - \xi R \\ \frac{dS_{\text{new}}}{dt} &= \xi R - \xi S_{\text{new}} \end{aligned} \tag{1.6.1}$$

where:

- β is the transmission rate (rate of infection).
- σ is the rate at which exposed individuals become infectious.
- γ is the recovery rate (rate of recovery or transition from infectious to recovered).
- ξ is the rate at which recovered individuals become susceptible again.
- N is the total population size.

1.6.2 Equilibrium Points

The equilibrium points of the SEIRS epidemic model can be found by setting the rates of change of all compartments to zero. Solving the resulting system of equations yields the equilibrium points.

For the SEIRS model, the equilibrium points are:

$$S^* = \frac{\gamma\xi}{\beta(\xi + \gamma)}$$

$$E^* = 0$$

$$I^* = \frac{\sigma}{\gamma} \left(1 - \frac{\gamma\xi}{\beta(\xi + \gamma)} \right)$$

$$R^* = \frac{\xi}{\xi + \gamma} N$$

$$S_{\text{new}}^* = N - S^* - I^* - R^*$$

where N is the total population size.

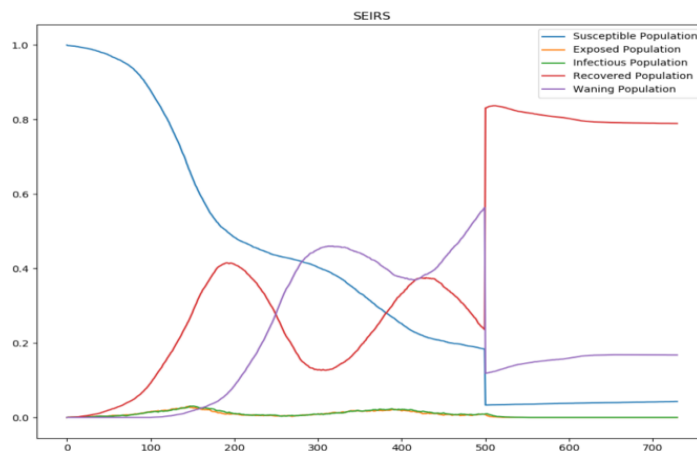


Figure 1.3: Trajectories of SEIRS model

1.6.3 Linearization

The Jacobian matrix of the system evaluated at the equilibrium points can be calculated and then used to determine the stability of the equilibrium points.

1.6.4 Eigenvalues

The eigenvalues of the Jacobian matrix determine the stability of the equilibrium points. If all eigenvalues have negative real parts, the equilibrium is stable. If any eigenvalue has a positive real part, the equilibrium is unstable.

1.6.5 Conclusion

In summary, the SEIRS epidemic model offers a nuanced understanding of disease dynamics by incorporating a temporary immunity period. By comprehensively analyzing the model's behavior, equilibrium points, and stability, one can glean valuable insights into the transmission and control of infectious diseases within populations. This holistic approach aids in devising effective strategies for disease management and public health interventions, ultimately contributing to the safeguarding of community well-being.

Unit 2

Course Structure

- General Epidemic Model
 - Approximate Solution
 - Recurring Epidemic
 - Behaviour of Seasonal Dynamics in Recurrent Epidemics
-

2.1 General Epidemic Model

The study of general epidemic involves with infection as well as removal. Let us assume that $S(t)$, $I(t)$ and $R(t)$ be the respective population sizes of susceptible, infected and removal individual at time t .

Let us make few assumption about the nature of S , I and R as follows:

- The population is treated as closed (constant) and continuous which can be represented by S moving over to I moving over to R (we ignore both birth and immigration).
- The rate of change of susceptible population is proportional to the number of contacts between the members of the class S and I , in which we take in term, the number of contacts to be proportional to the product of the numbers of S and I . This assumption takes care of uniform mixing of the population.
- Individuals are recovered at a rate proportional to the number I .

Let $r > 0$ be the infective rate and $\gamma > 0$ be the removed rate and if S_0, I_0 be the initial number of members of S and I respectively, then the governing equations are given by

$$\frac{dS}{dt} = -rSI \quad (2.1.1)$$

$$\frac{dI}{dt} = rSI - \gamma I \quad (2.1.2)$$

$$\frac{dR}{dt} = \gamma I \quad (2.1.3)$$

We are to study these equation with the following conditions given by $S = S_0$, $I = I_0$ and $R = 0$ initially at $t = 0$. In addition to these we have

$$S(t) + I(t) + R(t) = \text{constant} \quad \text{i.e.,} \quad \frac{d}{dt}(S + I + R) = 0 \quad (2.1.4)$$

From Eq. (2.1.2), we have

$$\frac{dI}{dt} = r \left(S - \frac{\gamma}{r} \right) I \quad (2.1.5)$$

If $S_0 < \frac{\gamma}{r}$ then $\frac{dI}{dt} < 0$ and since $S(t) < S_0$, one can conclude that $\frac{dI}{dt} < 0$ for all t . Therefore, it is such a case in which the infection dies out, i.e., non epidemic takes place. This is known as a “*Threshold Phenomena*”. We therefore conclude that there exist a critical value for which the initial susceptible has to exceed for their to be an epidemic, in other words the relative removal rate $\frac{\gamma}{r}$ must be sufficiently small so as to allow the epidemic to spread.

The Eqs. (2.1.1)–(2.1.4) also enable us to study another behaviour relative to spread of the disease. Since $S(t)$ is non-increasing and positive $\lim_{t \rightarrow \infty} S(t) \rightarrow S(\infty)$ exists and since $\frac{dR}{dt} \geq 0$ and $R(t) \leq N$ then $R(\infty)$ exists. Again we have $I(t) = N - R(t) - S(t)$ is follows the $\lim_{t \rightarrow \infty} I(t) \rightarrow 0$.

Now we consider some other values in dividing Eq. (2.1.1) by Eq. (2.1.3) when we have

$$\frac{dS}{dR} = -\frac{r}{\gamma} S \quad (2.1.6)$$

On integration we have

$$S = S_0 \exp \left\{ -\frac{r}{\gamma} R \right\} \quad (2.1.7)$$

Now since $R \leq N$ which implies $-R \geq -N$, so that

$$S = S_0 \exp \left\{ -\frac{r}{\gamma} R \right\} \geq S_0 \exp \left\{ -\frac{r}{\gamma} N \right\} > 0 = \alpha \quad (\text{say}). \quad (2.1.8)$$

Therefore, $\lim_{t \rightarrow \infty} S(t)$ is always positive, one can interpreted this by saying that there will always be susceptible remaining in the population. Thus we conclude that some individual will escape the disease all together and in particular the spread of disease does not stop for the lack of susceptible population. Let us consider a function

$$f(z) = S_0 \exp \left\{ -\frac{1}{\rho}(N - z) \right\} - z \quad \text{in which} \quad \rho = \frac{\gamma}{r} \quad (2.1.9)$$

Now, $f(0) > 0$ and $f(N) = S_0 - N < 0$. Therefore, there must be a positive root for $f(z) = 0$. Let z_0 be the root, then we have

$$f'(z) = \frac{1}{\rho} S_0 \exp \left\{ -\frac{1}{\rho}(N - z) \right\} - 1 \quad (2.1.10)$$

$$\text{and } f''(z) = \frac{1}{\rho^2} S_0 \exp \left\{ -\frac{1}{\rho}(N - z) \right\} \quad (2.1.11)$$

Now since $f''(z) > 0$ and $f(N) < 0$, there is only one such root $z_0 < N$. Now we have seen that

$$S = S_0 \exp \left(-\frac{R}{\rho} \right) \quad \text{i.e.,} \quad S_\infty = S_0 \exp \left\{ -\frac{1}{\rho}(N - S_\infty) \right\} \quad (2.1.12)$$

Hence, we can say that S_∞ is the root of the equation $f(z) = 0$. Now we can sum up all the results in the form of a theorem as follows:

Theorem 2.1.1. If $S_0 < \rho$ then $I(t)$ decreases monotonically to zero. If $S_0 > \rho$ then the number of infective increases as time t increases and then tends monotonically to zero. Further $\lim_{t \rightarrow \infty} S(t)$ exists and S_∞ is a root of the transcendental equation.

Remark 2.1.1. The equation $\frac{dS}{dR} = -\frac{r}{\gamma}S$ can be solved under certain approximations when R is known.

2.2 Approximate Solution

We have the Eq. (2.1.6) as

$$\frac{dS}{dR} = -\frac{r}{\gamma}S \quad (2.2.1)$$

where S is given by the Eq. (2.1.7) as $S = S_0 \exp\left(-\frac{r}{\gamma}R\right)$. Now substituting Eq. (2.1.7) in the Eq. (2.1.3), we have

$$\frac{dR}{dt} = \gamma \left[N - S_0 \exp\left(-\frac{r}{\gamma}R\right) - R \right] \quad (2.2.2)$$

The Eq. (2.2.2) can be solved by standard method by taking some approximate value after expanding upto some power of R . But we are interested in looking for values of R when $t \rightarrow \infty$. We note that as $t \rightarrow \infty$, $\frac{dR}{dt} \rightarrow 0$. Further as $t \rightarrow \infty$, taking $S_0 \approx N$, we have

$$\begin{aligned} 0 &= \gamma \left[N - N \exp\left(-\frac{r}{\gamma}R\right) - R \right] \\ \text{or, } 0 &= \gamma \left[N - N \exp\left(-\frac{R}{\rho}R\right) - R \right] \quad (\because \rho = \frac{\gamma}{r}) \end{aligned}$$

Now we expand the exponential term in the right hand side in powers of $\frac{R}{\rho}$, which becoming smaller and smaller as $t \rightarrow \infty$ and can be approximate upto second power of $\frac{R}{\rho}$. Therefore, we have

$$\begin{aligned} 0 &\approx \gamma \left[N - N \left(1 - \frac{R}{\rho} + \frac{R^2}{2\rho^2} \right) - R \right] \\ \Rightarrow R &\approx N \left(\frac{R}{\rho} - \frac{R^2}{2\rho^2} \right) \\ \Rightarrow \frac{1}{N} &\approx \frac{2\rho - R}{2\rho^2} \\ \Rightarrow \frac{2\rho^2}{N} &\approx 2\rho - R \\ \Rightarrow R &\approx 2\rho \left(1 - \frac{\rho}{N} \right) \end{aligned}$$

This is approximate as $t \rightarrow \infty$ and hence one should get the ultimate size of the epidemic. If $\rho > N$, there is no true epidemic and hence the appearance of epidemic will be there only when $\rho < N$, i.e., when the effective removal rate is less than the initial number of susceptible and in this case all persons do not get infected. A stage may be reached when all the infected person are immediately removed. So in order of epidemic may

occur, we have $N = \rho + \gamma$, where $\gamma > 0$ is small. Thus we have

$$\begin{aligned} R(\infty) &\approx 2\rho \left(1 - \frac{\rho}{\rho + \gamma}\right) \\ &\approx 2\rho \left[1 - \left(1 + \frac{\gamma}{\rho}\right)^{-1}\right] \\ &\approx 2\rho \left[1 - 1 + \frac{\gamma}{\rho}\right] \\ &\approx 2\gamma \end{aligned}$$

This shows that the initial density of susceptible namely $S_0 (= N = \rho + \gamma)$ is reduced to $S_\infty (= \rho - \gamma)$ which means that the final number of susceptible falls at a point as far below the threshold value ρ as originally it was above it. This is known as “*Kermack & McKendric Threshold Theorem*” .

Remark 2.2.1. • The above theorem corresponds to the general observation of the epidemic tends to built up more rapidly for the density of susceptible is high on account of over crowding and the removal rate is relatively low because of the factors that ignorance and inadequate isolation.

- The Eq. (2.2.2) can also be integrated when the approximation is taken upto second powers to R .

Integration leading to approximate solution. We have

$$\frac{dR}{dt} = \gamma \left[N - R - S_0 \exp\left(-\frac{R}{\rho}\right) \right] \quad (2.2.3)$$

Substituting $\exp\left(-\frac{R}{\rho}\right) = 1 - \frac{R}{\rho} + \frac{R^2}{2\rho^2}$ into the above equation, one get

$$\begin{aligned} \frac{dR}{dt} &= \gamma \left[N - R - S_0 \left(1 - \frac{R}{\rho} + \frac{R^2}{2\rho^2}\right) \right] \\ \Rightarrow \frac{dR}{dt} &= \gamma \left[N - S_0 + R \left(\frac{S_0}{\rho} - 1\right) - \frac{S_0}{2} \frac{R^2}{\rho^2} \right] \\ \Rightarrow \frac{dR}{dt} &= a + bR - cR^2 \end{aligned}$$

where $a = \gamma(N - S_0)$, $b = \gamma \left(\frac{S_0}{\rho} - 1\right)$ and $c = \frac{\gamma S_0}{2\rho^2}$. On integration, we obtain

$$\begin{aligned} \frac{2}{q} \tanh^{-1} \left(\frac{2cR - b}{q} \right) &= t + c_1, \quad c_1 \text{ being a constant and } q = \sqrt{b^2 + 4ac} \\ \Rightarrow R(t) &= \frac{1}{2c} \left[b + q \tanh \left(\frac{qt}{2} + c_2 \right) \right], \quad c_2 \text{ is a different constant} \\ \Rightarrow R(t) &= \frac{1}{2c} \left[b + q \left\{ \frac{1 - e^{-qt+c_3}}{1 + e^{-qt+c_3}} \right\} \right] \end{aligned}$$

Since $q > b$ and since $\tanh x$ increases monotonically from -1 to $+1$ when x increases from $-\infty$ to $+\infty$, it follows that the constant c_2 and c_3 exists and have real values. These constants can also be chosen in such a way that $R(0) = 0$. Behaviour of $R(t)$ for large values of time or in other words asymptotic behaviour of $R(t)$ can be found as

$$\lim_{t \rightarrow \infty} R(t) = \frac{1}{2c} (b + q) \quad (2.2.4)$$

or in terms of the old parameters of the mode we have,

$$R_\infty = \frac{1}{S_0} \left[\rho(S_0 - \rho) + \rho \{ (S_0 - \rho)^2 + 2S_0 I_0 \}^{1/2} \right] \quad (2.2.5)$$

Let us now see if some additional assumption regarding the relative size of the parameter gives some result of the threshold theorem mention early.

In particular, it is customary to assume that an epidemic is generated through the introduction of a small number of infected individuals to a population of susceptible. Mathematically, $S_0 > \rho$ and $I_0 > 0$. We now use the quantity

$$\lim_{I_0 \rightarrow 0} R(\infty) = \frac{2(S_0 - \rho)\rho}{S_0} \quad (2.2.6)$$

to represents the asymptotic size of an epidemic resulted from the introduction of a small number of infective into a group of susceptible.

Finally, let us assume that $S - 0$ is closed to the threshold value ρ , then the epidemic develop only of $S_0 > \rho$, i.e., $S_0 = \rho + \gamma$, where $\gamma > 0$ is small. Therefore,

$$\lim_{I_0 \rightarrow \infty} R_\infty = \frac{2\gamma R}{\rho + \gamma} = 2\gamma \left(1 + \frac{\gamma}{\rho} \right)^{-1} \approx 2\gamma \quad (2.2.7)$$

Therefore the asymptotic size of the epidemic is approximately equal to 2γ . Hence, we can state as follows:

The total size of the epidemic resulting from an introduction of trace infection into a population of susceptible whose size S_0 is closed to the threshold value ρ is approximately equal to $2(S_0 - \rho)$.

Remark 2.2.2. • It may be remarked that this result is also taken as a part of threshold theorem of epidemiology.

- We can rewrite the expression of $R(t)$ also in the form

$$R(t) = \frac{\rho^2}{S_0} \left[\frac{S_0}{\rho} - 1 + \alpha \tanh \left(\frac{\alpha \gamma t}{2} - \phi \right) \right] \quad (2.2.8)$$

$$\text{where } \alpha = \left[\left(\frac{S_0}{\rho} - 1 \right)^2 + \frac{2S_0}{\rho^2} (N - S_0) \right]^{1/2} \text{ and } \phi = \tanh^{-1} \frac{1}{\alpha} \left(\frac{S_0}{\rho} - 1 \right).$$

Differentiating, we get

$$\frac{dR}{dt} = \frac{\gamma \rho^2 \alpha^2}{2S_0} \operatorname{sech}^2 \left(\frac{1}{2} \alpha \gamma t - \phi \right) \quad (2.2.9)$$

This equation defines a *symmetrical bell-shaped* curve in $t - \frac{dR}{dt}$ plane (see Fig. 2.1). It may be noted that “Kermack & McKendric” compared the values of $\frac{dR}{dt}$ from this equation and found complete agreement with the data from an actual plague which occur during 1905-06 in Bombay. The typical variations of $S(t)$, $I(t)$ and $R(t)$ can be represented graphically in Fig. 2.2.

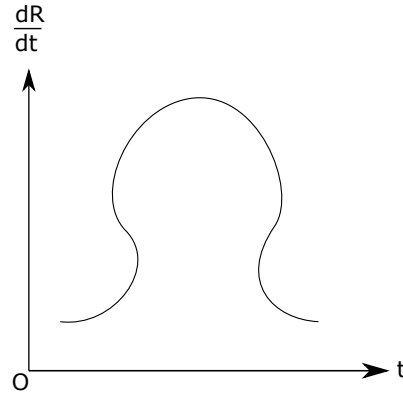
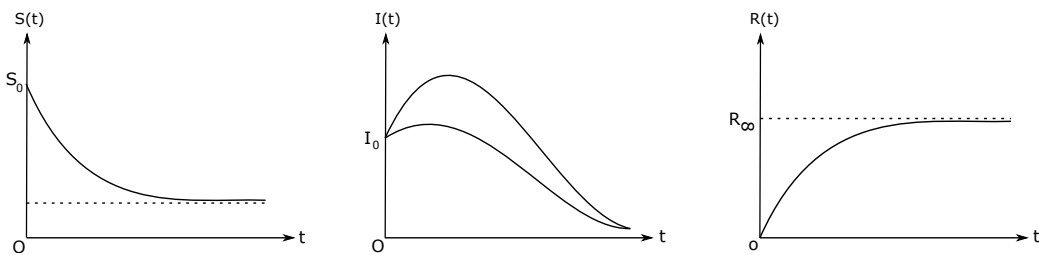


Figure 2.1: Symmetrical bell-shaped curve

Figure 2.2: Variation of $S(t)$, $I(t)$ and $R(t)$ with time t .

2.3 Recurring epidemic

There are many disease that tend to recur in various population with a certain amount of regularity often assuming the character of an epidemic. For example, measles. We assume that the stock of susceptible is replenished at a constant rate μ in time Δt , so that we can take the group of susceptible to be increase by the amount $\mu\Delta t$, which losing $rSI\Delta t$ due to new infections. We can take the total population size to remain constant. By assuming the influx of the new susceptible balanced by an appropriate death rate affecting only the removed individuals. We can then have the governing equation as

$$\frac{dS}{dt} = -rSI + \mu \quad (2.3.1)$$

$$\frac{dI}{dt} = rSI - \gamma I \quad (2.3.2)$$

The steady state conditions are given by

$$\frac{dS}{dt} = 0 = \frac{dI}{dt}$$

Therefore the steady states are given by

$$S = \frac{\gamma}{r} = S_0 \quad \text{and} \quad I = \frac{\mu}{\gamma} = I_0$$

Let us now study about the equilibrium position through the use of

$$S = S_0(1 + u) \quad \text{and} \quad I = I_0(1 + v)$$

where u and v are small quantities. Substituting the above quantities in Eqs. (2.3.1) and (2.3.2), we have

$$\frac{1}{rI_0} \frac{du}{dt} = -(u + v + uv) \Rightarrow \sigma \frac{du}{dt} = -(u + v + uv) \text{ where } \sigma = \frac{\gamma}{r\mu} \quad (2.3.3)$$

$$\frac{dv}{dt} = \gamma u(1 + v) \Rightarrow \tau \frac{dv}{dt} = u(1 + v) \text{ where } \tau = \frac{1}{\gamma} \quad (2.3.4)$$

Since u and v are small, so their products may be neglected so that the Eqs. (2.3.3) and (2.3.4) reduced to

$$\sigma \frac{du}{dt} = -(u + v) \quad (2.3.5)$$

$$\tau \frac{dv}{dt} = u \quad (2.3.6)$$

From these equations, we get

$$\begin{aligned} \tau \frac{d^2v}{dt^2} &= \frac{du}{dt} = -\frac{1}{\sigma}(u + v) = -\frac{1}{\sigma} \left(\tau \frac{dv}{dt} + v \right) \\ \Rightarrow \frac{d^2v}{dt^2} + \frac{1}{\sigma} \frac{dv}{dt} + \frac{1}{\tau\sigma} v &= 0 \end{aligned} \quad (2.3.7)$$

The general solution of the Eq. (2.3.7) is given by

$$v(t) = Ae^{-t/2\sigma} \cos \xi t + Be^{-t/2\sigma} \sin \xi t, \quad (2.3.8)$$

where $\xi = \sqrt{\frac{1}{\sigma\tau} - \frac{1}{4\sigma^2}}$. Using the initial conditions $v = v_0$ and $\frac{dv}{dt} = 0$ at $t = 0$, we have $v_0 = A$ and $B = \frac{v_0}{2\sigma\xi}$. Therefore,

$$\begin{aligned} v(t) &= v_0 e^{-t/2\sigma} \cos \xi t + \frac{v_0}{2\sigma\xi} e^{-t/2\sigma} \sin \xi t \\ &= v_0 e^{-t/2\sigma} \left[\cos(\xi t) + \frac{1}{2\sigma\xi} \sin \xi t \right] \end{aligned} \quad (2.3.9)$$

Using Eq. (2.3.9), from Eq. (2.3.6) we get

$$\begin{aligned} u(t) &= \tau \frac{dv}{dt} \\ &= \tau v_0 \left[-\frac{1}{2\sigma} \left(\cos \xi t + \frac{1}{2\sigma\xi} \sin \xi t \right) + \left(-\xi \sin \xi t + \frac{1}{2\sigma} \cos \xi t \right) \right] e^{-t/2\sigma} \\ &= \tau v_0 e^{-t/2\sigma} \left[\frac{1}{4\sigma^2\xi} \sin \xi t - \xi \sin \xi t \right] \\ &= \tau v_0 e^{-t/2\sigma} \left(\frac{1}{4\sigma^2\xi} - \xi \right) \sin \xi t \end{aligned}$$

This clearly represents damp harmonic motion to discuss the small departure from equilibrium.

2.4 Behaviour of Seasonal Dynamics in Recurrent Epidemics

Seasonality is a driving force that has a major effect on the spatio-temporal dynamics of natural systems and their populations. This is especially true for the transmission of common infectious diseases (such as influenza,

measles, chickenpox and pertussis), and is of great relevance for host–parasite relationships in general. Here we gain further insights into the nonlinear dynamics of recurrent diseases through the analysis of the classical seasonally forced SIR (susceptible, infectious or recovered) epidemic model. Our analysis differs from other modelling studies in that the focus is more on post-epidemic dynamics than the outbreak itself. Despite the mathematical intractability of the forced SIR model, we identify a new threshold effect and give clear analytical conditions for predicting the occurrence of either a future epidemic outbreak, or a ‘skip’—a year in which an epidemic fails to initiate. The threshold is determined by the population’s susceptibility measured after the last outbreak and the rate at which new susceptible individuals are recruited into the population. Moreover, the time of occurrence (that is, the phase) of an outbreak proves to be a useful parameter that carries important epidemiological information. In forced systems, seasonal changes can prevent late-peaking diseases (that is, those having high phase) from spreading widely, thereby increasing population susceptibility, and controlling the triggering and intensity of future epidemics. These principles yield forecasting tools that should have relevance for the study of newly emerging and re-emerging diseases controlled by seasonal vectors.

The driving force maintaining recurrent epidemic dynamics has long been recognized to be the continuous birth and recruitment of new susceptible individuals into the population. As an outbreak progresses, susceptibles (S) become infected, drop to a minimum level (S_0) in the wake of the epidemic, and then grow in number as the birth process begins to dominate once again. The pattern of epidemics from year to year is controlled by the population’s periodically changing annual contact rate. Mathematical analysis has shown it useful to focus on S_0 , defined as the local minimum number of susceptibles left in the wake of an epidemic. S_0 controls whether there will be an outbreak in the year ahead or the number of ensuing skips that follow. To a good approximation, it is obligatory to show that to generate k or more consecutive skips in successive years requires that S_0 fall below:

$$S_c(k) = \frac{\gamma + \mu}{\beta_0} - \frac{(k + 1)\mu\chi}{2}. \quad (2.4.1)$$

The critical threshold is defined in terms of classical epidemiological parameters: γ represents the rate at which infected individuals recover; μ is the per capita rate at which members of the population reproduce and die; and β_0 is the rate of effective contacts between infected and susceptible individuals averaged over the year. The seasonal forcing modulates the contact rate and is taken to be annual with period $\chi = 1$ (χ having time units of years). For example, the commonly used sinusoidally forced contact rate changes annually in time (t) according to the relation $\beta(t) = \beta_0[1 + \delta \sin 2\pi t]$, with δ setting the strength of the forcing. More specifically, for $k = 0$, one obtains:

$$S_0 > S_c = \frac{\gamma + \mu}{\beta_0} - \frac{\mu\chi}{2} \Rightarrow \text{Epidemic} \quad (2.4.2)$$

whereas if $S_0 < S_c$, there is a skip in the following year.

The above threshold rests on the principle that after a large epidemic the infected population recovers and passes through a period of long-term immunity. A large epidemic is able to exhaust the susceptible pool (S_0), and should the latter fall below the critical threshold level (S_c), there is a skip—it becomes impossible for a major epidemic to be triggered in the following year. Interestingly, the above criteria (equations (2.4.1) and (2.4.2)) go beyond the predictions of the classical theory based on the unforced epidemic model, which sometimes proves to be a misleading guide. For instance, during the skip marked in Fig. 2.4a, there is a period in which infectives begin to increase rapidly owing to favourable seasonal conditions (high disease transmission). This increase is an indicator that the reproductive number R_0 is greater than unity ($R_0 > 1$) and thus, according to the classical theory, suggests a major epidemic is under way. But instead, the growth of infectives is cut short, owing to a change of seasons (diminished disease transmission) which curtails the build-up of the

epidemic process, and results in a skip. Whereas predictions based on R_0 prove unhelpful here, the criterion of equation (2.4.2) is able to correctly differentiate skips from large-scale outbreaks.

The effectiveness of the threshold prediction may be demonstrated through the study of simulated epidemic time series. The seasonally forced SIR model was integrated in the chaotic regime, which advantageously generates time series with skips and variability similar to real world data. The threshold point (S_c) may thus be easily checked. at ant time t between two successive large-scale epidemics A and B, as a function of the susceptibles S_0 left after the first outbreak A. For the given model parameters, the theoretical critical susceptible threshold ($S_c = 0.031$ from equation (2.4.2)) corresponds to the number of susceptibles that separates the annual dynamics ($\tau \approx 1$) from the biennial dynamics ($\tau \approx 2$) in which there is a skip between two outbreaks. Our formalism provides an exact topological distinction that differentiates a skip from an outbreak, even if small. During a skip, susceptibles always increase in time, whereas during an outbreak they must decrease (Fig. 2.4 legend). This overall analysis shows explicitly how S_0 , which characterizes population susceptibility, gives accurate predictions of future outbreaks.

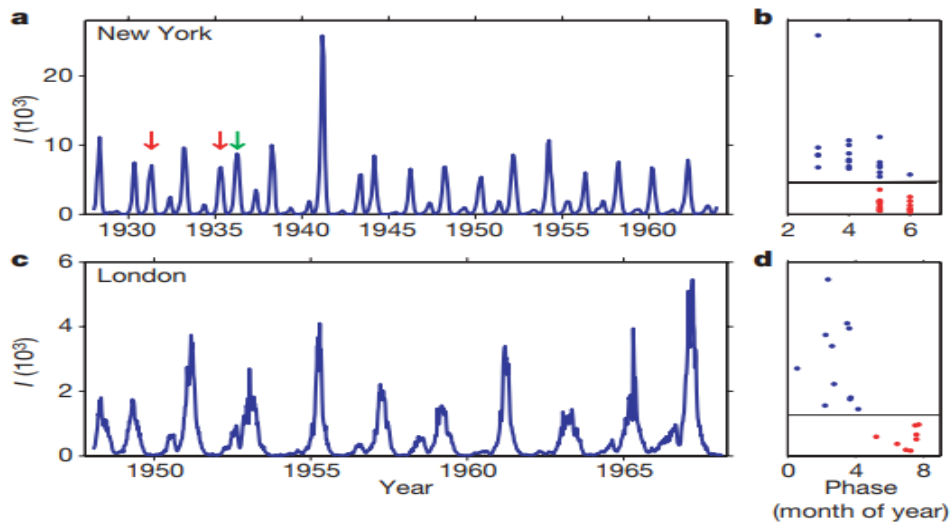


Figure 2.3: **Epidemic time series together with their associated phase relationship and synchronization effects.** **a, c,** Time series of reported measles infective cases (I , in thousands) from the largest city in the US (New York, monthly sampling) and in the UK (London, weekly sampling) in the pre-vaccination era. **b, d,** The maximum number of infectives of each epidemic is plotted as a function of the time of year (phase in months) at which this maximum occurred. Minor epidemic peaks (skips) have been plotted in red to emphasize that all skips occur at the end of the ‘high’ season, and are thus synchronized. The probability of finding all red points only in the late phase regime is $P < 0.001$, making the synchronization significant. Limitations of conventional prediction schemes are as follows. Consider the New York time-series (**a**) where two similar sized ‘intermediate’ outbreaks occurred in 1931 and 1935 (red arrows). The former was followed by a skip, whereas the latter was followed by another intermediate outbreak in 1936 (green arrow). Given the very different outcomes, peak-to-peak predictions become untenable. The problem intensifies when trying to predict outbreaks that occur after skips. The latter skips can be followed by a variety of different sized peaks, ranging from a successive skip (for example, New York in 1940) to extremely large epidemics (for example, New York in 1941).

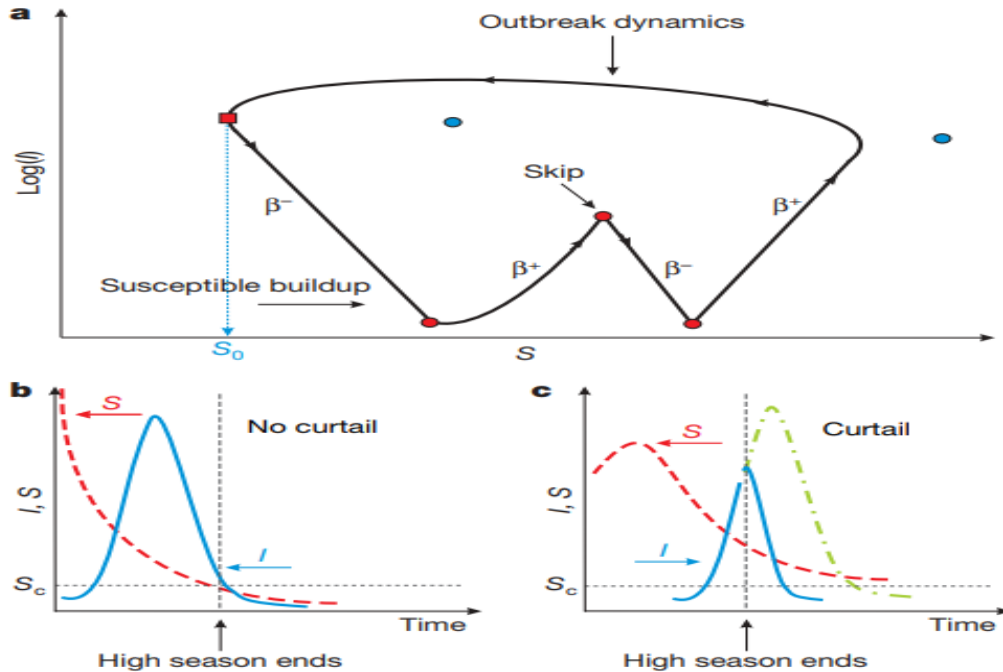


Figure 2.4: **Effects of seasonality on population dynamics.** **a**, Phase plane diagram with the number of infectives $\log(I)$ plotted as a function of susceptible numbers (S) for a typical biennial cycle. The trajectory of the SIR model (system (2.4.3)) rotates anti-clockwise around the phase plane. The trajectory is attracted to the quasi-equilibrium associated with each season (each marked as a filled blue circle). As the seasons (and contact rates β^\pm) change, the trajectory is kicked from one equilibrium to the next. The symbols β^+ and β^- are marked on the curve to indicate those periods of time when the contact rates are associated with high and low seasons respectively. In this biennial cycle, an epidemic occurs in the upper part of phase plane, after which susceptibles pass through a minimum (S_0 , marked by the red square), with a skip occurring in the following year (lower part of phase plane). During a skip, the susceptibles slowly build up, and a small maximum in infective numbers develops one year after the major outbreak. This maximum is prevented from reaching large numbers, as it is curtailed by the change of seasons ($\beta^+ \rightarrow \beta^-$). In contrast to a skip, susceptibles decrease in number during an outbreak. We now consider the relationship between peak outbreak magnitude and initiation time. **b**, An infected individual enters the population early in the high season, and a full scale epidemic develops (solid line). Susceptible numbers fall below the critical level S_c . **c**, An infected individual enters the population very late in the high season. The epidemic (solid line) is cut short at the end of the high season, and prevented from reaching its full potential (dashed-dotted line). Susceptible numbers remain above the critical level S_c . Although the outbreak is curtailed, it should not be viewed as a skip (as susceptible levels decrease over the epidemic).

2.4.1 Classical Forced SIR Model

The classical forced SIR model has the following equations:

$$\begin{aligned}
 \dot{S} &= \mu - \mu S \beta(t) S(I + \epsilon), \\
 \dot{I} &= \beta(t) S(I + \epsilon) - \gamma I - \mu I, \\
 \dot{R} &= \gamma I - \mu R.
 \end{aligned}
 \tag{2.4.3}$$

where the population is composed of susceptible (S), infected (I) and recovered (R) individuals, and are scaled here as proportions. The rate of birth and mortality is μ , infected individuals recover at rate γ . Here, we consider $\epsilon = 10^{-12}$ is a small immigration term. For the case of two seasons each year, the contact rate $\beta(t)$ may be approximated as $\beta^+ = \beta_0(1 + \delta)$ in the high season and as $\beta^- = \beta_0(1 - \delta)$ in the low season, where $0 < \delta < 1$ represents the strength of the seasonal forcing. Over time, the seasons change sequentially: high \rightarrow low \rightarrow high \rightarrow low \rightarrow

A mathematical analysis of the forced ($\delta > 0$) model's epidemic dynamics is worthy noting. The effects of forcing, but do not develop a language of skips attempted here. For a given S_0 , it is possible to derive mathematical expressions for the model's orbit in the lower part of phase plane in Fig. 2.4, and calculate the resulting number of skips. The analysis uncovers the threshold point separating annual and biennial (or higher-order) dynamics. An intuitive understanding may be gained by removing seasonal forcing ($\delta = 0$) altogether. Let $w = \log(I)$, and consider the model's trajectory in the lower part of the S - w phase plane. Beginning in the wake of a large epidemic, with $(S, w) = (S_0, w_0)$, equations (2.4.3) may be approximated as: $\dot{w} = \beta_0 S - \gamma - \mu$ and $\dot{S} \approx \mu$. Susceptibles build up linearly, $S(t) \approx S_0 + \mu t$, and $w(t)$ follows a simple parabola, first descending to very low numbers, and later increasing when the turning point is reached. The recovery time between major epidemics is approximately

$$t_\tau = \frac{2(\gamma + \mu - \beta_0 S_0)}{\beta_0 \mu}, \quad (2.4.4)$$

the time needed for $w(t)$ to return to $w = w_0$. The number of skips is $k = \frac{t_\tau}{\chi} - 1$ where $\chi = 1$ - year. Rearranging the last equation for t_τ gives the maximum level of S_0 susceptibles required to generate k consecutive skips, namely $S_c(k) = \frac{\gamma + \mu}{\beta_0} - (k + 1)\mu \frac{\chi}{2}$. We have shown that the above results hold when forcing $\delta > 0$ is fully taken into account.

Unit 3

Course Structure

- Discrete Mathematical Modelling
 - Stochastic Epidemic Model without Removal
 - Basic System of Equations
 - Solution of the System of Equation
-

3.1 Discrete Mathematical Modelling

A basic three dimensional ODE-based mathematical model for exploring the fundamental features of the disease leprosy is presented. While dealing with continuous systems, a discrete cell dynamical model of leprosy has not yet been proposed and investigated previously. In this regard, recent experimental studies suggests that population growth rate plays a synergistic effect in describing the various aspects of the proliferation of *Mycobacterium leprae* bacteria. It is necessary to understand the density-dependent growth to forecast a more realistic population trend of *M. leprae* into the human body.

Introducing theta logistic growth rate instead of classical logistic growth makes the dynamics of a living system more complicated but it adds more pliability and flexibility in terms of the key relationship of per capita growth rate with the population density of *M. leprae*. Indeed, the intraspecific competition for a safe and sustainable intracellular environment with necessary metabolic activities performed by the organism inside Schwann cells ensure the density dependency when abundance in the bacterial concentration increases. Theta logistic equation is represented generally in the form of density dependence where introduction of a new parameter θ in the growth term is necessary. Here, we denote the curvature of relationship by the parameter θ and more formally, it is called the shape parameter. In fact, θ determines the shape of the curve of per capita growth rate (PGR) vs. population density for the bacterial population. It plays a deterministic role on how abruptly the per capita growth rate of *M. leprae* declines whenever abundance interacts with the intraspecific competition for the available intracellular resources. The pattern of the growth response is concave for $\theta < 1$. The convex relationship between per capita growth rate (PGR) and population density is noted for $\theta > 1$. For the specific case of $\theta = 1$, the growth term actually reflects the classical logistic growth.

Also, this approach is mathematically more practical and plausible as it considers the bacteria population not to grow unboundedly. In this Section, we have considered a three-dimensional non-linear mathematical model with healthy Schwann cell, infected Schwann cell, and *M. leprae* bacteria population. We have incorporated a theta logistic growth in the *M. leprae* bacteria population due to its vital density dependence property. We have discussed how different values of the shape parameter θ plays a key role on interpreting the impacts for the infection and dissemination of leprosy through cell-to-cell interactions into the human body. The stability of the system and also bifurcation analysis has been investigated in detail.

3.1.1 Model Formulation with Suitable Assumptions

Firstly, we have reconsidered the following three dimensional mathematical model.

$$\begin{aligned}\frac{dx_h}{dt} &= r_1 x_h \left(1 - \frac{x_h}{K}\right) - \lambda x_h M_l, \\ \frac{dx_i}{dt} &= \lambda x_h M_l - \delta x_i, \\ \frac{dM_l}{dt} &= r_2 M_l \left(1 - \frac{M_l}{N}\right) - \gamma x_h M_l + \nu x_i.\end{aligned}\tag{3.1.1}$$

Here, $x_h(t)$, $x_i(t)$ and $M_l(t)$ are the concentrations of healthy Schwann cells, infected Schwann cells and *M. leprae* bacteria, respectively, for any time t . Logistic growth rate is assumed for both healthy Schwann cells and bacteria population where we have denoted the intrinsic growth rate and the carrying capacity of the healthy Schwann cell population by r_1 and K and the same for the bacteria population are denoted by r_2 and N respectively. The rate at which healthy Schwann cells getting infected by the *M. leprae* bacteria is represented by λ . New free bacteria proliferates from infected cells at a rate ν . The natural mortality rate of infected Schwann cells and the rate of bacterial clearance due to infection are represented by δ and γ , respectively.

Theta logistic growth curve is more realistic and accurate than the classical logistic growth model. Here, we incorporate the discrete version of the model (3.1.1). Based on the above perception along with the theta logistic growth in *M. leprae* bacteria population using the Forward Euler Scheme for discretization, we have revised the system (3.1.1) as follows:

$$\begin{aligned}x_{h_{t+1}} &= x_{h_t} + p \left[r_1 x_{h_t} \left(1 - \frac{x_{h_t}}{K}\right) - \lambda x_{h_t} M_{l_t} \right], \\ x_{i_{t+1}} &= x_{i_t} + p \left[\lambda x_{h_t} M_{l_t} - \delta x_{i_t} \right], \\ M_{l_{t+1}} &= M_{l_t} + p \left[r_2 M_{l_t} \left[1 - \left(\frac{M_{l_t}}{N} \right)^\theta \right] - \gamma x_{h_t} M_{l_t} + \nu x_{i_t} \right].\end{aligned}\tag{3.1.2}$$

Here, $\theta (> 0)$ describes the curvature of the relationship and the parameter $p (> 0)$ denotes the step size.

3.1.2 Equilibria and Stability Analysis

System (3.1.2) has two equilibrium points, namely, the disease-free equilibrium $E_0 = (K, 0, 0)$ and the unique positive interior equilibrium $E^* = (x_h^*, x_i^*, M_l^*)$, where the values of x_h^* , x_i^* , M_l^* are given by

$$x_i^* = \frac{r_1}{\delta} x_h^* \left(1 - \frac{x_h^*}{K}\right), \quad M_l^* = \frac{r_1}{\lambda} \left(1 - \frac{x_h^*}{K}\right)$$

and x_h^* is the positive root of the following equation,

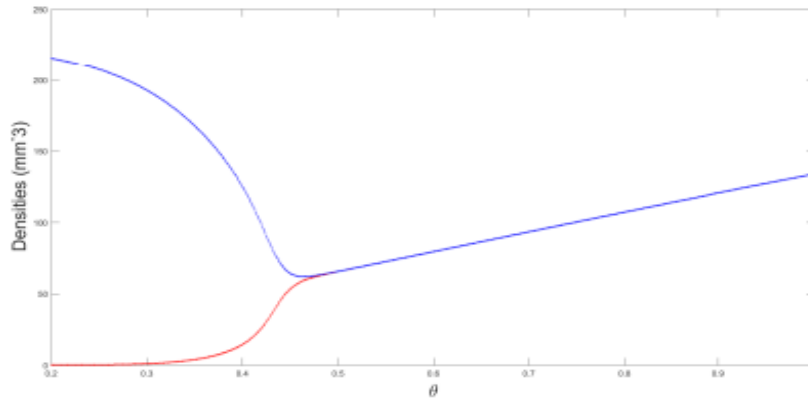


Figure 3.1: Bifurcation diagram of the densities of x_h cells, x_i cells and M_l bacteria with respect to the shape parameter θ for system (3.1.2). Values of the parameters used here are given as: $r_1 = 0.4$, $r_2 = 0.1$, $K = 780$, $N = 550$, $\lambda = 0.00036$, $\nu = 0.31$, $\gamma = 0.0003$.

$$g(x_h^*) = r_2 \left[1 - \left\{ 1 - \frac{r_1}{\lambda N} \left(1 - \frac{x_h^*}{K} \right) \right\}^\theta \right] + \left(\frac{\nu \lambda}{\delta} - \gamma \right) x_h^* = 0.$$

Here, it is important to note that both $x_i^* > 0$ and $M_l^* > 0$ because $x_h^* < K$ always holds true as the density of healthy Schwann cells can never exceed its carrying capacity K at the endemic steady state. Now, from the second equation of system (3.1.2), it follows that the values of x_h^* , x_i^* , M_l^* are interconnected and actually, x_h^* can be written as

$$x_h^* = \frac{\delta}{\lambda} \frac{x_i^*}{M_l^*}. \quad (3.1.3)$$

Now, as we have already obtained $x_i^* > 0$, $M_l^* > 0$, we can see that equation (3.1.3) clearly ensures the positivity of x_h^* .

3.1.3 Stability of the Disease-free Equilibrium

The Jacobian matrix of the system (3.1.2) at the disease-free equilibrium point $E_0 = (K, 0, 0)$ is as follows:

$$\mathcal{J}_0 = \begin{pmatrix} 1 - pr_1 & 0 & -p\lambda K \\ 0 & 1 - p\delta & p\lambda K \\ 0 & p\nu & 1 + p(r_2 - \gamma K) \end{pmatrix}. \quad (3.1.4)$$

The eigenvalues of \mathcal{J}_0 are ζ_i for $i = 1, 2, 3$ where $\zeta_1 = 1 - pr_1$ and ζ_2, ζ_3 are the roots of the following equation:

$$f(\zeta) = \zeta^2 + A_1\zeta + A_2 = 0. \quad (3.1.5)$$

Here,

$$\begin{aligned} A_1 &= p(\gamma K + \delta - r_2) - 2, \\ A_2 &= 1 + p(r_2 - \gamma K - \delta) - p^2(\lambda \nu K + \delta(r_2 - \gamma K)). \end{aligned}$$

Now, by analyzing the nature of the roots ζ_i for $i = 1, 2, 3$ of equation (3.1.5) according to the well-known Jury conditions, we can conclude the following theorem about the stability situation of E_0 .

Theorem 3.1.1. The disease-free equilibrium $E_0 = (K, 0, 0)$ of system (3.1.2) will be locally asymptotically stable if $|\zeta_1| < 1$ and also if the following three conditions are satisfied:

$$f(1) > 0, \quad f(-1) > 0 \quad \text{and} \quad A_2 < 1. \quad (3.1.6)$$

3.1.4 Stability Analysis of the Interior Equilibrium

Here, we will discuss the stability of the system (3.1.2) at the interior equilibrium point $E^* = (x_h^*, x_i^*, M_l^*)$. The Jacobian matrix of system (3.1.2) at E^* is given by,

$$\mathcal{J}(E^*) = \begin{pmatrix} M_{11} & 0 & -p\lambda x_h^* \\ p\lambda M_l^* & 1 - p\delta & p\lambda x_h^* \\ -p\gamma M_l^* & p\nu & M_{33} \end{pmatrix} \quad (3.1.7)$$

where,

$$M_{11} = 1 + p\left(r_1 - \frac{2r_1}{K}x_h^* - \lambda M_l^*\right),$$

$$M_{33} = p[r_2 - r_2(\theta + 1)\left(\frac{M_l^*}{N}\right) - \gamma x_h^*].$$

From the Jacobian matrix $\mathcal{J}(E^*)$ given by (3.1.7), we get the characteristic equation of system (3.1.2) at E^* as follows:

$$|\mathcal{J}(E^*) - \xi I| = 0. \quad (3.1.8)$$

Expanding equation (3.1.8), we get

$$\xi^3 + \varphi_1\xi^2 + \varphi_2\xi + \varphi_3 = 0 \quad (3.1.9)$$

where,

$$\begin{aligned} \varphi_1 &= \delta p - M_{11} - M_{33} - 1, \\ \varphi_2 &= M_{11} + M_{33} + M_{11}M_{33} - \delta p(M_{11} + M_{33}) - p^2\lambda x_h^*(\nu + \gamma M_l^*), \\ \varphi_3 &= M_{11}M_{33}(\delta p - 1) + p^2\lambda x_h^*(\nu M_{11} + \gamma M_l^*) + p^3\lambda x_h^*M_l^*(\lambda\nu + \gamma\delta). \end{aligned}$$

Hence, using the Jury conditions, we now obtain the following theorem which ensures the stability of E^* . This clearly indicates the following theorem.

Theorem 3.1.2. System (3.1.2) will be locally asymptotically stable at the the interior equilibrium E^* if and only if

$$|\varphi_1 + \varphi_3| < 1 + \varphi_2, \quad |\varphi_3| < 1 \quad \text{and} \quad |\varphi_2 - \varphi_1\varphi_3| < |1 - \varphi_3^2|. \quad (3.1.10)$$

3.1.5 Bifurcation Analysis

In this Section, we will derive conditions for which Hopf bifurcation occurs around the interior equilibrium E^* as θ varies in the open interval $(0, 1)$.

Let, $\Psi : (0, \infty) \rightarrow \mathbb{R}$ be a continuously differentiable function of θ defined by

$$\Psi(\theta) = \varphi_1(\theta)\varphi_2(\theta) - \varphi_3(\theta). \quad (3.1.11)$$

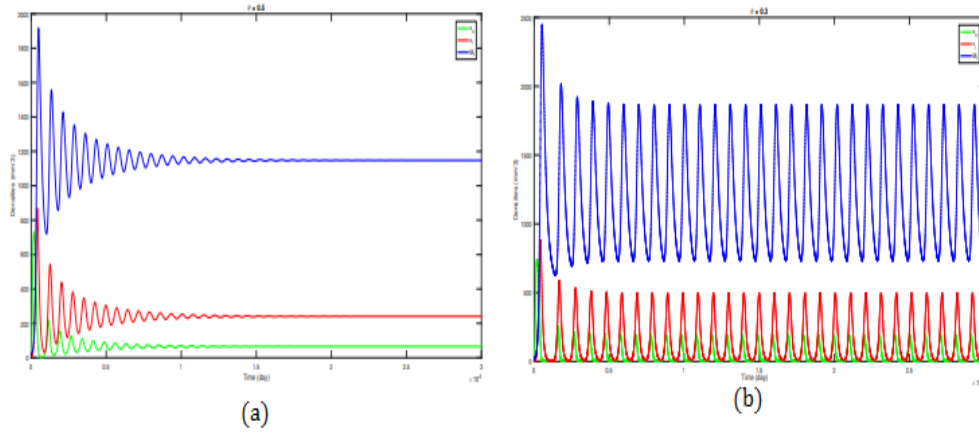


Figure 3.2: (a) Time series plot of the densities of x_h , x_i and M_l for $\theta = 0.5$ for system (3.1.2). Values of the parameters are chosen as $K = 800$, $N = 530$, $\lambda = 0.00038$, $\nu = 0.34$, $\gamma = 0.0003$. (b) Time series plot of the densities of x_h , x_i and M_l for $\theta = 0.3$ for system (3.1.2). We choose the values of the parameters as $K = 800$, $N = 530$, $\lambda = 0.00038$, $\nu = 0.34$, $\gamma = 0.0003$.

For the occurrence of Hopf bifurcation there should exist a $\theta^* \in (0, 1)$ such that $Re \xi(\theta^*) = 0$ and $Im \xi(\theta^*) = \omega_0 > 0$ where the complex conjugate pair of eigenvalues $\xi(\theta^*)$, $\bar{\xi}(\theta^*) \in \sigma(\theta)$. The transversality condition is given by

$$\left. \frac{d(Re\xi(\theta))}{d\theta} \right|_{\theta=\theta^*} \neq 0; \quad (3.1.12)$$

Also, let us define $\sigma(\theta) = \{\rho : D(\rho) = 0\}$ is the spectrum of the characteristic equation (3.1.9). For the appearance of Hopf bifurcation, it is necessary for all the other elements of $\sigma(\theta)$ to have negative real parts.

To prove the existence of such θ^* , we have to solve the equation for $\xi(\theta^*)$. Now using equation (3.1.11), we can rewrite the characteristic equation (3.1.9) as

$$\begin{aligned} \xi^3 + \varphi_1 \xi^2 + \varphi_2 \xi + \varphi_1 \varphi_2 &= 0 \quad [As \varphi_1 \varphi_2 - \varphi_3 = 0] \\ \Rightarrow \xi^2(\xi + \varphi_1) + \varphi_2(\xi + \varphi_1) &= 0 \\ \Rightarrow (\xi + \varphi_1)(\xi^2 + \varphi_2) &= 0. \end{aligned} \quad (3.1.13)$$

This equation contains three roots ξ_i for $i = 1, 2, 3$ which are given by

$$\begin{aligned} \xi_1 &= +i\sqrt{\varphi_2}, \\ \xi_2 &= -i\sqrt{\varphi_2}, \\ \xi_3 &= -\varphi_1. \end{aligned}$$

So, there exists a pair of purely imaginary eigenvalues for $\varphi_1 \varphi_2 - \varphi_3 = 0$. To obtain the transversality condition, differentiating equation (3.1.9) with respect to θ , we get that

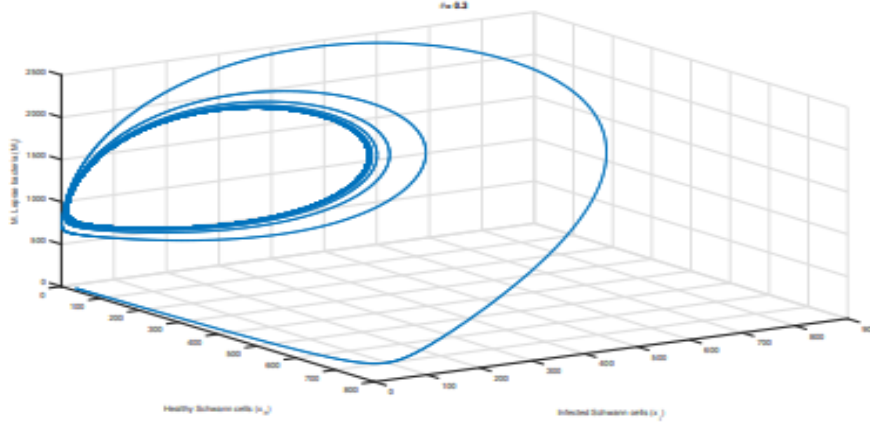


Figure 3.3: Phase plot of x_h cells, x_i cells and M_l for system (3.1.2) for the value of $\theta = 0.3$ for system (3.1.2). The initial values are taken as $(x_h, x_i, M_l) = (30, 5, 15)$.

$$\begin{aligned}
 \frac{d\xi}{d\theta} &= -\frac{\xi^2\dot{\varphi}_1 + \xi\dot{\varphi}_2 + \dot{\varphi}_3}{3\xi^2 + 2\xi\varphi_1 + \varphi_2} \Big|_{\xi=i\sqrt{\varphi_2}} \\
 &= -\frac{(\dot{\varphi}_3 - \varphi_2\dot{\varphi}_1 + i\sqrt{\varphi_2}\dot{\varphi}_2)}{(-2\varphi_2 + 2i\sqrt{\varphi_2}\varphi_1)} \\
 &= \frac{(\dot{\varphi}_3\sqrt{\varphi_2} - \varphi_2\sqrt{\varphi_2}\dot{\varphi}_1 - \sqrt{\varphi_2}\varphi_1\dot{\varphi}_2) + i(\varphi_1\dot{\varphi}_3 - \varphi_1\varphi_2\dot{\varphi}_1 + \varphi_2\dot{\varphi}_2)}{2\sqrt{\varphi_2}(\varphi_1^2 + \varphi_2)} \\
 &= \frac{\dot{\varphi}_3 - (\dot{\varphi}_1\varphi_2 + \dot{\varphi}_2\varphi_1)}{2(\varphi_1^2 + \varphi_2)} + i\frac{\sqrt{\varphi_2}(\varphi_1\dot{\varphi}_3 + \varphi_2\dot{\varphi}_2 - \dot{\varphi}_1\varphi_1\varphi_2)}{2\varphi_2(\varphi_1^2 + \varphi_2)}. \tag{3.1.14}
 \end{aligned}$$

Now, using (3.1.14),

$$\begin{aligned}
 \operatorname{Re}\left(\frac{d\xi}{d\theta}\right) \Big|_{\theta=\theta^*} &= \frac{d(\operatorname{Re}\xi)}{d\theta} \Big|_{\theta=\theta^*} \\
 &= \frac{\dot{\varphi}_3 - (\dot{\varphi}_1\varphi_2 + \dot{\varphi}_2\varphi_1)}{2(\varphi_1^2 + \varphi_2)} > 0. \tag{3.1.15}
 \end{aligned}$$

i.e.

$$\dot{\varphi}_3 > (\dot{\varphi}_1\varphi_2 + \dot{\varphi}_2\varphi_1). \tag{3.1.16}$$

Thus, we achieve the transversality condition (3.1.16) for which Hopf bifurcation occurs at the critical value of $\theta = \theta^*$.

In view of the above discussion, we now present the following theorem.

Theorem 3.1.3. The system (3.1.2) exhibits Hopf bifurcation around the interior equilibrium E^* at $\theta = \theta^* \in (0, 1)$ if and only if the following conditions hold:

1. $\Psi(\theta^*) = 0$
2. $\dot{\varphi}_3 > (\dot{\varphi}_1\varphi_2 + \dot{\varphi}_2\varphi_1)$

3. All the other eigenvalues have negative real parts

where $\xi(\theta)$ is purely imaginary at the critical value of $\theta = \theta^*$.

This discrete mathematical model emphasizes a special importance for the investigation of Hopf bifurcation for our discrete-time based system (3.1.2). The bifurcation diagram of the densities of our model populations with respect to the shape parameter θ has been depicted in Figure 3.1. From the appearance of periodic solutions and presence of limit cycles in the phase diagram, we can confirm that system (3.1.2) undergoes a Hopf bifurcation whenever the value of θ crosses the critical value $\theta = \theta^* = 0.48$, which completely clarifies our analytical findings in section 3.1.5.

In Figure 3.2, we have shown that for $\theta = 0.5$, trajectories of the cell populations oscillate more rapidly about 1.2×10^4 days and then gradually tend to proceed toward its stable region. If the value of θ is decreased further to $\theta = 0.3$ then behaviour of the system trajectories suddenly alters which is illustrated in Figure 3.2. For $\theta = 0.3 < 0.48$, the system (3.1.2) becomes unstable and periodic oscillations are observed after almost 2000 days. From this findings, it is evident that for $\theta > 0.48$, our system is asymptotically stable at the interior equilibrium point $E^* = (x_h^*, x_i^*, M_l^*)$ and for $\theta < 0.48$, Hopf-bifurcating periodic solution begins to exist. Hence, we can interpret that our system (3.1.2) exhibits a rich dynamics if the value of θ decreases from the value of $\theta = 1$. Thus incorporating theta-logistic growth instead of classical logistic one for the growth rate of *M. leprae* bacteria is more realistic and flexible in nature.

The phase portrait of the system populations displayed in Figure 3.3 indicates occurrence of limit cycles. In particular, it reflects the periodic oscillatory behaviour of the densities of the model cell populations starting from the same initial values.

3.2 Stochastic Epidemic Model Without Removal

A stochastic epidemic model without removal is a mathematical framework used to study the spread of infectious diseases in populations where infected individuals do not leave the system after recovering. In this model, recovered individuals do not acquire immunity or are immediately susceptible again.

3.3 Essence in Mathematics

The essence of using stochastic epidemic models without removal in mathematical biology lies in their ability to capture the inherent randomness and complexity of infectious disease transmission dynamics.

1. **Realism:** Stochastic models more accurately reflect the unpredictable nature of disease outbreaks in real populations by considering stochastic transmission events, population heterogeneity, and variability in disease progression.
2. **Population Heterogeneity:** These models allow for the incorporation of population heterogeneity, such as variations in contact rates, susceptibility, and infectiousness among individuals, which can significantly impact disease dynamics.
3. **Small Population Sizes:** Stochastic effects can play a crucial role in determining the trajectory of an outbreak, especially in small populations or early stages of an epidemic. Stochastic models provide insights into the probability of different outcomes and the likelihood of rare events.
4. **Effect of Interventions:** Stochastic models are useful for evaluating the impact of interventions, such as vaccination campaigns or social distancing measures, on disease transmission dynamics. They can assess the effectiveness of interventions under different scenarios and account for uncertainty in their implementation.

5. **Understanding Uncertainty:** By explicitly accounting for randomness in the system, stochastic models help quantify uncertainty in disease forecasts and predictions. This is crucial for decision-making and risk assessment in public health planning and policy-making.

Overall, stochastic epidemic models without removal provide a more realistic and nuanced understanding of disease transmission dynamics compared to deterministic models. They are valuable tools for understanding infectious disease dynamics, assessing the effectiveness of control measures, and informing public health interventions in real-world settings. They provide a more realistic and nuanced understanding of disease transmission dynamics compared to deterministic models, allowing researchers to better predict and manage disease outbreaks.

3.4 Basic System of Equation

Let us suppose that $p_n(t)$ be the probability that there are n susceptible individuals at time t in the system. Let $f_j(n)\Delta t + o(\Delta t)$ be the probability that the number changes from n to $n + j$ in the time interval $(t, t + \Delta t)$. Here, j is any positive or negative integers, and $o(\Delta t)$ denotes an infinitesimal which is such that

$$\frac{o(\Delta t)}{\Delta t} \rightarrow 0 \quad \text{as} \quad \Delta t \rightarrow 0. \quad (3.4.1)$$

The probability that there is no change in the time interval $(t, t + \Delta t)$ is then given by

$$1 - \sum_j f_j(n)\Delta t + o(\Delta t) \quad (3.4.2)$$

Using the theorem of total and compound probabilities, we get

$$p_n(t + \Delta t) = p_n(t) \left[1 - \sum_j f_j(n)\Delta t \right] + \sum_j p_{n-j}(t) f_j(n-j)\Delta t + o(\Delta t) \quad (3.4.3)$$

so that

$$\frac{p_n(t + \Delta t) - p_n(t)}{\Delta t} = -p_n(t) \sum_j f_j(n) + \sum_j p_{n-j}(t) f_j(n-j) + \frac{o(\Delta t)}{\Delta t}. \quad (3.4.4)$$

Proceeding to the limit as $\Delta t \rightarrow 0$, we obtain

$$\frac{dp_n}{dt} = -p_n(t) \sum_j f_j(n) + \sum_j p_{n-j}(t) f_j(n-j). \quad (3.4.5)$$

Multiplying (3.4.5) by x^n , summing for all n , and using the definition of the probability generating function, namely,

$$\phi(x, t) = \sum_{n=0}^{\infty} p_n(t) x^n, \quad (3.4.6)$$

we get

$$\frac{\partial \phi}{\partial t} = - \sum_j \sum_n f_j(n) p_n(t) x^n + \sum_j \sum_n p_{n-j}(t) f_j(n-j) x^{n-j} \quad (3.4.7)$$

which gives the partial differential equation

$$\frac{\partial \phi}{\partial t} = \sum_j (x^{-j} - 1) f_j \left(x \frac{\partial}{\partial x} \right) \phi(x, t). \quad (3.4.8)$$

Now we make use of the relations

$$\begin{aligned}
 \left(x \frac{\partial}{\partial x}\right) \phi &= \sum_n n p_n(t) x^n \\
 \left(x \frac{\partial}{\partial x}\right)^2 \phi &= \sum_n n^2 p_n(t) x^n \\
 &\dots \dots \dots \\
 \left(x \frac{\partial}{\partial x}\right)^m \phi &= \sum_n n^m p_n(t) x^n, \quad m = 1, 2, 3, \dots
 \end{aligned} \tag{3.4.9}$$

to get

$$\psi \left(x \frac{\partial}{\partial x}\right) \phi = \sum_n \psi(n) p_n(t) x^n, \tag{3.4.10}$$

where $\psi(x)$ is any polynomial functions of x . In order to find all the probabilities, we either solve the finite system of differential-difference equations (3.4.5) or solve the partial differential equation (3.4.8) subject to the initial conditions

$$\phi(x, 0) = \sum_n p_n(0) x^n = x^{n_0}, \tag{3.4.11}$$

where n_0 is the number of susceptible in the system at $t = 0$.

3.4.1 Solution of the System of Equation

Initially, at $t = 0$, let there be n susceptibles and one infective in the system. Also, let the probability that there are r susceptible person at time t be $p_r(t)$. We assume that the probability of one more person becoming infected in time Δt is

$$\beta(n + 1 - r)\Delta t + o(\Delta t) \tag{3.4.12}$$

so that

$$\begin{aligned}
 f_j(r) &= \beta r(n + 1 - r) \quad (j = 1) \\
 &= 0 \quad (j \neq 1)
 \end{aligned} \tag{3.4.13}$$

Substituting (3.4.13) in (3.4.8), we get

$$\begin{aligned}
 \frac{\partial \phi}{\partial t} &= \beta(x^{-1} - 1) \left[x \frac{\partial}{\partial x} \left(n + 1 - x \frac{\partial}{\partial x} \right) \phi \right] \\
 \Rightarrow \frac{\partial \phi}{\partial t} &= \beta(x^{-1} - 1) \left[x \frac{\partial}{\partial x} (n + 1)\phi - x \frac{\partial \phi}{\partial x} \right] \\
 \Rightarrow \frac{\partial \phi}{\partial t} &= \beta(1 - x) \left[(n + 1) \frac{\partial \phi}{\partial x} - \frac{\partial \phi}{\partial x} - x \frac{\partial^2 \phi}{\partial x^2} \right] \\
 \Rightarrow \frac{\partial \phi}{\partial t} &= \beta(1 - x) \left(n \frac{\partial \phi}{\partial x} - x \frac{\partial^2 \phi}{\partial x^2} \right)
 \end{aligned} \tag{3.4.14}$$

Since there are n susceptibles at time $t = 0$,

$$\phi(x, t) = \sum_r p_r(0) x^r = p_n(0) x^n = x^n. \tag{3.4.15}$$

Substituting $\phi(x, t) = \sum_{r=0}^n p_r(t)x^r$ in (3.4.14) and equating the coefficients of the various powers of x , we get

$$\frac{dp_r}{dt} = \beta(r+1)(n-r)p_{r+1} - \beta r(n-r+1)p_r \quad (r = 0, 1, 2, \dots, n-1), \quad (3.4.16)$$

$$\frac{dp_n}{dt} = -\beta n p_n \quad (3.4.17)$$

with initial conditions

$$p_n(0) = 1, \quad p_r(0) = 0 \quad (r = 0, 1, 2, \dots, n-1). \quad (3.4.18)$$

We can now follow either of the two procedures:

- We can solve the partial differential equation (3.4.14) subject to initial condition (3.4.15), or
- We can solve the system of $n+1$ differential equations, namely, (3.4.16) and (3.4.17), subject to initial conditions (3.4.18). We adopt the second procedure here.

Solving (3.4.17) subject to (3.4.18), we get

$$p_n(t) = e^{-\beta n t} \quad (3.4.19)$$

Equation (3.4.16) then gives

$$\frac{dp_{n-1}}{dt} + 2\beta(n-1)p_{n-1} = n\beta e^{-n\beta t}. \quad (3.4.20)$$

Integrating (3.4.20) subject to (3.4.18), we obtain

$$p_{n-1}(t) = e^{-2\beta(n-1)t} \int_0^t n\beta e^{-n\beta t} e^{2(n-1)\beta t} dt = \frac{n}{n-2} [e^{-n\beta t} - e^{-(2n-2)\beta t}]. \quad (3.4.21)$$

We can proceed in this way systematically step by step to find $p_{n-2}(t)$, $p_{n-3}(t)$, \dots , $p_0(t)$.

Alternatively, we can use the Laplace transform method to solve (3.4.16) and (3.4.17) subject to (3.4.18). Let

$$q_r(s) = \int_0^{\infty} e^{-st} p_r(t) dt. \quad (3.4.22)$$

Multiplying both sides of (3.4.16) and (3.4.17) by e^{-st} and integrating over the range 0 to ∞ , we get

$$\int_0^{\infty} e^{-st} \frac{dp_r}{dt} dt = \beta \int_0^{\infty} e^{-st} (r+1)(n-r)p_{r+1} dt - \beta r(n-r+1) \int_0^{\infty} e^{-st} p_r dt$$

$$\int_0^{\infty} e^{-st} \frac{dp_n}{dt} dt = -\beta n \int_0^{\infty} e^{-st} p_n dt.$$

Using the conditions given by (3.4.18), we obtain

$$s q_r(s) = \beta(r+1)(n-1)q_{r+1}(s) - \beta r(n-r+1)q_r(s), \quad r = 0, 1, 2, \dots, n-1, \quad (3.4.23)$$

$$s q_n(s) = 1 - \beta n q_n(s) \quad (3.4.24)$$

From (3.4.23),

$$\begin{aligned}
 q_r(s) &= \frac{\beta(r+1)(n-r)}{[s+r(n-r+1)\beta]} q_{r+1}(s) \\
 &= \frac{\beta^2(r+1)(n-r)(r+2)(n-r-1)}{[s+r(n-r+1)\beta][s+(r+1)(n-r)\beta]} q_{r+2} \\
 &\vdots \\
 &= \frac{\beta^{n-r}[(r+1)(r+2)\cdots(r+n-r)][(n-r)!]}{\prod_{j=1}^{n-r+1} [s+j(n-j+1)\beta]} \\
 &= \frac{\beta^{n-r} [n!] [(n-r)!]}{r!} \prod_{j=1}^{n-r+1} \frac{1}{[s+j(n-j+1)\beta]} \quad (r = 0, 1, 2, \dots, n-1) \quad (3.4.25)
 \end{aligned}$$

$$q_n(s) = \frac{1}{s+n\beta}. \quad (3.4.26)$$

By inverting the Laplace transforms, we can find $p_r(t)$. This can be easily done by splitting the product on the right-hand side of Eq. (3.4.25) into partial fractions.

- If $r > n/2$, there are no repeated factors, and this is relatively easier.
- If $r \leq n/2$, repeated factors occur, and care has to be exercised.

The mean of the distribution is found by using

$$m(t) = \sum_{r=1}^n r p_r(t). \quad (3.4.27)$$

Unit 4

Course Structure

- Stochastic Epidemic Model with Multiple Infections
 - Stochastic Epidemic Model with Removal
 - Stochastic Epidemic Model with Removal, Immigration and Emigration
 - Stochastic Epidemic Model with Carriers
 - Stochastic Epidemic Model with Infectives and Carriers
-

4.1 Other Stochastic Epidemic Models

The Essence of Stochastic Epidemic Model with Multiple Infections

The essence of a stochastic epidemic model with multiple infections lies in its ability to capture the complexity of infectious disease dynamics in populations where individuals can be infected with multiple strains or types of the pathogen. Here are some key aspects that highlight the essence of such a model:

1. **Realistic Representation:** In many real-world scenarios, infectious diseases can involve multiple variants, strains, or types of the pathogen circulating simultaneously within a population. A stochastic epidemic model with multiple infections provides a realistic representation of this complexity.
2. **Dynamic Interactions:** The model allows for dynamic interactions between different strains of the pathogen, including competition, coexistence, and potential interactions such as cross-immunity or cross-enhancement.
3. **Emergence of New Variants:** By considering the co-circulation of multiple strains, the model can help in understanding the emergence of new variants through processes such as genetic reassortment, recombination, or mutation.
4. **Epidemiological Implications:** The model enables the investigation of epidemiological implications of multiple infections, such as the impact on disease transmission dynamics, the effectiveness of interventions, and the potential for outbreaks or pandemics.

5. **Public Health Strategies:** Insights from the model can inform public health strategies and interventions aimed at controlling the spread of infectious diseases with multiple variants, including vaccination strategies, surveillance efforts, and targeted control measures.
6. **Uncertainty and Stochasticity:** Stochasticity inherent in the model accounts for uncertainty and randomness in transmission events, individual behavior, and other factors affecting disease spread. This stochastic component allows for the exploration of uncertainty in epidemic outcomes and the assessment of intervention effectiveness under different scenarios.
7. **Research and Policy Decision Support:** Stochastic epidemic models with multiple infections serve as valuable tools for researchers, policymakers, and public health officials to better understand and mitigate the impact of complex infectious disease dynamics on public health.

In essence, a stochastic epidemic model with multiple infections provides a comprehensive framework for studying the intricate interplay between different strains of a pathogen, offering valuable insights into disease transmission, evolution, and control in real-world populations.

4.1.1 Epidemics with Multiple Infections

Particular case for the epidemics with multiple infections. When epidemics with multiple infection occur, there can be j infections in the time interval $(t + \Delta t)$ with the probability $\beta_j s(n + 1 - s)\Delta t + o(\Delta t)$ where $j = 1, 2, \dots, m$ and s be the number of susceptibles at time t and n be the initial number of susceptibles.

Here r_j be the contact rates for j infections. In such a case, the basic partial differential equation will have the form

$$\begin{aligned}
 \frac{\partial \phi}{\partial t} &= \sum_{j=1}^m (x^{-j} - 1)\beta_j x \frac{\partial}{\partial x} \left[\left(n + 1 - x \frac{\partial}{\partial x} \right) \phi \right] \\
 \Rightarrow \frac{\partial \phi}{\partial t} &= \sum_{j=1}^m \frac{1}{x^{j-1}} (1 - x^j)\beta_j \left[(n + 1) \frac{\partial \phi}{\partial x} - \frac{\partial \phi}{\partial x} - x \frac{\partial^2 \phi}{\partial x^2} \right] \\
 \Rightarrow \frac{\partial \phi}{\partial t} &= \sum_{j=1}^m \frac{1 - x^j}{x^{j-1}} \beta_j \left[n \frac{\partial \phi}{\partial x} - x \frac{\partial^2 \phi}{\partial x^2} \right] \\
 \Rightarrow \frac{\partial \phi}{\partial t} &= \left(n \frac{\partial \phi}{\partial x} - x \frac{\partial^2 \phi}{\partial x^2} \right) \left[\beta_1(1 - x) + \beta_2 \left(\frac{1}{x} - x \right) + \beta_3 \left(\frac{1}{x^2} - x \right) + \dots + \beta_m \left(\frac{1}{x^{m+1}} - x \right) \right]
 \end{aligned}$$

This results is equivalent to (3.4.14) if one takes for $m = 1$ and $\beta_m = \beta$. We can also write the system of differential difference equations from first principle and solve those one-by-one directly or by using Laplace transformation technique.

4.1.2 Stochastic Epidemic Model with Removal

Stochastic epidemic models with removal (or recovery) are used in mathematical biology for several reasons, each contributing to a more comprehensive understanding of infectious disease dynamics. Here's why they are commonly used:

1. **Realism in Modeling:** Stochastic epidemic models with removal reflect the real-world dynamics of infectious diseases, where individuals who have been infected can recover and become immune to the disease. This reflects the natural course of many infectious diseases and allows for more realistic modeling of disease spread and control strategies.

2. **Incorporation of Recovery Dynamics:** Including a removal (or recovery) component in the model allows for the explicit modeling of the recovery process, including the duration of infectiousness and the rate at which individuals recover from the disease. This is essential for accurately capturing the dynamics of disease transmission over time.
3. **Assessment of Disease Control Measures:** Stochastic epidemic models with removal allow researchers to assess the impact of various disease control measures, such as vaccination, treatment, isolation, and social distancing, on disease spread and population-level outcomes. This helps policymakers and public health officials make informed decisions about disease control strategies.
4. **Study of Endemic and Epidemic Dynamics:** These models can be used to study both endemic diseases (those that persist at a relatively constant level in a population) and epidemic outbreaks (sudden increases in disease incidence). By incorporating removal dynamics, researchers can investigate the factors influencing the transition between endemic and epidemic states and the conditions under which outbreaks occur.
5. **Exploration of Stochastic Effects:** Stochastic epidemic models with removal capture the inherent randomness and uncertainty in disease transmission and recovery processes. This allows researchers to explore the role of stochastic effects in shaping epidemic outcomes, such as the probability of outbreak occurrence, the size and duration of outbreaks, and the effectiveness of interventions.
6. **Comparison with Empirical Data:** These models can be compared with empirical data on disease incidence, prevalence, and recovery rates to validate model predictions and improve our understanding of disease dynamics. By calibrating model parameters to fit observed data, researchers can gain insights into the underlying mechanisms driving disease transmission and recovery.

In summary, stochastic epidemic models with removal are used in mathematical biology to provide a realistic and flexible framework for studying infectious disease dynamics, assessing disease control measures, and understanding the complex interplay between pathogens, hosts, and the environment. They play a crucial role in informing public health policies and interventions aimed at controlling and mitigating the impact of infectious diseases on populations.

Let $p_{m,n}(t)$ be the probability that there are m susceptibles and n infectives in the population at time t . If N is the total size of the population, then the number of persons in the removed category is $N - m - n$.

Let the probability of susceptible being infected in the time interval $(t, t + \Delta t)$ be $\beta mn\Delta t + o(\Delta t)$, and let the corresponding probability of one infected being removed in the same time interval be $\gamma n\Delta t + o(\Delta t)$. The probability of not having any change in this time interval is

$$1 - \beta mn\Delta t - \gamma n\Delta t + o(\Delta t). \quad (4.1.1)$$

Now there can be m susceptibles and n infected persons at time $t + \Delta t$ if there are

- (i) $m + 1$ susceptibles and $n - 1$ infectives at time t and if one person has become infected in time Δt , or
- (ii) m susceptibles and $n + 1$ infectives at time t and if one infected person has been removed in time Δt ,
or
- (iii) m susceptibles and n infectives at time t and if there is no change in time Δt .

We assume, as usual, that the probability of more than one change in time Δt is $o(\Delta t)$. Then, using the theorem of total and compound probability, we get

$$\begin{aligned} p_{m,n}(t + \Delta t) &= p_{m+1,n-1}(t)\beta(m+1)(n-1)\Delta t + p_{m,n+1}(t)\gamma(n+1)\Delta t \\ &\quad + p_{m,n}(t)(1 - \beta mn\Delta t - \gamma n\Delta t) + o(\Delta t) \\ \Rightarrow \frac{p_{m,n}(t + \Delta t) - p_{m,n}(t)}{\Delta t} &= \beta(m+1)(n-1)p_{m+1,n-1}(t) - \beta mn p_{m,n}(t) \\ &\quad + \gamma(n+1)p_{m,n+1}(t) - \gamma n p_{m,n}(t) + \frac{o(\Delta t)}{\Delta t}. \end{aligned}$$

Proceeding to the limit as $\Delta t \rightarrow 0$, we get

$$\begin{aligned} \frac{d}{dt} [p_{m,n}(t)] &= \beta(m+1)(n-1)p_{m+1,n-1}(t) - \beta mn p_{m,n}(t) \\ &\quad + \gamma(n+1)p_{m,n+1}(t) - \gamma n p_{m,n}(t). \end{aligned} \quad (4.1.2)$$

Initially, let there be s susceptibles and a infectives. Then we define the probability generating function by

$$\phi(x, y, t) = \sum_{m=0}^s \sum_{n=0}^{s+a-m} p_{m,n}(t) x^m y^n. \quad (4.1.3)$$

Multiplying (4.1.2) by $x^m y^n$ and summing over n from 0 to $s+a-m$ and m from 0 to s , we get

$$\begin{aligned} \frac{\partial}{\partial t} \sum_{m=0}^s \sum_{n=0}^{s+a-m} p_{m,n}(t) x^m y^n &= \beta y^2 \sum_{m=0}^s \sum_{n=0}^{s+a-m} p_{m+1,n-1}(t) (m+1)(n-1) x^m y^{n-2} \\ &\quad - \beta x y \sum_{m=0}^s \sum_{n=0}^{s+a-m} p_{m,n}(t) m n x^{m-1} y^{n-1} \\ &\quad + \gamma \sum_{m=0}^s \sum_{n=0}^{s+a-m} p_{m,n-1}(t) (n+1) x^m y^n \\ &\quad - \gamma y \sum_{m=0}^s \sum_{n=0}^{s+a-m} p_{m,n}(t) n x^m y^{n-1}. \end{aligned} \quad (4.1.4)$$

From (4.1.3) and (4.1.4), we get

$$\frac{\partial \phi}{\partial t} = \beta(y^2 - xy) \frac{\partial^2 \phi}{\partial x \partial y} + \gamma(1 - y) \frac{\partial \phi}{\partial y}. \quad (4.1.5)$$

Now the equation (4.1.5) can be solved subject to the initial condition

$$\phi(x, y, 0) = x^s y^a \quad \text{since} \quad p_{m,n}(0) = \begin{cases} 1; & m = s, n = a \\ 0; & \text{otherwise.} \end{cases} \quad (4.1.6)$$

An Alternative Derivation of the Partial Differential Equation

The stochastic model with removal can be represented as follows:

Event	Transition	Transition rate	Probability
a susceptible becomes infected	$(m, n) \rightarrow (m-1, n+1)$	βmn	$\beta mn \Delta t + o(\Delta t)$
an infective becomes removed	$(m, n) \rightarrow (m, n-1)$	γn	$\gamma n \Delta t + o(\Delta t)$
there is no change	$(m, n) \rightarrow (m, n)$	$-(\beta mn + \gamma n)$	$1 - (\beta mn + \gamma n) \Delta t + o(\Delta t)$

From the tabular representation, we get

$$f_{-1,1}(m, n) = \beta mn, \quad f_{0,-1}(m, n) = \gamma n \quad (4.1.7)$$

so that the partial differential equation representing the model becomes

$$\begin{aligned} \frac{\partial \phi}{\partial t} &= (x^{-1}y^1 - 1)\beta xy \frac{\partial^2 \phi}{\partial x \partial y} + (x^0y^{-1} - 1)\gamma y \frac{\partial \phi}{\partial y} \\ \Rightarrow \frac{\partial \phi}{\partial t} &= \beta(y^2 - xy) \frac{\partial^2 \phi}{\partial x \partial y} + \gamma(1 - y) \frac{\partial \phi}{\partial y} \end{aligned} \quad (4.1.8)$$

It is worthwhile to note here that Eq. (4.1.5) and Eq. (4.1.8) are identical.

Stochastic Epidemic Model with Removal, Immigration, and Emigration

The model can be represented as follows:

Event	Transition	Transition rate	Probability
a susceptible is removed	$(m, n) \rightarrow (m - 1, n + 1)$	βmn	$\beta mn \Delta t + o(\Delta t)$
an infective is removed	$(m, n) \rightarrow (m, n - 1)$	γn	$\gamma n \Delta t + o(\Delta t)$
a new susceptible joins	$(m, n) \rightarrow (m + 1, n)$	μ	$\mu \Delta t + o(\Delta t)$
an infective joins	$(m, n) \rightarrow (m, n + 1)$	ν	$\nu \Delta t + o(\Delta t)$
a susceptible leaves	$(m, n) \rightarrow (m - 1, n)$	δm	$\delta m \Delta t + o(\Delta t)$

This model gives

$$f_{-1,-1}(m, n) = \beta mn, \quad f_{0,-1}(m, n) = \gamma n, \quad f_{1,0}(m, n) = \mu, \quad f_{0,1}(m, n) = \gamma, \quad f_{-1,0}(m, n) = \delta n$$

so that the partial differential equation representing the model becomes

$$\begin{aligned} \frac{\partial \phi}{\partial t} &= (x^{-1}y^1 - 1)\beta xy \frac{\partial^2 \phi}{\partial x \partial y} + (x^0y^{-1} - 1)\gamma y \frac{\partial \phi}{\partial y} + (xy^0 - 1)\mu \phi \\ &\quad + (x^0y^1 - 1)\nu \phi + (x^{-1}y^0 - 1)\delta x \frac{\partial \phi}{\partial x} \\ \Rightarrow \frac{\partial \phi}{\partial t} &= \beta(y^2 - xy) \frac{\partial^2 \phi}{\partial x \partial y} + \gamma(1 - y) \frac{\partial \phi}{\partial y} + \mu(x - 1)\phi + \nu(y - 1)\phi + \delta(1 - x) \frac{\partial \phi}{\partial x}. \end{aligned} \quad (4.1.9)$$

In the absence of immigration and emigration, (4.1.9) gives

$$\frac{\partial \phi}{\partial t} = \beta(y^2 - xy) \frac{\partial^2 \phi}{\partial x \partial y} + \gamma(1 - y) \frac{\partial \phi}{\partial y}. \quad (4.1.10)$$

It is worthwhile to note here that Eq. (4.1.8) and Eq. (4.1.10) are identical.

Stochastic Epidemic Model with Carriers

Here we consider a disease spread only by carriers so that our interest is in the two classes of individuals, namely, susceptibles and carriers. Carriers are eliminated by external action. Thus we get the following model:

Event	Transition	Transition rate	Probability
a susceptible becomes infective	$(m, n) \rightarrow (m - 1, n)$	βmn	$\beta mn \Delta t + o(\Delta t)$
a carrier is removed	$(m, n) \rightarrow (m, n - 1)$	γn	$\gamma n \Delta t + o(\Delta t)$

From the tabular representation, we get

$$f_{-1,0}(m, n) = \beta mn, \quad f_{0,-1}(m, n) = \gamma n \quad (4.1.11)$$

so that the partial differential equation representing the model becomes

$$\begin{aligned} \frac{\partial \phi}{\partial t} &= (x^{-1}y^0 - 1)\beta xy \frac{\partial^2 \phi}{\partial x \partial y} + (x^0y^{-1} - 1)\gamma y \frac{\partial \phi}{\partial y} \\ \Rightarrow \frac{\partial \phi}{\partial t} &= \beta y(1-x) \frac{\partial^2 \phi}{\partial x \partial y} + \gamma(1-y) \frac{\partial \phi}{\partial y} \end{aligned} \quad (4.1.12)$$

If we allow immigration and emigration of susceptibles and carriers, we get

$$\frac{\partial \phi}{\partial t} = \beta y(1-x) \frac{\partial^2 \phi}{\partial x \partial y} + \gamma(1-y) \frac{\partial \phi}{\partial y} + \mu(x-1) + \nu(y-1)\phi + \delta(1-x) \frac{\partial \phi}{\partial x}. \quad (4.1.13)$$

Further Discussion on Epidemic with Carriers

In Eq. (4.1.12), we allow β and γ to be functions of t so that we get

$$\frac{\partial \phi}{\partial t} = \beta(t)y(1-x) \frac{\partial^2 \phi}{\partial x \partial y} + \gamma(t)(1-y) \frac{\partial \phi}{\partial y}. \quad (4.1.14)$$

We have to solve this subject to the initial condition

$$\phi(x, y, 0) = x^M y^N, \quad (4.1.15)$$

where M and N are the initial number of susceptibles and carriers. We try the solution

$$\phi(x, y, t) = \sum_{r=0}^n M_{c_r} (x-1)^r f_r(y, t). \quad (4.1.16)$$

Substituting (4.1.16) in (4.1.14), we obtain

$$\sum_{r=0}^n M_{c_r} (x-1)^r \left\{ \frac{\partial f_r}{\partial t} + [(r\beta + \gamma)y - \gamma] \frac{\partial f_r}{\partial y} \right\} = 0 \quad (4.1.17)$$

Since the polynomials $P_r(x) = M_{c_r} (x-1)^r$, $r = 0, 1, 2, \dots, n$ are linearly independent, we get

$$\frac{\partial f_r}{\partial t} + [(r\beta + \gamma)y - \gamma] \frac{\partial f_r}{\partial y} = 0, \quad (r = 0, 1, 2, \dots, n) \quad (4.1.18)$$

For each r , this is a linear partial differential equation of the first order. The auxiliary equations for solving (4.1.18) are

$$\frac{dt}{1} = \frac{dy}{(r\beta + \gamma)y - \gamma} = \frac{df}{0}. \quad (4.1.19)$$

An intermediate integral is obtained by solving

$$\frac{dy}{dt} - (r\beta + \gamma)y = -\gamma \quad (4.1.20)$$

so that if $F_r(t) = \int_0^t [r\beta(t) + \gamma(t)] dt$, the solution of (4.1.20) is

$$f_r(y, t) = \psi_r \left[ye^{-F_r(t)} + \int_0^t \gamma(t) e^{-F_r(t)} dt \right]. \quad (4.1.21)$$

Stochastic Epidemic Model with Infectives and Carriers

A stochastic epidemic model with infectives and carriers is a mathematical framework used to study the spread of infectious diseases within a population, taking into account both individuals who are actively infectious (infectives) and those who are carriers (asymptomatic or subclinical individuals who can transmit the disease). This type of model is particularly useful for understanding the dynamics of diseases where individuals may be infectious before showing symptoms.

A common way to represent the dynamics of such a model is through a transition table, which outlines the possible transitions between different states of individuals within the population. The states typically include susceptible individuals, infectives, carriers, and recovered individuals. Each transition is associated with a certain rate, representing the probability of that transition occurring within a given time interval. Let m , n , p denote the number of susceptibles, infectives and carriers respectively. A susceptible can become infective by contact with either an infected or a carrier. The result is represented in the following model:

Event	Transition	Transition rate	Probability
a susceptible becomes an infective	$(m, n, p) \rightarrow (m - 1, n + 1, p)$	βmn	$\beta mn \Delta t + o(\Delta t)$
a susceptible becomes an infective due to contact with a carrier	$(m, n, p) \rightarrow (m - 1, n + 1, p)$	γmp	$\gamma mp \Delta t + o(\Delta t)$
a carrier is removed	$(m, n, p) \rightarrow (m, n, p - 1)$	δp	$\delta p \Delta t + o(\Delta t)$

From the tabular representation, we get

$$f_{-1,1,0}(m, n, p) = \beta mn + \gamma mp, \quad f_{0,0,-1}(m, n, p) = \gamma p \quad (4.1.22)$$

so that the partial differential equation representing the model becomes

$$\begin{aligned} \frac{\partial \phi}{\partial t} &= (x^{-1}y^1z^0 - 1) \left(\beta xy \frac{\partial^2 \phi}{\partial x \partial y} + xz \frac{\partial^2 \phi}{\partial x \partial z} \right) + (x^0y^0z^{-1} - 1) \delta z \frac{\partial \phi}{\partial z} \\ \Rightarrow \frac{\partial \phi}{\partial t} &= (y - x) \left(\beta y \frac{\partial^2 \phi}{\partial x \partial y} + \gamma z \frac{\partial^2 \phi}{\partial x \partial z} \right) + \delta(1 - z) \frac{\partial \phi}{\partial z}. \end{aligned} \quad (4.1.23)$$

Unit 5

Course Structure

- Basic model for inheritance of genetic characteristic
 - Hardy Wienberg law
 - Solved Examples on the Application of the Hardy-Weinberg Law
-

5.1 Introduction

Population genetics deals with genetic differences within and between populations, and is a part of evolutionary biology. Studies in this branch of biology examine such phenomena as adaptation, speciation, and population structure. Population genetics was a vital ingredient in the emergence of the modern evolutionary synthesis. Traditionally a highly mathematical discipline, modern population genetics encompasses theoretical, lab, and field work. Population genetic models are used both for statistical inference from DNA sequence data and for proof/disproof of concept.

5.2 Basic Model for Inheritance

The basic model for the inheritance of genetic characteristics is provided by Gregor Mendel's laws of inheritance, which laid the foundation for modern genetics. Mendel conducted experiments with pea plants in the mid-19th century and formulated several principles that describe how traits are passed from parents to offspring.

The key components of Mendel's model include:

- **Dominance and Recessiveness:** Mendel observed that certain traits, such as tallness and yellow seed color in pea plants, appeared to dominate over other traits, such as shortness and green seed color. He referred to the dominant trait as the one that was expressed in the offspring's phenotype (physical appearance), while the recessive trait was not expressed when paired with the dominant trait.
- **Segregation:** Mendel proposed that each individual possesses two alleles (variants of a gene) for a particular trait, one inherited from each parent. During gamete formation (the process of producing sex cells), these alleles segregate randomly into separate gametes. As a result, each gamete carries only one allele for each trait.

- Independent Assortment: Mendel also observed that the inheritance of one trait is independent of the inheritance of other traits. In other words, the alleles for different traits assort independently during gamete formation, leading to a variety of possible combinations in the offspring.
- To represent these principles mathematically, geneticists often use Punnett squares and probability calculations. Punnett squares are grids that show all possible combinations of alleles from two parents and predict the genotypes (genetic makeup) and phenotypes of their offspring.

For example, if we consider a single trait controlled by a pair of alleles, where capital letters represent dominant alleles and lowercase letters represent recessive alleles, we can use a Punnett square to illustrate the possible outcomes of a cross between two heterozygous individuals (individuals with different alleles for the trait). In this example, there is a 3 : 1 ratio of dominant to recessive phenotypes among the offspring, reflecting Mendel's principle of dominance.

Overall, Mendel's model provides a basic framework for understanding how genetic characteristics are inherited and passed from one generation to the next. While modern genetics has uncovered more complexity in inheritance patterns, Mendel's laws remain fundamental principles in the field of genetics.

Table 5.1: Punnett square for a single genetic trait

	Dominant allele	Recessive allele
Dominant allele	DD	Dd
Recessive allele	Dd	dd

Genetic Matrices

In genetics, a genetic matrix is essentially a table or grid used to predict the outcomes of a cross between two individuals, usually in terms of their genetic makeup and the traits they carry. It's a tool to visualize and understand how genetic traits are inherited from parents to offspring.

Here's a simplified example of a genetic matrix for a single genetic trait, such as flower color in pea plants, where capital letters represent dominant alleles and lowercase letters represent recessive alleles:

	Pp	pp
PP	Pp	Pp
Pp	Pp	pp

In this example:

- The letters represent the alleles for the flower color trait.
- "P" represents the dominant allele for purple flowers.
- "p" represents the recessive allele for white flowers.
- The rows and columns represent the alleles contributed by each parent.
- The cells in the matrix show the possible genotype combinations and their probabilities in the offspring.

So, if you cross two plants heterozygous for flower color (Pp), you'd expect a 1 in 4 chance of getting a homozygous dominant offspring (PP), a 2 in 4 chance of getting a heterozygous offspring (Pp), and a 1 in 4 chance of getting a homozygous recessive offspring (pp).

This is a basic example, and genetic matrices can become much more complex when considering multiple traits or multiple alleles for a single trait. Additionally, factors like genetic linkage, incomplete dominance, or codominance can add further complexity to the matrix. But the basic principle remains the same: using a grid to predict the possible outcomes of genetic crosses.

Each characteristic (e.g., height, colour of the eye and type of blood) of an individual is determined by two *genes*, either of these being received from each of the parents. Each gene may be in two forms, the *dominant* G or the *recessive* g . Thus an individual may belong to one of the following three *genotypes*:

- (i) (G, G) which is called *dominant* and denoted by D .
- (ii) (G, g) or (g, G) which is termed *hybrid* and denoted by H .
- (iii) (g, g) which is called *recessive* and denoted by R .

When two individuals mate, the offspring gets from each parent either of the two forms of genes with the same probability $1/2$. Thus, if (G, G) is crossed with (G, g), there are four possibilities:

- (i) The offspring gets the first G from the first parent and G from the second parent. The probability of this is $1/2 \times 1/2 = 1/4$, and the offspring is D .
- (ii) The offspring gets the first G from the first parent and g from the second parent. The probability of this is $1/2 \times 1/2 = 1/4$, and the offspring is H .
- (iii) The offspring gets the second G from the first parent and G from the second parent. The probability of this is $1/2 \times 1/2 = 1/4$, and the offspring is D .
- (iv) The offspring gets the second G from the first parent and g from the second parent. The probability of this is $1/2 \times 1/2 = 1/4$, and the offspring is H .

Thus the probabilities of the offspring being D, H, R are $1/2, 1/2, 0$ respectively. Arguing in the same way, we get the results given in below which gives the probabilities of the offspring being D, H, R when these are crossed with D, H, R , in that order.

Results of Crossing by Two Genotypes

	D			H			R		
	D	H	R	D	H	R	D	H	R
D	1	0	0	1/2	1/2	0	0	1	0
H	1/2	1/2	0	1/4	1/2	1/4	0	1/2	1/2
R	0	1	0	0	1/2	1/2	0	0	1

The three fundamental *genetic matrices* which refer to mating with D, H, R , respectively, are obtained as follows:

$$A = \begin{bmatrix} 1 & 0 & 0 \\ 1/2 & 1/2 & 0 \\ 0 & 1 & 1 \end{bmatrix}, \quad B = \begin{bmatrix} 1/2 & 1/2 & 0 \\ 1/4 & 1/2 & 1/4 \\ 0 & 1/2 & 1/2 \end{bmatrix}, \quad C = \begin{bmatrix} 0 & 1 & 0 \\ 0 & 1/2 & 1/2 \\ 0 & 0 & 1 \end{bmatrix}. \quad (5.2.1)$$

Each of these matrices is a *stochastic matrix* since all of its elements are non-negative and the row sums are unity (this is so because in each case the probability that the offspring is a *D* or *H* or *R* is unity).

Let us consider a population in which the probabilities of a person being *D*, *H*, *R* are p , q , r , respectively, so that $p + q + r = 1$. We shall call $P = (p, q, r)$ the *probability vector* of the population.

If each individual in this population is mated with a dominant, then the first matrix gives:

the probability of the *dominant* (*D*) offspring as

$$1 \cdot p + \frac{1}{2} \cdot q + 0 \cdot r = p + \frac{1}{2}q; \quad (5.2.2)$$

the probability of the *hybrid* (*H*) offspring as

$$0 \cdot p + \frac{1}{2} \cdot q + 1 \cdot r = \frac{1}{2}q + r; \quad (5.2.3)$$

the probability of the *recessive* (*R*) offspring as

$$0 \cdot p + 0 \cdot q + 0 \cdot r = 0. \quad (5.2.4)$$

Thus the probability vector for the first generation, on population being mated with pure dominants, is obtained by taking the product of the row matrix P with the first matrix A , i.e., it is given by PA . Similarly, the probability vector for the first generation when population with the probability vector P is mated with pure hybrids (pure recessives) is given by PB (PC).

If the original population is mated with dominants, hybrids, dominants, recessives, hybrids, in that order, the probability vector for the fifth generation is given by $PABACB$.

When mated with dominants, the first generation has the same probability vector as the original probability vector if $PA = P$ i.e., if $\left(p + \frac{1}{2}q, \frac{1}{2}q + r, 0\right) = (p, q, r)$. In other words, if $p = 1, q = 0, r = 0$, then

$$PA = P \Rightarrow P = (1, 0, 0). \quad (5.2.5)$$

Similarly,

$$PB = P \Rightarrow P = \left(\frac{1}{4}, \frac{1}{2}, \frac{1}{4}\right), \quad (5.2.6)$$

$$PC = P \Rightarrow P = (0, 0, 1). \quad (5.2.7)$$

Now, if the population with the probability vector P is crossed with pure dominant n times, the probability vector of the n -th generation is given by PA^n . To find this, A^n has to be determined, and this is easily done by first diagonalising the matrix A . Thus, since the eigenvalues of the matrix A are easily found to be $\left(1, \frac{1}{2}, 0\right)$ and the corresponding eigenvectors are $(1, 1, 0)$, $(0, 1, 2)$ and $(0, 0, 1)$, we can write

$$A = \begin{bmatrix} 1 & 0 & 0 \\ 1 & 1 & 0 \\ 1 & 2 & 1 \end{bmatrix} \begin{bmatrix} 1 & 0 & 0 \\ 0 & 1/2 & 0 \\ 1 & 0 & 0 \end{bmatrix} \begin{bmatrix} 1 & 0 & 0 \\ -1 & 1 & 0 \\ 1 & -2 & 1 \end{bmatrix} = S \Lambda S^{-1} \quad (5.2.8)$$

so that

$$\begin{aligned}
 A^n &= (S \wedge S^{-1})(S \wedge S^{-1}) \cdots (S \wedge S^{-1}) = S \wedge^n S^{-1} \\
 &= \begin{bmatrix} 1 & 0 & 0 \\ 1 & 1 & 0 \\ 1 & 2 & 1 \end{bmatrix} \begin{bmatrix} 1 & 0 & 0 \\ 0 & 1/2^n & 0 \\ 1 & 0 & 0 \end{bmatrix} \begin{bmatrix} 1 & 0 & 0 \\ -1 & 1 & 0 \\ 1 & -2 & 1 \end{bmatrix} \\
 &= \begin{bmatrix} 1 & 0 & 0 \\ 1 - \frac{1}{2^n} & \frac{1}{2^n} & 0 \\ 1 - \frac{1}{2^{n-1}} & \frac{1}{2^{n-1}} & 0 \end{bmatrix}, \tag{5.2.9}
 \end{aligned}$$

Therefore,

$$PA^n = \left(1 - \frac{q}{2^n} - \frac{r}{2^{n-1}}, \frac{q}{2^n} + \frac{r}{2^{n-1}}, 0\right) \tag{5.2.10}$$

As n tends to infinity, PA^n approaches to the vector $(1, 0, 0)$.

Thus, if any population is mated at random with only dominants successively, we find that (i) the recessives never appear, (ii) the proportion of hybrids tends to zero, and (iii) the proportion of dominants tends to unity.

Even if the original population consists of only recessives, we shall have a proportion 15/16 of dominants in the fifth generation and a proportion of 511/512 of dominants in the tenth generation. Thus, if dominants are desired, we can transform even a breed of recessives into a breed of dominants in a number of generations by repeated mating with dominants.

- Exercise 5.2.1.**
1. Prove that $PAB \neq PBA$, $PBC \neq PCB$, and $PCA \neq PAC$. What conclusions can you draw?
 2. Suppose an individual of unknown genotype is crossed with a recessive and the offspring is again crossed with a recessive, and so on. Show that, after a long period of such breeding, it is almost certain that the offspring will be a recessive genotype.
 3. Find A^n , B^n , C^n , PA^n , PB^n , PC^n , and consider the limiting cases when n approaches infinity. Do the limiting vector depend on P ? Interpret the results obtained.
 4. Find $P(AB)^n$, and interpret the limit of this as n tends to infinity.

5.3 Hardy-Weinberg Law

The Hardy-Weinberg law, also known as the Hardy-Weinberg equilibrium, is a fundamental principle in population genetics that describes the relationship between allele frequencies and genotype frequencies in a population that is not evolving. It provides a baseline against which we can measure evolutionary changes in populations over time.

5.3.1 Assumptions

The Hardy-Weinberg law is based on several key assumptions:

1. **Random Mating:** Individuals in the population mate randomly with respect to the gene in question.

2. **Large Population Size:** The population is infinitely large, or at least large enough to prevent genetic drift.
3. **No Mutation:** There are no new mutations occurring in the population.
4. **No Migration:** There is no migration of individuals into or out of the population.
5. **No Natural Selection:** There is no natural selection acting on the gene in question.

5.3.2 Equations

The Hardy-Weinberg law is described by two equations:

Allele Frequency Equation

The frequency of alleles in a population can be described by the equation:

$$p + q = 1$$

where:

p = frequency of the dominant allele

q = frequency of the recessive allele

5.3.3 Genotype Frequency Equation

The frequency of genotypes in a population can be described by the equation:

$$p^2 + 2pq + q^2 = 1$$

where:

p^2 = frequency of homozygous dominant individuals

$2pq$ = frequency of heterozygous individuals

q^2 = frequency of homozygous recessive individuals

5.3.4 Applications

The Hardy-Weinberg law has several important applications in population genetics, including:

- Estimating allele frequencies in populations.
- Detecting evolutionary forces such as genetic drift, gene flow, mutation, and natural selection.
- Testing for deviations from expected genotype frequencies, which may indicate the presence of evolutionary forces.

5.3.5 Conclusion

The Hardy-Weinberg law provides a useful framework for understanding how allele and genotype frequencies are maintained in populations over time in the absence of evolutionary forces. It serves as a null hypothesis against which we can test for evolutionary change.

Consider random mating or *panmixia* in a population with probability vector P . The probability vectors for mating with D , H , R are given by PA , PB , PC , but the relative proportions of D , H , R in the population are p , q , r so that the probability vector for the first generation, say F_1 , is given by

$$\begin{aligned} p PA + q PB + r PC &= \left[\left(p + \frac{1}{2}q \right)^2, 2 \left(p + \frac{1}{2}q \right) \left(r + \frac{1}{2}q \right), \left(r + \frac{1}{2}q \right)^2 \right] \\ &= (p', q', r') = P' \text{ (say).} \end{aligned} \quad (5.3.1)$$

The three components of the probability vector for the second generation, say F_2 , are then given by

$$\begin{aligned} \left(p' + \frac{1}{2}q' \right)^2 &= \left[\left(p + \frac{1}{2}q \right)^2 + \frac{1}{2} \cdot 2 \left(p + \frac{1}{2}q \right) \left(r + \frac{1}{2}q \right) \right]^2 \\ &= \left(p + \frac{1}{2}q \right)^2 \left(p + \frac{1}{2}q + r + \frac{1}{2}q \right)^2 \\ &= \left(p + \frac{1}{2}q \right)^2 \\ &= p', \end{aligned} \quad (5.3.2)$$

$$\begin{aligned} 2 \left(p' + \frac{1}{2}q' \right) \left(r' + \frac{1}{2}q' \right) &= 2 \left[\left(p + \frac{1}{2}q \right)^2 + \left(p + \frac{1}{2}q \right) \left(r + \frac{1}{2}q \right) \right] \\ &\quad \times \left[\left(r + \frac{1}{2}q \right)^2 + \left(p + \frac{1}{2}q \right) \left(r + \frac{1}{2}q \right) \right] \\ &= 2 \left[\left(p + \frac{1}{2}q \right) \left(p + \frac{1}{2}q + r + \frac{1}{2}q \right) \left(r + \frac{1}{2}q \right) \left(r + \frac{1}{2}q + p + \frac{1}{2}q \right) \right] \\ &= 2 \left(p + \frac{1}{2}q \right) \left(r + \frac{1}{2}q \right) \\ &= q', \end{aligned} \quad (5.3.3)$$

$$\begin{aligned} \left(r' + \frac{1}{2}q' \right)^2 &= \left[\left(r + \frac{1}{2}q \right)^2 + \left(p + \frac{1}{2}q \right) \left(r + \frac{1}{2}q \right) \right]^2 \\ &= \left(r + \frac{1}{2}q \right)^2 \left(r + \frac{1}{2}q + p + \frac{1}{2}q \right)^2 \\ &= \left(r + \frac{1}{2}q \right)^2 \\ &= r', \end{aligned} \quad (5.3.4)$$

Thus the probability vector for F_2 is the same as that for F_1 . This shows that, due to random mating, the probability vectors for the first generation and all succeeding generations are the same. This is known as the

Hardy-Weinberg law, called after the mathematician G. H. Hardy and the geneticist W. Weinberg.

In any population in which random mating takes place, we have $P = P'$ so that

$$p = \left(p + \frac{1}{2}q\right)^2, \quad q = 2\left(p + \frac{1}{2}q\right)\left(r + \frac{1}{2}q\right), \quad r = \left(r + \frac{1}{2}q\right)^2. \quad (5.3.5)$$

Simplifying (5.3.5), we get

$$p = (1 - \sqrt{r})^2, \quad q = 2\sqrt{r}(1 - \sqrt{r}), \quad r = r. \quad (5.3.6)$$

The ratios $p : q : r$ in a genetically stable population are known as *Hardy-Weinberg ratios*. There is only one parameter r that depends on the particular gene under consideration.

Note: We may note that the Hardy-Weinberg law holds for a gene if the mating is random with respect to that gene. Thus, in human populations, the law is likely to hold for genes for blood groups, since, in general, people do not worry about blood groups when marrying, but the law may not hold for the gene determining heights since tall people, in general, tend to marry tall people.

Note: If we can identify the three genotypes for a particular gene in a population and if their relative proportions verify (5.3.6), then it confirms that mating is likely to be random for that gene. If (5.3.6) can not be verified, it may be due to non-random mating or differential mortality of dominant and recessive genes.

Note: In general, however, it is not easy to distinguish between the three genotypes. If G is dominant to g , then individuals having (G, G) (G, g) have the same appearance and belong to the same *phenotype*. Thus, while there are three genotypes, only two distinct phenotypes exist, namely, $\{(G, G), (G, g)\}$ and $\{(g, g)\}$, with respect to a gene.

The individuals with (G, G) , (g, g) are said to be *homozygous* and the individual with (G, g) are said to be *heterozygous*.

The Hardy-Weinberg law can also be stated in terms of gene frequencies. If P, Q are the relative gene frequencies in a population and (p, q, r) are the relative frequencies of (G, G) , (G, g) and (g, g) , then it is easily seen that

$$P = p + \frac{1}{2}q, \quad Q = \frac{1}{2}q + r. \quad (5.3.7)$$

Knowing p, q, r , we can find P and Q uniquely, but knowing P and Q , we cannot find p, q, r uniquely. However, for random mating, (5.3.6) and (5.3.7) give

$$P = 1 - \sqrt{r}, \quad Q = \sqrt{r}. \quad (5.3.8)$$

Now, in any generation, if the relative frequencies of genes G and g are P and Q provided $P + Q = 1$, in both males and females, then, in random mating, the probability of an offspring getting G from both parents is P^2 , the probability of its getting G from one parent and g from the other parent is $2PQ$, and the probability of its getting g from both parent is Q^2 , so that the proportions in F_1 are

$$(G, G) : P^2, \quad (G, g) : 2PQ, \quad (g, g) : Q^2. \quad (5.3.9)$$

From (5.3.2) - (5.3.4) and (5.3.7), we get the Hardy-Weinberg ratio. The relative gene frequencies in F_1 are

$$G : 2P^2 + 2PQ = 2P(P + Q) = 2P, \quad g : 2PQ + 2Q^2 = 2Q(P + Q) = 2Q \quad (5.3.10)$$

so that the proportions of genes are the same as in the original population and F_2 has the ratios given by (5.3.9). This again confirms the Hardy-Weinberg law.

The Hardy-Weinberg principle is a fundamental concept in population genetics that describes the relationship between allele frequencies and genotype frequencies in a population that is not evolving. Here, some solved examples regarding this are presented.

Solved Examples on the Application of the Hardy-Weinberg Law

Example 1:

In a population of rabbits, the frequency of the dominant allele (A) for coat color is 0.6, and the frequency of the recessive allele (a) is 0.4. According to the Hardy-Weinberg principle, what are the expected genotype frequencies?

Solution: Let p = frequency of allele $A = 0.6$

Let q = frequency of allele $a = 0.4$

According to the Hardy-Weinberg equation:

$$\text{Genotype frequency of } AA = p^2 = (0.6)^2 = 0.36$$

$$\text{Genotype frequency of } Aa = 2pq = 2 \times 0.6 \times 0.4 = 0.48$$

$$\text{Genotype frequency of } aa = q^2 = (0.4)^2 = 0.16$$

So, the expected genotype frequencies are 0.36 (AA), 0.48 (Aa), and 0.16 (aa).

Example 2:

In a population of 500 individuals, 250 are homozygous dominant (AA), 200 are heterozygous (Aa), and 50 are homozygous recessive (aa). What are the allele frequencies?

Solution:

$$\text{Total number of individuals} = 500$$

$$\text{Frequency of } AA = \frac{250}{500} = 0.5$$

$$\text{Frequency of } Aa = \frac{200}{500} = 0.4$$

$$\text{Frequency of } aa = \frac{50}{500} = 0.1$$

Allele frequencies:

$$\text{Frequency of } A = p = \text{frequency of } AA + 0.5 \times \text{frequency of } Aa = 0.5 + 0.5 \times 0.4 = 0.7$$

$$\text{Frequency of } a = q = \text{frequency of } aa + 0.5 \times \text{frequency of } Aa = 0.1 + 0.5 \times 0.4 = 0.3$$

Example 3:

In a population of 1000 individuals, 360 are homozygous dominant (AA), 480 are heterozygous (Aa), and 160 are homozygous recessive (aa). What are the allele frequencies?

Solution:

$$\text{Total number of individuals} = 1000$$

$$\text{Frequency of } AA = \frac{360}{1000} = 0.36$$

$$\text{Frequency of } Aa = \frac{480}{1000} = 0.48$$

$$\text{Frequency of } aa = \frac{160}{1000} = 0.16$$

Allele frequencies:

$$\text{Frequency of } A = p = \text{frequency of } AA + 0.5 \times \text{frequency of } Aa = 0.36 + 0.5 \times 0.48 = 0.6$$

$$\text{Frequency of } a = q = \text{frequency of } aa + 0.5 \times \text{frequency of } Aa = 0.16 + 0.5 \times 0.48 = 0.4$$

Example 4:

In a population of butterflies, the frequency of the recessive allele for wing color (b) is 0.3. According to the Hardy-Weinberg principle, what is the frequency of the homozygous dominant genotype (BB)?

Solution: Let q = frequency of allele $b = 0.3$.

Since, $p + q = 1$, $p = 1 - q = 1 - 0.3 = 0.7$,

According to the Hardy-Weinberg equation:

$$\text{Genotype frequency of } BB = p^2 = (0.7)^2 = 0.49.$$

So, the frequency of the BB genotype is 0.49.

Example 5:

In a population of 800 birds, 400 are homozygous for a particular gene (AA), and 200 are heterozygous (Aa). What are the allele frequencies?

Solution:

$$\text{Total number of individuals} = 800$$

$$\text{Frequency of } AA = \frac{400}{800} = 0.5$$

$$\text{Frequency of } Aa = \frac{200}{800} = 0.25$$

$$\text{Frequency of } aa \text{ can be calculated as } 1 - 0.5 - 0.25 = 0.25$$

Allele frequencies:

$$\text{Frequency of } A = p = \text{frequency of } AA + 0.5 \times \text{frequency of } Aa = 0.5 + 0.5 \times 0.25 = 0.625$$

$$\text{Frequency of } a = q = \text{frequency of } aa + 0.5 \times \text{frequency of } Aa = 0.25 + 0.5 \times 0.25 = 0.375$$

Example 6:

In a population of 5000 individuals, 2250 are homozygous recessive (bb). If the population is in Hardy-Weinberg equilibrium, what is the frequency of the dominant allele (B)?

Solution: Since 2250 individuals are homozygous recessive (bb), $q^2 = \frac{2250}{5000} = 0.45$.

Solving for q , we find $q = \sqrt{0.45} \approx 0.67$.

Since $p + q = 1$, $p = 1 - q = 1 - 0.67 = 0.33$

So, the frequency of the dominant allele (B) is 0.33.

Example 7:

In a population of 2000 individuals, 900 are heterozygous (Aa) for a particular gene. What are the expected genotype frequencies in the population?

Solution: Similar to Example 1, you can use the Hardy-Weinberg equation to calculate the expected genotype frequencies using the allele frequencies.

Example 8:

In a population of plants, 25% are homozygous dominant (AA), 50% are heterozygous (Aa), and 25% are homozygous recessive (aa). What are the allele frequencies?

Solution: Similar to Example 2, you can calculate the allele frequencies using the given genotype frequencies.

Example 9:

In a population of 3000 individuals, 700 are homozygous dominant (AA), and 500 are homozygous recessive (aa). What is the frequency of the heterozygous genotype (Aa)?

Solution: Similar to previous examples, you can use the given genotype frequencies to calculate the frequency of the heterozygous genotype (Aa).

Example 10:

In a population of mice, 70% are homozygous dominant (AA) for a particular trait. What is the frequency of the recessive allele (a)?

Solution: Since 70% are homozygous dominant (AA), $p^2 = 0.7$.

Solving for p , we find that $p = \sqrt{0.7} \approx 0.84$.

Since $p + q = 1$, $q = 1 - p = 1 - 0.84 = 0.16$

So, the frequency of the recessive allele (a) is 0.16.

Unit 6

Course Structure

- Correlation between Genetic Composition of Siblings
 - Bayes Theorem and Its Applications in Genetics
-

6.1 Correlation between Genetic Composition of Siblings

As an example of the use of our basic model, we find the correlation between genetic composition of offsprings from the same parents, assuming random mating and a genetically stable population. In the original population, let the proportion of dominants, hybrids and recessives be given by (5.3.6), i.e.,

$$p = (1 - \sqrt{r})^2, \quad q = 2\sqrt{r}(1 - \sqrt{r}), \quad r = r. \quad (6.1.1)$$

Let Y_1, Y_2 be the offspring from parents X_1, X_2 . Then using the theorems of total and compound probabilities, we get

$$\begin{aligned} P(Y_1 = D, Y_2 = D) &= P(Y_1 = D, Y_2 = D; X_1 = D, X_2 = D) \\ &\quad + P(Y_1 = D, Y_2 = D; X_1 = D, X_2 = H) \\ &\quad + P(Y_1 = D, Y_2 = D; X_1 = H, X_2 = D) \\ &\quad + P(Y_1 = D, Y_2 = D; X_1 = H, X_2 = H) \\ &= P(X_1 = D, X_2 = D)P(Y_1 = D, Y_2 = D/X_1 = D, X_2 = D) \\ &\quad + P(X_1 = D, X_2 = H)P(Y_1 = D, Y_2 = D/X_1 = D, X_2 = H) \\ &\quad + P(X_1 = H, X_2 = D)P(Y_1 = D, Y_2 = D/X_1 = H, X_2 = D) \\ &\quad + P(X_1 = H, X_2 = H)P(Y_1 = D, Y_2 = D/X_1 = H, X_2 = H) \\ &= p^2 \cdot 1 + pq \cdot \frac{1}{2} \cdot \frac{1}{2} + pq \cdot \frac{1}{2} \cdot \frac{1}{2} + q^2 \cdot \frac{1}{4} \cdot \frac{1}{4} \\ &= p^2 + \frac{1}{2}pq + \frac{1}{16}q^2 \\ &= (1 - \sqrt{r})^4 + \sqrt{r}(1 - \sqrt{r})^3 + \frac{1}{4}r(1 - \sqrt{r})^2 \\ &= \frac{1}{4}(1 - \sqrt{r})^2(2 - \sqrt{r})^2. \end{aligned} \quad (6.1.2)$$

Similarly,

$$P(Y_1 = D, Y_2 = H) = P(Y_1 = H, Y_2 = D) = \frac{1}{2}\sqrt{r}(1 - \sqrt{r})^2(2 - \sqrt{r}), \quad (6.1.3)$$

$$P(Y_1 = D, Y_2 = R) = P(Y_1 = R, Y_2 = D) = \frac{1}{4}r(1 - \sqrt{r})^2, \quad (6.1.4)$$

$$P(Y_1 = H, Y_2 = R) = P(Y_1 = R, Y_2 = H) = \frac{1}{2}r(1 - \sqrt{r})(1 + \sqrt{r}), \quad (6.1.5)$$

$$P(Y_1 = H, Y_2 = H) = \sqrt{r}(1 - \sqrt{r})(1 + \sqrt{r} - r), \quad (6.1.6)$$

$$P(Y_1 = R, Y_2 = R) = \frac{1}{4}r(1 + \sqrt{r})^2, \quad (6.1.7)$$

If we assign arbitrary values 1, 0, -1 to D , H and R , respectively, we get the bivariate probability distribution as follows:

Y_1	Y_2	Probability
1	1	$\frac{1}{4}(1 - \sqrt{r})^2(2 - \sqrt{r})^2$
-1	-1	$\frac{1}{4}r(1 + \sqrt{r})^2$
0	0	$\sqrt{r}(1 - \sqrt{r})(1 + \sqrt{r} - r)$
1	0	$\frac{1}{2}\sqrt{r}(1 - \sqrt{r})^2(2 - \sqrt{r})$
0	1	$\frac{1}{2}\sqrt{r}(1 - \sqrt{r})^2(2 - \sqrt{r})$
1	-1	$\frac{1}{4}r(1 - \sqrt{r})^2$
-1	1	$\frac{1}{4}r(1 - \sqrt{r})^2$
0	-1	$\frac{1}{2}r(1 - \sqrt{r})(1 + \sqrt{r})$
-1	0	$\frac{1}{2}r(1 - \sqrt{r})(1 + \sqrt{r})$

The marginal distributions of Y_1 and Y_2 are the same and are given by

Y_1 or Y_2	1	0	-1
Probability	$(1 - \sqrt{r})^2$	$2\sqrt{r}(1 - \sqrt{r})$	r

From these we easily deduce

$$\bar{Y}_1 = \bar{Y}_2 = 1 - 2\sqrt{r}, \quad (6.1.8)$$

$$\sigma_{Y_1}^2 = \sigma_{Y_2}^2 = 2\sqrt{r}(1 - \sqrt{r}), \quad (6.1.9)$$

$$\text{cov}(Y_1, Y_2) = \sqrt{r}(1 - \sqrt{r}), \quad (6.1.10)$$

$$\rho_{Y_1, Y_2} = \frac{1}{2}. \quad (6.1.11)$$

Thus, the correlation coefficient comes out to be independent of the value of r , i.e., it is the same for all genes.

6.2 Bayes Theorem and Its Applications in Genetics

At any time, we have some hypotheses to explain genetic events and probabilities associated with these hypotheses to measure our degrees of confidence in the hypotheses. These probabilities are called *a priori*

probabilities. The occurrence of an event changes our degrees of confidence in the sense that the probabilities of some hypotheses may increase and of other may decrease. The new probabilities are called *a posteriori probabilities*. Bayes theorem connects a posteriori and a priori probabilities.

Let H_1, H_2, \dots, H_n be n mutually exclusive hypothesis, and let their a priori probabilities be $P(H_1), P(H_2), \dots, P(H_n)$. Now let an event A happen, and let the probabilities of happening of this event on the basis of various hypotheses be given by $P(A/H_1), P(A/H_2), \dots, P(A/H_n)$. Our object is to find the posteriori probabilities $P(H_1/A), P(H_2/A), \dots, P(H_n/A)$ in terms of the known probabilities $P(H_i), P(A/H_i), i = 1, 2, \dots, n$.

From the theorem of compound probability,

$$P(AH_i) = P(H_i)P(A/H_i) = P(A)P(H_i/A)$$

so that

$$P(H_i/A) = \frac{P(H_i)P(A/H_i)}{P(A)}, \quad i = 1, 2, \dots, n. \quad (6.2.1)$$

Since H_1, H_2, \dots, H_n are mutually exclusive and exhaustive hypotheses under consideration, we have, by the theorem of total probability,

$$P(A) = P(AH_1) + P(AH_2) + \dots + P(AH_n) = \sum_{j=1}^n P(AH_j) = \sum_{j=1}^n P(H_j)P(A/H_j). \quad (6.2.2)$$

From (6.2.1) and (6.2.2), we get

$$P(H_i/A) = \frac{P(H_i)P(A/H_i)}{\sum_{j=1}^n P(H_j)P(A/H_j)} \quad (6.2.3)$$

which is the required *Bayes theorem*.

Illustration - I

As an illustration of Bayes theorem in genetics, we investigate the probability that two blue-eyed boy twins are monovular (i.e., from the same egg). Here we have two possible hypothesis:

(i) H_1 : Both are from the same egg, i.e., both are monovular;

(ii) H_2 : Both are from the different eggs, i.e., both are binovular.

To find $P(H_1)$ and $P(H_2)$, we remember that observation that 32 percent of all twin pairs are of unlike sex; of the remaining 68 percent, half are expected to be monovular and the other half are expected to be binovular so that

$$P(H_1) = \frac{0.36}{0.68} = \frac{9}{17}, \quad P(H_2) = \frac{0.32}{0.68} = \frac{8}{17}. \quad (6.2.4)$$

To find $P(A/H_1)$ and $P(A/H_2)$, we assume that mating is random and is genetically stable so that the proportions of D, H, R are given by

$$p = (1 - \sqrt{r})^2, \quad q = 2\sqrt{r}(1 - \sqrt{r}), \quad r = r \quad (6.2.5)$$

Also, blue eyes are known to arise due to a recessive gene so that:

$$\begin{aligned} P(A/H_1) &= \text{probability that both boys are recessive when they are from the same egg} \\ &= r, \end{aligned} \tag{6.2.6}$$

$$\begin{aligned} P(A/H_2) &= \text{probability that both boys are recessive when they are from the different egg} \\ &= P(\text{parents are } Bb, Bb, \text{ and both children are } bb) \\ &\quad + P(\text{parents are } Bb, bb, \text{ and both children are } bb) \\ &\quad + P(\text{parents are } bb, Bb, \text{ and both children are } bb) \\ &\quad + P(\text{parents are } bb, bb, \text{ and both children are } bb) \\ &= q^2 \cdot \frac{1}{4} \cdot \frac{1}{4} + qr \cdot \frac{1}{2} \cdot \frac{1}{2} + qr \cdot \frac{1}{2} \cdot \frac{1}{2} + r^2 \cdot 1 \cdot 1 \\ &= \frac{r(1 - \sqrt{r})^2}{4} + \frac{r\sqrt{r}(1 - \sqrt{r})}{1} + r^2 \\ &= \frac{1}{4}r(1 + r - 2\sqrt{r} + 4\sqrt{r} - 4r + 4r) \\ &= \frac{1}{4}r(1 + \sqrt{r})^2. \end{aligned} \tag{6.2.7}$$

Using (6.2.3), (6.2.4), (6.2.6) and (6.2.7), we can find $P(H_1/A)$ and $P(H_2/A)$.

Illustration - II

To illustrate another application of Bayes theorem, we consider the following problem. For mating of two dominant-looking individuals, a dominant-looking individual is obtained. What is the probability that both the parents are real dominants?

There are four possible hypotheses about parents:

- H_1 : parents are GG, GG ,
- H_2 : parents are GG, Gg ,
- H_3 : parents are Gg, GG ,
- H_4 : parents are Gg, Gg .

The event A is that the offspring is GG or Gg , so that

$$P(A/H_1) = 1, \quad P(A/H_2) = 1, \quad P(A/H_3) = 1, \quad P(A/H_4) = \frac{3}{4}.$$

Also, in the absence of any knowledge, we make use of *Bayes hypotheses* which postulates that all the four hypotheses have the same a priori probability so that

$$P(H_1) = \frac{1}{4}, \quad P(H_2) = \frac{1}{4}, \quad P(H_3) = \frac{1}{4}, \quad P(H_4) = \frac{1}{4}.$$

Therefore, on making use of (6.2.3), we get

$$P(H_1/A) = \frac{\frac{1}{4} \cdot 1}{\frac{1}{4} \cdot 1 + \frac{1}{4} \cdot 1 + \frac{1}{4} \cdot 1 + \frac{1}{4} \cdot \frac{3}{4}} = \frac{4}{15}.$$

Illustration - III : Genetic Testing for a Rare Disease

Suppose a rare genetic disease affects 1 in 10,000 individuals in the population. A genetic test for this disease has a sensitivity of 95% (probability of a positive test result given that the individual has the disease) and a specificity of 99% (probability of a negative test result given that the individual does not have the disease).

If an individual tests positive for the disease, what is the probability that they actually have the disease?

Solution:

Let's denote the following events:

- A : Individual has the disease. - B : Individual tests positive for the disease.

We are asked to find $P(A|B)$, the probability that the individual has the disease given a positive test result.

Using Bayes' theorem:

$$P(A|B) = \frac{P(B|A) \times P(A)}{P(B)}$$

We have:

- $P(B|A) = 0.95$ (sensitivity) - $P(A) = 1/10,000 = 0.0001$ (prevalence of the disease) - $P(B|A') = 1 - P(\text{Negative test}|A') = 1 - 0.99 = 0.01$ (complement of specificity) - $P(A') = 1 - P(A) = 1 - 0.0001 = 0.9999$ (complement of prevalence)

$$P(B) = P(B|A) \times P(A) + P(B|A') \times P(A')$$

$$P(B) = (0.95 \times 0.0001) + (0.01 \times 0.9999)$$

$$P(B) = 0.000095 + 0.009999$$

$$P(B) = 0.010094$$

Now, we can calculate $P(A|B)$:

$$P(A|B) = \frac{0.95 \times 0.0001}{0.010094}$$

$$P(A|B) \approx 0.0009414$$

So, the probability that an individual has the disease given a positive test result is approximately 0.09414%.

Illustration - IV : DNA Evidence in Criminal Investigations

Suppose a DNA test is conducted in a criminal investigation. The DNA evidence matches the DNA profile of the suspect. However, it is known that the DNA profile occurs in 1 out of 1000 individuals in the population.

Given that the suspect is known to be in the group that matches the DNA profile, what is the probability that the suspect is actually guilty?

Solution:

Let's denote the following events:

- G : Suspect is guilty. - M : Suspect's DNA matches the DNA evidence.

We are asked to find $P(G|M)$, the probability that the suspect is guilty given a DNA match.

Using Bayes' theorem:

$$P(G|M) = \frac{P(M|G) \times P(G)}{P(M)}$$

We have:

- $P(M|G) = 1$ (if the suspect is guilty, then the DNA must match) - $P(G) = 1$ (since we are considering only the group of individuals where the DNA profile matches) - $P(M|G') = 1/1000 = 0.001$ (probability of a DNA match in an innocent person) - $P(G') = 1 - P(G) = 0$ (probability of innocence for an individual in the group)

$$P(M) = P(M|G) \times P(G) + P(M|G') \times P(G')$$

$$P(M) = 1 \times 1 + 0.001 \times 0$$

$$P(M) = 1$$

Now, we can calculate $P(G|M)$:

$$P(G|M) = \frac{1 \times 1}{1} = 1$$

So, the probability that the suspect is guilty given a DNA match is 100%.

Illustration - V

Suppose a screening test is used to detect a genetic disorder that affects 1 in 500 individuals in the population. The test has a sensitivity of 90% (probability of a positive test result given that the individual has the disorder) and a specificity of 95% (probability of a negative test result given that the individual does not have the disorder).

If an individual tests negative for the disorder, what is the probability that they actually do not have the disorder?

Solution:

Let's denote the following events:

- A : Individual has the disorder. - B : Individual tests negative for the disorder.

We are asked to find $P(A'|B)$, the probability that the individual does not have the disorder given a negative test result.

Using Bayes' theorem:

$$P(A'|B) = \frac{P(B|A') \times P(A')}{P(B)}$$

We have:

- $P(B|A') = 0.95$ (specificity) - $P(A') = 1 - P(A) = 1 - (1/500) = 499/500$ - $P(B|A) = 1 - P(\text{Positive test}|A) = 1 - 0.90 = 0.10$ - $P(B) = P(B|A) \times P(A) + P(B|A') \times P(A')$ - $P(B) = (0.10) \times (1/500) + (0.95) \times (499/500)$

Now, we can calculate $P(A'|B)$:

$$P(A'|B) = \frac{(0.95) \times (499/500)}{(0.10) \times (1/500) + (0.95) \times (499/500)}$$

$$P(A'|B) \approx 0.999$$

So, the probability that an individual does not have the disorder given a negative test result is approximately 99.9%.

Illustration - VI

Suppose a paternity test is conducted to determine the father of a child. The test examines specific genetic markers. The alleged father shares the same genetic markers with the child at 15 out of 20 markers tested.

Given that the alleged father is not the biological father, what is the probability of observing this level of genetic similarity by chance?

Solution:

Let's denote the following events:

- F : Alleged father is the biological father. - M : Genetic markers match between the alleged father and the child.

We are asked to find $P(M|F')$, the probability of observing genetic similarity between the alleged father and the child given that the alleged father is not the biological father.

Using Bayes' theorem:

$$P(M|F') = \frac{P(F'|M) \times P(M)}{P(F')}$$

We have:

- $P(F'|M) = 0$ (since the alleged father is not the biological father) - $P(M)$ is the probability of observing genetic similarity by chance, which may vary depending on the specific genetic markers and population frequencies. - $P(F') = 1 - P(F)$ (probability that the alleged father is not the biological father)

Now, we can calculate $P(M|F')$ based on the specific context and population data.

- Exercise 6.2.1.**
1. A flock of certain species of fowls consists of 117, 191 and 16 with blue, black, and white plumages. Assuming that black and white plumages are the phenotypes corresponding to the homozygous genotypes (b, b) and (w, w) and the blue plumage corresponds to the heterozygous genotype (w, b) , find the genotype and gene frequencies.
 2. In a certain human population, dominants, hybrids and recessives are 16 per cent, 48 per cent and 36 per cent, respectively. Given that a man is recessive and has a brother, show that the probability of the brother being recessive is 0.66. What are the probabilities of the brother being a dominant or a hybrid?
 3. Assuming Mendel's law of independent assortment which postulates that, when there are two or more gene pair segregating at the same time, they do independently, prove that the double inter-cross $AaBb \times AaBb$ results in four phenotypes, namely, AB , Ab , aB , and ab , in the ratios 9 : 3 : 3 : 1.
 4. From the mating of two hybrids Gg and Gg , a dominant-looking offspring Gx is obtained. This individual is mated with another hybrid, and as a result, n individuals are obtained, all of whom look dominant. What is the a posteriori probability that $x = G$?
 5. From the mating of two dominant-looking individuals, n offspring are produced, of which r are recessives. What is the probability that both the parents are hybrid?

Unit 7

Course Structure

- Extension of basic model for inheritance of genetic characteristics
 - Models for genetic improvement: Selection and Mutation
-

7.1 Further Discussion of Basic Model for Inheritance of Genetic Characteristics

7.1.1 Phenotype Ratios

For one gene, there are 4 possible genetic constitutions, namely, $\{(G, G), (G, g), (g, G), (g, g)\}$; there are 3 genotypes, viz, dominant $D : (G, G)$, hybrid $H : (G, g), (g, G)$, and recessive $R : (g, g)$; and there 2 phenotypes, viz, dominant-looking: $\{(G, G), (G, g), (g, G)\}$ and recessive-looking $\{(g, g)\}$. The ratio of the two phenotypes is 3 : 1.

For two genes, there are 16 possibilities:

$G_1 G_1 G_2 G_2$			
$G_1 g_1 G_2 G_2$			
$G_1 g_1 G_2 G_2$			
$G_1 g_1 G_2 G_2$			

There are 9 genotypes:

$$D_1 D_2, D_1 H_2, D_1 R_2, H_1 D_2, H_1 H_2, H_1 R_2, R_1 D_2, R_1 H_2, R_1 R_2$$

with frequencies 1, 2, 1, 2, 4, 2, 1, 2, 1, respectively. There are 4 phenotypes:

$$D_1 D_2, D_1 R_2, R_1 D_2, R_1 R_2$$

with frequencies 9 : 3 : 3 : 1.

Let us now generalize the case of n genes. For each gene, there are 4 possibilities and so the total number of possibilities for n gene is 4^n . For each gene, there are 3 genotypes and so the total number of genotypes is 3^n . For each gene, there are 2 phenotypes and so the total number of phenotypes for n genes is 2^n . With respect to each gene, there are 3 dominant phenotypes for each recessive phenotype.

Let us find how many phenotypes are dominant with respect to r genes. We can choose r genes in $\binom{n}{r}$ ways and, corresponding to each of these, there are 3 dominant phenotypes and 1 recessive phenotype so that the frequency of genotypes, which are dominant with respect to r genes and recessives with respect to $n - r$ genes, is $\binom{n}{r} 3^r 1^{n-r}$, and the total of all these frequencies is

$$\sum_{r=0}^n \binom{n}{r} 3^r = (3 + 1)^n = 4^n. \quad (7.1.1)$$

Thus of the 4^n possibilities with n genes, we have $\binom{n}{r}$ groups of 3^{n-r} , each dominant with respect to $n - r$ genes for $r = 0, 1, 2, \dots, n$.

Thus we have one group of 3^n , $\binom{n}{1}$ groups of 3^{n-1} each, \dots $\binom{n}{r}$ groups of 3^{n-r} each, \dots and one group of 1 so that the phenotype ratios are:

$$\underbrace{3^n}_{\binom{n}{0}}, \quad \underbrace{3^{n-1}, 3^{n-1}, \dots, 3^{n-1}}_{\binom{n}{1}}, \quad \dots \quad \underbrace{3, 3, \dots, 3}_{\binom{n}{n-1}}, \quad \underbrace{3^0}_{\binom{n}{n}}$$

The frequencies of phenotypes are given by coefficients in the expansion of $(3x + y)^n$. Similarly, the frequencies of genotypes are given by coefficients of $(x + 2y + z)^n$, and the frequency of a genotype dominant with respect to r genes, hybrid with respect to s genes, and recessive with respect to $n - r - s$ genes is

$$\frac{n!}{r! s! (n - r - s)!} 2^n.$$

7.2 Multiple Alleles and Application to Blood Groups

In genetics, multiple alleles refer to the existence of more than two alleles (variants of a gene) for a particular trait in a population. The classic example of multiple alleles is the ABO blood group system in humans.

ABO Blood Group System

The ABO blood group system is controlled by three main alleles located on chromosome 9: **A**, **B**, and **O**. Each individual inherits two alleles, one from each parent, resulting in six possible genotypes: AA, AO, BB, BO, AB, and OO.

- Allele **A** codes for the A antigen on the surface of red blood cells.
- Allele **B** codes for the B antigen on the surface of red blood cells.
- Allele **O** codes for neither A nor B antigens, often referred to as the absence of antigen.

The A and B alleles are co-dominant, meaning that when both alleles are present (genotype AB), both antigens are expressed equally on the surface of red blood cells. The O allele is recessive to both A and B alleles, so individuals with genotype OO have neither A nor B antigens.

Genotype-Phenotype Relationships

The genotype of an individual determines their blood type, which is characterized by the presence or absence of A and B antigens on the surface of red blood cells. The following genotype-phenotype relationships exist in the ABO blood group system:

- **Blood type A:** Genotypes AA and AO
- **Blood type B:** Genotypes BB and BO
- **Blood type AB:** Genotype AB
- **Blood type O:** Genotype OO

Application to Blood Transfusions and Organ Transplantation

Understanding the genetics of the ABO blood group system is crucial in medicine, particularly in blood transfusions and organ transplantation. Compatibility in blood transfusions is determined by the presence or absence of A and B antigens and antibodies in the recipient’s blood.

- Individuals with blood type A can receive blood from donors with blood types A and O.
- Individuals with blood type B can receive blood from donors with blood types B and O.
- Individuals with blood type AB can receive blood from any blood type (universal recipient).
- Individuals with blood type O can only receive blood from donors with blood type O (universal donor).

Similarly, compatibility in organ transplantation is assessed based on ABO blood group compatibility between the donor and recipient.

The ABO blood group system serves as a practical application of multiple alleles in determining blood compatibility, thereby ensuring the safety and efficacy of blood transfusions and organ donations.

So far we have considered the case of two alleles G and g only, but there may be a number of *alleles* corresponding to a given locus. The most important and elementary example is the gene determining blood groups, which has three alleles A, B, O giving rise to 9 possibilities (A,A), (A,B), (A,O), (B,A), (B,B), (B,O), (O,A), (O,B) and (O,O). There are, however, only 6 genotypes since (A,B), (B,A); (A,O), (O,A); and (B,O), (O,B) give the same genotypes. Since A and B dominate over O, there are only four phenotype groups, namely, $\{(A, A), (A, O), (O, A)\}$, $\{(B, B), (B, O), (O, B)\}$, $\{(A, B), (B, A)\}$, and $\{O, O\}$. These are denoted by A, B, AB and O, respectively.

Table 2 : Possible Blood Groups of Father in terms of Blood Groups of Mother and Child

Child	A	B	AB	O
Mother	A, B, AB, O	B, AB	B, AB	A, B, O
B	A, AB	A, B, AB, O	A, AB	AB, O
AB	A, B, AB, O	A, B, AB, O	A, B, AB	ϕ
O	A, AB	B, AB	ϕ	A, B, O

We now get the results given in Table 1 for genotypes and blood groups of offspring. From Table 1, we can deduce the table for the possible blood groups for the father when we know the blood group of mother and child (Table 2). Table 2 is used in certain disputed legal cases to decide whether a certain child born of a certain mother can be the child of a given male.

Again, if the proportions of alleles A, B, O in the population are p , q , r , then the proportions of persons with blood groups A, B, AB, and O in the population are

$$p^2 + 2pr, q^2 + 2qr, 2qr, r^2 \quad [p^2 + 2pq + q^2 + 2qr + 2pq + r^2 = (p + q + r)^2 = 1]$$

If we know the division of the population according to blood groups, we can calculate p , q , r .

Table 1: Genotypes and Blood Groups of Offspring

Mother	Father		A		B		AB	O
	(A, A)	(A, O)	(A, B)	(A, O)	(B, B)	(B, O)	(A, B)	(O, O)
A	(A, A)	(A, A), (A, O)	(A, B)	(A, B), (A, O)	(A, A), (A, B)	(A, O)	(A, A), (A, B)	(A, O)
	A	A	AB	AB, A	A, AB	A	A, AB	A
	(A, A), (A, O)	(A, A), (A, O), (O, O)	(A, B), (B, O)	(A, B), (A, O), (B, O)	(A, A), (A, O), (A, B), (B, O)	(A, O), (O, O)	(A, A), (A, O), (A, B), (B, O)	(A, O), (O, O)
	A	A, O	AB, B	AB, A, B, O	A, AB, B	A, O	A, AB, B	A, O
B	(A, B)	(A, B), (B, O)	(B, B)	(B, B), (B, O)	(A, B), (B, B)	(B, O)	(A, B), (B, B)	(B, O)
	AB	AB, B	B	B	AB, B	B	AB, B	B
	(A, B), (A, O)	(A, B), (A, O), (B, O), (O, O)	(B, B), (B, O)	(B, B), (B, O), (O, O)	(A, B), (B, B), (A, O), (B, O)	(B, O), (O, O)	(A, B), (B, B), (A, O), (B, O)	(B, O), (O, O)
	AB, A	AB, A, B, O	B	B, O	AB, B, A	B, O	AB, B, A	B, O
AB	(A, A), (A, B)	(A, A), (B, O), (A, O), (A, B)	(A, B), (B, B)	(A, B), (A, O), (B, O)	(A, A), (A, B), (B, B)	(A, O)	(A, A), (A, B), (B, B)	(A, O), (B, O)
	A, AB	A, B, AO	AB, B	AB, A, B	A, AB, B	A, B	A, AB, B	A, B
O	(A, O)	(A, O), (O, O)	(B, O)	(B, O), (O, O)	(A, O), (B, O)	(O, O)	(A, O), (B, O)	(O, O)
	A	A, O	B	B, O	A, B	B, O	A, B	O

7.3 Models for Genetic Improvement: Selection and Mutation

Description of models for genetic improvement involving selection and mutation is crucial in understanding evolutionary dynamics and population genetics. Here's an overview of these two fundamental processes:

Selection:

Selection is a key mechanism in evolutionary biology where certain heritable traits become more or less common in a population over generations. It occurs when individuals with advantageous traits have a higher chance of survival and reproduction, leading to the increase in frequency of those traits in the population.

Models for Selection:

1. **Hard Selection Model:** Also known as deterministic or directional selection, this model assumes that individuals with the highest fitness have the highest chance of survival and reproduction. It predicts a continuous increase or decrease in the frequency of advantageous or disadvantageous traits, respectively, until fixation or loss occurs.
2. **Soft Selection Model:** Soft selection considers variations in fitness within a population due to environmental heterogeneity. It accounts for differences in survival and reproduction rates among individuals with the same trait, leading to a more nuanced understanding of selection dynamics.
3. **Frequency-Dependent Selection:** In this model, the fitness of a trait depends on its frequency within the population. Traits that are rare may have a fitness advantage due to reduced competition or predator avoidance, leading to oscillations in trait frequencies over time.

Mutation:

Mutation is the ultimate source of genetic variation, providing raw material for evolutionary change. It involves changes in the DNA sequence of an organism, leading to new alleles and phenotypic diversity within populations.

Models for Mutation:

1. **Point Mutation Model:** Point mutations involve changes in single nucleotides within the DNA sequence. This model describes the substitution of one nucleotide for another (e.g., A to T), leading to the creation of new alleles and potentially altering the phenotype of individuals.
2. **Insertion-Deletion (Indel) Mutation Model:** Indel mutations involve the insertion or deletion of nucleotides within the DNA sequence. They can lead to frameshift mutations, causing significant changes in the amino acid sequence and protein function.
3. **Duplication Mutation Model:** Duplication mutations result in the duplication of genomic regions, leading to the creation of gene copies. These duplicated genes may undergo further divergence and specialization, contributing to genetic novelty and adaptation.

Interaction between Selection and Mutation:

Selection and mutation are intertwined processes that shape the genetic composition of populations over time. Selection acts on existing genetic variation, favoring alleles that confer higher fitness, while mutation introduces new variation into the population. The balance between these processes determines the rate and

direction of evolutionary change.

Models for genetic improvement involving selection and mutation provide valuable insights into the mechanisms driving evolutionary dynamics and population genetics. By understanding the interplay between selection and mutation, researchers can better predict how populations evolve and adapt to changing environments, leading to advancements in fields such as agriculture, medicine, and conservation biology.

7.3.1 Genetic Improvement through Cross Breeding

We have already discussed the results of crossing a breed successively with a dominant breed, a recessive breed, or a hybrid breed. We now consider the case when genes carrying undesirable characteristics are to be eliminated from a race and are to be replaced by genes with desirable characteristics. Thus let

$$g_1g_1, \quad g_2g_2, \quad g_3g_3, \quad \cdots \quad g_n g_n \quad (7.3.1)$$

denote n pairs of genes which we want to replace by the n pairs of genes

$$G_1G_1, \quad G_2G_2, \quad G_3G_3, \quad \cdots \quad G_n G_n. \quad (7.3.2)$$

We shall call the individual having gene pairs (7.3.2) as belonging to the G -race. We are not implying here that G 's are dominant and g 's are recessive. On crossing the given generation F_0 with the G -race, we get the first generation F_1 , namely,

$$G_1g_1, \quad G_2g_2, \quad G_3g_3, \quad \cdots \quad G_n g_n, \quad (7.3.3)$$

so that one g in each pair is replaced by the corresponding G . Our object is to replace the other g also by successive crossing with the G -race. Successive crosses give us the generations

$$F_2, \quad F_3, \quad \cdots \quad F_{m+1}, \quad \dots \quad (7.3.4)$$

In every generation, there is a probability $1/2$ that g_i has been replaced G_i , and there is a probability $1/2$ that g_i has not been replaced by G_i , and so the probability that $(m+1)$ -th generation still has g_i is $(1/2)^m$. Also, the probability that r of the n replacements of genes have not taken place is given by the binomial distribution, as

$$\binom{n}{r} \left(\frac{1}{2^m}\right)^r \left(1 - \frac{1}{2^m}\right)^{n-r}. \quad (7.3.5)$$

If $r = 0$, all the genes g_i have replaced by G_i , and the probability of this is

$$\binom{n}{0} \left(\frac{1}{2^m}\right)^0 \left(1 - \frac{1}{2^m}\right)^{n-0} = \left(1 - \frac{1}{2^m}\right)^n. \quad (7.3.6)$$

As m approaches infinity, the probability approaches unity, regardless of the value of n . Thus, ultimately all genes g_i will be replaced by genes G_i for $i = 1, 2, \dots, n$.

Solved Examples on Genetic Improvement through Cross Breeding

Example 1

A plant breeder is performing crossbreeding experiments to introduce a specific trait into a crop species. In each breeding experiment, there is a 30% chance that the desired gene replacement occurs. If the breeder conducts 10 independent crossbreeding experiments, what is the probability that exactly 2 of the gene replacements have not taken place?

Solution:

Let X be the number of gene replacements that have not taken place in 10 experiments. Since each experiment is independent and has a fixed probability of success (gene replacement), we can model this scenario using the binomial distribution.

Given:

$$\begin{aligned}n &= 10 \\p &= 0.30 \\r &= 2\end{aligned}$$

Using the probability mass function (PMF) of the binomial distribution:

$$P(X = r) = \binom{n}{r} \times p^r \times (1 - p)^{n-r}$$

Substituting the given values:

$$P(X = 2) = \binom{10}{2} \times (0.30)^2 \times (1 - 0.30)^{10-2}$$

Using the binomial coefficient $\binom{n}{r} = \frac{n!}{r!(n-r)!}$:

$$P(X = 2) = \frac{10!}{2!(10 - 2)!} \times (0.30)^2 \times (0.70)^8$$

$$P(X = 2) = \frac{10 \times 9}{2 \times 1} \times (0.30)^2 \times (0.70)^8$$

$$P(X = 2) = 45 \times 0.09 \times 0.05764801$$

$$P(X = 2) \approx 0.3089$$

So, the probability that exactly 2 of the gene replacements have not taken place is approximately 0.3089.

Example 2

A livestock breeder is conducting crossbreeding experiments to introduce a specific trait into a population of animals. In each experiment, there is a 20% chance that the desired gene replacement occurs. If the breeder conducts 15 independent crossbreeding experiments, what is the probability that at least 10 of the gene replacements have taken place?

Solution:

Similar to Example 1, we can model this scenario using the binomial distribution.

Given:

$$\begin{aligned}n &= 15 \\p &= 0.20 \\r &\geq 10\end{aligned}$$

We are interested in finding $P(X \geq 10)$.

Using the cumulative distribution function (CDF) of the binomial distribution:

$$P(X \geq 10) = 1 - \sum_{k=0}^9 P(X = k)$$

$$P(X \geq 10) = 1 - (P(X = 0) + P(X = 1) + P(X = 2) + \dots + P(X = 9))$$

We can calculate each term using the binomial distribution formula and subtract their sum from 1 to find $P(X \geq 10)$.

This method allows us to find the probability that at least 10 of the gene replacements have taken place in 15 experiments.

Some Solved Examples on the ABO Blood Group System and its Genetics

Important Formulas

Genotype Frequencies under Hardy-Weinberg Equilibrium:

$$\begin{aligned}\text{Genotype AA: } & p(A)^2 \\ \text{Genotype AB: } & 2 \times p(A) \times p(B) \\ \text{Genotype AO: } & 2 \times p(A) \times p(O) \\ \text{Genotype BB: } & p(B)^2 \\ \text{Genotype BO: } & 2 \times p(B) \times p(O) \\ \text{Genotype OO: } & p(O)^2\end{aligned}$$

Where:

- $p(A)$, $p(B)$, and $p(O)$ are the frequencies of the A, B, and O alleles, respectively.

Example 1:

Sarah's parents both have blood type O. What is the probability that Sarah has blood type O?

Solution:

Given that both parents have blood type O, they can only pass on the O allele to their offspring. Therefore, Sarah must inherit an O allele from each parent.

Since blood type O is determined by the genotype OO, Sarah's genotype must be OO. Thus, the probability that Sarah has blood type O is 100%.

Example 2:

John has blood type AB. What are the possible blood types of his parents?

Solution:

Blood type AB is only possible when an individual inherits one A allele from one parent and one B allele from the other parent. Therefore, one of John's parents must have blood type A (genotype AO) and the other parent must have blood type B (genotype BO).

Example 3:

A couple has two children, one with blood type A and the other with blood type O. What are the possible blood types of the parents?

Solution:

Since the children have blood types A and O, we can deduce the genotypes of the parents based on the inheritance patterns:

1. Child with blood type A: - Genotype: AA or AO 2. Child with blood type O: - Genotype: OO

From the genotype possibilities of the children, we can conclude that both parents must carry at least one O allele. Therefore, both parents must have blood type O (genotype OO).

Example 4:

In a population, the frequencies of the A, B, and O alleles are 0.4, 0.3, and 0.3, respectively. What are the expected genotype frequencies in the population?

Solution:

Given: - Frequency of allele A ($p(A)$) = 0.4 - Frequency of allele B ($p(B)$) = 0.3 - Frequency of allele O ($p(O)$) = 0.3

Using Hardy-Weinberg equilibrium, we can calculate the expected genotype frequencies:

- i. Genotype AA: $p(A)^2 = 0.4^2 = 0.16$,
- ii. Genotype AB: $2 \times p(A) \times p(B) = 2 \times 0.4 \times 0.3 = 0.24$,
- iii. Genotype AO: $2 \times p(A) \times p(O) = 2 \times 0.4 \times 0.3 = 0.24$,
- iv. Genotype BB: $p(B)^2 = 0.3^2 = 0.09$,
- v. Genotype BO: $2 \times p(B) \times p(O) = 2 \times 0.3 \times 0.3 = 0.18$,
- vi. Genotype OO: $p(O)^2 = 0.3^2 = 0.09$.

These genotype frequencies represent the expected distribution of ABO blood types in the population under Hardy-Weinberg equilibrium.

Example 5

In a population, the frequencies of the A, B, and O alleles are 0.4, 0.3, and 0.3, respectively. Calculate the expected genotype frequencies under Hardy-Weinberg equilibrium.

Solution:

Using the formulas for genotype frequencies under Hardy-Weinberg equilibrium:

$$p(A) = 0.4, \quad p(B) = 0.3, \quad p(O) = 0.3$$

Substitute these values into the formulas to find the expected genotype frequencies.

Example 6

A couple with blood types AB and O have a child with blood type B. What are the possible blood types of their other children?

Solution:

Since the parents have blood types AB and O, we can determine the possible genotypes and blood types of their children based on Mendelian inheritance patterns.

Example 7

In a population, 16% of individuals have blood type AB. What are the frequencies of the A and B alleles in the population?

Solution:

Given that the frequency of blood type AB is 16%, we can use this information to determine the frequencies of the A and B alleles in the population.

Example 8

A population has the following genotype frequencies: AA (25%), AO (50%), and OO (25%). Calculate the frequencies of the A and O alleles.

Solution:

Given the genotype frequencies, we can use them to calculate the frequencies of the A and O alleles using the Hardy-Weinberg equilibrium.

Solved Examples on Phenotype ratios

Example 1

Consider a cross between two heterozygous parents (Aa) for a trait where A is dominant over a. What are the expected genotype and phenotype ratios in their offspring?

Solution:

Given:

- Genotype of parent 1: Aa
- Genotype of parent 2: Aa

Using the Punnett square, we can determine the genotype ratios:

	A	a
A	AA	Aa
a	Aa	aa

From the Punnett square, we see that the genotype ratio is 25% AA, 50% Aa, and 25% aa.

For the phenotype ratio, 75% display the dominant trait (A), and 25% display the recessive trait (a).

Example 2

In a population, 40% of individuals have the homozygous dominant genotype (AA), and 30% have the heterozygous genotype (Aa) for a certain trait. What are the expected phenotype ratios in the population?

Solution:

Given:

- Frequency of genotype AA: $P(AA) = 0.40$
- Frequency of genotype Aa: $P(Aa) = 0.30$

Using the information provided, we can calculate the phenotype ratios:

- Dominant phenotype ratio = $P(AA) + P(Aa)$
- Recessive phenotype ratio = Frequency of genotype aa

Substitute the given values to find the phenotype ratios.

Example 3

In a genetic experiment, a cross between two parents (AA and aa) results in all offspring having the Aa genotype. What are the expected genotype and phenotype ratios in the offspring?

Solution:

Given:

- Genotype of parent 1: AA
- Genotype of parent 2: aa

Since all offspring have the Aa genotype, the genotype ratio is 100% Aa .
For the phenotype ratio, 100% display the dominant trait (A).

Unit 8

Course Structure

- Genetic Improvement through Elimination Recessives
 - Selection and Mutation
 - An Alternative Discussion of Selection
-

8.1 Genetic Improvement through Elimination Recessives

Genetic improvement strategies aim to enhance desirable traits in populations over successive generations. One approach involves eliminating undesirable recessive alleles from the gene pool through selective breeding. This strategy can lead to the improvement of specific traits and overall genetic fitness within a population.

Understanding Recessive Alleles

In genetics, recessive alleles are variants of genes that are masked by dominant alleles in heterozygous individuals. Recessive alleles only manifest their effects when present in a homozygous state. Undesirable traits associated with recessive alleles may include susceptibility to diseases, malformations, or other undesirable characteristics.

Selective Breeding for Recessive Elimination

Selective breeding aims to increase the frequency of desirable alleles while decreasing the frequency of undesirable alleles in a population. The elimination of recessive alleles involves identifying carriers of the recessive allele through genetic testing or phenotypic screening and avoiding mating between carriers. By preventing the transmission of recessive alleles to offspring, their frequency in the population decreases over time.

Examples of Recessive Elimination

1. **Cystic Fibrosis:** Cystic fibrosis is a genetic disorder caused by mutations in the CFTR gene. The condition is inherited in an autosomal recessive manner. Selective breeding strategies aim to reduce the frequency of the mutated CFTR allele in populations to decrease the incidence of cystic fibrosis.

2. **Hemophilia:** Hemophilia is a genetic disorder characterized by impaired blood clotting due to deficiencies in clotting factors. The disorder is caused by mutations in genes encoding clotting factors VIII or IX and is inherited in an X-linked recessive manner. Selective breeding can help reduce the frequency of the mutated alleles in populations to decrease the incidence of hemophilia.

Challenges and Considerations

While genetic improvement through the elimination of recessives can be effective, several challenges and considerations should be taken into account:

- **Genetic Diversity:** Selective breeding may reduce genetic diversity within a population, increasing the risk of inbreeding depression and susceptibility to new diseases or environmental changes.
- **Complex Traits:** Some traits influenced by multiple genes or environmental factors may be challenging to improve through recessive elimination alone.
- **Ethical Considerations:** Ethical concerns may arise regarding the selection of individuals for breeding and the potential impact on biodiversity and ecosystem dynamics.

Genetic improvement through the elimination of recessive alleles is a valuable strategy for enhancing desirable traits and genetic fitness within populations. However, careful consideration of genetic diversity, trait complexity, and ethical implications is essential to ensure the sustainability and welfare of populations undergoing selective breeding.

Another method of improving genetic composition in plants and animals is repeated elimination of recessives in each generation (e.g., by destroying recessive plants or by not allowing recessive animals to breed) and allowing random mating within the remaining members of the population.

In the n -th generation, if the proportions of dominants, hybrids, and recessives are p_n , q_n and r_n , then, in the $(n + 1)$ -th generation, these proportions are

$$p_{n+1} = \left(p_n + \frac{1}{2}q_n\right)^2, \quad q_{n+1} = 2\left(p_n + \frac{1}{2}q_n\right)\left(r_n + \frac{1}{2}q_n\right), \quad r_{n+1} = \left(r_n + \frac{1}{2}q_n\right)^2. \quad (8.1.1)$$

In the n -th generation, if recessives are eliminated, then the new proportions in the $(n + 1)$ -th generation are given by

$$p_{n+1} = \left(p'_n + \frac{1}{2}q'_n\right)^2, \quad q_{n+1} = 2\left(p'_n + \frac{1}{2}q'_n\right)\left(\frac{1}{2}q'_n\right), \quad r_{n+1} = \left(\frac{1}{2}q'_n\right)^2. \quad (8.1.2)$$

where p'_n, q'_n are the new proportions in the n -th generation after elimination of the recessives so that

$$\frac{p'_n}{q'_n} = \frac{p_n}{q_n}, \quad p'_n + q'_n = 1. \quad (8.1.3)$$

From (8.1.2) and (8.1.3),

$$p_{n+1} = \left(1 - \frac{1}{2}q'_n\right)^2, \quad q_{n+1} = q'_n\left(1 - \frac{1}{2}q'_n\right), \quad r_{n+1} = \left(\frac{1}{2}q'_n\right)^2. \quad (8.1.4)$$

After eliminating the recessives from the population, we get

$$\begin{aligned} \frac{p'_{n+1}}{1 - \frac{1}{2}q'_n} &= \frac{q'_{n+1}}{q'_n} = \frac{1}{1 + \frac{1}{2}q'_n} \\ \Rightarrow q'_{n+1} &= \frac{q'_n}{1 + \frac{1}{2}q'_n} \end{aligned} \quad (8.1.5)$$

This is a difference equation for solving for q'_n . Substituting

$$u_n = \frac{1}{q_n} \quad (8.1.6)$$

in (8.1.5), we get

$$u_{n+1} = u_n + \frac{1}{2} \quad (8.1.7)$$

whose solution is

$$u_n = A + \frac{1}{2}n \quad (8.1.8)$$

so that

$$q'_n = \frac{1}{A + \frac{1}{2}n}. \quad (8.1.9)$$

To determine A , we make use of $p = (1 - \sqrt{r})^2$, $q = 2\sqrt{r}(1 - \sqrt{r})$, $r = r$, to get

$$q'_1 = \frac{1}{p + q} = \frac{2\sqrt{r}}{1 + \sqrt{r}} \quad (8.1.10)$$

so that

$$A = \frac{1}{2\sqrt{r}}. \quad (8.1.11)$$

Also,

$$q'_n = \frac{2\sqrt{r}}{1 + n\sqrt{r}}, \quad (8.1.12)$$

$$r'_{n+1} = \left(\frac{1}{2}q'_n\right)^2 = \frac{r}{(1 + n\sqrt{r})^2}. \quad (8.1.13)$$

This gives the proportion of recessives in the $(n + 1)$ -th generation. Given the proportion of recessives in the original stable population, we can find, by using (8.1.13), the number of generation in which we can reduce the proportion of recessives below any given limit by elimination of recessives at all stages. We can also find that $p_n \rightarrow 1$, $q_n \rightarrow 0$, $r_n \rightarrow 0$ as $n \rightarrow \infty$.

Instead of eliminating all the recessives, we may keep a fraction k of the recessives. The basic equations in this case are

$$p'_n = \frac{1 - kr_n}{1 - r_n} p_n, \quad q'_n = \frac{1 - kr_n}{1 - r_n} q_n, \quad r'_n = kr_n, \quad (8.1.14)$$

$$p'_n + q'_n + r'_n = 1, \quad (8.1.15)$$

$$p_{n+1} \left(p'_n + \frac{1}{2}q'_n\right)^2 = \left(\frac{1 - kr_n}{1 - r_n}\right)^2 \left(p_n + \frac{1}{2}q_n\right)^2, \quad (8.1.16)$$

$$q_{n+1} = 2 \left(p'_n + \frac{1}{2}q'_n\right) \left(r'_n + \frac{1}{2}q'_n\right) = 2 \left(\frac{1 - kr_n}{1 - r_n}\right) \left(p_n + \frac{1}{2}q_n\right) \left(kr_n + \frac{1}{2} \frac{1 - kr_n}{1 - r_n} q_n\right) \quad (8.1.17)$$

$$r_{n+1} = \left(r'_n + \frac{1}{2}q'_n\right)^2 = \left(kr_n + \frac{1}{2} \frac{1 - kr_n}{1 - r_n} q_n\right)^2, \quad (8.1.18)$$

$$p'_{n+1} = \frac{1 - kr_{n+1}}{1 - r_{n+1}} p_{n+1} = \frac{1 - kr_{n+1}}{1 - r_{n+1}} \left(p'_n + \frac{1}{2}q'_n\right)^2, \quad (8.1.19)$$

$$q'_{n+1} = \frac{1 - kr_{n+1}}{1 - r_{n+1}} q_{n+1} = 2 \frac{1 - kr_{n+1}}{1 - r_{n+1}} \left(p'_n + \frac{1}{2}q'_n\right) \left(r'_n + \frac{1}{2}q'_n\right) \quad (8.1.20)$$

$$r'_{n+1} = kr_{n+1} = k \left(r'_n + \frac{1}{2}q'_n\right). \quad (8.1.21)$$

From (8.1.16)-(8.1.18), we get two simultaneous nonlinear difference equations of the first order for determining p_n and q_n and from (8.1.19)-(8.1.21), we obtain two nonlinear simultaneous difference equations to determine p'_n and q'_n . However, the equations are complicated, and closed-form solutions cannot be easily determined.

8.2 Selection and Mutation

Let the proportions of genes G and g in the n -th generation be P_n and Q_n so that in the $(n + 1)$ -th generation, the proportions of GG , Gg , and gg are P_n^2 , $2P_nQ_n$, and Q_n^2 . Suppose the probabilities of survival of these are $S(1 - K)$, S and $S(1 - k)$, respectively, where $|k|$ and $|K|$ are less than unity. Then the relative proportions in the $(n + 1)$ -th generation are

$$S(1 - K)P_n^2, \quad 2SP_nQ_n, \quad S(1 - k)Q_n^2 \quad (8.2.1)$$

so that the relative proportions of G and g in this generation are

$$2S(1 - K)P_n^2 + 2SP_nQ_n, \quad 2SP_nQ_n + 2S(1 - k)Q_n^2 \quad (8.2.2)$$

and hence

$$\frac{P_{n+1}}{Q_{n+1}} = \frac{(1 - K)(P_n^2/Q_n^2) + (P_n/Q_n)}{(P_n/Q_n) + (1 - k)} \quad (8.2.3)$$

$$\Rightarrow u_{n+1} = \frac{(1 - K)u_n^2 + u_n}{u_n + (1 - k)}, \quad \text{where } u_n = \frac{P_n}{Q_n}. \quad (8.2.4)$$

This is a nonlinear difference equation of the first order. Knowing u_1 , we can find, step by step, u_n . The equilibrium solution is obtained by putting $u_n = u_{n+1} = u$ which gives

$$\begin{aligned} u &= \frac{(1 - K)u^2 + u}{u + 1 - k} \\ \Rightarrow u(uK - k) &= 0 \end{aligned} \quad (8.2.5)$$

so that $u = 0$, or $u = k/K$, $1/u = 0$ i.e. either dominants or recessives survive. However, a non-trivial equilibrium solution is

$$u = k/K. \quad (8.2.6)$$

Since this equilibrium solution has to be positive, both k and K have to be either positive or negative, i.e., either the heterozygotes have to be the fittest or they have to be the least fit. If $K = k$, the equilibrium of G and g are the same.

To discuss the stability of the equilibrium solution of (8.2.5), we note that (8.2.4) give

$$u_{n+1} - u_n = \frac{Ku_n}{u_n + 1 - k} \left(\frac{k}{K} - u_n \right) \quad (8.2.7)$$

or

$$\frac{u_{n+1} - u_n}{k/K - u_n} = \frac{Ku_n}{u_n + 1 - k} \quad (8.2.8)$$

and

$$\frac{u_{n+1} - k/K}{u_n - k/K} = \frac{u_n(1 - K) + (1 - k)}{u_n + 1 - k} \quad (8.2.9)$$

From (8.2.9), we deduce the following results:

- (i) If $0 < k < K < 1$ when $u_n > k/K$, we find that $u_{n+1} < u_n$ and $u_{n+1} > k/K$, i.e., u_{n+1} is nearer to k/K than u_n , and the sequence $\{u_n\}$ monotonically decreases to k/K . On the other hand, if $u_n < k/K$, then $u_{n+1} > u_n$ and $u_{n+1} < k/K$ so that the sequence $\{u_n\}$ monotonically increases to k/K . In the first case, we get a monotonically decreasing sequence bounded below; in the second case, we get a monotonically increasing sequence bounded above. In either case, we find that, if $0 < k < K < 1$, then the equilibrium solution is stable.
- (ii) If k and K are both negative and $k/K < 1$, then (8.2.8) and (8.2.9) show that $u_{n+1} - u_n$, $u_n - k/K$, and $u_{n+1} - k/K$ have the same sign so that, if $u_n > k/K$, then $u_{n+1} > k/K$ and $u_{n+1} > k/K$ and $u_{n+1} > u_n$, and hence u_{n+1} is farther from k/K than u_n . Similarly, if $u_n < k/K$, then $u_{n+1} < k/K$ and $u_{n+1} < u_n$ so that here too u_{n+1} is farther from k/K than u_n . Thus, when k and K are both negative, the equilibrium solution is unstable.

Thus, when the hybrids are the fittest, we get a stable equilibrium; when these are the least fit, we obtain an unstable equilibrium. Now (8.2.8) can be written as

$$\frac{u_{n+1} - u_n}{(n+1) - 1} = \frac{Ku_n}{u_n + 1 - k} \left(\frac{k}{K} - u_n \right). \quad (8.2.10)$$

When the change in one generation is not substantially different from the changes in the preceding or succeeding generations (e.g., when K is very small or when there are small oscillations about the equilibrium position), we can replace (8.2.10) by the differential equation

$$\frac{du}{dn} = \frac{Ku}{u + 1 - k} \left(\frac{k}{K} - u \right) \quad (8.2.11)$$

which gives, on integration,

$$\left(\frac{1}{k} - 1 \right) \ln u + \left(\frac{1}{K} + \frac{1}{k} - 1 \right) \ln \left| \frac{k}{K} - u \right| = n + \text{constant}. \quad (8.2.12)$$

From this we can discuss the variation of u from generation to generation.

Similarly, we can discuss the *balance between selection and mutation*. Let the probabilities of survival of D , H , R be $S(1 - K)$, $S(1 - K)$, and S , respectively, and let μ be the probability of a mutation from g to G in one generation. Then we get

$$\begin{aligned} \frac{P_{n+1}}{Q_{n+1}} &= \frac{2S(1 - K)P_n + 2S(1 - K)P_nQ_n + \mu[2S(1 - K)P_nQ_n + 2SQ_n^2]}{[2S(1 - K)P_nQ_n + 2SQ_n^2](1 - \mu)} \\ &= \frac{\left(\frac{P_n}{Q_n} + 1 \right) (1 - K) \frac{P_n}{Q_n} + \mu \left(\frac{P_n}{Q_n} + 1 - K \frac{P_n}{Q_n} \right)}{\left(\frac{P_n}{Q_n} - 1 - K \frac{P_n}{Q_n} \right) (1 - \mu)} \end{aligned} \quad (8.2.13)$$

so that

$$u_{n+1} = \frac{(u_n + 1)(1 - K)u_n + \mu(u_n + 1 - Ku_n)}{(u_n + 1 - Ku_n)(1 - \mu)}. \quad (8.2.14)$$

If we assume that u_n is very small (which is justified since mutation rates are small, i.e., of the order of 10^{-5} or less), then genes with lower fitness level can be maintained only at very low frequency by mutation. Equation (8.2.14) can now be written as

$$u_{n+1} = u_n(1 - K) + \mu, \quad (8.2.15)$$

In equilibrium, this gives

$$u = \mu/K. \quad (8.2.16)$$

8.3 An Alternative Discussion of Selection

In §8.2, we have discussed the problem of selection in terms of the ratio $\frac{P_n}{Q_n}$. We can also discuss the same problem in terms of P_n alone. If $\sigma_1, \sigma_2, \sigma_3$ denote the proportions of D, H, R which survive from birth to reproduction, we get

$$P_{n+1} = \frac{\sigma_1 P_n^2 + \sigma_2 P_n Q_n}{\sigma_1 P_n^2 + 2\sigma_2 P_n Q_n + \sigma_3 Q_n^2} = f(P_n). \quad (8.3.1)$$

If $n \rightarrow \infty$, then $P_n \rightarrow P$, $P_{n+1} \rightarrow P$, and $Q_n \rightarrow 1 - P$, so that

$$\sigma_1 P^3 + 2\sigma_2 P^2(1 - P) + \sigma_3(1 - P)^2 P - \sigma_1 P^2 - \sigma_2 P(1 - P) = 0 \quad (8.3.2)$$

which gives the three equilibrium solutions

$$P = 0, \quad P = 1, \quad P_e = \frac{\sigma_2 - \sigma_3}{2\sigma_2 - \sigma_1 - \sigma_3}. \quad (8.3.3)$$

The third solution exists if $0 < P_e < 1$, and is of special significance, because, in this case, all the three forms, namely, D, H, R survive. We can now write Eq.(8.3.1) as

$$\left(P_{n+1} - \frac{\sigma_2 - \sigma_3}{2\sigma_2 - \sigma_1 - \sigma_3} \right) = \frac{\sigma_1 P_n + \sigma_3 Q_n}{\sigma_1 P_n^2 + 2\sigma_2 P_n Q_n + \sigma_3 Q_n^2} \left[P_n - \frac{\sigma_2 - \sigma_3}{2\sigma_2 - \sigma_1 - \sigma_3} \right]. \quad (8.3.4)$$

This also shows that, if $P_n \rightarrow P_e$, then P_{n+1} also approaches P_e . Now

$$\begin{aligned} \frac{\sigma_1 P_n + \sigma_3 Q_n}{\sigma_1 P_n^2 + 2\sigma_2 P_n Q_n + \sigma_3 Q_n^2} &= \frac{\sigma_1 P_n + \sigma_3 Q_n}{(\sigma_1 P_n + \sigma_3 Q_n)(P_n + Q_n) + (2\sigma_2 - \sigma_1 - \sigma_3)P_n Q_n} \\ &= \frac{1}{1 + \frac{2\sigma_2 - \sigma_1 - \sigma_3}{\sigma_1 P_n + \sigma_3 Q_n} P_n Q_n} \end{aligned} \quad (8.3.5)$$

From (8.3.4) and (8.3.5), we deduce the following results:

- (i) If $\sigma_2 > \sigma_1, \sigma_3$, then the first factor on the right-hand side of (8.3.4) is less than unity and

$$|P_{n+1} - P_e| < |P_n - P_e| \quad (8.3.6)$$

so that $P_n \rightarrow P_e$ as $n \rightarrow \infty$, regardless of the initial value P_0 . Therefore, the equilibrium point is stable (see Fig. 1).

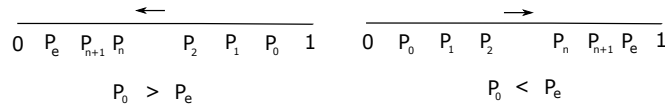


Fig. 1: $\sigma_2 > \sigma_1, \sigma_3$: Stable equilibrium

- (ii) If $\sigma_2 < \sigma_1, \sigma_3$, then the first factor on the right-hand side of (8.3.4) is greater than unity and

$$|P_{n+1} - P_e| > |P_n - P_e|. \quad (8.3.7)$$

Hence the equilibrium is unstable. If $P_0 < P_e$, then $P_n \rightarrow 0$, and if $P_0 > P_e$, then $P_n \rightarrow 1$ (see Fig. 2).

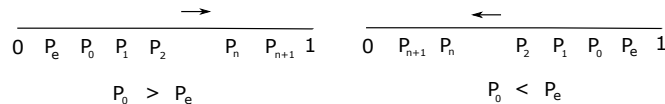


Fig. 2: $\sigma_2 < \sigma_1, \sigma_3$: Unstable equilibrium

These results are the same as those of §8.2 and show that the equilibrium is stable if the heterozygotes have the greatest chance of survival and is unstable if the heterozygotes have the least chance of survival.

For the stability of the equilibrium, it is necessary that

$$\begin{aligned} 2\sigma_2 - \sigma_1 - \sigma_3 > 0, & \quad \frac{\sigma_2 - \sigma_3}{2\sigma_2 - \sigma_1 - \sigma_3} > 0, & \quad \sigma_2 - \sigma_3 > 0, \\ \frac{\sigma_2 - \sigma_3}{2\sigma_2 - \sigma_1 - \sigma_3} < 1, & \quad \sigma_2 - \sigma_3 < 2\sigma_2 - \sigma_1 - \sigma_3, & \quad \sigma_2 - \sigma_1 > 0. \end{aligned} \quad (8.3.8)$$

Thus, for P_e to represent an equilibrium solution, it is both necessary and sufficient that $\sigma_2 > \sigma_1, \sigma_3$.

The convergence of a sequence $\{P_n\}$ to a limit P_e is said to be *geometric* at the rate c for $0 < |c| < 1$, $0 < a < |c|$ if

$$\lim_{n \rightarrow \infty} \frac{|P_n - P_e|}{c^n} < \infty, \quad \lim_{n \rightarrow \infty} \frac{|P_n - P_e|}{a^n} = \infty. \quad (8.3.9)$$

The convergence is said to be *algebraic* if

$$\lim_{n \rightarrow \infty} n^k |P_n - P_e| = \text{a positive constant}. \quad (8.3.10)$$

Using (8.3.9) and (8.3.10), we find that, when $\sigma_2 > \sigma_1, \sigma_3$, the convergence is geometric at the rate

$$1 / \left[1 + \frac{2\sigma_2 - \sigma_1 - \sigma_3}{\sigma_1 P_e + \sigma_3 Q_e} P_e Q_e \right] = \frac{\sigma_2(\sigma_1 + \sigma_3) - 2\sigma_1\sigma_3}{\sigma_2^2 - \sigma_1\sigma_3}. \quad (8.3.11)$$

Unit 9

Course Structure

- Navier-Stokes Equations
 - Hagen-Poiseuille Flow
 - Inlet Length Flow
 - Reynolds Number Flow
 - Non-Newtonian Fluids
-

9.1 Introduction

In large and medium sized arteries, those more typically affected by vascular diseases, blood can be modelled by means of the Navier-Stokes (NS) equation for incompressible homogeneous Newtonian fluids. Non-Newtonian rheological models are necessary for describing some specific flow processes, such as clotting or sickle cell diseases, or more generally flow in capillaries. Let us recall some preliminary concepts of fluid dynamics.

9.2 Navier-Stokes Equations for the Flow of a Viscous Incompressible Fluid

Let $u(x, y, z, t)$, $v(x, y, z, t)$, $w(x, y, z, t)$, and $p(x, y, z, t)$ denote respectively the three velocity components and pressure at the point (x, y, z) at time t in a fluid with constant density ρ and viscosity coefficient μ . Then the *equation of continuity*, which expresses the fact that the amount of fluid entering a unit volume per unit time is the same as the amount of the fluid leaving it per unit time, is given by

$$\frac{\partial u}{\partial x} + \frac{\partial v}{\partial y} + \frac{\partial w}{\partial z} = 0. \quad (9.2.1)$$

The *equations of motion* are obtained from Newton's second law of motion which states that the product of mass and acceleration of any fluid element is equal to the resultant of all the external body forces acting on the element and to the surface forces acting on the fluid volume due to the action of the remaining fluid on

the element. The equations of motion, known as *Navier-Stokes* equations, for the flow of a Newtonian viscous incompressible fluid are

$$\rho \left(\frac{\partial u}{\partial t} + u \frac{\partial u}{\partial x} + v \frac{\partial u}{\partial y} + w \frac{\partial u}{\partial z} \right) = X - \frac{\partial p}{\partial x} + \mu \left(\frac{\partial^2 u}{\partial x^2} + \frac{\partial^2 u}{\partial y^2} + \frac{\partial^2 u}{\partial z^2} \right) \quad (9.2.2)$$

$$\rho \left(\frac{\partial v}{\partial t} + u \frac{\partial v}{\partial x} + v \frac{\partial v}{\partial y} + w \frac{\partial v}{\partial z} \right) = Y - \frac{\partial p}{\partial y} + \mu \left(\frac{\partial^2 v}{\partial x^2} + \frac{\partial^2 v}{\partial y^2} + \frac{\partial^2 v}{\partial z^2} \right) \quad (9.2.3)$$

$$\rho \left(\frac{\partial w}{\partial t} + u \frac{\partial w}{\partial x} + v \frac{\partial w}{\partial y} + w \frac{\partial w}{\partial z} \right) = Z - \frac{\partial p}{\partial z} + \mu \left(\frac{\partial^2 w}{\partial x^2} + \frac{\partial^2 w}{\partial y^2} + \frac{\partial^2 w}{\partial z^2} \right) \quad (9.2.4)$$

If the external body forces X , Y , Z form a conservative system, there exists a potential function Ω such that

$$\begin{aligned} X &= -\frac{\partial \Omega}{\partial x}, & Y &= -\frac{\partial \Omega}{\partial y}, & Z &= -\frac{\partial \Omega}{\partial z} \\ X - \frac{\partial p}{\partial x} &= -\frac{\partial}{\partial x}(\Omega + p), & Y - \frac{\partial p}{\partial y} &= -\frac{\partial}{\partial y}(\Omega + p), & Z - \frac{\partial p}{\partial z} &= -\frac{\partial}{\partial z}(\Omega + p) \end{aligned} \quad (9.2.5)$$

so that p is effectively replaced by $p + \Omega$.

If X , Y , Z are known or are absent, (9.2.1)-(9.2.4) give a system of four coupled nonlinear partial differential equations for the four unknown functions u , v , w , and p . These equations have to be solved subject to certain *initial conditions* giving the motion of the fluid at time $t = 0$ and certain prescribed *boundary conditions* on the surfaces with which the fluid may be in contact or conditions which may hold at very large distances from the surfaces. Usually, the boundary conditions are provided by the *no-slip condition* according to which both tangential and normal components of the fluid velocity vanish at all points of the surfaces of the stationary bodies with which the fluid may be in contact. However, if a body is moving, then the tangential and normal components of the fluid velocity at any point of contact are the same as those of the moving body at that point.

We can simplify the basic equations (9.2.2)-(9.2.4) when

- (i) there are *no external body forces*, i.e., when $X = 0$, $Y = 0$, $Z = 0$, or when the external forces form a conservative system
- (ii) the motion is *steady*, i.e., when there is no variation with respect to time so that u , v , w , and p are functions of x , y , z only and $\frac{\partial u}{\partial t}$, $\frac{\partial v}{\partial t}$, $\frac{\partial w}{\partial t}$ and $\frac{\partial p}{\partial t}$ are all zero.
- (iii) the motion is *two dimensional*, i.e., when it is the same in all places parallel to $z = 0$ plane and, in particular, when $w = 0$ and when there is no variation with respect to z . In this case, the three equations we get for the three unknowns, namely, $u(x, y, t)$, $v(x, y, t)$ and $p(x, y, t)$, are

$$\frac{\partial u}{\partial x} + \frac{\partial v}{\partial y} = 0, \quad (9.2.6)$$

$$\rho \left(\frac{\partial u}{\partial t} + u \frac{\partial u}{\partial x} + v \frac{\partial u}{\partial y} \right) = -\frac{\partial p}{\partial x} + \mu \left(\frac{\partial^2 u}{\partial x^2} + \frac{\partial^2 u}{\partial y^2} \right), \quad (9.2.7)$$

$$\rho \left(\frac{\partial v}{\partial t} + u \frac{\partial v}{\partial x} + v \frac{\partial v}{\partial y} \right) = -\frac{\partial p}{\partial y} + \mu \left(\frac{\partial^2 v}{\partial x^2} + \frac{\partial^2 v}{\partial y^2} \right). \quad (9.2.8)$$

Equation (9.2.6) can be satisfied by introducing the *stream function* $\psi(x, y)$ which is such that

$$u = \frac{\partial \psi}{\partial y}, \quad v = -\frac{\partial \psi}{\partial x}. \quad (9.2.9)$$

Substituting in (9.2.7) and (9.2.8) and eliminating p between them, we get

$$\frac{\partial}{\partial t} \nabla^2 \psi + \frac{\partial \psi}{\partial y} \frac{\partial}{\partial x} \nabla^2 \psi - \frac{\partial \psi}{\partial x} \nabla^2 \psi + \nu \nabla^4 \psi, \quad (9.2.10)$$

where $\nu = \mu/\rho$ is the kinematic viscosity and ∇^2 is the Laplacian operator defined by

$$\nabla^2 \equiv \frac{\partial^2}{\partial x^2} + \frac{\partial^2}{\partial y^2}, \quad \nabla^4 \equiv \nabla^2(\nabla^2). \quad (9.2.11)$$

The *vorticity* of this two dimensional flow is defined by

$$\omega = \frac{1}{2} \left(\frac{\partial v}{\partial x} - \frac{\partial u}{\partial y} \right) = -\frac{1}{2} \nabla^2 \psi. \quad (9.2.12)$$

From (9.2.10) and (9.2.12), we get

$$\frac{\partial \omega}{\partial t} + \frac{\partial \psi}{\partial y} \frac{\partial \omega}{\partial x} - \frac{\partial \psi}{\partial x} \frac{\partial \omega}{\partial y} = \frac{\partial \omega}{\partial t} + \frac{\partial(\omega, \psi)}{\partial(x, y)} = \nu \nabla^4 \psi. \quad (9.2.13)$$

- (iv) The basic equations (9.2.2)-(9.2.4) can also be simplified when the motion is axially symmetric, i.e., when it is symmetrical about an axis. Here we use the cylindrical polar coordinate (r, θ, z) , where the axis of symmetry is taken as the axis of z . There are, in general, three components of velocity, namely, v_r along the radius vector perpendicular to the axis, v_θ perpendicular to the axis and the radius vector, and v_z parallel to the axis of z . For the axi-symmetric case, we take $v_\theta = 0$, and we also take v_r, v_z and p to be independent of θ . In this case, the equation of continuity and the equations of motion are given by

$$\frac{1}{r} \frac{\partial}{\partial r} (r v_r) + \frac{\partial}{\partial z} v_z = 0, \quad (9.2.14)$$

$$\rho \left(\frac{\partial v_r}{\partial t} + v_r \frac{\partial v_r}{\partial r} + v_z \frac{\partial v_r}{\partial z} \right) = -\frac{\partial p}{\partial r} + \mu \left(\frac{\partial^2 v_r}{\partial r^2} + \frac{\partial^2 v_r}{\partial z^2} + \frac{1}{r} \frac{\partial v_r}{\partial r} - \frac{v_r}{r^2} \right), \quad (9.2.15)$$

$$\rho \left(\frac{\partial v_z}{\partial t} + v_r \frac{\partial v_z}{\partial r} + v_z \frac{\partial v_z}{\partial z} \right) = -\frac{\partial p}{\partial z} + \mu \left(\frac{\partial^2 v_z}{\partial r^2} + \frac{\partial^2 v_z}{\partial z^2} + \frac{1}{r} \frac{\partial v_r}{\partial r} \right). \quad (9.2.16)$$

We can satisfy (9.2.14) by introducing the stream function ψ defined by

$$\frac{1}{r} \frac{\partial \psi}{\partial r} = v_z, \quad \frac{1}{r} \frac{\partial \psi}{\partial z} = -v_r \quad (9.2.17)$$

Substituting (9.2.17) in (9.2.15) and (9.2.16) and eliminating p , we get the fourth-order partial differential equation for ψ , as

$$\frac{\partial}{\partial t} (D^2 \psi) - \frac{1}{r} \frac{\partial(\psi, D^2 \psi)}{\partial(r, z)} - \frac{2}{r^2} \frac{\partial \psi}{\partial z} D^2 \psi = \nu D^4 \psi, \quad (9.2.18)$$

where

$$D^2 \equiv \frac{\partial^2}{\partial r^2} - \frac{1}{r} \frac{\partial}{\partial r} + \frac{\partial^2}{\partial z^2}, \quad D^2 \psi = D^2(D^2 \psi). \quad (9.2.19)$$

After solving for ψ , we can obtain pressure p and vorticity ω by using the equation

$$\frac{\partial^2 p}{\partial r^2} + \frac{\partial^2 p}{\partial z^2} + \frac{1}{r} \frac{\partial p}{\partial r} = \frac{2}{r} \left[\frac{\partial^2 \psi}{\partial z^2} \left(\frac{\partial^2 \psi}{\partial r^2} - \frac{1}{r} \frac{\partial \psi}{\partial r} \right) - \left(\frac{\partial \psi}{\partial z} \right)^2 + \frac{\partial^2 \psi}{\partial z \partial r} \left(\frac{1}{r} \frac{\partial \psi}{\partial r} - \frac{\partial^2 \psi}{\partial z^2} \right) \right] \quad (9.2.20)$$

$$\omega = -D^2 \psi = -\frac{1}{r^2} \left(\frac{\partial^2 \psi}{\partial z^2} - \frac{1}{r} \frac{\partial \psi}{\partial r} + \frac{\partial^2 \psi}{\partial z^2} \right). \quad (9.2.21)$$

Solved Problems on Flow of a Viscous Incompressible Fluid

Problem 1 Consider the steady, laminar flow of an incompressible fluid between two parallel plates separated by a distance h . The top plate is stationary, while the bottom plate moves with a constant velocity U . Neglecting gravitational effects, derive the simplified Navier-Stokes equations governing the flow and determine the velocity profile and shear stress distribution.

Solution

We consider two-dimensional flow in the x -direction only. The simplified Navier-Stokes equations governing the flow are:

$$\frac{\partial u}{\partial x} + \frac{\partial v}{\partial y} = 0 \quad (\text{Continuity equation})$$

$$\rho u \frac{\partial u}{\partial x} + \rho v \frac{\partial u}{\partial y} = -\frac{\partial p}{\partial x} + \mu \left(\frac{\partial^2 u}{\partial x^2} + \frac{\partial^2 u}{\partial y^2} \right) \quad (\text{Momentum equation})$$

where:

- $u(x, y)$ is the velocity component in the x -direction.
- $v(x, y)$ is the velocity component in the y -direction (zero in this case).
- $p(x, y)$ is the pressure.
- ρ is the fluid density.
- μ is the dynamic viscosity of the fluid.

The boundary conditions are $u(0, y) = 0$ (no-slip condition at the bottom plate) and $u(h, y) = U$ (no-slip condition at the top plate).

To solve the equations, we first integrate the continuity equation with respect to y and apply the boundary conditions to find $u(x, y)$. Then, we substitute the velocity profile into the momentum equation and solve for the pressure distribution $p(x, y)$.

Solution for Velocity Profile

Integrating the continuity equation with respect to y , we have:

$$\frac{\partial u}{\partial x} = -\frac{\partial v}{\partial y}$$

Integrating again with respect to y and applying the boundary conditions, we find:

$$u(x, y) = \frac{U}{h}y$$

Solution for Pressure Distribution

Substituting the velocity profile into the x -momentum equation, we obtain:

$$\frac{\partial p}{\partial x} = -\mu \frac{U}{h}$$

Integrating with respect to x , we find:

$$p(x, y) = -\mu \frac{U}{h} x + C(y)$$

where $C(y)$ is the integration constant.

Applying the boundary condition $u(h, y) = U$, we find $C(y) = 0$, so:

$$p(x, y) = -\mu \frac{U}{h} x$$

Shear Stress Distribution

The shear stress at the top plate ($y = h$) is given by:

$$\tau(x, y) = \mu \left. \frac{\partial u}{\partial y} \right|_{y=h} = \mu \frac{U}{h}$$

We have derived the velocity profile, pressure distribution, and shear stress distribution for the steady, laminar flow of an incompressible fluid between two parallel plates. These results provide insights into the fluid behavior and are valuable for understanding the flow characteristics and designing engineering systems.

9.3 Hagen-Poiseuille Flow

The equation of fluid flow we have obtained are rather complicated and, in general, have to be integrated either by using approximations or numerically with the help of computers. There are, however, a few exact solutions. One of these was investigated by physician Poiseuille because of his interest in the flow of blood in arteries (see Fig. 9.1).

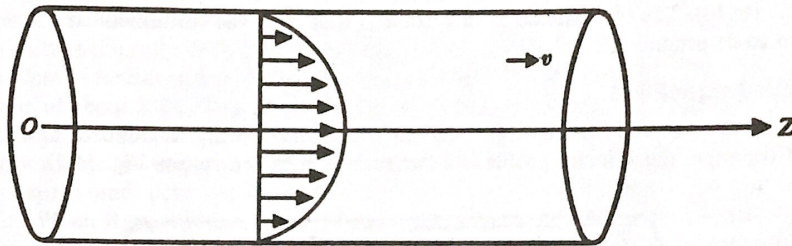


Figure 9.1: Velocity profile for Poiseuille flow

We consider steady flow when there is only one velocity component parallel to the axis so that $v_r = 0$, $v_\theta = 0$, and $v_z = v$. Then the equation of continuity gives

$$v_z = v(r). \quad (9.3.1)$$

The equations of motion, (9.2.15) and (9.2.16), now give

$$\frac{\partial p}{\partial r} = 0, \quad \frac{d^2 v}{dr^2} + \frac{1}{r} \frac{dv}{dr} = \frac{1}{\mu} \frac{\partial p}{\partial z}. \quad (9.3.2)$$

From (9.3.2), $-\frac{\partial p}{\partial z}$ must be a constant. Let us denote this constant pressure gradient by P . Then (9.3.2) gives

$$\frac{1}{r} \frac{d}{dr} \left(r \frac{dv}{dr} \right) = -\frac{P}{\mu}. \quad (9.3.3)$$

Integrating (9.3.3) twice, we get

$$r \frac{dv}{dr} = -\frac{1}{2\mu} P r^2 + A, \quad v(r) = -\frac{P r^2}{4\mu} + A \ln r + B, \quad (9.3.4)$$

but velocity on the axis (i.e., at $r = 0$) must be finite, giving $A = 0$, and it should vanish on $r = a$ because of the no-slip condition so that

$$B = \frac{P a^2}{4\mu}, \quad v = \frac{P}{4\mu} (a^2 - r^2). \quad (9.3.5)$$

The velocity is zero on the surface and is maximum on the axis. In fact, the velocity profile is parabolic and in the three-dimensional space, it may be regarded as a paraboloid of revolution.

The total flux across any section, i.e., the total volume of the fluid crossing any section per unit time, is given by

$$Q = \int_0^a 2\pi r v \, dr = \frac{\pi a^4}{8\mu} P. \quad (9.3.6)$$

The result that the flux is proportional to the pressure gradient and to the fourth power of the radius of the tube was discovered experimentally by Hagen and rediscovered independently by Poiseuille. The importance of this result is that it can be confirmed experimentally and can be used to determine μ .

Solved Problem on Hagen-Poiseuille Flow

Hagen-Poiseuille flow describes the steady, laminar flow of an incompressible and Newtonian fluid through a cylindrical pipe of radius R . The flow is driven by a constant pressure gradient along the pipe.

Derivation

The simplified Navier-Stokes equations governing the flow in cylindrical coordinates are:

$$\begin{aligned} \frac{1}{r} \frac{\partial}{\partial r} (r \cdot u) &= 0 \quad (\text{Radial continuity}) \\ -\frac{\partial p}{\partial z} + \mu \left(\frac{1}{r} \frac{\partial}{\partial r} (r \cdot u) + \frac{\partial^2 u}{\partial z^2} \right) &= 0 \quad (\text{Axial momentum}) \end{aligned}$$

where:

- $u(r, z)$ is the velocity of the fluid.

- $p(r, z)$ is the pressure.
- μ is the dynamic viscosity of the fluid.

Given that the flow is axisymmetric and there is no dependence on the azimuthal coordinate, the velocity u is only a function of the radial coordinate r and the axial coordinate z , i.e., $u = u(r, z)$.

Radial Continuity Equation

Integrating the radial continuity equation with respect to r , we have:

$$r \cdot u = \text{constant}$$

which implies that the velocity profile is parabolic.

Axial Momentum Equation

Substituting the velocity profile $u = \frac{1}{4\mu}(R^2 - r^2)\frac{\partial p}{\partial z}$ into the axial momentum equation, we obtain:

$$-\frac{\partial p}{\partial z} + \frac{\mu}{r} \frac{\partial}{\partial r} \left(r \cdot \frac{1}{4\mu} (R^2 - r^2) \frac{\partial p}{\partial z} \right) = 0$$

Simplifying, we get:

$$\frac{\partial^2 p}{\partial z^2} = 0$$

which implies that the pressure p varies linearly along the axial direction.

Velocity Profile

The velocity profile for Hagen-Poiseuille flow is given by:

$$u(r) = \frac{1}{4\mu}(R^2 - r^2)$$

Flow Rate

The flow rate Q through the pipe can be calculated by integrating the velocity profile over the cross-sectional area A of the pipe:

$$Q = \int_0^R u(r) \cdot 2\pi r \, dr = \frac{\pi R^4}{8\mu}$$

Conclusion

Hagen-Poiseuille flow describes the laminar flow of an incompressible fluid through a cylindrical pipe. The flow velocity varies parabolically across the pipe cross-section, and the pressure varies linearly along the pipe axis. The flow rate through the pipe is proportional to the fourth power of the pipe radius and inversely proportional to the fluid viscosity.

9.4 Inlet Length Flow

When a fluid enters a tube from a large reservoir where the velocity is uniform and parallel to the axis of the tube, the velocity profile is a flat surface at the entry (see Fig. 9.2). Immediately after entry, the velocity near the surface is affected by the friction of the surface, but the velocity profile near the axis still remains flat. As the fluid moves further in the tube, the flat portion decreases, and at the section corresponding to A , the paraboloidal velocity profile for the fully developed flow is reached. The flow in the region OA is called the *entry region* (or *inlet*) flow and the flow beyond A (in region III) is called the *fully developed flow*. The length OA is called the entry length. the flow in the entry length portion itself consists two parts. The flow in region I near the surface is called the *boundary layer flow*; the flow in region II is called the *core flow* or the *plug flow*. In fact, the flow approaches the parabolic velocity profile asymptotically, and we may define the entry length as the length in which 99 per cent of the final velocity profile is attained.

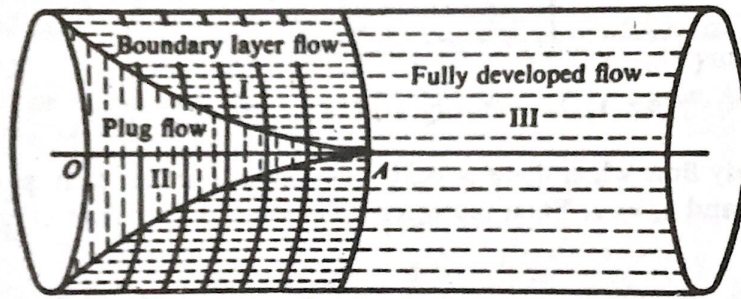


Figure 9.2: Inlet length velocity profiles

9.5 Reynolds Number of Flows

In (9.2.12)-(9.2.14), the terms on the left-hand sides represent the *inertial forces* (mass \times acceleration) while the three terms on the right-hand side of each equation represent respectively the *body forces*, *pressure forces* and *viscous forces*. If U is a typical velocity and L is a typical length, the inertial forces are of the order $\frac{\rho U}{L}$ and the viscous forces are of the order $\frac{\mu U}{L}$. The ratio of these forces is of the order

$$Re = \frac{\rho U^2 L^2}{\mu L U} = \frac{\rho U L}{\mu} = \frac{U L}{\mu} \quad (9.5.1)$$

where $\mu = \mu/\rho$ is called the *kinematic viscosity* of the fluid. Now the dimensions of μ and $\rho U L$ are given by

$$\mu = \frac{\text{stress}}{\text{strain rate}} = \frac{\text{force per unit area}}{\text{velocity/length}} = \frac{MLT^{-2}L^{-2}}{T^{-1}} = ML^{-1}T^{-1}, \quad (9.5.2)$$

$$\rho U L = ML^{-3}LT^{-1}L = ML^{-1}T^{-1}. \quad (9.5.3)$$

Thus, Re is a dimensionless number. It is called *Reynold's number*, after Osborn Reynold who in 1890 showed that the fully developed Poiseuille flow in a circular tube changes from stream line or *laminar flow* to *turbulent flow* when this number, based on the diameter of the tube, exceed a critical value of about 2000.

When Reynold number is small, viscous forces dominate over inertial forces. If we neglect the inertial forces, which we can justifiably do when $Re \ll 1$, (9.2.13) and (9.2.18) give

$$\nabla^4 \psi = 0. \quad (9.5.4)$$

Low Reynold number flows are also characteristic of

- (i) *lubrication theory*, which we shall find useful in our study of lubrication of human joints;
- (ii) *microcirculation* or flows of blood in blood vessel of diameter less than $100 \mu\text{m}$;
- (iii) *air flows* in alveolar passages of diameter less than a few hundred micron; and
- (iv) *swimming of microorganisms* with Re of the order 10^{-3}

Solved Example 1

Consider the flow of water ($\rho = 1000 \text{ kg/m}^3$) through a pipe with a diameter of 0.1 m at a velocity of 2 m/s . The dynamic viscosity of water is $0.001 \text{ Pa} \cdot \text{s}$. Calculate the Reynolds number of this flow.

Solution

Substituting the given values into the Reynolds number formula, we get:

$$Re = \frac{(1000 \text{ kg/m}^3) \times (2 \text{ m/s}) \times (0.1 \text{ m})}{0.001 \text{ Pa} \cdot \text{s}} = 2000$$

Since $2000 < Re < 4000$, the flow is in the transitional regime.

The Reynolds number is a crucial parameter in fluid mechanics that helps determine the flow regime of a fluid flow. It is used extensively in engineering and physics to understand and analyze fluid behavior.

Solved Example 2

Consider the flow of air ($\rho = 1.225 \text{ kg/m}^3$) through a pipe with a diameter of 0.05 m at a velocity of 20 m/s . The dynamic viscosity of air is $1.85 \times 10^{-5} \text{ Pa} \cdot \text{s}$. Calculate the Reynolds number of this flow and determine the flow regime.

Solution

The Reynolds number (Re) is given by:

$$Re = \frac{\rho u D}{\mu}$$

where:

- ρ is the density of the fluid,
- u is the characteristic velocity of the flow,
- D is a characteristic length (diameter of the pipe), and
- μ is the dynamic viscosity of the fluid.

Substituting the given values into the Reynolds number formula, we get:

$$Re = \frac{(1.225 \text{ kg/m}^3) \times (20 \text{ m/s}) \times (0.05 \text{ m})}{1.85 \times 10^{-5} \text{ Pa} \cdot \text{s}} \approx 131351.35$$

Since $Re > 4000$, the flow is generally turbulent.

The Reynolds number of the flow is approximately 131351.35, indicating turbulent flow. The Reynolds number is an important parameter in fluid mechanics used to predict flow regimes and analyze fluid behavior.

9.6 Non-Newtonian Fluids

For the simple motions we shall consider, there is only one non-zero component τ of the stress tensor and only one non-zero component e of the rate of strain. In general, each of these tensor has six distinct components. The functional relations between the components of the two tensors depend on the fluid under consideration and determine the *constitutive equations* for the fluid. For Newtonian viscous fluids,

$$\tau = \mu e, \tag{9.6.1}$$

where μ is the constant coefficient of viscosity. We have fluids for which μ itself may be a function of strain rate, i.e., for which stress becomes a non-linear or non-homogeneous function of strain rate (see Fig. 9.3). Such fluids are called *non-Newtonian fluids*. One important class of non-Newtonian fluids is that of *power-law fluids* with constitutive equations

$$\tau = \mu e^n = \mu e^{n-1} e. \tag{9.6.2}$$

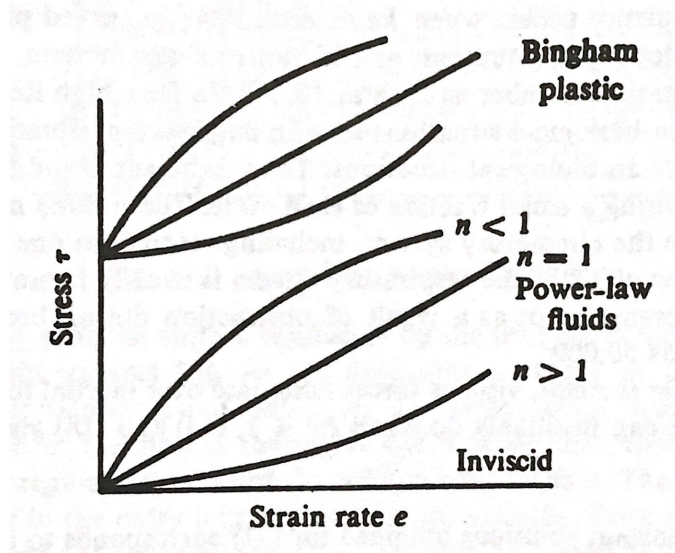


Figure 9.3: Inlet length velocity profiles

- If $n < 1$, we get a *pseudo-plastic power-law fluid* in which the effective viscosity coefficient μe^{n-1} decreases with increasing strain rate.
- If $n > 1$, we get a *dilatant power-law fluid* in which the effective viscosity coefficient increases with increasing strain rate.

- If $n = 1$, Eq.(9.6.2) gives the Newtonian viscous fluid as a special case.

Another important non-Newtonian fluid, namely, the Bingham plastic, has the constitutive equation

$$\begin{aligned}\tau &= \mu e + \tau_0 & (\tau \geq \tau_0), \\ e &= 0 & (\tau \leq \tau_0).\end{aligned}\tag{9.6.3}$$

It shows an yield stress τ_0 and, if $\tau < \tau_0$, no flow takes place. Some other laws which have been proposed for special non-Newtonian fluids are:

- Herschel-Bulkley fluid

$$\begin{aligned}\tau &= \mu e^n + \tau_0 & (\tau \geq \tau_0), \\ e &= 0 & (\tau \leq \tau_0).\end{aligned}\tag{9.6.4}$$

- Casson fluid

$$\begin{aligned}\tau^{\frac{1}{2}} &= \mu^{\frac{1}{2}} e^{\frac{1}{2}} + \tau_0^{\frac{1}{2}} & (\tau \geq \tau_0), \\ e &= 0 & (\tau \leq \tau_0).\end{aligned}\tag{9.6.5}$$

- Prandtl fluid

$$\tau = A \sin^{-1} \left(\frac{e}{c} \right)\tag{9.6.6}$$

- Prandtl-Eyring fluid

$$\tau = Ae + B \sin^{-1} \left(\frac{e}{c} \right)\tag{9.6.7}$$

Exercise 9.6.1. 1. Verify (9.2.10), (9.2.12), (9.2.18), (9.2.20) and (9.2.21).

2. Discuss the steady motion of a Newtonian viscous incompressible fluid between two parallel plates when
 - (i) the plates are at rest and there is an external pressure gradient;
 - (ii) one plate is moving in relation to the other and there is no external constant pressure gradient;
 - (iii) one plate is moving in relation to the other and there is also an external constant pressure gradient.
3. For steady motion between coaxial circular cylinders, show that

$$v = V \frac{\ln(r/b)}{\ln(a/b)} - \frac{\rho}{4\pi} \left[r^2 - \frac{b^2 \ln(r/a) - a^2 \ln(r/b)}{\ln(b/a)} \right],$$

where the inner cylinder moves with velocity V and the outer cylinder is at rest. Show also that

$$Q = \pi V \left[\frac{\frac{1}{2}(b^2 - a^2)}{\ln(b/a)} - a^2 \right] + \frac{\pi \rho}{8\mu} \left[b^4 - a^4 - \frac{(b^2 - a^2)}{\ln(b/a)} \right].\tag{9.6.8}$$

Unit 10

Course Structure

- Basic Concepts about Blood
 - Cardiovascular System and Blood Flow
 - Special Characteristics of Blood Flow
 - Structure, Function and Mechanical properties of Blood Vessels
-

10.1 Basic Concepts about Blood, Cardiovascular System and Blood Flow

10.1.1 Constitution of Blood

Blood consists of a *suspension of cells* in an aqueous solution called *plasma* which is composed of about 90 per cent water and 7 per cent protein. There are about 5×10^9 cells in a millilitre (1 cc) of healthy human blood, of which about 95 per cent are *red cells* or *erythrocytes* whose main function is to transport oxygen from the lungs to all the cells of the body and the removal of carbon-dioxide formed by metabolic processes in the body to the lungs. About 45 per cent of the blood volume in an average man is occupied by red cells. This fraction is known as the *hematocrit*. Of the remaining, *white cells* or *leucocytes* constitute about one-sixth or 1 per cent of the total, and these play a role in the resistance of the body to infection; *platelets* form 5 per cent of the total, and they perform a function related to blood clotting.

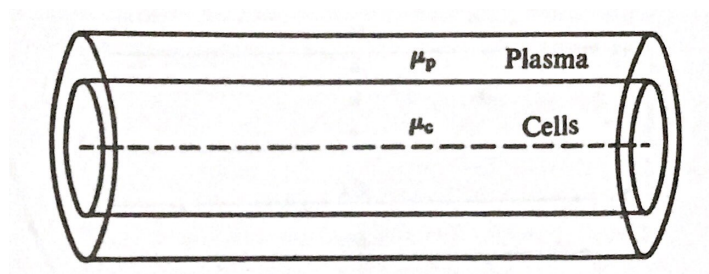


Figure 10.1: Two layer flow

Composition of Blood

Blood is a specialized bodily fluid that circulates through the cardiovascular system, delivering essential nutrients and oxygen to tissues and removing metabolic waste products. It is composed of various cellular and non-cellular components that work together to maintain homeostasis and support physiological functions.

Cellular Components

Red Blood Cells (Erythrocytes)

- Red blood cells are the most abundant cellular component of blood, comprising approximately 40-45
- Their primary function is to transport oxygen from the lungs to tissues and carbon dioxide from tissues to the lungs for elimination.
- Red blood cells contain hemoglobin, a protein that binds oxygen and gives blood its red color.

White Blood Cells (Leukocytes)

- White blood cells are a diverse group of cells involved in the immune response and defense against pathogens and foreign substances.
- There are several types of white blood cells, including neutrophils, lymphocytes, monocytes, eosinophils, and basophils, each with specific functions in immunity.
- White blood cells can migrate out of blood vessels into tissues to combat infection and inflammation.

Platelets (Thrombocytes)

- Platelets are small, disc-shaped cell fragments derived from megakaryocytes in the bone marrow.
- They play a crucial role in hemostasis, the process of blood clotting, by forming a plug at the site of blood vessel injury and initiating the coagulation cascade.
- Platelets release various factors and enzymes that promote clot formation and repair damaged blood vessels.

Non-cellular Components

Plasma

- Plasma is the liquid portion of blood, making up approximately 55-60
- It is a complex mixture of water, proteins, electrolytes, hormones, nutrients, waste products, and gases.
- Plasma proteins, such as albumin, globulins, and fibrinogen, play roles in maintaining osmotic balance, transporting substances, and participating in immune responses and clotting mechanisms.

Clinical Significance

- Blood composition is closely monitored in clinical settings to assess overall health and diagnose various medical conditions.
- Abnormalities in blood cell counts, such as anemia (low red blood cell count) or leukocytosis (high white blood cell count), may indicate underlying diseases or disorders.
- Blood tests, including complete blood count (CBC), blood chemistry analysis, and blood typing, provide valuable information for evaluating organ function, detecting infections, and guiding treatment decisions.

The composition of blood is remarkably complex, consisting of cellular elements, such as red blood cells, white blood cells, and platelets, as well as non-cellular components, including plasma proteins and other solutes. This intricate balance of components is essential for maintaining physiological functions and responding to internal and external challenges.

10.1.2 Viscosity of Blood

Blood is neither homogeneous nor Newtonian. Plasma in isolation may be considered Newtonian with a viscosity of about 1.2 times that of water. For whole blood, we can measure effective viscosity, and this found to depend on shear rate. The constitutive equations proposed for whole blood are as follows:

(i) $\tau = \mu e^n$ (power law equation). This is found to hold good for strain rates between 5 and 200 sec^{-1} , with n having a value between 0.68 and 0.80.

(ii) $\tau = \mu e^n + \tau_0$ ($\tau \geq \tau_0$) (Herschel-Bulkley equation).

(iii) $\tau^{1/2} = \mu^{1/2} e^{1/2} + \tau_0^{1/2}$ (Casson equation). This holds for strain rate between 0 and 100000 sec^{-1} .

The yield stress arises because, at low shear stress, red cells form aggregates in the form of rouleaux which are stacks of red cells in the shape of a roll of coins (see Fig. 10.2). At some finite stress, which is usually small (of the order of 0.005 dyne/cm^2), the aggregate is disrupted and blood begins to flow.

For hematocrits exceeding 5.8 per cent, it has been found that the yield stress is given by

$$\tau_0^{1/2} = A(H - H_m)/100, \quad (10.1.1)$$

where $A = (0.008 \pm 0.002 \text{ dyne/cm}^2)^{1/3}$, H is the normal hematocrit, and H_m is the hematocrit below which there is no yield stress. Taking H as 45 per cent and H_m as 5 per cent, the yield stress of normal human blood should be between 0.01 and 0.06 dyne/cm^2 .

Not only τ_0 , but also τ and effective viscosity, depend significantly on the hematocrit. The effective viscosity is also apparently found to depend on capillary radius when measurements are made in capillaries of diameters less than 300 μm . This apparent dependence of viscosity on capillary radius is known as *Fahraeus-Lindqvist effect*. We shall explain this effect which is based on the hypothesis of a two layer flow (a plasma layer and a core layer) with different viscosities.

Solved Problem: Constitutive Equations for Whole Blood

Whole blood exhibits complex rheological behavior due to its heterogeneous composition and non-Newtonian nature. Constitutive equations are mathematical models used to describe the relationship between stress and strain in blood flow. Consider the following constitutive equation proposed for whole blood:

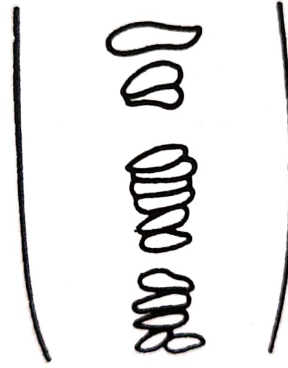


Figure 10.2: Rouleaux formation.

$$\tau = \eta \left(\frac{\partial v}{\partial r} \right)^n$$

where:

- τ is the shear stress,
- η is the viscosity coefficient,
- v is the velocity gradient,
- r is the radial distance from the center of the vessel, and
- n is the power-law index.

Problem

Given a blood flow experiment in a cylindrical tube with a radius of $R = 0.1$ cm, the measured shear stress (τ) at the vessel wall is 0.5 dyn/cm². The velocity profile (v) is given by $v(r) = V \left(1 - \frac{r^2}{R^2} \right)$, where $V = 1$ cm/s. Assuming a power-law index (n) of 0.7, determine the viscosity coefficient (η) of the blood.

Solution

First, we need to calculate the velocity gradient $\left(\frac{\partial v}{\partial r} \right)$ using the given velocity profile:

$$\frac{\partial v}{\partial r} = \frac{d}{dr} \left(V \left(1 - \frac{r^2}{R^2} \right) \right) = -\frac{2Vr}{R^2}$$

Now, we can use the constitutive equation to solve for the viscosity coefficient (η):

$$\tau = \eta \left(\frac{\partial v}{\partial r} \right)^n$$

Substituting the given values and solving for η :

$$0.5 = \eta \left(\frac{-2Vr}{R^2} \right)^{0.7}$$

$$\eta = \frac{0.5}{\left(\frac{-2Vr}{R^2}\right)^{0.7}}$$

$$\eta = \frac{0.5}{\left(\frac{-2 \times 1 \times r}{0.1^2}\right)^{0.7}} = \frac{0.5}{(-2000r)^{0.7}}$$

The viscosity coefficient (η) of the blood is given by this expression.

Conclusion

We have determined the viscosity coefficient (η) of the blood using the constitutive equation proposed for whole blood. This coefficient represents the resistance of blood to flow and is essential for understanding and modeling blood rheology in various physiological and pathological conditions.

10.1.3 Cardiovascular System

The cardiovascular system consists of the following:

- (i) The *heart* (which acts as a pump, whose elastic muscular walls contract rhythmically, making possible the pulsatile flow of blood through the vascular system)
- (ii) The *distributory system* (comprising arteries and arterioles for sending blood to the various organs of the body)
- (iii) The *diffusing system* (made up of fine capillaries which are in contact with the cells of the body)
- (iv) The *collecting system of veins* (which collects blood depleted of oxygen and full of products of metabolic processes of the system).

The organs which supplement the function of the cardiovascular system are (i) the lungs which provide a region of inter-phase transfer of O_2 to the blood and removal of CO_2 from it, and (ii) the kidney, liver, and spleen, which help in maintaining the chemical quality of blood under normal conditions and under conditions of extreme stress.

Deoxygenated blood enters the *right atrium* (RA) from where it goes to the *right ventricle* (RV), as shown in Fig. 10.3. When the heart contracts, the *tricuspid valve* between the RA and RV closes and blood is pushed out to the lung through the *pulmonary artery* (PA) which branches to the right and left lungs where CO_2 is removed and blood is oxygenated. The blood returns from the lungs through the *pulmonary vein* (PV) to *left atrium* (LA) and then it goes to the *left ventricle* (LV) and from there, due to contraction of the heart, it enters the aorta from which it travels to other arteries and the rest of the vascular system.

10.1.4 Special Characteristics of Blood Flow

Blood flow problems are more complicated than the problems of fluid flows in engineering situations for the following reasons:

- (i) Unusually high Reynolds number of flows. The flows remain laminar at Reynolds numbers as high as 5000 - 10000. This causes the entry length (which is proportional to the Reynolds number) to be so large that in most cases the fully developed flow is never reached since tube branching start before this stage is attained.
- (ii) Unusual curvature of blood vessels. In some cases, this leads to secondary flows and these become more marked at high Reynolds numbers in some of the tubes.

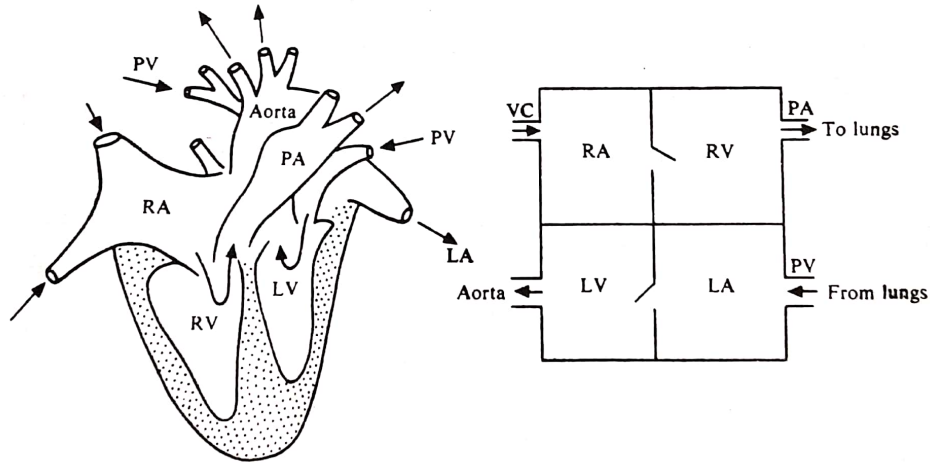


Figure 10.3: The heart.

- (iii) Unusually large number of branches. Bifurcation takes place 20 - 30 times, leading to millions of blood vessels.
- (iv) Unusual distensible properties of containing vessels. These properties arise from the fact that the vessel walls are formed of different substances such as elastin, collagen, and smooth muscles, with entirely different properties.
- (v) Unusual fluid properties of blood. These properties are due to the fact that blood is a suspension of millions of cells of different shapes in plasma and these cells can deform when passing through vessels of diameter smaller than their own.
- (vi) Unusual pulsatility of flows. This arises from the rhythmic action of the heart.

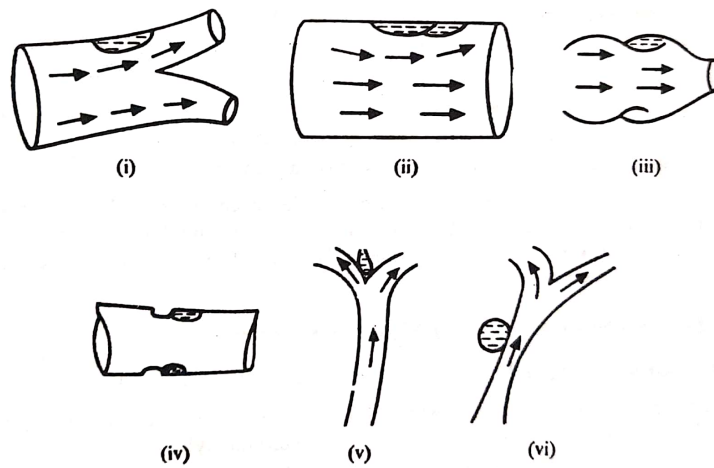


Figure 10.4: Examples of separation of flows in blood vessels.

There is also an unusual separation of flows, leading to increased resistance to flow and undesirable effects,

e.g., hardening of arteries. The separation occurs due to various reasons, some of which are as follows (see Fig. 10.7):

- (i) Bifurcation of blood vessel
- (ii) Atheroma of blood vessels or fatty degeneration of the inner walls of the blood vessel
- (iii) Stenosis of heart valve or narrowing of the heart valve when the valve is fully open
- (iii) Stenosis of blood vessels or narrowing of blood vessels
- (iv) Secular aneurysm or a sac-like permanent abnormal blood-filled dilatation of blood vessel, resulting from a disease of the vessel wall
- (v) Aortic aneurysm of abnormal blood-filled dilatation of the aortic vessel.

10.1.5 Structure and function of Blood Vessels

Blood vessels are well-arranged sophisticated network of branching tubes or pipes conveying blood to the all parts of the body. There are several types of blood vessels, namely aorta, arteries, arterioles, veins, venules, capillaries etc. The arteries are those blood vessels which carry away from the heart. The blood vessel is composed of three layers.

- (i) The innermost layer called *Tunica-Intima*, consists of thin layer of endothelial cells,
- (ii) The middle layer called *Tunica-Media* consists of plain muscles and a network of elastic fibres, and
- (iii) The outer most layer, called *Tunica-Adventitia*, is made up of fibrous tissues and elastic tissue.

Veins are the blood vessels which carry blood to the heart. The venous cross-sectional area at any point is larger than of arteries and the velocity of blood is considerably lower when the arteries break up into minute vessels, they are turned to capillaries.

10.1.6 Principal of Blood Vessels

Blood vessels are essential components of the circulatory system, responsible for transporting blood throughout the body. The principal constituents of blood vessels are collagen, smooth muscles and elastin.

Collagen: It is the most important structure element of animal. There is a high amount of collagen present in bone materials. Collagen is relatively inextensible fibrous protein. The fibres can be identified by light or electron microscope.

Elastin: Unlike collagen elastin is an extensible fibrous protein present in large amount in skin, blood vessels, lung etc. The elastic behaviour of this structure is solely due to the presence of elastin. The fact that elastin never appears without collagen, leads us to think that there must be resemblance in structure of both.

Smooth muscles: Muscles consist of many fibres held together by connective tissues. Their structure and function vary widely in different organ and animal. One of the basic structures they are divided into smooth and striated muscles.

Arteries: Arteries are blood vessels that carry oxygen-rich blood away from the heart to various parts of the body. They have thick, elastic walls composed of three layers: the tunica intima, tunica media, and tunica

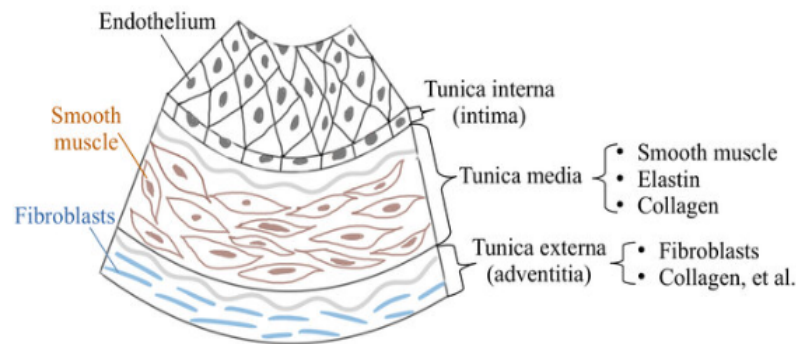


Figure 10.5: The basic structure of a hollow blood vessel. Note that only a tiny segment of the vessel is used to show the microstructure. The tunica intima is the inner supporting tissue layer that contains the endothelium, a flat single layer of cells, the basement membrane, and the supporting connective tissue. The connective tissue consists of elastic and collagenous fibers. The tunica media represents the muscle layer. The tunica externa is the outer supporting tissue layer with its own epithelium (which is a thin tissue forming the outer layer of the blood vessel surface). The collagen is present in the tunica media and the tunica externa to maintain the elasticity of the blood vessel.

externa. Arteries have a thick muscular layer (tunica media) that allows them to withstand high blood pressure and regulate blood flow.

Veins: Veins are blood vessels that carry oxygen-depleted blood back to the heart from various parts of the body. They have thinner walls compared to arteries and contain valves to prevent the backflow of blood. Veins rely on the contraction of surrounding muscles and the respiratory pump to propel blood towards the heart.

Capillaries: Capillaries are the smallest and most numerous blood vessels in the body. They connect arterioles to venules and facilitate the exchange of gases, nutrients, and waste products between the blood and tissues. Capillary walls are thin and composed of a single layer of endothelial cells, allowing for efficient diffusion.

Blood Flow Regulation: Blood flow through blood vessels is regulated by various factors, including:

- Autoregulation: Local control mechanisms that adjust blood flow based on tissue metabolic demands.
- Neural regulation: Sympathetic and parasympathetic nervous systems regulate blood vessel diameter and blood pressure.
- Hormonal regulation: Hormones such as adrenaline, angiotensin II, and vasopressin influence blood vessel constriction and dilation.

Clinical Significance

Understanding the principles of blood vessels is crucial in diagnosing and treating various cardiovascular diseases, such as hypertension, atherosclerosis, and peripheral artery disease. Medical interventions, includ-

ing angioplasty, stent placement, and bypass surgery, aim to restore blood flow and prevent complications associated with vascular disorders.

10.1.7 Mechanical Properties of Blood Vessels

In view of the diverse elastic properties of the components of the arterial wall, a number of theoretical and experimental investigation in the relevant field have established that vascular wall are non-homogeneous, anisotropy, incompressible and visco-elastic. The mechanical properties of blood vessels play a crucial role in maintaining proper cardiovascular function. These properties describe how blood vessels deform and respond to changes in pressure, volume, and flow.

Inhomogeneity: Usually the wall of blood vessels are inhomogeneous. But experimental investigations showed that the outermost layer, adventesia has a very loose network and merges externally with the surrounding tissues. The inner most layer intima, is very thin and can be easily neglected. The remaining layer, the media, is considered homogeneous containing a matrix of smooth muscles elastic and collagen.

Compressibility: A material is said to be compressible if it changes its volume when it subjected to stress. It is said to be incompressible if the change of the volume is ignorable. The experimental studied showed that there is 20-40% change in volume and hence, for practical purpose the compressibility of vascular tissue can be considerably very small.

Anisotropy: Healthy arteries are highly deformable comfit structures and show a non-linear stress strain response with a typical stiffening effect at high pressure. This stiffening effect, common to all biological tissues is based on the recruitment of embedded wavy collagen fibrils which leads to the characteristics of anisotropic behaviour of artery.

Visco-elasticity: For a perfectly elastic body, there must be a single valued relationship between the applied strain and resulting stress. But when artery is subject to a cyclically varying strain the stress response exhibits a hysteresis loop called it cycle. The rate of decreases is very rapid in the beginning, but a steady state is observed after a numbers of cycles. Visco-elasticity describes the combination of elastic and viscous properties in blood vessel walls. While elasticity allows blood vessels to store and release energy, viscosity determines the rate of deformation and relaxation. The viscoelastic behavior of blood vessels influences their response to pulsatile blood flow and contributes to damping oscillations in blood pressure.

Elasticity: Elasticity refers to the ability of blood vessels to deform under stress and return to their original shape when the stress is removed. Arteries exhibit high elasticity due to the presence of elastic fibers in their walls, primarily in the tunica media. This elasticity allows arteries to expand and recoil in response to changes in blood pressure, ensuring continuous blood flow and reducing the workload on the heart.

Compliance: Compliance, also known as distensibility, measures the ability of blood vessels to accommodate changes in blood volume without significant changes in pressure. Arteries have higher compliance than veins, meaning they can stretch more easily to accommodate increased blood volume. Compliance is an important factor in regulating blood pressure and maintaining proper tissue perfusion.

Stiffness: Stiffness is the opposite of compliance and refers to the resistance of blood vessels to deformation. As blood vessels age or undergo pathological changes such as atherosclerosis, they become stiffer, leading to increased systolic blood pressure and decreased diastolic blood pressure. Stiffness is often quantified using parameters such as pulse wave velocity and arterial stiffness index.

Clinical Significance: Understanding the mechanical properties of blood vessels is essential for diagnosing and managing cardiovascular diseases. Alterations in vessel elasticity, compliance, and stiffness are associated with conditions such as hypertension, atherosclerosis, and arterial aneurysms. Therapeutic interventions, including lifestyle modifications, pharmacotherapy, and surgical procedures, aim to preserve or restore the mechanical integrity of blood vessels and prevent adverse cardiovascular events.

Moreover, two main characteristics of visco-elastic material as for example creep and stress relaxation were also observed in vascular tissue.

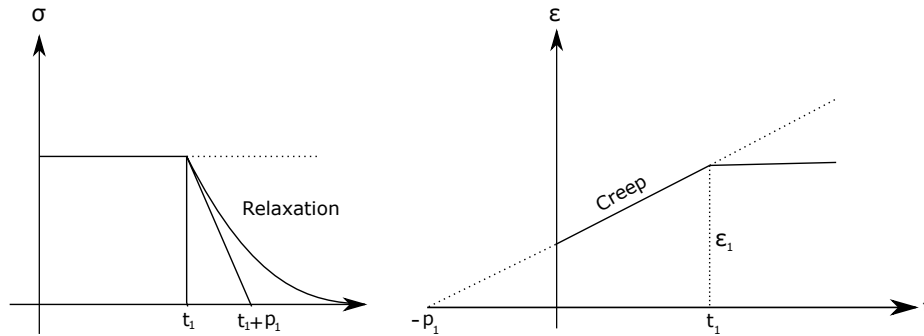


Figure 10.6: Relaxation and Creep.

In the first stage, ϵ increases under the constant stress. This phenomena is called creep. In the second stage, the stress decrease under constant strain, i.e., the material relaxes. This phenomena is called stress relaxation.

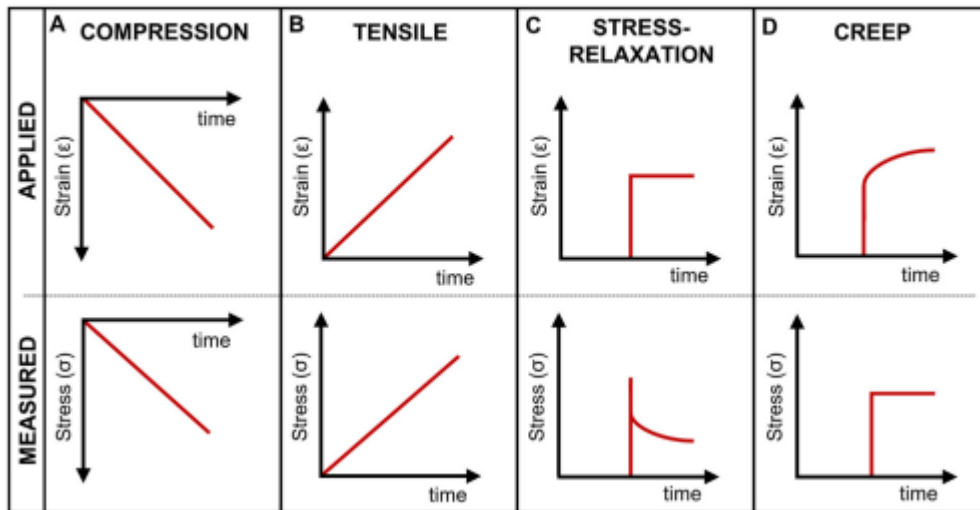


Figure 10.7: Stress and strain curves in function of time for (A) compression, (B) tensile, (C) tensile stress-relaxation, and (D) creep tests. First row represents the applied strain or stress, and the second row represents the corresponding strain or stress response measured.

Solved Problem on Mechanical Properties of Blood Vessels

Consider a cylindrical blood vessel with a radius of $R = 0.1$ cm and a length of $L = 10$ cm. The vessel wall is composed of elastic tissue with a Young's modulus (E) of 2×10^6 dyn/cm². Calculate the change in vessel diameter (ΔD) when the pressure inside the vessel increases by $\Delta P = 100$ mmHg.

Solution

The change in vessel diameter (ΔD) can be calculated using the formula for the change in length (ΔL) due to an increase in pressure:

$$\Delta L = \frac{\Delta P \cdot V}{E}$$

where V is the volume of the vessel wall.

The volume (V) of the vessel wall can be approximated as the product of the cross-sectional area (A) and the length (L) of the vessel:

$$V = A \cdot L$$

The cross-sectional area (A) of the vessel can be calculated using the formula for the area of a circle:

$$A = \pi R^2$$

Substituting the values into the equations:

$$A = \pi(0.1 \text{ cm})^2 = 0.0314 \text{ cm}^2$$

$$V = 0.0314 \text{ cm}^2 \times 10 \text{ cm} = 0.314 \text{ cm}^3$$

Now, we can calculate the change in length (ΔL):

$$\Delta L = \frac{(100 \text{ mmHg}) \times (0.314 \text{ cm}^3)}{2 \times 10^6 \text{ dyn/cm}^2} = 0.00157 \text{ cm}$$

Since the change in diameter (ΔD) is twice the change in length (ΔL) due to the vessel's cylindrical shape:

$$\Delta D = 2 \times \Delta L = 2 \times 0.00157 \text{ cm} = 0.00314 \text{ cm}$$

Conclusion

The change in vessel diameter (ΔD) due to an increase in pressure of 100 mmHg is 0.00314 cm. This calculation demonstrates the elastic properties of blood vessels and their ability to deform in response to changes in pressure.

Unit 11

Course Structure

- Steady non-Newtonian fluid flow in circular tubes
 - Flow in Power-Law fluid in circular tubes
 - Flow in Herschel-Bulkley fluid in circular tubes
 - Flow in Casson fluid in circular tubes
-

11.1 Steady Non-Newtonian Fluid Flow in Circular Tubes

11.1.1 Basic Equations for Fluid Flow

We consider the laminar flow of a non-Newtonian in a circular tube under a constant pressure gradient. Let the control volume be bounded by two coaxial cylinders of radii r and $r + dr$ and let it be of unit length, as shown in Fig. 11.1.

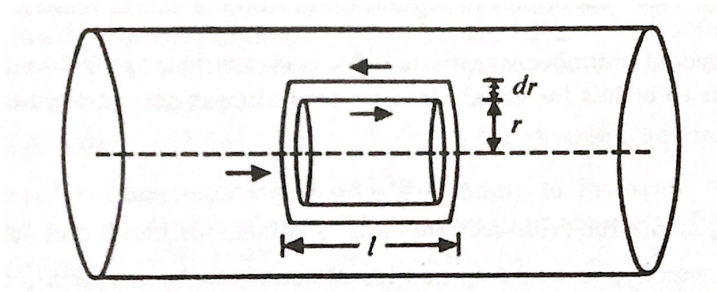


Figure 11.1: Forces on control volume

Due to the pressure gradient, there is a forward force $P \times 2\pi[(r + r dr) - r] = P \times 2\pi r dr$ on it. Let the stress be $\tau(r)$ at a distance r from the axis. Then the force on the inner cylindrical surface is $2\pi r \tau$, and the

force on the outer cylindrical surface is

$$\begin{aligned}
 2\pi(r + dr)\tau(r + dr) &= 2\pi(r + dr) \left[\tau(r) + \frac{d\tau(r)}{dr} dr \right] \\
 &= 2\pi \left[r\tau(r) + \tau(r) dr + r \frac{d\tau(r)}{dr} dr \right] \\
 &= 2\pi \left[[r\tau(r)] + \frac{d}{dr} [r\tau(r)] dr \right]
 \end{aligned} \tag{11.1.1}$$

Balancing the force in the axial direction in the control volume, we get

$$\begin{aligned}
 2\pi \frac{d}{dr} [r\tau(r)] &= 2\pi r P \\
 \Rightarrow \frac{d}{dr} [r\tau(r)] &= r P.
 \end{aligned} \tag{11.1.2}$$

Integrating (11.1.2), we obtain

$$\begin{aligned}
 r\tau(r) &= \frac{1}{2} r^2 P + A \\
 \Rightarrow \tau(r) &= \frac{1}{2} P \left[r + \frac{D}{r} \right] \quad \text{where } D = 2A.
 \end{aligned} \tag{11.1.3}$$

Since the stress $\tau(r)$ is finite on the axis (i.e. at $r = 0$), we have

$$A = 0, \quad D = 0, \quad \tau = \frac{r}{2} P. \tag{11.1.4}$$

The velocity v is parallel to the axis which is also a function of r only and is expected to decrease from a maximum on the axis to zero on the surface so that the only non-zero component of strain rate is

$$e(r) = -\frac{dv}{dr}. \tag{11.1.5}$$

For a non-Newtonian fluid,

$$\tau = f(e) \tag{11.1.6}$$

so that from Eq.(11.1.3), we have

$$\frac{r}{2} P = f\left(-\frac{dv}{dr}\right). \tag{11.1.7}$$

Integrating (11.1.7) subject to the condition that $v = 0$ when $r = R$, we get v as a function of r . Then we can obtain the flux Q by using

$$Q = \int_0^R 2\pi r v dr. \tag{11.1.8}$$

Integrating the right-hand side of (11.1.8) by parts, we get

$$Q = 2\pi \left[\left(\frac{1}{2} r^2 v \right)_0^R - \int_0^R \frac{1}{2} r^2 \frac{dv}{dr} dr \right]. \tag{11.1.9}$$

Since $v = 0$ at $r = R$, we have

$$Q = \pi \int_0^R r^2 e(r) dr. \tag{11.1.10}$$

Solved Problem: Steady Non-Newtonian Fluid Flow in Circular Tubes

Consider the flow of a non-Newtonian fluid with the following velocity profile through a long circular tube with radius R :

$$v(r) = \frac{1}{2\eta_0} (R^2 - r^2)^2$$

where:

- $v(r)$ is the velocity of the fluid at radial position r ,
- R is the radius of the tube, and
- η_0 is the viscosity of the fluid.

Determine the maximum velocity (v_{\max}) and the volumetric flow rate (Q) of the non-Newtonian fluid through the tube.

Solution

To find the maximum velocity (v_{\max}), we need to determine the maximum value of the velocity profile. The maximum velocity occurs at $r = 0$, so:

$$v_{\max} = \frac{1}{2\eta_0} (R^2)^2 = \frac{1}{2\eta_0} R^4$$

Now, let's find the volumetric flow rate (Q). The volumetric flow rate (Q) can be calculated by integrating the velocity profile over the cross-section of the tube and multiplying by the cross-sectional area:

$$Q = \int_0^R v(r) \cdot 2\pi r \, dr$$

Substituting the given velocity profile:

$$Q = \int_0^R \frac{1}{2\eta_0} (R^2 - r^2)^2 \cdot 2\pi r \, dr$$

$$Q = \frac{\pi}{\eta_0} \int_0^R (R^2 - r^2)^2 r \, dr$$

Performing the integration:

$$Q = \frac{\pi}{\eta_0} \int_0^R (R^4 - 2R^2r^2 + r^4) r \, dr$$

$$Q = \frac{\pi}{\eta_0} \int_0^R (R^5 - 2R^2r^4 + r^5) \, dr$$

$$Q = \frac{\pi}{\eta_0} \left[\frac{1}{6}R^6 - \frac{2}{7}R^6 + \frac{1}{6}R^6 \right]$$

$$Q = \frac{\pi}{\eta_0} \left[\frac{1}{6}R^6 - \frac{2}{7}R^6 + \frac{1}{6}R^6 \right]$$

$$Q = \frac{\pi}{\eta_0} \left[\frac{1}{6} R^6 - \frac{2}{7} R^6 + \frac{1}{6} R^6 \right]$$

$$Q = \frac{\pi}{\eta_0} \left[\frac{1}{3} R^6 - \frac{2}{7} R^6 \right]$$

$$Q = \frac{\pi}{\eta_0} \left[\frac{7}{21} R^6 - \frac{6}{21} R^6 \right]$$

$$Q = \frac{\pi}{\eta_0} \left[\frac{1}{21} R^6 \right]$$

$$Q = \frac{\pi R^6}{21 \eta_0}$$

Conclusion

The maximum velocity (v_{\max}) of the non-Newtonian fluid through the tube is $\frac{1}{2\eta_0} R^4$, and the volumetric flow rate (Q) is $\frac{\pi R^6}{21\eta_0}$. These calculations provide insights into the flow characteristics of non-Newtonian fluids in circular tubes.

11.2 Flow of Power-Law Fluid in Circular Tube

Here $\tau = \mu e^n$, Eq.(11.1.7) gives

$$\frac{dv}{dr} = - \left(\frac{1}{2} \frac{P}{\mu} r \right)^{1/n} \quad (11.2.1)$$

Integrating (11.2.1), we obtain

$$v = \left(\frac{P}{2\mu} \right)^{1/n} \frac{n}{n+1} \left[R^{\frac{1}{n}+1} - r^{\frac{1}{n}+1} \right] \quad (11.2.2)$$

Also,

$$Q = \int_0^R 2\pi r v dr = \left(\frac{1}{2} \frac{P}{\mu} \right)^{1/n} \frac{n\pi}{3n+1} R^{\frac{1}{n}+3}. \quad (11.2.3)$$

Solved Problem: Flow of Power-Law Fluid in a Circular Tube

Consider the flow of a power-law fluid through a long circular tube with radius R . The power-law fluid model describes non-Newtonian fluids with a shear-thinning behavior characterized by a power-law index (n) and consistency coefficient (K). The velocity profile for laminar flow in the tube can be expressed as:

$$v(r) = \frac{K}{n+1} (R^{n+1} - r^{n+1})$$

where:

- $v(r)$ is the velocity of the fluid at radial position r ,
- R is the radius of the tube,

- n is the power-law index of the fluid, and
- K is the consistency coefficient of the fluid.

Given that $R = 0.1$ m, $n = 0.5$, and $K = 2$ Pa s ^{n} , determine the maximum velocity (v_{\max}) and the volumetric flow rate (Q) of the power-law fluid through the tube.

Solution

First, let's find the maximum velocity (v_{\max}) by substituting $r = 0$ into the velocity profile:

$$v_{\max} = \frac{K}{n+1} (R^{n+1})$$

$$v_{\max} = \frac{2}{0.5+1} (0.1^{0.5+1})$$

$$v_{\max} = \frac{2}{1.5} (0.1^{1.5})$$

$$v_{\max} = \frac{2}{1.5} \times 0.0316$$

$$v_{\max} = \frac{0.0632}{1.5}$$

$$v_{\max} \approx 0.0421 \text{ m/s}$$

Now, let's find the volumetric flow rate (Q). The volumetric flow rate (Q) can be calculated by integrating the velocity profile over the cross-section of the tube and multiplying by the cross-sectional area:

$$Q = \int_0^R v(r) \cdot 2\pi r \, dr$$

Substituting the given values into the equation and performing the integration:

$$Q = \int_0^{0.1} \frac{2}{0.5+1} (0.1^{0.5+1} - r^{0.5+1}) \cdot 2\pi r \, dr$$

$$Q = \int_0^{0.1} \frac{2}{1.5} (0.1^{1.5} - r^{1.5}) \cdot 2\pi r \, dr$$

$$Q = \frac{2}{1.5} \left(\int_0^{0.1} (0.001 - r^{1.5}) \cdot 2\pi r \, dr \right)$$

$$Q = \frac{2}{1.5} \left(\int_0^{0.1} (0.001 \cdot 2\pi r - r^{1.5} \cdot 2\pi r) \, dr \right)$$

$$Q = \frac{2}{1.5} \left(0.001 \cdot 2\pi \int_0^{0.1} r \, dr - 2\pi \int_0^{0.1} r^{2.5} \, dr \right)$$

$$Q = \frac{2}{1.5} \left(0.001 \cdot 2\pi \left[\frac{1}{2} r^2 \right]_0^{0.1} - 2\pi \left[\frac{2}{3.5} r^{3.5} \right]_0^{0.1} \right)$$

$$\begin{aligned}
Q &= \frac{2}{1.5} \left(0.001 \cdot 2\pi \left[\frac{1}{2}(0.1)^2 - \frac{1}{2}(0)^2 \right] - 2\pi \left[\frac{2}{3.5}(0.1)^{3.5} - \frac{2}{3.5}(0)^{3.5} \right] \right) \\
Q &= \frac{2}{1.5} \left(0.001 \cdot 2\pi \left[\frac{1}{2}(0.01) - 0 \right] - 2\pi \left[\frac{2}{3.5}(0.1)^{3.5} - 0 \right] \right) \\
Q &= \frac{2}{1.5} \left(0.001 \cdot 2\pi [0.005] - 2\pi \left[\frac{2}{3.5}(0.1)^{3.5} \right] \right) \\
Q &= \frac{2}{1.5} \left(0.001 \cdot 2\pi \times 0.005 - 2\pi \times \frac{2}{3.5}(0.1)^{3.5} \right) \\
Q &\approx \frac{2}{1.5} (0.00003142 - 0.00001073) \\
Q &\approx \frac{2}{1.5} \times 0.00002069 \\
Q &\approx 0.00002758 \text{ m}^3/\text{s}
\end{aligned}$$

Conclusion

The maximum velocity (v_{\max}) of the power-law fluid through the tube is approximately 0.0421 m/s, and the volumetric flow rate (Q) is approximately 0.00002758 m³/s. These calculations provide insights into the flow characteristics of non-Newtonian fluids with shear-thinning behavior in circular tubes.

11.3 Flow of Herschel-Bulkley Fluid in Circular Tube

In this case, we have $e = 0$ when $\tau \leq \tau_0$, and there is a core region which flows as a plug (see Fig. 11.2). Let the radius of the plug region be r_p . At the surface of the plug, the stress is τ_0 so that, considering the forces on the plug, we get

$$\begin{aligned}
P \times \pi r_p^2 &= \tau_0 \times 2\pi r_p \\
\Rightarrow r_p &= 2\tau_0/P
\end{aligned} \tag{11.3.1}$$

In the non-core region, $\tau \geq \tau_0$, and

$$\tau = \mu e^n + \tau_0 \tag{11.3.2}$$

so that (11.1.7) gives

$$\left(\frac{\frac{r}{2}P - \tau_0}{\mu} \right)^{1/n} = e = -\frac{dv}{dr} \tag{11.3.3}$$

or, on using (11.3.1), we get

$$\frac{dv}{dr} = - \left(\frac{1}{2} \frac{P}{\mu} \right)^{1/n} (r - r_p)^{1/n}. \tag{11.3.4}$$

Integrating (11.3.4), we obtain

$$v = \frac{n}{n+1} \left(\frac{P}{2\mu} \right)^{1/n} \left[(R - r_0)^{\frac{1}{n}+1} - (r - r_0)^{\frac{1}{n}+1} \right]. \tag{11.3.5}$$

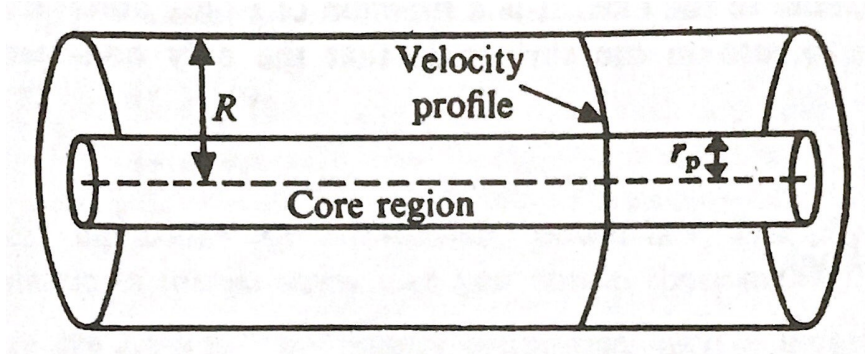


Figure 11.2: Plug flow

If $r = r_p$, then $v = v_p$ (the velocity of the plug flow) so that

$$v_p = \frac{n}{n+1} \left(\frac{P}{2\mu} \right)^{1/n} (R - r_p)^{\frac{1}{n}+1}. \quad (11.3.6)$$

Eq. (11.3.1) determines the radius of the plug, and then using this value of the plug, (11.3.6) determines the velocity of the plug and (11.3.5) determines the velocity in the non-core region. Also,

$$\begin{aligned} Q &= \pi r_p^2 v_p + \int_{r_p}^R 2\pi r v \, dr \\ &= \pi r_p^2 \frac{n}{n+1} \left(\frac{P}{2\mu} \right)^{1/n} (R - r_p)^{\frac{1}{n}+1} + \frac{n}{n+1} \left(\frac{P}{2\mu} \right)^{1/n} 2\pi \left[\frac{1}{2} (R - r_p)^{\frac{1}{n}+2} (R + r_p) \right. \\ &\quad \left. - \frac{(R - r_p)^{\frac{1}{n}+3}}{\frac{1}{n}+3} - r_p \frac{(R - r_p)^{\frac{1}{n}+2}}{\frac{1}{n}+3} \right] \end{aligned} \quad (11.3.7)$$

$$\begin{aligned} &= \pi \frac{n}{n+1} \left(\frac{P}{2\mu} \right)^{1/n} R^{\frac{1}{n}+3} \left[c_p^2 (1 - c_p)^{\frac{1}{n}+1} + (1 + c_p)(1 - c_p)^{\frac{1}{n}+2} \right. \\ &\quad \left. - \frac{2}{\frac{1}{n}+3} (1 - c_p)^{\frac{1}{n}+3} - \frac{2c_p}{\frac{1}{n}+2} (1 - c_p)^{\frac{1}{n}+2} \right] \end{aligned} \quad (11.3.8)$$

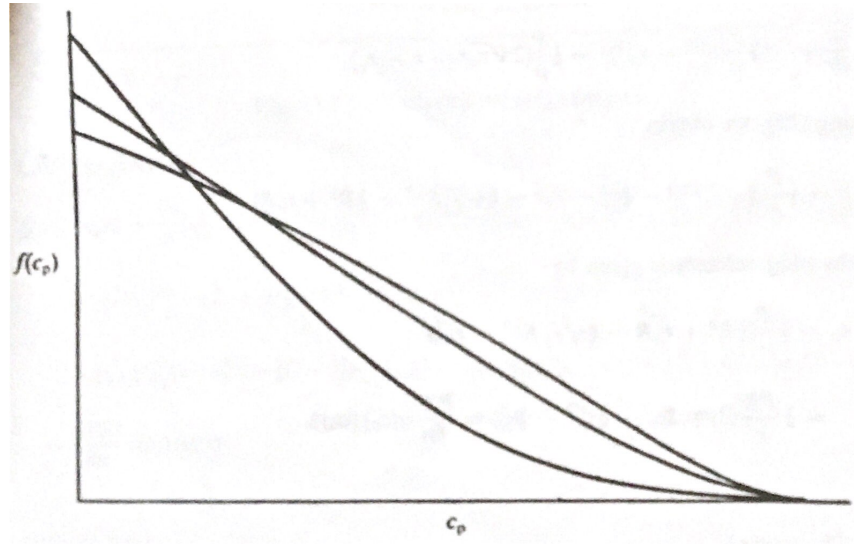
$$= \pi \frac{n}{3n+1} \left(\frac{P}{2\mu} \right)^{1/n} R^{\frac{1}{n}+3} f(c_p) \quad (\text{say}), \quad (11.3.9)$$

where $c_p = \frac{r_p}{R} = \frac{2\tau_0}{PR}$, $f(0) = 1$.

If Q_0 denotes the flux when there is no plug flow (i.e., when $\tau_0, c_p = 0$), we get

$$\frac{Q}{Q_0} = f(c_p) = f\left(\frac{r_p}{R}\right) = f\left(\frac{2\tau_0}{PR}\right). \quad (11.3.10)$$

This gives the relative change in Q with τ_0 . Fig. 11.3 illustrates the variation of $f(c_p)$ with c_p for various values of n . The figure shows that:

Figure 11.3: Variation of flux with τ_0

- (i) As τ_0 increases (μ and n remaining the same), the flux decreases rapidly and approaches zero as c_p approaches unity.
- (ii) If $n < 1$, the curve is always concave upwards; when $n = 1$, the curve is always a straight line in the beginning and becomes concave upwards; and when $n > 1$, the curve is convex in the beginning and becomes concave near $c_p = 1$, and, therefore, it has a point of inflexion.
- (iii) If τ_0 and μ are constant, the decline in Q is more when $n < 1$ and less when $n > 1$. If we put $n = 1$ in (11.3.8) and (11.3.9), we get the results for the special case of a Bingham plastic.
- (iv) If we put $\tau_0 = 0, r_p = 0$ in (11.3.8), we get results for the special case of a power-law fluid. Further, if we put $n = 1$, we obtain results for Poiseuille flow.

11.4 Flow of Casson Fluid in Circular Tube

Here

$$\tau^{\frac{1}{2}} = \mu^{\frac{1}{2}} e^{\frac{1}{2}} + \tau_0^{\frac{1}{2}} \quad (\tau \geq \tau_0) \quad (11.4.1)$$

so that for the non-core region, (11.3.4) gives

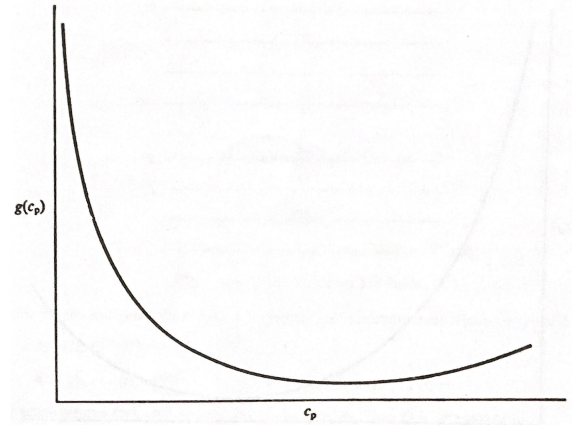
$$-\frac{dv}{dr} = e = \frac{1}{\mu^{1/2}} \left[\left(\frac{1}{2} r P \right)^{1/2} - \left(\frac{1}{2} r_p P \right)^{1/2} \right] \quad (11.4.2)$$

or

$$\frac{dv}{dr} = -\frac{1}{2} \frac{P}{\mu} \left[r^{1/2} - r_p^{1/2} \right]^2 = \frac{1}{2} \frac{P}{\mu} \left[2\sqrt{r_p r} - r - r_p \right]. \quad (11.4.3)$$

Integrating (11.4.3), we obtain

$$v = \frac{1}{2} \frac{P}{\mu} \left[\frac{4}{3} \sqrt{r_p} r^{3/2} - \frac{1}{2} r^2 - r_p r - \frac{4}{3} \sqrt{r_p} R^{3/2} + \frac{1}{2} R^2 + r_p R \right] \quad (11.4.4)$$

Figure 11.4: Variation of $g(c_p)$ with c_p

so that the plug velocity is given by

$$\begin{aligned}
 v_p &= \frac{1}{2} \frac{P}{\mu} \left[\frac{1}{2} R^2 + r_p R - \frac{4}{3} \sqrt{r_p} R^{3/2} - \frac{1}{6} r_p^2 \right] \\
 &= \frac{1}{4} \frac{P R^2}{\mu} \left[1 + 2c_p - \frac{8}{3} c_p^{1/2} - \frac{1}{6} c_p^2 \right] \\
 &= \frac{P R^2}{4\mu} g(c_p) \quad (\text{say}).
 \end{aligned} \tag{11.4.5}$$

Thus

$$\frac{v_p}{(v_p)_0} = g(c_p). \tag{11.4.6}$$

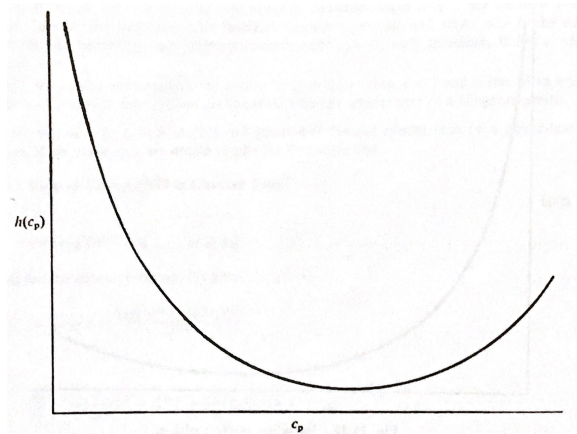
Figure 11.5: Variation of $h(c_p)$ with c_p

Figure 11.4 shows the variation of $g(c_p)$ with c_p . This shows that, as τ_0 increases (μ remaining the same), the plug velocity or the maximum velocity of flow decreases rapidly till c_p reaches 0.6 when the velocity is reduced to about 6 per cent of the value and then it rises slightly. For blood, small changes in τ_0 lead to significant changes in maximum velocity.

The flux Q is given by

$$\begin{aligned}
 Q &= \pi v_p r_p^2 + \frac{P\pi}{\mu} \left[\frac{8}{21} \sqrt{r_p} (R^{7/2} - r_p^{7/2}) - \frac{1}{8} (R^4 - r_p^4) - \frac{1}{3} r_p (R^3 - r_p^3) \right. \\
 &\quad \left. - \frac{2}{3} \sqrt{r_p} R^{3/2} (R^2 - r_p^2) + \frac{1}{4} R^2 (R^2 - r_p^2) + \frac{1}{2} r_p R (R^2 - r_p^2) \right] \\
 &= \frac{\pi P R^4}{4 \mu} c_p^2 g(c_p) + \frac{\pi P R^4}{\mu} \left[\frac{8}{21} \sqrt{c_p} (1 - c_p^{7/2}) - \frac{1}{8} (1 - c_p^4) - \frac{1}{3} c_p (1 - c_p^3) \right. \\
 &\quad \left. - \frac{2}{3} \sqrt{c_p} (1 - c_p^2) + \frac{1}{4} (1 - c_p^2) + \frac{1}{2} c_p (1 - c_p^2) \right] \\
 &= \frac{\pi P R^4}{8 \mu} h(c_p), \quad (\text{say})
 \end{aligned} \tag{11.4.7}$$

so that

$$\frac{Q}{Q_0} = h(c_p). \tag{11.4.8}$$

Figure 11.5 gives the graph of $h(c_p)$ against c_p . It shows that, as τ_0 increases (μ remaining the same), the flux decreases rapidly till $c_p = 0.6$ and till it has fallen to about 5 per cent of Q_0 and then it rises again. For blood, small changes in τ_0 can make significant changes in Q . The Casson fluid flows in the tube takes place only if $r_p < R$, i.e., if

$$2\tau_0 < PR. \tag{11.4.9}$$

Solved Problem: Flow of Casson Fluid in a Circular Tube

Consider the flow of a Casson fluid through a long circular tube with radius R . The Casson fluid model describes non-Newtonian fluids with a yield stress (τ_y) and a plastic viscosity (μ_p). The velocity profile for laminar flow in the tube can be expressed as:

$$v(r) = \frac{1}{4\mu_p} \left(R^2 - r^2 + \frac{\tau_y}{3\mu_p} \right)$$

where:

- $v(r)$ is the velocity of the fluid at radial position r ,
- R is the radius of the tube,
- μ_p is the plastic viscosity of the fluid, and
- τ_y is the yield stress of the fluid.

Determine the average velocity (\bar{v}) and the volumetric flow rate (Q) of the Casson fluid through the tube.

Solution

To find the average velocity (\bar{v}), we need to calculate the mean velocity over the cross-section of the tube. The average velocity (\bar{v}) can be calculated by integrating the velocity profile ($v(r)$) over the cross-section and dividing by the area:

$$\bar{v} = \frac{1}{A} \int_0^R v(r) \cdot 2\pi r \, dr$$

Substituting the given velocity profile:

$$\bar{v} = \frac{1}{A} \int_0^R \frac{1}{4\mu_p} \left(R^2 - r^2 + \frac{\tau_y}{3\mu_p} \right) \cdot 2\pi r \, dr$$

$$\bar{v} = \frac{\pi}{2\mu_p} \left(\int_0^R R^2 r - r^3 \, dr + \frac{\tau_y}{3\mu_p} \int_0^R r \, dr \right)$$

$$\bar{v} = \frac{\pi}{2\mu_p} \left(\left[\frac{1}{3}R^3 - \frac{1}{4}R^4 \right] + \frac{\tau_y}{3\mu_p} \left[\frac{1}{2}R^2 \right] \right)$$

$$\bar{v} = \frac{\pi}{2\mu_p} \left(\frac{1}{3}R^3 - \frac{1}{4}R^4 + \frac{1}{6}\tau_y R^2 \right)$$

Now, let's find the volumetric flow rate (Q). The volumetric flow rate (Q) is given by:

$$Q = \bar{v} \cdot A$$

Substituting the expression for \bar{v} and the cross-sectional area ($A = \pi R^2$):

$$Q = \frac{\pi}{2\mu_p} \left(\frac{1}{3}R^3 - \frac{1}{4}R^4 + \frac{1}{6}\tau_y R^2 \right) \cdot \pi R^2$$

$$Q = \frac{\pi^2}{2\mu_p} \left(\frac{1}{3}R^5 - \frac{1}{4}R^6 + \frac{1}{6}\tau_y R^4 \right)$$

$$Q = \frac{\pi^2}{6\mu_p} R^5 - \frac{\pi^2}{8\mu_p} R^6 + \frac{\pi^2}{12\mu_p} \tau_y R^4$$

Conclusion

We have derived expressions for the average velocity (\bar{v}) and the volumetric flow rate (Q) of a Casson fluid through a circular tube. These expressions provide insights into the flow characteristics of non-Newtonian fluids with yield stress. The calculations demonstrate the importance of rheological properties in determining fluid behavior in various engineering and biomedical applications.

Unit 12

Course Structure

- Fahraeus-Lindqvist Effect
 - Pulsatile Flow in Circular Rigid Tube
 - Blood Flow through Artery with Mild Stenosis
-

12.1 Newtonian Fluid Models

12.1.1 Fahraeus-Lindqvist Effect

Fahraeus-Lindqvist effect is an effect where the viscosity of a fluid, in particular blood, changes with the diameter of the tube, it travels through. More precisely, there is a decrease of viscosity as tubes diameter decreases (only if the vessel diameter is between 10 to 300 micrometers).

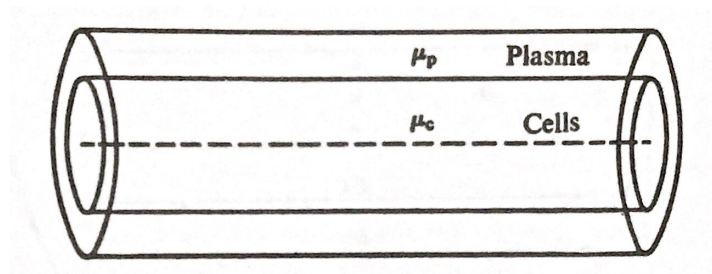


Figure 12.1: Two layer flow

In arteries, blood flows in two layers, a plasma layer near the walls consisting of only the plasma and almost no cells and a core layer consisting of red cells in plasma (see Fig. 12.1). If μ_p and μ_c are the viscosities of the two fluids, which are assumed Newtonian, we get

$$v_p = \frac{P}{4\mu_p}(R^2 - r^2), \quad R - \delta \leq r \leq R, \quad (12.1.1)$$

$$v_c = \frac{P}{4\mu_c}(R^2 - r^2) + \frac{P}{\mu_c} [R^2 - (R - \delta)^2] \left(\frac{\mu_c}{\mu_p} - 1 \right), \quad 0 \leq r \leq R - \delta. \quad (12.1.2)$$

Thus the velocity in the plasma layer is the same as it would be when the whole tube is filled with plasma, but the velocity in the core layer is more than it would be when the whole tube is filled with the core fluid. This is what is expected.

Now,

$$\begin{aligned} Q &= \int_0^{R-\delta} 2\pi r v_c dr + \int_{R-\delta}^R 2\pi r v_p dr \\ &= \frac{\pi P R^4}{8\mu_p} \left[1 - \left(1 - \frac{\delta}{R} \right)^4 \left(1 - \frac{\mu_p}{\mu_c} \right) \right]. \end{aligned} \quad (12.1.3)$$

If the whole tube were filled with a single Newtonian fluid with viscosity coefficient μ , we would have

$$Q = \frac{\pi P R^4}{8\mu}. \quad (12.1.4)$$

The two fluxes would be the same if

$$\mu = \mu_p \left[1 - \left(1 - \frac{\delta}{R} \right)^4 \left(1 - \frac{\mu_p}{\mu_c} \right) \right]^{-1}, \quad (12.1.5)$$

where μ is the *effective viscosity* of the two fluids taken together. From (12.1.5), it can be seen that the effective viscosity depends on R . In practice, $\frac{\delta}{R} \ll 1$, and hence (12.1.5) gives

$$\mu = \mu_p \left[1 - \frac{4\delta}{R} \left(\frac{\mu_c}{\mu_p} - 1 \right) \right]. \quad (12.1.6)$$

We find that, as R decreases, μ decreases. This explains the Fahraeus-Lindqvist effect. Here it has been assumed that δ is independent of R .

Pulsatile Flow in Circular Rigid Tube

We consider axially-symmetric flow in a rigid circular tube of radius R for which

$$v_r = 0, \quad v_\theta = 0, \quad v_z = v(r, z, t), \quad p = p(r, z, t) \quad (12.1.7)$$

so that the equation of continuity and the equation of motion are given by

$$\frac{\partial v}{\partial z} = 0, \quad \frac{\partial p}{\partial r} = 0, \quad (12.1.8)$$

$$\frac{\partial v}{\partial t} + v \frac{\partial v}{\partial z} = -\frac{1}{\rho} \frac{\partial p}{\partial z} + \nu \left(\frac{\partial^2 v}{\partial r^2} + \frac{1}{r} \frac{\partial v}{\partial r} + \frac{\partial^2 v}{\partial z^2} \right). \quad (12.1.9)$$

By using (12.1.8) and (12.1.9) becomes

$$\frac{\partial v}{\partial t} = -\frac{1}{\rho} \frac{\partial p}{\partial z} + \nu \frac{\partial}{\partial r} \left(r \frac{\partial v}{\partial r} \right). \quad (12.1.10)$$

From (12.1.7) and (12.1.8), v is a function of r and t only and p is a function of z and t only. From (12.1.10), $\partial p/\partial z$ is a function of t only. Thus for a pulsatile sinusoidal flow, we take

$$\frac{\partial p}{\partial z} = -P e^{i\omega t}, \quad (i = \sqrt{-1}), \quad (12.1.11)$$

$$v(r, t) = V(r) e^{i\omega t}. \quad (12.1.12)$$

This means that the real part gives the velocity for pressure gradient $P \cos(\omega t)$ and the imaginary part gives the velocity for the pressure gradient $P \sin \omega t$.

From (12.1.10)-(12.1.12),

$$i\omega V \rho = P + \mu \left(\frac{d^2 V}{dr^2} + \frac{1}{r} \frac{dV}{dr} \right) \quad (12.1.13)$$

$$\Rightarrow \frac{d^2 V}{dr^2} + \frac{1}{r} \frac{dV}{dr} - \frac{i\omega}{\mu} \rho V = -\frac{P}{\mu}. \quad (12.1.14)$$

Now the general solution of the equation

$$\frac{d^2 y}{dx^2} + \frac{1}{x} \frac{dy}{dx} - k^2 y = 0 \quad (12.1.15)$$

is

$$y = A J_0(ikx) + B Y_0(ikx), \quad (12.1.16)$$

where both $J_0(x)$ and $Y_0(x)$ are Bessel functions of zero order and are of the first and second kind, respectively.

Thus the solution of (12.1.14) is

$$V = A J_0 \left[\left(i^{\frac{3}{2}} \sqrt{\frac{\omega \rho}{\mu}} \right) r \right] + B Y_0 \left[\left(i^{\frac{3}{2}} \sqrt{\frac{\omega \rho}{\mu}} \right) r \right] + \frac{P}{\omega \rho i}. \quad (12.1.17)$$

Since v and V have to be finite on the axis (i.e., at $r = 0$) and $Y_0(0)$ is not finite, B has to be zero. Also, because of the no-slip condition $v(r) = 0$ when $r = R$, we have

$$A J_0 \left[\left(i^{\frac{3}{2}} \sqrt{\frac{\omega \rho}{\mu}} \right) R \right] + \frac{P}{\omega \rho i} = 0, \quad B = 0. \quad (12.1.18)$$

Let

$$\alpha^2 = \frac{\omega \rho}{\mu} R^2 = \frac{\omega R^2}{\nu} \quad (12.1.19)$$

so that

$$A = \frac{P}{\omega \rho} i \frac{1}{J_0(i^{3/2} \alpha)}, \quad (12.1.20)$$

$$V(r) = -\frac{P}{\omega \rho} i \left[1 - \frac{J_0(i^{3/2} \alpha s)}{J_0(i^{3/2} \alpha)} \right], \quad (12.1.21)$$

where

$$s = \frac{r}{R}. \quad (12.1.22)$$

Finally, we get

$$v(r, t) = -\frac{PR^2}{\mu\alpha^2} i \left[1 - \frac{J_0(i^{3/2}\alpha s)}{J_0(i^{3/2}\alpha)} \right] e^{i\omega t}. \quad (12.1.23)$$

The volumetric flow rate Q is given by

$$\begin{aligned} Q &= \int_0^R v 2\pi r \, dr \\ &= 2\phi R^2 \int_0^1 v s \, ds \\ &= -\frac{2\pi PR^4}{\mu\alpha^2} i e^{i\omega t} \left[\int_0^1 s \, ds - \frac{1}{J_0(i^{3/2}\alpha)} \int_0^1 J_0(i^{3/2}\alpha s) s \, ds \right] \\ &= -\frac{\pi PR^4}{\mu\alpha^2} i e^{i\omega t} \left[1 - \frac{2}{J_0(i^{3/2}\alpha)} \int_0^{i^{3/2}\alpha} \left(\frac{x J_0(x)}{i^3 \alpha^2} \right) dx \right]. \end{aligned} \quad (12.1.24)$$

But

$$\int x J_0(x) \, dx = x J_1(x) \quad (12.1.25)$$

so that

$$\begin{aligned} Q &= -\frac{\pi PR^4}{\mu\alpha^2} i e^{i\omega t} \left[1 - \frac{2i}{J_0(i^{3/2}\alpha)} \frac{i^{3/2}\alpha J_1(i^{3/2}\alpha)}{\alpha^2} \right] \\ &= -\frac{\pi R^4}{\mu\alpha^2} i P \left[1 - \frac{2J_1(i^{3/2}\alpha)}{i^{3/2}\alpha J_0(i^{3/2}\alpha)} \right] e^{i\omega t} \\ &= \frac{\pi R^4 P}{\mu\alpha^2 i} X(\alpha) e^{i\omega t} \quad (\text{say}). \end{aligned} \quad (12.1.26)$$

Now the series expansion for $J_0(x)$ and $J_1(x)$ are given by

$$J_0(x) = 1 - \frac{1}{2}x^2 + \dots, \quad (12.1.27)$$

$$J_1(x) = \frac{x}{2} - \frac{(x/2)^3}{1^2 \cdot 2} + \frac{(x/2)^5}{1^2 \cdot 2^2 \cdot 3} - \dots \quad (12.1.28)$$

For small values of α ,

$$X(\alpha) = 1 - \frac{2 \left[\frac{i^{3/2}\alpha}{2} - \left(\frac{i^{3/2}\alpha}{2/2} \right)^3 + \dots \right]}{i^{3/2} \left[1 - \left(\frac{i^{3/2}\alpha}{2} \right)^2 + \dots \right]} = 1 - \frac{1 - \frac{i^3\alpha^2}{8} + \dots}{1 - \frac{i^3\alpha^2}{4} + \dots} = \frac{i\alpha^2}{8} + O(\alpha^4) \quad (12.1.29)$$

From (12.1.24) and (12.1.29), we have

$$Q = \left[\frac{\pi R^4 P}{8} + O(\alpha^2) \right] e^{i\omega t}. \quad (12.1.30)$$

From (12.1.19) as $\alpha \rightarrow 0$, $\omega \rightarrow 0$ and then from (12.1.30), $Q \rightarrow Q_0$, where

$$Q_0 = \frac{\pi R^4 P}{8\mu} e^{i\omega t}, \quad |Q_0| = \frac{\pi R^4 P}{8\mu}, \quad (12.1.31)$$

and $|Q_0|$ is the volumetric flow rate for a constant pressure gradient and is the same as for Poiseuille law for steady flow. If

$$X(\alpha) = X_1(\alpha) + iX_2(\alpha), \quad (12.1.32)$$

(12.1.24) gives

$$Q = \frac{\pi R^4}{\mu \alpha^2} \left[\left\{ X_2(\alpha) \cos \omega t + X_1(\alpha) \sin \omega t \right\} - i \left\{ X_1(\alpha) \cos(\omega t) - X_2(\alpha) \sin \omega t \right\} \right] \quad (12.1.33)$$

The real part gives the flux when the pressure gradient is $P \cos \omega t$ and the imaginary part gives the flux when it is $P \sin \omega t$.

12.2 Blood Flow through Artery with Mild Stenosis

12.2.1 Effect of Stenosis

The term *stenosis* denotes the narrowing of the artery due to the development of arteriosclerotic plaques or other types of abnormal tissue development. As the growth projects into the lumen (cavity) of the artery, blood flow is obstructed. The obstruction may damage the internal cells of the wall and may lead to further growth of the stenosis. Thus there is a coupling between the growth of a stenosis and the flow of blood in the artery since each affects the other.

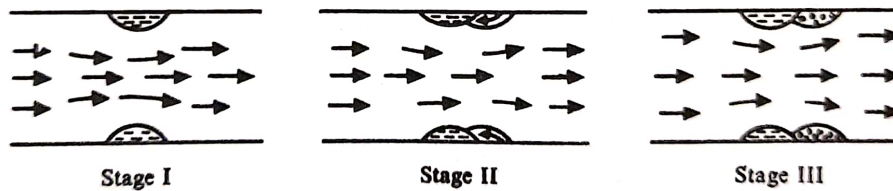


Figure 12.2: Three stages of stenosis growth.

The stenosis growth usually passes through three stages, as shown in Fig. 12.2. In stage I, there is no separation of flow and there is no back flow. In stage II, the flow is laminar, but separation occurs and there is back flow. In stage III, turbulence develops in a certain region of the down stream. We shall discuss here only Stage I, called *mild stenosis*.

The development of stenosis in artery can have serious consequences and can disrupt the normal functioning of the circulatory system. In particular, it may lead to

- (i) increased resistance to flow, with possible severe reduction in blood flow;
- (ii) increased danger of complete occlusion (obstruction);
- (iii) abnormal cellular growth in the vicinity of the stenosis, which increases the intensity of the stenosis; and
- (iv) tissue damage leading to post-stenosis dilatation.

12.2.2 Analysis of Mild Stenosis

We shall consider the steady flow of a Newtonian fluid past an axially-symmetric stenosis whose surface is given by

$$\frac{R}{R_0} = 1 - \frac{\delta}{2R_0} \left(1 + \cos \frac{\pi z}{z_0} \right), \quad (12.2.1)$$

where the notations are clear from Fig. XX. We shall assume further that

$$\frac{\delta}{R_0} \ll 1, \quad \frac{R_0}{z_0} \approx 0(T), \quad Re \frac{\delta}{z_0} \ll 1, \quad (12.2.2)$$

where Re is the Reynolds number of fluid flow. By carrying out an order of magnitude analysis on these basic

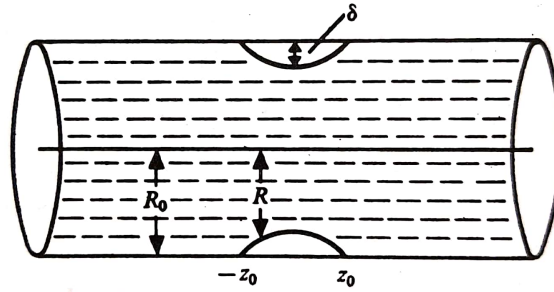


Figure 12.3: Mild stenosis.

equations of motion in cylindrical polar coordinates, it can be shown that the radial velocity can be neglected in relation to axial velocity v which is determined by

$$0 = -\frac{\partial p}{\partial z} + \mu \left(\frac{\partial^2 v}{\partial r^2} + \frac{1}{r} \frac{\partial v}{\partial r} \right), \quad (12.2.3)$$

$$0 = -\frac{\partial p}{\partial r}, \quad (12.2.4)$$

or

$$-P(z) = \frac{\mu}{r} \frac{\partial}{\partial r} \left(r \frac{\partial v}{\partial r} \right). \quad (12.2.5)$$

The no-slip condition on the stenosis surface gives

$$\begin{aligned} v = 0 & \quad \text{at} \quad r = R(z), \quad -z_0 \leq z \leq z_0, \\ v = 0 & \quad \text{at} \quad r = R_0, \quad |z| \geq z_0. \end{aligned} \quad (12.2.6)$$

Thus for a mild stenosis, the main difference from the usual Poiseuille flow is that the pressure gradient and axial velocity are functions of z also. However, for a stenosis in stage II or stage III, the radial velocity can be significant, and turbulence may have to be considered. Obviously then, the analysis is more complicated.

Integrating (12.2.5), we get

$$r \frac{\partial v}{\partial r} = -P(z) \frac{r^2}{2\mu} + A(z), \quad (12.2.7)$$

but $A(z) = 0$ since $\frac{\partial v}{\partial r} = 0$ on the axis. Integrating again and using (12.2.6), we get

$$v = -\frac{P(z)}{4\mu} \left[r^2 - R^2(z) \right]. \quad (12.2.8)$$

If Q is the flux through the tube, then

$$Q = \int_0^{R(z)} v 2\pi r \, dr = \frac{\pi P(z)}{8\mu} R^4(z). \quad (12.2.9)$$

Since Q is constant for all section of the tube, the pressure gradient varies inversely as the fourth power of the surface distance of the stenosis from the axis of the artery so that it (the pressure gradient) is minimum at the middle of the stenosis and is maximum at the ends.

Unit 13

Course Structure

- Peristaltic Flows in Tubes and Channel
 - Peristaltic Motion in a Channel
 - Long-wavelength Approximation
 - Further discussion on Long-wavelength Approximation
-

13.1 Peristaltic Flows in Tubes and Channel

Peristaltic flows occur in biological systems and engineering applications where fluids are transported through tubes or channels due to rhythmic contractions and relaxations of the tube walls. This phenomenon is commonly observed in biological processes such as digestion, blood circulation, and urine propulsion in the ureters. Peristaltic pumping is also utilized in various engineering applications, including microfluidics, biotechnology, and medical devices.

The mechanism of peristaltic flow involves the periodic compression and expansion of the tube or channel, which propels the fluid in the desired direction. This rhythmic motion creates traveling waves along the tube, leading to the transport of fluid particles. The fluid motion induced by peristalsis is characterized by complex flow patterns, including axial flow, secondary flows, and mixing effects.

Mathematically modeling peristaltic flows often involves solving nonlinear partial differential equations describing fluid dynamics, coupled with equations governing the deformation of the tube walls. Simplified analytical solutions can be obtained under certain assumptions, such as the long-wavelength approximation or low Reynolds number flow.

Peristaltic flows exhibit unique features compared to other types of fluid transport mechanisms. For example, peristalsis can generate net flow against pressure gradients, enabling fluid transport in uphill directions. This property is exploited in biological systems to overcome obstacles and transport fluids efficiently.

In engineering applications, peristaltic pumping offers advantages such as precise control of flow rates, gentle handling of sensitive fluids, and compatibility with microscale devices. These characteristics make peristaltic pumps suitable for a wide range of applications, including drug delivery systems, chemical processing, and lab-on-a-chip devices.

Overall, peristaltic flows play a crucial role in both biological processes and engineering applications, providing an efficient and versatile method for fluid transport in tubes and channels.

13.1.1 Peristaltic Flows in Biomechanics

Peristaltic flow is the motion generated in the fluid contained in a distensible tube when a progressive wave of area contraction and expansion travels along the wall of the tube. The elasticity of the tube wall does not directly enter into our calculations, but it affects the flow through the progressive wave travelling along its length. This wave determines the boundary conditions since the no-slip condition has to be used now on a moving undulating wall surface.

Peristaltic motion is involved in

- (i) expansion and contractions (or vasomotion) of small blood vessels,
- (ii) cilia transport through the ducts efferents of the male reproductive organ,
- (iii) transport of spermatozoa in cervical canal,
- (iv) transport of chyme in small intestines,
- (v) functioning of ureter, and
- (i) transport of bile.

The wide occurrence of peristaltic motion should not be surprising since it results physiologically from neuro-muscular properties of any tubular smooth muscle.

We now consider peristaltic motion in channels or tubes. The fluid involved may be non-Newtonian (e.g., power-law, viscoelastic, or micropolar fluid) or Newtonian, and the flow may take place in two layers (a core layer and a peripheral layer). The equations of motion in their complete generality do not admit of simple solutions and we have to look for reasonable approximations. For this we first transform these equations in terms of dimensionless variables.

Peristaltic Motion in a Channel : Characteristic Dimensionless Parameters

We consider the flow of a homogeneous Newtonian fluid through a channel of width $2a$. Travelling sinusoidal waves are supposed on the elastic walls of the channel. Taking the x -axis along the centre line of the channel and the y -axis normal to it, the equations of the walls are given by

$$Y = \eta(X, T) = \pm a \left[1 + \epsilon \cos \left\{ \frac{2\pi}{\lambda} (x - ct) \right\} \right] \quad (13.1.1)$$

where ϵ is the amplitude ratio, λ the wavelength, and c the phase velocity of the waves. Now using Eq. 9.10 of Unit 9, the stream function $\psi(X, Y)$ for the two-dimensional motion satisfies the equation

$$\nu \nabla^4 \psi = \nabla^2 \Psi_T + \Psi_Y \nabla^2 \Psi_X - \Psi_X \nabla^2 \Psi_Y, \quad (13.1.2)$$

where the velocity components are given by

$$U = \Psi_Y, \quad V = -\Psi_X. \quad (13.1.3)$$

Assuming that the walls have only transverse displacements at all times, we get the boundary conditions as

$$U = 0, \quad V = \pm \frac{2\pi ac\epsilon}{\lambda} \sin \left\{ \frac{2\pi}{\lambda}(X - cT) \right\} \quad \text{at} \quad Y = \pm \eta(X, T). \quad (13.1.4)$$

We now introduce the dimensionless variables and parameters

$$x = \frac{X}{\lambda}, \quad y = \frac{Y}{a}, \quad t = \frac{cT}{\lambda}, \quad \psi = \frac{\Psi}{ac}, \quad \delta = \frac{a}{\lambda}, \quad Re = \frac{ac}{\nu} \quad (13.1.5)$$

so that (13.1.2) becomes

$$\frac{1}{\delta Re} \left[\delta^2 \frac{\partial^2}{\partial x^2} + \frac{\partial^2}{\partial y^2} \right]^2 \psi = \left[\delta^2 \frac{\partial^2}{\partial x^2} + \frac{\partial^2}{\partial y^2} \right] \psi_t + \psi_y \left[\delta^2 \frac{\partial^2}{\partial x^2} + \frac{\partial^2}{\partial y^2} \right] \psi_x - \psi_x \left[\delta^2 \frac{\partial^2}{\partial x^2} + \frac{\partial^2}{\partial y^2} \right] \psi_y. \quad (13.1.6)$$

The boundary conditions becomes

$$\psi_y = 0, \quad \psi_x = 2\pi\epsilon \sin(x - \epsilon). \quad (13.1.7)$$

Thus the basic partial differential equations and the boundary condition together involve three dimensionless parameters:

- (i) The Reynolds number, Re determined by the phase velocity, half the mean distance between the plates, and the kinematic viscosity. (This number is small if the distance between the walls is small or the phase velocity is small or the kinematic viscosity is large.)
- (ii) The wave number δ which is small if the wavelength is large as compared to the distance between the walls.
- (iii) The amplitude ratio ϵ which is small if the amplitude of the wave is small as compared to the distance between the walls.

In obtaining the equations for the stream function, the pressure gradient was eliminated. Hence there may arise a fourth dimensionless parameter, depending on the pressure gradient. Non-Newtonian fluids give rise to additional dimensionless parameters, depending on the parameters occurring in the constitutive equations of the fluids.

It is not possible to solve (13.1.2) for arbitrary values of δ, ϵ, Re and, therefore, this equation is solved under, among others, the following alternative sets of assumptions:

- (i) $\epsilon \ll 1$, and Stoke's assumption of slow motion so that inertial terms can be neglected.
- (ii) $\epsilon \ll 1, \delta \ll 1$.
- (iii) $\delta \ll 1, Re \ll 1$, but ϵ is arbitrary
- (iv) $\epsilon \ll 1, Re \ll 1$, but δ is arbitrary.

The initial flow may be taken as the Hagen-Poiseuille flow.

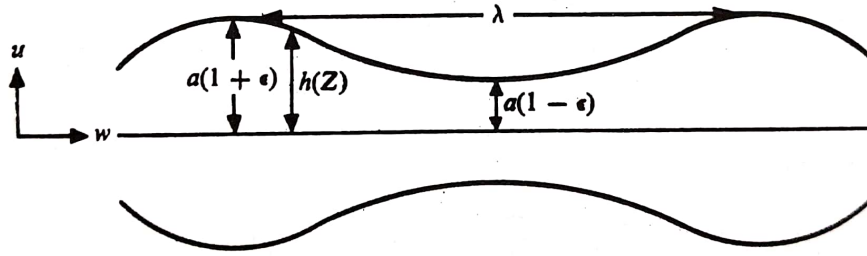


Figure 13.1: Tube geometry.

Long-wavelength Approximation to Peristaltic Flow in a Tube

Let the equation of the tube surface be given by

$$h(Z, t) = a \left[1 + \epsilon \sin \left\{ \frac{2\pi}{\lambda} (Z - ct) \right\} \right], \quad (13.1.8)$$

where a is the undisturbed radius of the tube and ϵ the amplitude ratio, $a(1 + \epsilon)$ and $a(1 - \epsilon)$ are the maximum and minimum disturbed radii, and λ is the wave velocity and c the phase velocity (see Fig. 13.1). Under the assumptions $\frac{a}{\lambda} \ll 1$ and $\frac{ac}{\nu} \ll 1$, we conduct an order of magnitude study of the various terms in the equation of continuity and equations of motion in cylindrical polar coordinates to find

$$\frac{\partial p}{\partial R} \ll \frac{\partial p}{\partial Z} \quad (13.1.9)$$

so that p is only weakly dependent on R and we can take

$$p = p(Z, t). \quad (13.1.10)$$

Now it is convenient to use the moving coordinate system (r, z) travelling with the wave so that

$$r = R, \quad z = Z - ct. \quad (13.1.11)$$

In this system, p is a function of z only. The equations of continuity and motion reduce respectively to

$$\frac{\partial}{\partial r}(ru) + \frac{\partial}{\partial z}(rw) = 0, \quad (13.1.12)$$

$$\frac{dp}{dz} = \mu \left(\frac{\partial^2 w}{\partial r^2} + \frac{1}{r} \frac{\partial w}{\partial r} \right) = \frac{\mu}{r} \frac{\partial}{\partial r} \left(r \frac{\partial w}{\partial r} \right), \quad (13.1.13)$$

where u and w are the velocity components for the motion of the fluid in relation to the moving coordinate system.

The boundary conditions for solving (13.1.12) and (13.1.13) are

$$u = \frac{\partial h}{\partial t}, \quad w = -c \quad \text{at} \quad r = h. \quad (13.1.14)$$

Integrating (13.1.13) at the constant z , we obtain

$$w = -c - \frac{1}{4\mu} \frac{dp}{dz} (h^2 - r^2). \quad (13.1.15)$$

To an observer moving with velocity c in the axial direction, the pressure and flow appear stationary. Hence the flow rate q measured in the moving coordinate system is a constant, independent of position and time. Now

$$q = 2\pi \int_0^h r w \, dr. \quad (13.1.16)$$

Using (13.1.15) we have

$$q = \pi h^2 c - \frac{\pi h^4}{8\mu} \frac{dp}{dz} \quad (13.1.17)$$

or

$$\frac{dp}{dz} = -\frac{8\mu q}{\pi h^4} - \frac{8\mu c}{h^2}. \quad (13.1.18)$$

Substituting in (13.1.15), we get

$$w = -c + 2(h^2 - r^2) \left[\frac{q}{\pi h^4} + \frac{c}{h^2} \right]. \quad (13.1.19)$$

To find the transverse velocity component u , we integrate the continuity equation (13.1.12) at the constant z . Remembering that $u = 0$ at $r = 0$, we obtain

$$ru = - \int_0^r r \frac{\partial w}{\partial z} dr. \quad (13.1.20)$$

Using (13.1.19) and remembering that $u(0, z) = 0$, we get

$$u = -\frac{dh}{dz} \left(\frac{cr^3}{h^3} - \frac{2qr}{\pi h^3} + \frac{2qr^3}{\pi h^5} \right). \quad (13.1.21)$$

We now revert to the stationary coordinate system with the coordinates R, Z , the velocity components U, W , and the flow rate Q so that

$$W = w + c, \quad U = u, \quad (13.1.22)$$

$$Q = 2\pi \int_0^h WR \, dR \quad \text{or} \quad Q = q + \pi ch^2. \quad (13.1.23)$$

Let \bar{Q} denote the time average of Q over a complete time period T for h so that

$$T = \frac{\lambda}{c} \quad (13.1.24)$$

$$\bar{Q} = \frac{1}{T} \int_0^T Q \, dt = q + \pi ca^2 \left(1 + \frac{1}{2}\epsilon^2 \right). \quad (13.1.25)$$

Further Discussion on Long-wavelength Approximation

From (13.1.8) and (13.1.11),

$$h(z) = a \left[1 + \epsilon \sin \left\{ \frac{2\pi}{\lambda} (Z - ct) \right\} \right] = a \left[1 + \epsilon \sin \left(\frac{2\pi}{\lambda} z \right) \right] \quad (13.1.26)$$

$$\frac{dh}{dz} = \frac{2\pi a\epsilon}{\lambda} \cos \left(\frac{2\pi}{\lambda} z \right) = \frac{2\pi a\epsilon}{\lambda} \cos \left\{ \frac{2\pi}{\lambda} (Z - ct) \right\}. \quad (13.1.27)$$

From (13.1.11), (13.1.19), (13.1.21) and (13.1.22) we have

$$U = -\frac{2\pi a\epsilon}{\lambda} \cos \left\{ \frac{2\pi}{\lambda}(Z - ct) \right\} \left[\frac{cR^3}{h^3} - \frac{2qR}{\pi h^3} + \frac{2qR^3}{\pi h^5} \right] \quad (13.1.28)$$

$$W = 2 \left[\frac{q}{\pi h^4} + \frac{c}{h^2} \right] (h^2 - R^2). \quad (13.1.29)$$

Here h is determined as a function of Z and t from (13.1.26), and q is known from (13.1.25) after \bar{Q} is determined experimentally.

To determine the pressure drop across a length equal to the wavelength λ , we integrate (13.1.18) to get

$$\begin{aligned} (\Delta p)_k &= -\frac{8\mu q}{\pi a^4} \int_0^\lambda \frac{dz}{[1 + \epsilon \sin(\frac{2\pi}{\lambda}z)]^4} - \frac{8\mu c}{\pi a^2} \int_0^\lambda \frac{dz}{[1 + \epsilon \sin(\frac{2\pi}{\lambda}z)]^2} \\ &= -\frac{4\mu\lambda}{\pi^2 a^4} \int_0^{2\pi} \left[\frac{q}{[1 + \epsilon \sin \tau]^4} + \frac{\pi c a^2}{[1 + \epsilon \sin \tau]^2} \right] d\tau \\ &= -\frac{4\mu\lambda}{\pi a^4} \left[q \frac{2 + 3\epsilon^2}{(1 - \epsilon^2)^{7/2}} + \frac{2\pi c a^2}{(1 - \epsilon^2)^{3/2}} \right]. \end{aligned} \quad (13.1.30)$$

The pressure drop across one wavelength would be zero if

$$q = -2\pi c \frac{a^2(1 - \epsilon^2)^2}{2 + 3\epsilon^2}, \quad (13.1.31)$$

and then from (13.1.25),

$$\bar{Q} = \frac{\pi a^2 c (16\epsilon^2 - \epsilon^4)}{2(2 + 3\epsilon^2)}. \quad (13.1.32)$$

Substituting (13.1.31) in (13.1.28) and (13.1.29), we get

$$U = -\frac{2\pi a c \epsilon R}{\lambda h^3} \cos \left\{ \frac{2\pi}{\lambda}(Z - ct) \right\} \left[R^2 + \frac{4c a^2 (1 - \epsilon^2)^2}{2 + 3\epsilon^2} \left(1 - \frac{R^2}{h^2} \right) \right], \quad (13.1.33)$$

$$W = 2c \left[1 - \frac{2a^2(1 - \epsilon^2)^2}{h^2(2 + 3\epsilon^2)} \right] \left(1 - \frac{R^2}{h^2} \right). \quad (13.1.34)$$

For every fixed z , we can draw the velocity profiles U/c and W/C in the special case $(\Delta p)_\lambda = 0$. If $(\Delta p)_\lambda \neq 0$, then velocity profiles will depend also on q .

Solved Problem: Long-wavelength Approximation to Peristaltic Flow in a Tube

Consider the peristaltic flow of an incompressible fluid with viscosity μ through a long circular tube of radius R . The long-wavelength approximation to the velocity profile of the fluid is given by:

$$v(r, t) = -\frac{a^2}{4\mu} \frac{\partial p}{\partial x} R^2$$

where:

- $v(r, t)$ is the velocity of the fluid at radial position r and time t ,

- a is the amplitude of the peristaltic wave,
- μ is the viscosity of the fluid,
- p is the pressure in the tube, and
- x is the axial coordinate.

Determine the volumetric flow rate (Q) of the fluid through the tube in terms of the amplitude a and the pressure gradient $\frac{\partial p}{\partial x}$.

Solution

The volumetric flow rate (Q) can be calculated by integrating the velocity profile over the cross-section of the tube and multiplying by the cross-sectional area:

$$Q = \int_0^R v(r, t) \cdot 2\pi r \, dr$$

Substituting the given velocity profile:

$$Q = \int_0^R -\frac{a^2}{4\mu} \frac{\partial p}{\partial x} R^2 \cdot 2\pi r \, dr$$

$$Q = -\frac{a^2}{4\mu} \frac{\partial p}{\partial x} R^2 \int_0^R 2\pi r \, dr$$

$$Q = -\frac{a^2}{4\mu} \frac{\partial p}{\partial x} R^2 [\pi r^2]_0^R$$

$$Q = -\frac{a^2}{4\mu} \frac{\partial p}{\partial x} R^2 [\pi R^2 - \pi \cdot 0^2]$$

$$Q = -\frac{a^2}{4\mu} \frac{\partial p}{\partial x} R^2 \cdot \pi R^2$$

$$Q = -\frac{a^2}{4\mu} \frac{\partial p}{\partial x} \pi R^4$$

$$Q = -\frac{a^2}{4\mu} \frac{\partial p}{\partial x} A$$

where A is the cross-sectional area of the tube.

Conclusion

The volumetric flow rate (Q) of the fluid through the tube in terms of the amplitude a and the pressure gradient $\frac{\partial p}{\partial x}$ is $Q = -\frac{a^2}{4\mu} \frac{\partial p}{\partial x} A$. This expression provides insights into the flow characteristics of peristaltic flow in long tubes.

Unit 14

Course Structure

- Two Dimensional Flow in Renal Tubule
 - Function of Renal Tubule
 - Basic Equations and Boundary Conditions
 - Solution When Radial Velocity at Wall Decreases Linearly with z
-

14.1 Two Dimensional Flow in Renal Tubule

Renal tubules are the functional units of the kidney responsible for the filtration, reabsorption, and secretion of substances from the blood to form urine. The flow of fluid through renal tubules exhibits complex dynamics, including two-dimensional flow patterns that play a crucial role in kidney function.

The two-dimensional flow in renal tubules refers to the flow of fluid along the length of the tubule as well as across its cross-section. This flow pattern is influenced by various factors, including the structure of the tubule, the properties of the fluid, and the physiological processes occurring within the kidney.

Mathematically modeling two-dimensional flow in renal tubules involves solving partial differential equations that describe fluid dynamics in two dimensions. These equations take into account factors such as fluid viscosity, tubule geometry, and boundary conditions imposed by the tubule walls.

Understanding two-dimensional flow in renal tubules is essential for elucidating key physiological processes in the kidney, such as tubular reabsorption and secretion. For example, the distribution of solutes and ions across the cross-section of the tubule affects their transport properties and determines their concentration gradients along the tubule length.

Two-dimensional flow in renal tubules also plays a role in the formation and regulation of urine volume and composition. By controlling the rate and direction of fluid flow, the kidney can adjust the concentration of solutes in the urine and maintain fluid balance in the body.

In addition to its physiological significance, the study of two-dimensional flow in renal tubules has practical implications for medical research and clinical practice. Insights gained from mathematical modeling and experimental studies of renal tubule flow can inform the development of therapies for kidney diseases and disorders.

Overall, two-dimensional flow in renal tubules is a complex yet essential aspect of kidney function, with implications for both basic science and clinical medicine.

14.1.1 Function of Renal Tubule

The functional unit of the kidney is called the *nephron* or *renal tubule*, and each kidney has about 1 million of these tubules. One major part of a nephron is the glomerular tuft through which blood coming from the renal artery and afferent arterioles is filtered. The glomerular filtrate is essentially identical to plasma, and no chemical separation occurs upto this point. If the kidneys deliver this filtrate for excretion, the body loses many valuable materials, including water, at a rate faster than the one at which they can be supplied by synthesis or feeding. The rest of the nephron therefore recovers these valuable materials and returns them to the blood. Thus about 80 per cent of the filtrate is reabsorbed in the proximal tubule, and of the remaining, about 95 per cent is further reabsorbed by the end of the collecting ducts.

This reabsorption or seepage creates a radial component of the velocity in the cylindrical tubule, which must be considered along with the axial component of the velocity (see Fig. 14.1). Due to loss of fluid from

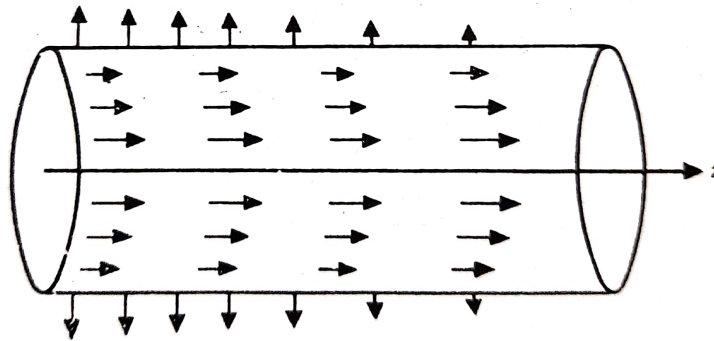


Figure 14.1: Two-dimensional flow in renal tubule.

the walls, both the radial and axial velocities decrease with z . Mathematically, we have to solve the problem of flow of viscous fluid in circular cylinder when there are axial and radial components of velocity and the radial velocity at all points on the surface of the cylinder is prescribed and is a decreasing function $\phi(z)$ of z .

14.1.2 Basic Equations and Boundary Conditions

At the outset, we may note that the equation of motion can be simplified since the inertial term in relation to the viscous terms can be neglected. The average tubular radius is about 10^{-3} cm, the average velocity is about 10^{-1} cm/sec, since this is very much less than one, we neglect the inertial terms to get the following equations of continuity and motion

$$\frac{1}{r} \frac{\partial}{\partial r}(rv_r) + \frac{\partial v_z}{\partial z} = 0, \quad (14.1.1)$$

$$\frac{1}{\mu} \frac{\partial p}{\partial r} = \frac{\partial}{\partial r} \left(\frac{1}{r} \frac{\partial}{\partial r}(rv_r) \right) + \frac{\partial^2 v_r}{\partial z^2}, \quad (14.1.2)$$

$$\frac{1}{\mu} \frac{\partial p}{\partial z} = \frac{\partial}{\partial r} \left(\frac{1}{r} \frac{\partial}{\partial r}(rv_z) \right) + \frac{\partial^2 v_z}{\partial z^2}, \quad (14.1.3)$$

The boundary conditions are

$$\frac{\partial v_z}{\partial r} = 0, \quad v_r = 0, \quad v_z = \text{finite} \quad \text{at} \quad r = 0, \quad (14.1.4)$$

$$v_z = 0, \quad v_r = \phi(z) \quad \text{at} \quad r = R, \quad (14.1.5)$$

$$p = p_0 \quad \text{at} \quad z = 0, \quad (14.1.6)$$

$$p = p_L \quad \text{at} \quad z = L. \quad (14.1.7)$$

Eliminating p between (14.1.2) and (14.1.3), we get

$$\frac{\partial^2}{\partial r \partial z} \left[\frac{1}{r} \frac{\partial}{\partial z} (r v_z) \right] + \frac{\partial^3 v_r}{\partial z^3} = \frac{\partial}{\partial r} \left[\frac{1}{r} \frac{\partial}{\partial r} \left(r \frac{v_z}{\partial r} \right) \right] + \frac{\partial^3 v_z}{\partial z^2 \partial r}. \quad (14.1.8)$$

Taking the partial derivative of this equation with respect to z and substituting from (14.1.1), we get

$$\left[\frac{\partial}{\partial r} \left(\frac{1}{r} \frac{\partial}{\partial r} \left(r \frac{\partial}{\partial r} \left(\frac{1}{r} \frac{\partial}{\partial r} \right) \right) \right) \right] + 2 \frac{\partial}{\partial r} \left(\frac{1}{r} \frac{\partial}{\partial r} \left(\frac{\partial^2}{\partial z^2} \right) \right) + \frac{1}{r} \frac{\partial^4}{\partial z^4} \right] (r v_r) = 0. \quad (14.1.9)$$

Alternatively, we can satisfy (14.1.1) by taking

$$v_r = \frac{1}{r} \frac{\partial \psi}{\partial z}, \quad v_z = -\frac{1}{r} \frac{\partial \psi}{\partial r}. \quad (14.1.10)$$

Substituting (14.1.9) in (14.1.7), we get

$$D^2(D^2\psi) = 0, \quad (14.1.11)$$

where the operator D^2 is defined by

$$D^2 \equiv \frac{\partial^2}{\partial r^2} - \frac{1}{r} \frac{\partial}{\partial r} + \frac{\partial^2}{\partial z^2}. \quad (14.1.12)$$

If

$$v_r = f(r)g(z), \quad (14.1.13)$$

then the form of (14.1.8) suggests that an analytical solution may be possible if

$$g(z) = A_0 + A_1 z \quad \text{or} \quad g(z) = A_2 e^{-\gamma z}. \quad (14.1.14)$$

From (14.1.5) since $v_r = \phi(z)$ when $r = R$, we get

$$f(R)g(z) = \phi(z). \quad (14.1.15)$$

This suggests that we may get an analytical solution when the radial component of velocity on the surface of the cylinder is given by

$$\phi(z) = a_0 + a_1 z \quad \text{or} \quad \phi(z) = ce^{\gamma z}. \quad (14.1.16)$$

We shall give the solutions for a special cases in §14.1.3.

14.1.3 Solution When Radial Velocity at Wall Decreases Linearly with z

For (14.1.11), we try the solution

$$\psi(r, z) = F(r) \left(a_0 z + \frac{1}{2} a_1 z^2 \right) + G(r) \quad (14.1.17)$$

so that using (14.1.10), we get

$$v_r = \frac{1}{r}F(r)(a_0 + a_1z), \quad (14.1.18)$$

$$v_z = -\frac{1}{r}F'(r)\left(a_0z + \frac{1}{2}a_1z^2\right) - \frac{1}{r}G'(r), \quad (14.1.19)$$

$$D^2\psi = \left(\frac{d^2}{dr^2} - \frac{1}{r}\frac{d}{dr}\right)F(r)\left(a_0z + \frac{1}{2}a_1z^2\right) + \left(\frac{d^2}{dr^2} - \frac{1}{r}\frac{d}{dr}\right)G(r) + a_1F(r), \quad (14.1.20)$$

$$\begin{aligned} D^2(D^2\psi) &= \left(\frac{d^2}{dr^2} - \frac{1}{r}\frac{d}{dr}\right)^2 F(r)\left(a_0z + \frac{1}{2}a_1z^2\right) + \left(\frac{d^2}{dr^2} - \frac{1}{r}\frac{d}{dr}\right)^2 G(r) \\ &\quad + 2a_1\left(\frac{d^2}{dr^2} - \frac{1}{r}\frac{d}{dr}\right)F(r) = 0. \end{aligned} \quad (14.1.21)$$

From (14.1.1) and (14.1.21), we get

$$\left(\frac{d^2}{dr^2} - \frac{1}{r}\frac{d}{dr}\right)^2 F(r) = 0, \quad (14.1.22)$$

$$\left(\frac{d^2}{dr^2} - \frac{1}{r}\frac{d}{dr}\right)^2 G(r) + 2a_1\left(\frac{d^2}{dr^2} - \frac{1}{r}\frac{d}{dr}\right)F(r) = 0. \quad (14.1.23)$$

Equation (14.1.22) gives

$$\left(\frac{d^2}{dr^2} - \frac{1}{r}\frac{d}{dr}\right)H(r) = 0, \quad \left(\frac{d^2}{dr^2} - \frac{1}{r}\frac{d}{dr}\right)F(r) = H(r). \quad (14.1.24)$$

Solving (14.1.24), we get

$$H(r) = Ar^2 + B, \quad (14.1.25)$$

$$r^2\frac{d^2F}{dr^2} - r\frac{dF}{dr} = Ar^4 - Br^2. \quad (14.1.26)$$

Integrating (14.1.26), we obtain

$$F(r) = C + Dr^2 + \frac{Ar^4}{8} + \frac{Br^2}{2}\ln r. \quad (14.1.27)$$

From (14.1.23) and (14.1.27), we have

$$\left(\frac{d^2}{dr^2} - \frac{1}{r}\frac{d}{dr}\right)\left[\left(\frac{d^2}{dr^2} - \frac{1}{r}\frac{d}{dr}\right)G(r) + 2a_1F(r)\right] = 0. \quad (14.1.28)$$

Using (14.1.24) and (14.1.25), we get

$$\left(\frac{d^2}{dr^2} - \frac{1}{r}\frac{d}{dr}\right)G(r) + 2a_1F(r) = Mr^2 + N. \quad (14.1.29)$$

Now from (14.1.24), (14.1.25), (14.1.18) and (14.1.19), we have

$$\frac{d}{dr}\left[\frac{1}{r}F'(r)\right] = 0 \quad \text{at } r = 0, \quad (14.1.30)$$

$$\frac{d}{dr}\left[\frac{1}{r}G'(r)\right] = 0 \quad \text{at } r = 0, \quad (14.1.31)$$

$$\frac{1}{r}F(r) = 0 \quad \text{at } r = 0, \quad (14.1.32)$$

$$\frac{1}{r}F'(r) \quad \text{and} \quad \frac{1}{r}G'(r) \quad \text{are finite at } r = 0, \quad (14.1.33)$$

$$F'(R) = 0, \quad G'(R) = 0, \quad F(R) = R. \quad (14.1.34)$$

From (14.1.27), (14.1.32) and (14.1.33), we obtain

$$C = 0, \quad B = 0. \quad (14.1.35)$$

From (14.1.27), (14.1.34) and (14.1.35)

$$2DR + \frac{1}{2}AR^3 = 0, \quad DR^2 + \frac{AR^4}{8} = R \quad (14.1.36)$$

so that

$$F(r) = \frac{2r^2}{R} - \frac{r^4}{R^3} = R \left[2 \left(\frac{r}{R} \right)^2 - \left(\frac{r}{R} \right)^4 \right]. \quad (14.1.37)$$

Substituting (14.1.37) in (14.1.29), we get

$$\frac{d^2G}{dr^2} - \frac{1}{r} \frac{dG}{dr} = Mr^2 + N - 4a_1 \frac{r^2}{R} + 2a_1 \frac{r^4}{R^3}. \quad (14.1.38)$$

Integrating (14.1.38), we obtain

$$G(r) = M_1 r^2 + N_1 + \frac{Mr^4}{8} + \frac{Nr^2 \ln r}{2} - \frac{a_1 r^4}{2R} + \frac{a_1 r^6}{12R^3}. \quad (14.1.39)$$

From (14.1.33) and (14.1.39), we have

$$N = 0. \quad (14.1.40)$$

From (14.1.34) and (14.1.39), we have

$$2M_1 R + \frac{1}{2}MR^3 - \frac{3a_1}{2}R^2 = 0. \quad (14.1.41)$$

Equation 14.1.41 can determine only one of the two unknown constants M and M_1 . To determine both of them, we need one more relation. This relation can be found in terms of Q_0 which is the total flux at $z = 0$. Using (14.1.18) and (14.1.19), we get

$$\begin{aligned} Q(z) &= \int_0^R 2\pi r v_z(r, z) dr \\ &= 2\pi \int_0^R \left[\left(\frac{4r^3}{R^3} - \frac{4r}{R} \right) \left(a_0 z + \frac{1}{2}a_1 z^2 \right) - 2M_1 r - \frac{Mr^3}{2} - \frac{2a_1}{R} r^3 + \frac{a_1 r^5}{2R^3} \right] dr \end{aligned} \quad (14.1.42)$$

$$\therefore \frac{Q_0}{2\pi R^2} = \frac{MR^2}{8} - \frac{a_1}{3}R, \quad (14.1.43)$$

$$\Rightarrow M = \frac{8}{R^2} \left(\frac{Q_0}{2\pi R^2} + \frac{a_1 R}{3} \right), \quad (14.1.44)$$

$$\Rightarrow M_1 = -\frac{Q_0}{\pi R^2} + \frac{a_1 R}{12}. \quad (14.1.45)$$

From (14.1.39), (14.1.40), 14.1.44 and 14.1.45,

$$G(r) = \left(\frac{a_1 R}{12} - \frac{Q_0}{\pi R^2} \right) r^2 + N_1 + \frac{1}{R^2} \left(\frac{Q_0}{2\pi R^2} + \frac{a_1 R}{3} \right) r^4 - \frac{a_1}{2} \frac{r^4}{R} + \frac{a_1}{12} \frac{r^6}{R^3}. \quad (14.1.46)$$

The constant N_1 need not to be determined since $\psi(r, z)$ can always contain an arbitrary constant without affecting the velocity components.

From (14.1.18) and (14.1.19), (14.1.27), (14.1.46), we have

$$v_r(r, z) = \left[2\frac{r}{R} - \left(\frac{r}{R}\right)^3 \right] (a_0 + a_1 z), \quad (14.1.47)$$

$$\begin{aligned} v_z(r, z) &= -4\left(\frac{r}{R} - \frac{r^3}{R^3}\right) \left(a_0 z + \frac{1}{2}a_1 z^2\right) - 2\left(\frac{a_1 R}{12} - \frac{Q_0}{\pi R^2}\right) \\ &\quad - \frac{4}{R^2} \left(\frac{Q_0}{2\pi R^2} + \frac{a_1 R}{3}\right) r^2 + 2a_1 \frac{r^2}{R} - \frac{a_1 r^4}{2R^3} \\ &= \left(1 - \frac{r^2}{R^2}\right) \left[\frac{2Q_0}{\pi R^2} - \frac{2}{R}(2a_0 z + a_1 z^2) - \frac{a_1 R}{2} \left(\frac{1}{3} - \frac{r^2}{R^2}\right) \right]. \end{aligned} \quad (14.1.48)$$

Differentiating (14.1.42), we obtain

$$\frac{dQ}{dz} = 8\pi(a_0 + a_1 z) \int_0^R \left(\frac{r^3}{R^3} - \frac{r}{R}\right) dr = -2\pi R(a_0 + a_1 z) \quad (14.1.49)$$

so that the decrease of flux is equal to the amount of the fluid coming out of the cylinder per unit length per unit time. Integrating (14.1.49), we get

$$Q(z) = Q_0 - \pi R(2a_0 z + a_1 z^2). \quad (14.1.50)$$

From (14.1.48) and (14.1.50), we have

$$v_z = \left(1 - \frac{r^2}{R^2}\right) \left[\frac{2Q(z)}{\pi R^2} - \frac{a_1 R}{2} \left(\frac{1}{3} - \frac{r^2}{R^2}\right) \right]. \quad (14.1.51)$$

For Hagen-Poiseuille flow in a circular tube, we have

$$v_z = \left(1 - \frac{r^2}{R^2}\right) \frac{2Q}{\pi R^2}. \quad (14.1.52)$$

Comparing (14.1.51) and (14.1.52), we find that there are two changes:

- (i) Q is replaced by the variable $Q(z)$, and
- (ii) there is further distortion due to the varying nature of the radial flow.

Using (14.1.2), (14.1.3), (14.1.47), (14.1.48) and (14.1.50), we get

$$\frac{\partial p}{\partial r} = -\frac{8\mu r}{R^2}(a_0 + a_1 z), \quad (14.1.53)$$

$$\frac{\partial p}{\partial z} = -\frac{4a_1\mu}{R} \left[\frac{r^2}{R^2} + \frac{2Q(z)}{a_1\pi R^3} + \frac{1}{2} \right]. \quad (14.1.54)$$

Integrating (14.1.53), we obtain

$$p(r, z) = -\frac{4\mu r^2}{R^3}(a_0 + a_1 z) + K(z). \quad (14.1.55)$$

Differentiating (14.1.55) partially with respect to z and then substituting $\partial p/\partial z$ in (14.1.54), we get

$$K'(z) = -\frac{4a_1\mu}{R} \left[\frac{1}{3} + \frac{2Q(z)}{a_1\pi R^2} \right] \quad (14.1.56)$$

so that

$$K(z) = -\frac{4a_1\mu}{R} \left[\frac{1}{3}z + \frac{2z\bar{Q}(z)}{a_1\pi R^3} \right] + K_0, \quad (14.1.57)$$

where

$$\bar{Q}(z) = \int_0^z Q(z) dz. \quad (14.1.58)$$

Substituting from (14.1.57) in (14.1.56), we get

$$p(r, z) - p(0, 0) = -\frac{4\mu}{R}(a_0 + a_1z)\frac{r^2}{R^2} - \mu \left(\frac{4a_1}{3R} + \frac{8\bar{Q}}{\pi R^4} \right) z. \quad (14.1.59)$$

The average pressure $\bar{p}(z)$ at any section is given by

$$\bar{p}(z) = \frac{\int_0^R p(r, z) 2\pi r dr}{\int_0^R 2\pi r dr} = -\mu \left[\frac{2a_0}{R} + \left(\frac{8\bar{Q}(z)}{\pi R^4} + \frac{10a_1}{3R} \right) z \right] \quad (14.1.60)$$

Thus the pressure drop over the tube length L is

$$\Delta\bar{p} = \bar{p}(0) - \bar{p}(L) = \mu \left[\frac{8\bar{Q}(L)}{\pi R^4} + \frac{10a_1}{3R} \right] L. \quad (14.1.61)$$

Unit 15

Course Structure

- Diffusion and Diffusion-Reaction Models
 - Fick's Laws of Diffusion
 - Solution of the One-dimensional Diffusion Equation
 - Solution of the Two-dimensional Diffusion Equation
-

15.1 The Diffusion Equation

15.1.1 Fick's Laws of Diffusion

Let $c(x, y, z, t)$ be the concentration of a solute or the amount of the solute per unit volume at the point (x, y, z) at time t . Due to the concentration gradient $\text{grad } c$, there is a flow of solute given by the current density vector \mathbf{j} , which, according to *Fick's first law of diffusion*, is given by

$$\mathbf{j} = D \text{ grad } c = -D \nabla c \quad (15.1.1)$$

or

$$j_x = -D \frac{\partial c}{\partial x}, \quad j_y = -D \frac{\partial c}{\partial y}, \quad j_z = -D \frac{\partial c}{\partial z}. \quad (15.1.2)$$

Here the quantities j_x, j_y, j_z give respectively the amounts of the solute crossing the planes perpendicular to x, y, z axes per unit area per unit time so that the dimensions of D are

$$\frac{ML^{-2}T^{-1}}{ML^{-3}L^{-1}} = L^2T^{-1}. \quad (15.1.3)$$

The negative signs in (15.1.1) and (15.1.2) indicate that the flow takes place in the direction of decreasing concentration. D can vary with x, y, z but we shall take it to be constant. Its values for some common biological solutes in water lie between 0.05×10^{-6} and $10 \times 10^{-6} \text{ cm}^2/\text{sec}$.

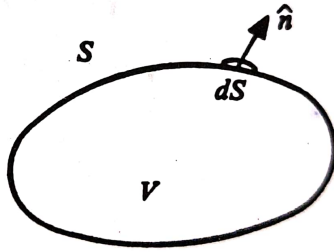


Figure 15.1: Control volume.

Now, consider a volume V with surface S (see Fig. 15.1). The rate of change of the amount of the solute is given by

$$\frac{\partial}{\partial t} \int_V c(x, y, z, t) dx dy dz. \quad (15.1.4)$$

The amount of the solute which comes out of the surface S per unit time is given by

$$\int_S \mathbf{j} \cdot \hat{\mathbf{n}} dS, \quad (15.1.5)$$

where $\hat{\mathbf{n}}$ is the unit normal vector to the surface. If there is no source or sink inside the volume, then on using (15.1.1), (15.1.4) and (15.1.5), and Gauss' divergence theorem, we get

$$\begin{aligned} \frac{\partial}{\partial t} \int_V c(x, y, z, t) dx dy dz &= - \int_S \mathbf{j} \cdot \hat{\mathbf{n}} dS \\ &= - \int_S (D \text{ grad } c) \cdot \hat{\mathbf{n}} dS \\ &= - \int_V \text{div} (D \text{ grad } c) dx dy dz \end{aligned} \quad (15.1.6)$$

so that

$$\int_V \left[\frac{\partial c}{\partial t} - \text{div} (D \text{ grad } c) \right] dx dy dz = 0. \quad (15.1.7)$$

Since (15.1.7) holds for all volumes, we get *Fick's second law of diffusion* as

$$\frac{\partial c}{\partial t} = \text{div} (D \text{ grad } c). \quad (15.1.8)$$

Since D is assumed to be constant, we get the diffusion equation

$$\frac{\partial c}{\partial t} = D \text{div} (\text{grad } c) = D \nabla^2 c = D \left(\frac{\partial^2 c}{\partial x^2} + \frac{\partial^2 c}{\partial y^2} + \frac{\partial^2 c}{\partial z^2} \right). \quad (15.1.9)$$

The equation governing the temperature θ of a heat-conducting homogeneous solid is given by

$$\frac{\partial \theta}{\partial t} = k \left(\frac{\partial^2 \theta}{\partial x^2} + \frac{\partial^2 \theta}{\partial y^2} + \frac{\partial^2 \theta}{\partial z^2} \right). \quad (15.1.10)$$

where k is called the *thermal diffusivity* of the solid. The diffusion equation is therefore also known as the *heat-conduction equation*.

15.1.2 Some Solution of the One-dimensional Diffusion Equation

Solution I

If there is diffusion only in the direction of the x -axis, (15.1.9) gives

$$\frac{\partial c}{\partial t} = D \frac{\partial^2 c}{\partial x^2}. \quad (15.1.11)$$

By differentiating and substituting in (15.1.11), it can be easily verified that

$$c = c(x, t) = \frac{m}{(4\pi Dt)^{1/2}} \exp\left[-\frac{x^2}{4Dt}\right] \quad (15.1.12)$$

is a solution of (15.1.11). Also,

$$\begin{aligned} \int_{-\infty}^{\infty} c(x, t) dx &= \frac{m}{(4\pi Dt)^{1/2}} \int_{-\infty}^{\infty} \exp\left[-\frac{x^2}{4Dt}\right] dx \\ &= \frac{m}{\sqrt{2\pi}} \int_{-\infty}^{\infty} \exp\left[-\frac{1}{2}y^2\right] dy = m \end{aligned} \quad (15.1.13)$$

so that m denotes the total amount of the diffusing solute. It is easily seen that $\frac{c}{m}$ is the density function for the normal probability distribution with mean zero and variance $2Dt$. The graphs of $\frac{c}{m}$ against x for $Dt = 4, 1, 1/4, 1/9$ and $1/16$ are given in Fig. 15.2.

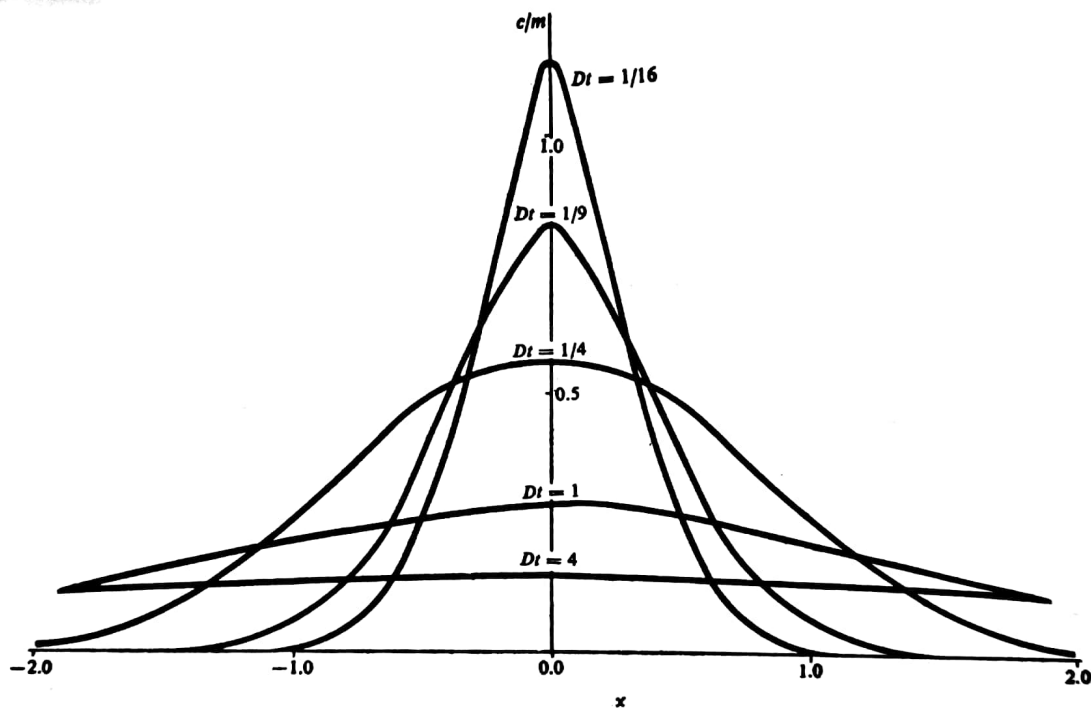


Figure 15.2: Graph of c/m against x .

The area under each of these curves is unity. As $t \rightarrow 0$, the variance tends to zero and we get Dirac delta-function $\delta(x)$ which vanishes everywhere except at $x = 0$ and is such that

$$\int_{-\infty}^{\infty} \delta(x) dx = 1, \quad \int_{-\infty}^{\infty} f(x)\delta(x) dx = f(0). \quad (15.1.14)$$

It thus appears that

$$\delta(x) = \lim_{t \rightarrow 0} \frac{1}{(4\pi Dt)^{1/2}} \exp\left[-\frac{x^2}{4Dt}\right]. \quad (15.1.15)$$

Thus (15.1.12) gives the concentration due to a solute mass m placed at $x = 0$ at time $t = 0$. If a unit mass of solute is placed at $x = \xi$, the concentration $c(x, t)$ is given by

$$c(x, t) = \frac{1}{(4\pi Dt)^{1/2}} \exp\left[-\frac{(x - \xi)^2}{Dt}\right]. \quad (15.1.16)$$

If the solute has an initial density distribution $A(\xi) d\xi$, then the concentration of the solute at time t is given by

$$c(x, t) = \frac{1}{(4\pi Dt)^{1/2}} \int_0^{\infty} A(\xi) \exp\left[-\frac{(x - \xi)^2}{Dt}\right] d\xi. \quad (15.1.17)$$

Solution II

For obtaining the second solution of (15.1.11), if $c(x, t)$ satisfies (15.1.11), then $\frac{\partial c}{\partial x}$ also satisfies it. Conversely, if (15.1.12) is a solution of (15.1.11), then

$$\frac{m}{(4\pi Dt)^{1/2}} \int_{-\infty}^x \exp\left[-\frac{x^2}{4Dt}\right] dx = \frac{m}{\sqrt{\pi}} \int_0^{\eta} \exp[-\eta^2] d\eta, \quad (15.1.18)$$

where

$$\eta = \frac{x}{(4Dt)^{1/2}}, \quad (15.1.19)$$

is also a solution of (15.1.11). If we define *error function* $\text{erf}(z)$ and *error function complement* $\text{erfc}(z)$ as

$$\text{erf}(z) = \frac{2}{\sqrt{\pi}} \int_0^z \exp[-\eta^2] d\eta, \quad (15.1.20)$$

$$\text{erfc}(z) = 1 - \text{erf}(z) = \frac{2}{\sqrt{\pi}} \int_z^{\infty} \exp[-\eta^2] d\eta,$$

then we find that $\text{erfc}\left[\frac{x}{(4Dt)^{1/2}}\right]$ is a solution of the one-dimensional diffusion equation. We may note that

$$\text{erf}(-z) = \text{erf}(z), \quad \text{erf}(0) = 0, \quad \text{erf}(\infty) = 1. \quad (15.1.21)$$

Since both $\text{erf}(z)$ and $\text{erfc}(z)$ are tabulated functions, we have a convenient solution of the one dimensional diffusion equation.

Solution III

For solving the boundary value problem for which there is no flux at $x = 0$ and $x = a$, i.e., for solving (15.1.11) subject to the boundary conditions

$$\frac{\partial c}{\partial x} = 0 \quad \text{at } x = 0, x = a, \quad (15.1.22)$$

we use the method of *separation of variables* and try the solution of the form

$$c(x, t) = X(x)T(t) \quad (15.1.23)$$

for (15.1.11) to get

$$\frac{1}{T} \frac{dT}{dt} = \frac{D}{X} \frac{d^2 X}{dx^2} = -k^2 \quad (\text{say}) \quad (15.1.24)$$

so that

$$c(x, t) = \sum_k \exp[-k^2 t] \left[A_k \cos\left(\frac{kx}{\sqrt{D}}\right) + B_k \sin\left(\frac{kx}{\sqrt{D}}\right) \right]. \quad (15.1.25)$$

Equation (15.1.22) then give

$$B_k = 0, \quad \frac{k}{\sqrt{D}} = \frac{n\pi}{a} \quad (15.1.26)$$

so that

$$c(x, t) = \sum_{n=0}^{\infty} C_n \exp\left[-\frac{n^2 \pi^2 D t}{a^2}\right] \cos\left[\frac{n\pi x}{a}\right]. \quad (15.1.27)$$

To determine the constants C_n , we make use of the knowledge of the initial distribution of concentration $c(x, 0) = f(x)$, so that

$$f(x) = \sum_{n=0}^{\infty} C_n \cos\left(\frac{n\pi x}{a}\right). \quad (15.1.28)$$

Expanding $f(x)$ in a half-range cosine series, we get

$$C_0 = \frac{1}{a} \int_0^a f(x) dx, \quad (15.1.29)$$

$$C_n = \frac{2}{a} \int_0^a f(x) \cos\left(\frac{n\pi x}{a}\right) dx \quad (n = 1, 2, 3, \dots). \quad (15.1.30)$$

As $t \rightarrow \infty$, we get, from (15.1.27) and (15.1.29),

$$\lim_{t \rightarrow \infty} c(x, t) = C_0 = \frac{1}{a} \int_0^a f(x) dx \quad (15.1.31)$$

which is only the average value of the initial concentration. This shows that, as $t \rightarrow \infty$, the concentration tends to become uniform and equal to the average value of the initial concentration. In fact, from (15.1.27),

$$\int_0^a c(x, t) dx = C_0 a = \int_0^a f(x) dx \quad (15.1.32)$$

so that the total amount of the solute at any time t is equal to the initial total amount. This result is expected since, according to boundary conditions (15.1.22), no solute enters or leaves the boundaries.

15.1.3 Some Solutions of the Two-dimensional Diffusion Equation

Solution I

By using the method of separation of variables, it is easily seen that the solution of the equation

$$\frac{\partial c}{\partial t} = D \left(\frac{\partial^2 c}{\partial x^2} + \frac{\partial^2 c}{\partial y^2} \right) \quad (15.1.33)$$

is

$$c(x, y, t) = \sum_{\lambda} \sum_{\mu} C_{\lambda\mu} \cos(\lambda x + \epsilon_k) \cos(\mu y + \epsilon_m) \exp[-(\lambda^2 + \mu^2)Dt]. \quad (15.1.34)$$

If the boundary conditions are

$$\begin{aligned} \frac{\partial c}{\partial x} &= 0 \quad \text{when } x = 0, a, \\ \frac{\partial c}{\partial y} &= 0 \quad \text{when } y = 0, b, \end{aligned} \quad (15.1.35)$$

we get

$$\epsilon_{\lambda} = 0, \quad \epsilon_{\mu} = 0, \quad \lambda = \frac{m\pi}{a}, \quad \mu = \frac{n\pi}{b} \quad (15.1.36)$$

so that

$$c(x, y, t) = \sum_{m=0}^{\infty} \sum_{n=0}^{\infty} C_{mn} \cos\left(\frac{m\pi x}{a}\right) \cos\left(\frac{n\pi y}{b}\right) \exp\left[-\left(\frac{m^2\pi^2}{a^2} + \frac{n^2\pi^2}{b^2}\right)Dt\right]. \quad (15.1.37)$$

If the initial concentration is $f(x, y)$, then we get

$$C_{00} = \frac{1}{ab} \int_0^b \int_0^a f(x, y) dy dx, \quad (15.1.38)$$

$$C_{m0} = \frac{2}{ab} \int_0^b \int_0^a f(x, y) \cos\left(\frac{m\pi x}{a}\right) dy dx, \quad (15.1.39)$$

$$C_{0n} = \frac{2}{ab} \int_0^b \int_0^a f(x, y) \cos\left(\frac{n\pi y}{b}\right) dy dx, \quad (15.1.40)$$

$$C_{mn} = \frac{4}{ab} \int_0^b \int_0^a f(x, y) \cos\left(\frac{m\pi x}{a}\right) \cos\left(\frac{n\pi y}{b}\right) dy dx, \quad (15.1.41)$$

so that, as expected

$$\lim_{t \rightarrow \infty} c(x, y, t) = C_{00} = \frac{1}{ab} \int_0^b \int_0^a f(x, y) dy dx, \quad (15.1.42)$$

$$\int_0^b \int_0^a c(x, y, t) dy dx = abC_{00} = \int_0^b \int_0^a f(x, y) dy dx. \quad (15.1.43)$$

Solution II

For the axially-symmetric case, the diffusion equation in cylindrical polar coordinates is

$$\frac{\partial c}{\partial t} = D \left(\frac{\partial^2 c}{\partial r^2} + \frac{1}{r} \frac{\partial c}{\partial r} + \frac{\partial^2 c}{\partial z^2} \right). \quad (15.1.44)$$

By using the method of separation of variables, we get a solution of (15.1.44), namely,

$$c(x, z, t) = \sum_{\mu} \sum_k A_{\lambda\mu} J_0(\sqrt{\lambda^2 + \mu^2} r) \exp(-\lambda^2 Dt \pm \mu z). \quad (15.1.45)$$

A solution independent of z is

$$c(r, t) = \sum_{\lambda} A_{\lambda} J_0(\lambda r) \exp(-\lambda^2 Dt). \quad (15.1.46)$$

If the flux $\frac{\partial c}{\partial r} = 0$ across the cylindrical boundary $r = a$, then

$$J_1(\lambda a) = 0 \quad \text{or} \quad \lambda = \frac{\xi}{a}, \quad (15.1.47)$$

where ξ is a zero of the first order Bessel function. Hence

$$c(r, t) = \sum_{n=1}^{\infty} B_n J_0 \left(\xi_n \frac{r}{a} \right) \exp \left[- \left(\frac{\xi_n^2}{a^2} \right) Dt \right], \quad (15.1.48)$$

where ξ_n is the n -th zero of $J_1(x)$. The constants B_n are to be determined from

$$c(r, 0) = f(r) = \sum_{n=1}^{\infty} B_n J_0 \left(\xi_n \frac{r}{a} \right). \quad (15.1.49)$$

If the boundary condition is $c = 0$ at $r = a$, then (15.1.46) gives

$$J_0(\lambda a) = 0 \quad (15.1.50)$$

so that

$$c(r, t) = \sum_{n=1}^{\infty} D_n \exp \left[- \frac{\eta_n^2 Dt}{a} J_0 \left(\frac{\eta_n r}{a} \right) \right], \quad (15.1.51)$$

where

$$D_n = \frac{2}{a^2 J_1^2(\eta_n)} \int_0^a r f(r) J_0 \left(\frac{\eta_n r}{a} \right) dr \quad (15.1.52)$$

and η_n is the n -th zero of zero order Bessel function.

Unit 16

Course Structure

- Ecological Application of Diffusion Models
 - Diffusion on the Stability of Single Species Model
 - Diffusion on the Stability of Two Species Model
 - Diffusion on the Stability of Prey-Predator Models
-

16.1 Application of Diffusion and Diffusion-Reaction Models in Population Biology

In the absence of diffusion, if an ecological model for n species is

$$\frac{dc_i}{dt} = Q_i(c_1, c_2, \dots, c_n), \quad (16.1.1)$$

then a model with diffusion is represented by

$$\frac{\partial c_i}{\partial t} = D_i \nabla^2 c_i + Q_i(c_1, c_2, \dots, c_n), \quad i = 1, 2, \dots, n, \quad (16.1.2)$$

where D_i is the coefficient of diffusion of the i -th substance and Q_i is the rate of its generation per unit time. Equation (16.1.2) is called *diffusion-reaction equation*. IN particular, if $N_1(x, t)$, $N_2(x, t)$ denote the densities of the two species at the point x at time t in a medium in which both species are diffusing in the direction of the x -axis only, then a *competition model with diffusion* is

$$\begin{aligned} \frac{\partial N_1}{\partial t} &= N_1(a_1 - b_{11}N_1 - b_{12}N_2) + D_1 \frac{\partial^2 N_1}{\partial x^2}, \\ \frac{\partial N_2}{\partial t} &= N_2(a_2 - b_{21}N_1 - b_{22}N_2) + D_2 \frac{\partial^2 N_2}{\partial x^2}, \end{aligned} \quad (16.1.3)$$

and a *prey-predator model with diffusion* is

$$\begin{aligned} \frac{\partial N_1}{\partial t} &= N_1(a_1 - b_{11}N_1 - b_{12}N_2) + D_1 \frac{\partial^2 N_1}{\partial x^2}, \\ \frac{\partial N_2}{\partial t} &= N_2(-a_2 - b_{21}N_1 - b_{22}N_2) + D_2 \frac{\partial^2 N_2}{\partial x^2}, \end{aligned} \quad (16.1.4)$$

Now we will discuss the stabilities of the equilibrium states of these models.

16.2 Absence of Diffusive Instability for Single Species

In the absence of diffusion, let a population grow according to the law

$$\frac{dN}{dt} = f(N). \quad (16.2.1)$$

Let the population be confined to the volume $0 \leq x \leq a$, $0 \leq y \leq b$, $0 \leq z \leq c$, and let there be diffusion. Let there be no flux across the faces of the rectangular parallelepiped so that (16.2.1) becomes

$$\frac{\partial N}{\partial t} = f(N) + D \left(\frac{\partial^2 N}{\partial x^2} + \frac{\partial^2 N}{\partial y^2} + \frac{\partial^2 N}{\partial z^2} \right). \quad (16.2.2)$$

The boundary conditions are

$$\begin{aligned} \frac{\partial N}{\partial x} &= 0 \quad \text{at } x = 0, a, \\ \frac{\partial N}{\partial y} &= 0 \quad \text{at } y = 0, b, \\ \frac{\partial N}{\partial z} &= 0 \quad \text{at } z = 0, c. \end{aligned} \quad (16.2.3)$$

If \bar{N} gives an equilibrium value for (16.2.1), it also gives an equilibrium value for (16.2.2). Let

$$N(x, y, z, t) = \bar{N} + u(x, y, z, t), \quad (16.2.4)$$

where u is sufficiently small so its squares and higher powers can be neglected. Then (16.2.2) gives

$$\frac{\partial u}{\partial t} = u \frac{\partial f}{\partial N} + D \left(\frac{\partial^2 u}{\partial x^2} + \frac{\partial^2 u}{\partial y^2} + \frac{\partial^2 u}{\partial z^2} \right). \quad (16.2.5)$$

where $\frac{\partial f}{\partial N}$ denote the value of $\frac{\partial f}{\partial N}$ at the equilibrium point \bar{N} . Now the boundary condition (16.2.3) becomes

$$\begin{aligned} \frac{\partial u}{\partial x} &= 0 \quad \text{at } x = 0, a, \\ \frac{\partial u}{\partial y} &= 0 \quad \text{at } y = 0, b, \\ \frac{\partial u}{\partial z} &= 0 \quad \text{at } z = 0, c. \end{aligned} \quad (16.2.6)$$

For (16.2.5), we try the solution

$$u(x, y, z, t) = e^{\lambda t} \sum_p \sum_n \sum_m A_{mnp} \cos\left(\frac{m\pi x}{a}\right) \cos\left(\frac{n\pi y}{b}\right) \cos\left(\frac{p\pi z}{c}\right) \quad (16.2.7)$$

which automatically satisfies boundary conditions (16.2.6). Substituting (16.2.7) in (16.2.5), we get

$$\lambda - \frac{\partial f}{\partial N} + D \left(\frac{m^2 \pi^2}{a^2} + \frac{n^2 \pi^2}{b^2} + \frac{p^2 \pi^2}{c^2} \right) = 0 \quad (16.2.8)$$

or

$$\lambda = \frac{\partial f}{\partial \bar{N}} - D\sigma^2, \quad \text{where } \sigma^2 = \left(\frac{m^2}{\partial a^2} + \frac{n^2}{b^2} + \frac{p^2}{\partial c^2} \right) \pi^2. \quad (16.2.9)$$

If, in the absence of diffusion, the equilibrium position is unstable, then $\frac{\partial f}{\partial \bar{N}}$ is negative, and so λ is also negative. Therefore, a position of equilibrium, which is stable in the absence of diffusion remains stable when there is diffusion in a finite domain with no flux across its surfaces. Thus there is no possibility of diffusion-induced instability when there is only one single species.

16.3 Possibility of Diffusive Instability for Two Species

If $N_1(x, y, z, t)$ and $N_2(x, y, z, t)$ are the populations of the two species, then the basic diffusion reaction equations are

$$\frac{\partial N_1}{\partial t} = f_1(N_1, N_2) + D_1 \left(\frac{\partial^2 N_1}{\partial x^2} + \frac{\partial^2 N_1}{\partial y^2} + \frac{\partial^2 N_1}{\partial z^2} \right), \quad (16.3.1)$$

$$\frac{\partial N_2}{\partial t} = f_2(N_1, N_2) + D_2 \left(\frac{\partial^2 N_2}{\partial x^2} + \frac{\partial^2 N_2}{\partial y^2} + \frac{\partial^2 N_2}{\partial z^2} \right). \quad (16.3.2)$$

The equilibrium position for these equations is given by

$$f_1(\bar{N}_1, \bar{N}_2) = 0, \quad f_2(\bar{N}_1, \bar{N}_2) = 0. \quad (16.3.3)$$

If

$$\begin{aligned} N_1(x, y, z, t) &= \bar{N}_1 + u_1(x, y, z, t), \\ N_2(x, y, z, t) &= \bar{N}_2 + u_2(x, y, z, t), \end{aligned} \quad (16.3.4)$$

then, after substituting (16.3.1) and (16.3.2) and linearizing, we get

$$\frac{\partial u_1}{\partial t} = u_1 \frac{\partial f_1}{\partial N_1} + u_2 \frac{\partial f_1}{\partial N_2} + D_1 \left(\frac{\partial^2 u_1}{\partial x^2} + \frac{\partial^2 u_1}{\partial y^2} + \frac{\partial^2 u_1}{\partial z^2} \right), \quad (16.3.5)$$

$$\frac{\partial u_2}{\partial t} = u_1 \frac{\partial f_2}{\partial N_1} + u_2 \frac{\partial f_2}{\partial N_2} + D_2 \left(\frac{\partial^2 u_2}{\partial x^2} + \frac{\partial^2 u_2}{\partial y^2} + \frac{\partial^2 u_2}{\partial z^2} \right) \quad (16.3.6)$$

where $\frac{\partial f_i}{\partial N_i}$, $i = 1, 2$, denotes the value of $\frac{\partial f_i}{\partial N_i}$ at the equilibrium point \bar{N}_1, \bar{N}_2 . When there is no flux, the boundary conditions are

$$\begin{aligned} \frac{\partial u_i}{\partial x} &= 0 \quad \text{at } x = 0, a, \\ \frac{\partial u_i}{\partial y} &= 0 \quad \text{at } y = 0, b, \\ \frac{\partial u_i}{\partial z} &= 0 \quad \text{at } z = 0, c. \end{aligned} \quad (16.3.7)$$

where $i = 1, 2$. Trying the solution

$$\begin{aligned} u_1 &= e^{\lambda t} \sum_p \sum_n \sum_m a_{mnp} \cos \frac{m\pi x}{a} \cos \frac{n\pi y}{b} \cos \frac{p\pi z}{c}, \\ u_2 &= e^{\lambda t} \sum_p \sum_n \sum_m b_{mnp} \cos \frac{m\pi x}{a} \cos \frac{n\pi y}{b} \cos \frac{p\pi z}{c}, \end{aligned} \quad (16.3.8)$$

we get

$$\begin{vmatrix} \lambda - \frac{\partial f_1}{\partial N_1} + D_1\sigma^2 & -\frac{\partial f_1}{\partial N_2} \\ -\frac{\partial f_2}{\partial N_1} & \lambda - \frac{\partial f_2}{\partial N_2} + D_2\sigma^2 \end{vmatrix} = 0 \quad (16.3.9)$$

where $\sigma^2 = \left(\frac{m^2}{a^2} + \frac{n^2}{b^2} + \frac{p^2}{c^2}\right)\pi^2$.

or

$$\begin{aligned} \lambda^2 + \lambda \left[(D_1 + D_2)\sigma^2 - \frac{\partial f_1}{\partial N_1} - \frac{\partial f_2}{\partial N_2} \right] + \left(\frac{\partial f_1}{\partial N_1} \frac{\partial f_2}{\partial N_2} - \frac{\partial f_1}{\partial N_2} \frac{\partial f_2}{\partial N_1} \right) \\ - \sigma^2 \left(D_1 \frac{\partial f_2}{\partial N_2} + D_2 \frac{\partial f_1}{\partial N_1} \right) + D_1 D_2 \sigma^4 = 0. \end{aligned} \quad (16.3.10)$$

In the absence of diffusion, the equation corresponding to (16.3.10) is

$$\lambda^2 - \lambda \left(\frac{\partial f_1}{\partial N_1} + \frac{\partial f_2}{\partial N_2} \right) + \left(\frac{\partial f_1}{\partial N_1} \frac{\partial f_2}{\partial N_2} - \frac{\partial f_1}{\partial N_2} \frac{\partial f_2}{\partial N_1} \right) = 0. \quad (16.3.11)$$

We assume that the equilibrium position (\bar{N}_1, \bar{N}_2) is stable in the absence of diffusion so that

$$\left(\frac{\partial f_1}{\partial N_1} + \frac{\partial f_2}{\partial N_2} \right) < 0, \quad \left(\frac{\partial f_1}{\partial N_1} \frac{\partial f_2}{\partial N_2} - \frac{\partial f_1}{\partial N_2} \frac{\partial f_2}{\partial N_1} \right) > 0. \quad (16.3.12)$$

Inequalities (16.3.12) show that the coefficient of λ in (16.3.10) is positive and the constant term in (16.3.10) is also positive if

$$D_1 \frac{\partial f_2}{\partial N_2} + D_2 \frac{\partial f_1}{\partial N_1} < 0. \quad (16.3.13)$$

Thus, if (16.3.13) is satisfied, the equilibrium position which is stable in the absence of diffusion remains stable when there is diffusion. In particular, in view of the first inequality in (16.3.12), if the diffusion coefficients are equal, diffusion fails to induce instability. Thus for diffusion-induced instability to occur, it is necessary that D_1 and D_2 should be unequal; but this condition is obviously not sufficient. Even when inequality (16.3.13) is reversed, the constant term in (16.3.10) may be (but need not to be) negative, and the equilibrium position may be unstable when there is diffusion. A sufficient condition for diffusion-induced instability is

$$\left(\frac{\partial f_1}{\partial N_1} \frac{\partial f_2}{\partial N_2} - \frac{\partial f_1}{\partial N_2} \frac{\partial f_2}{\partial N_1} \right) + D_1 D_2 \sigma^4 - \sigma^2 \left(D_1 \frac{\partial f_2}{\partial N_2} + D_2 \frac{\partial f_1}{\partial N_1} \right) < 0 \quad (16.3.14)$$

for some integral values of m, n, p . We may note that the stable equilibrium remain stable in spite of diffusion (16.3.13) is satisfied or if $D_1 = D_2$ or if

$$\frac{\partial f_1}{\partial N_1} < 0, \quad \frac{\partial f_2}{\partial N_2} < 0. \quad (16.3.15)$$

16.4 Influence of Diffusion on the Stability of Prey-Predator Models

Diffusion plays a crucial role in modifying the dynamics of prey-predator models by influencing the spatial distribution of populations and their interactions. In classical Lotka-Volterra-type models, populations are assumed to be well mixed, meaning that individuals have equal probability of encountering each other regardless of their spatial location. However, in real-world scenarios, populations are often distributed across space, and diffusion can lead to non-trivial effects on the stability and behavior of prey-predator systems. Here are some ways diffusion impacts the stability of these models:

1. **Spatial Heterogeneity:** Diffusion introduces spatial heterogeneity by allowing individuals to move from one location to another. This can lead to spatial variation in population densities, resource availability, and encounter rates between prey and predators. As a result, the stability of the system may be affected, with local variations in population dynamics influencing the overall behavior.
2. **Spatial Patterns:** Diffusion can give rise to spatial patterns in population distributions, such as traveling waves, patchiness, or spatial segregation. These patterns can emerge due to the interplay between local population dynamics and dispersal processes. The formation of spatial patterns can impact the stability of the system by altering the spatial distribution of resources and interactions between prey and predators.
3. **Stabilizing or Destabilizing Effects:** Diffusion can have both stabilizing and destabilizing effects on prey-predator systems. On one hand, dispersal can enhance stability by promoting the spatial averaging of population densities, reducing the likelihood of local extinctions or outbreaks. On the other hand, diffusion can also destabilize the system by facilitating the spread of perturbations or enabling the formation of spatially heterogeneous patterns that can lead to instability.
4. **Spatial Synchrony:** Diffusion can promote spatial synchrony, where populations in different locations become synchronized in their dynamics. This can occur through the dispersal of individuals carrying information about population fluctuations. Spatial synchrony can influence the stability of prey-predator systems by affecting the persistence and resilience of populations across space.
5. **Metapopulation Dynamics:** Diffusion transforms the classical prey-predator model into a metapopulation model, where local populations are connected through dispersal. Metapopulation dynamics can exhibit complex behaviors such as source-sink dynamics, spatial rescue effects, and spatially implicit Allee effects, which can have significant implications for the stability and persistence of populations.

In summary, diffusion can have profound effects on the stability of prey-predator models by introducing spatial heterogeneity, generating spatial patterns, influencing synchrony, and altering metapopulation dynamics. Understanding these effects is essential for predicting the dynamics of ecological systems and designing effective conservation and management strategies.

We now consider the influence of diffusion on the stability of three prey-predator models:

- (i) The simplest prey-predator model is

$$\frac{dN_1}{dt} = N_1(a_1 - \alpha_1 N_2), \quad \frac{dN_2}{dt} = N_2(-a_2 + \alpha_2 N_1) \quad (16.4.1)$$

so that

$$\begin{aligned}\bar{N}_1 &= \frac{a_2}{\alpha_2}, & \bar{N}_2 &= \frac{a_1}{\alpha_1}, \\ \frac{\partial f_1}{\partial \bar{N}_1} &= 0, & \frac{\partial f_2}{\partial \bar{N}_2} &= 0, \\ \frac{\partial f_1}{\partial \bar{N}_1} &= -\alpha_1 \frac{a_2}{\alpha_2}, & \frac{\partial f_2}{\partial \bar{N}_1} &= \alpha_2 \frac{a_1}{\alpha_1},\end{aligned}\tag{16.4.2}$$

Then (16.3.10) and (16.3.11) becomes

$$\lambda^2 + \lambda[(D_1 + D_2)\sigma^2] + a_1a_2 + \sigma^4D_1D_2 = 0,\tag{16.4.3}$$

$$\lambda^2 + a_1a_2 = 0,\tag{16.4.4}$$

so that the equilibrium is neutral without diffusion and is neutral or stable with diffusion. Thus diffusion may ‘increase’ stability; at least it does not ‘decrease stability’.

(ii) For the more general prey-predator model given by (16.3.1) and (16.3.2), we have

$$\frac{\partial f_1}{\partial \bar{N}_1} \geq 0, \quad \frac{\partial f_2}{\partial \bar{N}_2} \leq 0, \quad \frac{\partial f_1}{\partial \bar{N}_2} < 0, \quad \frac{\partial f_2}{\partial \bar{N}_1} > 0.\tag{16.4.5}$$

Thus, if the equilibrium is stable without diffusion and is unstable with diffusion, we get

$$\left| \frac{\partial f_2}{\partial \bar{N}_2} \right| \geq \left| \frac{\partial f_1}{\partial \bar{N}_1} \right|, \quad D_2 \left| \frac{\partial f_1}{\partial \bar{N}_1} \right| > D_1 \left| \frac{\partial f_2}{\partial \bar{N}_2} \right|\tag{16.4.6}$$

which give $D_1 < D_2$. Thus for diffusion-induced instability, it is necessary that the coefficient of diffusion for prey should be less than the diffusion coefficient for predator. Again, this condition is not sufficient.

(iii) Consider the model which, in the absence of diffusion, is given by

$$\begin{aligned}\frac{dN_1}{dt} &= N_1[f(N_1) - N_2], \\ \frac{dN_2}{dt} &= N_2[N_1 - g(N_2)].\end{aligned}\tag{16.4.7}$$

Then we have

$$\begin{aligned}f(\bar{N}_1) &= \bar{N}_2, & g(\bar{N}_2) &= \bar{N}_1, \\ \frac{\partial f_1}{\partial \bar{N}_1} &= \bar{N}_1 f'(\bar{N}_1), & \frac{\partial f_1}{\partial \bar{N}_2} &= -\bar{N}_1, \\ \frac{\partial f_2}{\partial \bar{N}_1} &= \bar{N}_2, & \frac{\partial f_2}{\partial \bar{N}_2} &= -\bar{N}_2 g'(\bar{N}_2).\end{aligned}\tag{16.4.8}$$

Now, (16.3.10) and (16.3.11) gives

$$\begin{aligned}\lambda^2 + \lambda[(D_1 + D_2)\sigma^2 - \bar{N}_1 f'(\bar{N}_1) + \bar{N}_2 g'(\bar{N}_2)] + [-\bar{N}_1 \bar{N}_2 f'(\bar{N}_1) g'(\bar{N}_2) + \bar{N}_1 \bar{N}_2] \\ + D_1 D_2 \sigma^4 - \sigma^2 [D_2 \bar{N}_1 f'(\bar{N}_1) - D_1 \bar{N}_2 g'(\bar{N}_2)] = 0,\end{aligned}\tag{16.4.9}$$

$$\Rightarrow \lambda^2 + \lambda[-\bar{N}_1 f'(\bar{N}_1) + \bar{N}_2 g'(\bar{N}_2)] + \bar{N}_1 \bar{N}_2 [1 - f'(\bar{N}_1) g'(\bar{N}_2)] = 0.\tag{16.4.10}$$

When there is no diffusion, the equilibrium is stable if

$$\bar{N}_2 g'(\bar{N}_2) - \bar{N}_1 f'(\bar{N}_1) > 0, \quad 1 - f'(\bar{N}_1) g'(\bar{N}_2) > 0.\tag{16.4.11}$$

When there is diffusion, the equilibrium can be unstable if

$$D_2 \bar{N}_1 f'(\bar{N}_1) > D_1 \bar{N}_2 g'(\bar{N}_2). \quad (16.4.12)$$

By the same reasoning as before, $D_1 < D_2$. If $f'(\bar{N}_1) > 0$, $g'(\bar{N}_2) > 0$, we can find the values of m , n , p so that the equilibrium with diffusion is unstable. However, if $f'(\bar{N}_1) < 0$, then $g'(\bar{N}_2) > 0$. This is not possible, and the equilibrium continues to be stable.

Unit 17

Course Structure

- Stochastic Model exploring Disease Dynamics
 - The Deterministic Model
 - The Way from Deterministic to Stochastic Model
 - Formulation of the Kolmogorov's Forward Equation
 - The Quasi-Stationary distribution
 - Distribution of the Time to Extinction
 - Diffusion approximation and approximation of Quasi-Stationary distribution
-

17.1 Stochastic Model Exploring Fundamentals of a Disease Dynamics

This Chapter aims to provide an overview of the terms and methods applied to form a mathematical model in sexually transmitted disease, specifically AIDS. This disease mainly spreads by attacking the immune system, particularly by depleting the CD4 cells. Antiretroviral treatment has significantly improved prognosis for HIV-1 infection, though life-long therapy remains a requirement for continuous viral suppression. Its long-term toxicity is also a medical concern for humans and the economic cost of such antiretroviral drugs is a major social problem. Application of highly specialized antigen-presenting dendritic cells (DCs) as a vaccine is thus a very promising approach to improve deteriorated immune function in HIV-1-infected individuals. DCs not only restore qualitative impairment of CTLs, but also stimulate naive CD8⁺T cells from the thymus during antiretroviral treatment in such complex immune system. The safety and efficacy of DC-based vaccine are thus investigated in this study, in stochastic point of view. In this following chapter, we obtain some analytical results for the stochastic model posed in this work. In particular, we derive expressions for the distribution function and expected time to extinction of the infected CD4⁺T cells.

Mathematical models play a significant role in such complex immunological systems. Mathematics provides an alternative way to make predictions about the behaviour of the system. Modelling the interaction between immune CD4 cells and HIV-1 virus has been a major area of research for many years.

While studying this mathematical model the first question that arises in our mind is: *why* we use stochastic approach? There are real advantages in using stochastic rather than deterministic models, particularly when we are modelling such an internal HIV dynamics. This is because different types of cells reacting in the same system can often give different results. Deterministic models predict an uniquely specified time at which the infected cell reaches any chosen level, whereas with a simple stochastic model we can successfully predict the distribution of values for this quantity. Having a distribution for the predicted outcomes is more versatile as it helps us examining important stochastic quantities, for example the variance of the number of infective particles at a given time and the probability that the infective cell particles have died out at a given time, which cannot be examined using deterministic models. Even quantities such as the expected values of the number of cells can be more accurately modelled using stochastic models because they include the effect of random variation on these quantities which deterministic models cannot.

There is a rich number of mathematical models which were developed to describe the viral dynamics of HIV-1. Some scientists estimated virion clearance rate and life-span the HIV-infected cells. Some researchers analysed a simplified version of the deterministic model where the interaction term between uninfected and infected cells is neglected as an approximation, but no stochastic study has been included in their study. observed 123 patients of transient viraemia and provided a statistical characterisation. They suggested that patients have different tendencies to show transient viraemia during the period of viral load suppression. Other researchers introduced a model of AIDS incorporating the concept of stochasticity via the technique of parameter perturbation which is standard in stochastic population modelling. They show that solutions of their described model are all non-negative and a certain type of stochastic perturbation may help in stabilising the system. have developed a mathematical model to find out the effect of the DC-based vaccination in the system to control the disease progression.

17.2 The Deterministic Model

We consider a mathematical model in a long term dynamics with anti-retroviral treatment and *in vitro* dendritic cell vaccination i.e. with monocyte derived dendritic cells (D_{mo}) or DC-based vaccine loaded with HIV-1 derived cytotoxic T lymphocytes (CTL) peptides in a complex immunological system. Here, we assume that the efficacy (ε_{ART}) of ART is very high and therefore the number of uninfected T-cells remains approximately constant and equal to T_S . This model consists three compartments: (I) the number of infected $CD4^+$ T cells, $I(t)$, which can replicate at a rate β_1 and die at a rate, μ_I ; (II) the activated dendritic cells concentration, $D_C(t)$, which becomes mature from premature stage at a rate s , migrate into the lymph and die at an average per capita death rate, μ_D ; (III) the CTL concentration, $C(t)$ which is reduced at rate μ_C .

The interaction between infected $CD4^+$ T helper cells and activated DCs may result in infection of the former at a rate, β_2 . This infection is mediated via DC-sign which allows DCs to transport HIV from peripheral regions of the body to $CD4^+$ T lymphocytes. The mature DCs also interact with $CD8^+$ T-cells at a rate $k\theta$, where k is the average peptide specific T-cell receptor (TCR) and θ represents the average number of the cognate pMHC complexes per DC. The $CD8^+$ T-cell proliferation is induced by cognate antigen presenting DC at a rate r . Based on the above assumptions we construct a non-linear system as given below:

$$\begin{aligned}
\frac{dI}{dt} &= \beta_1(1 - \varepsilon_{ART})T_S I + \beta_2 D_C I - \mu_I I - pIC, \\
\frac{dD_C}{dt} &= s - \mu_D D_C - knD_C C - \beta_2 D_C I, \\
\frac{dC}{dt} &= rkn(D_C + D_{mo})C - \mu_C C.
\end{aligned} \tag{17.2.1}$$

Now, at the equilibrium state we assume that $\frac{dC}{dt} = 0$. Thus, the third equation of (17.2.1) implies $C = 0$. Using this proviso we can transform the system (17.2.1) into two dimensional so that $I(t)$ and $D_C(t)$ satisfy

$$\begin{aligned}
\frac{dD_C}{dt} &= s - \mu_D D_C - \beta_2 D_C I, \\
\frac{dI}{dt} &= \beta_1(1 - \varepsilon_{ART})T_S I + \beta_2 D_C I - \mu_I I.
\end{aligned} \tag{17.2.2}$$

17.3 Analysis of the Stochastic Model

There are two state variables, namely the number of in vitro dendritic cells and the number of infected $CD4^+$ T-cells at time t . They jointly take values in the state space $S = \{(m, n) : m = 0, 1, 2, \dots; n = 0, 1, 2, \dots\}$. The joint distribution of $D_C(t)$, $I(t)$ at time t is denoted by $p_{m,n}(t) = P\{D_C(t) = m, I(t) = n\}$.

We use this notation even when m and/or n are negative, with the convention that $p_{m,n}(t)$ is then equal to 0. The model is based on the following four basic events, i.e. influx rate of in vitro $D_C(t)$ -cells, clearance rate of $D_C(t)$ -cells, production of infected $CD4^+$ T-cells and death of infected such cells. The transition rates of the model are shown in **Table 17.1**.

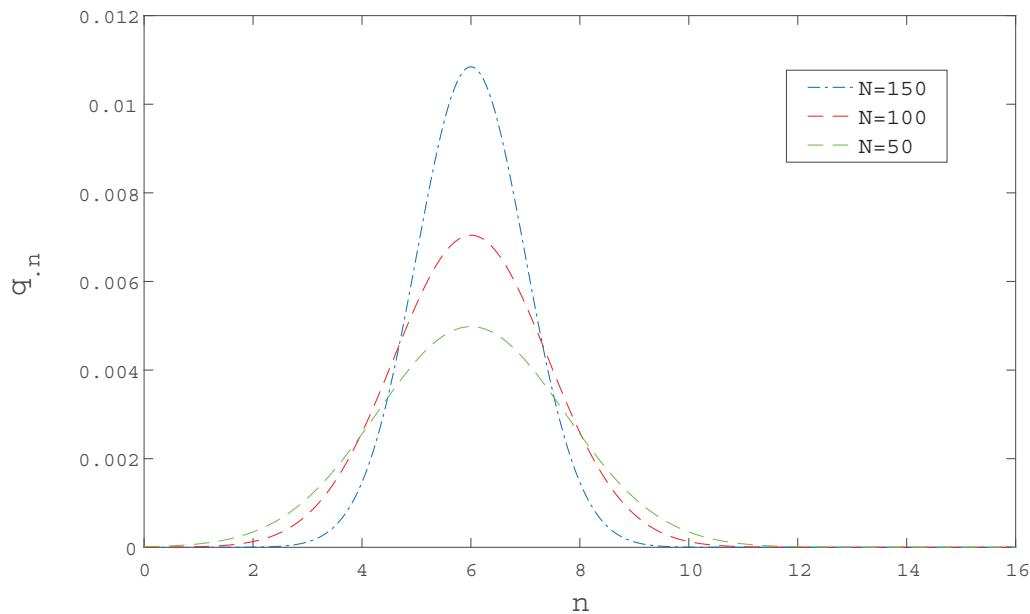


Figure 17.1: Quasi-stationary distribution of the infected cell density for different values of N (combined density of DCs and infected $CD4^+$ T cells).

Table 17.1: Hypothesized transition rates for stochastic version.

Event	Transition	Transition rates
Influx rate of in vitro $D_C(t)$	$(m, n) \rightarrow (m + 1, n)$	$\lambda_1(m, n) = s$
clearance rate of $D_C(t)$ -cells	$(m, n) \rightarrow (m - 1, n)$	$\mu_1(m, n) = \mu_D m$
Production of infected $CD4^+$ T-cells	$(m, n) \rightarrow (m, n + 1)$	$\lambda_2(m, n) = \beta_1(1 - \varepsilon_{ART})T_S n$
Death of infected $CD4^+$ T-cells	$(m, n) \rightarrow (m, n - 1)$	$\mu_2(m, n) = \mu_I n$

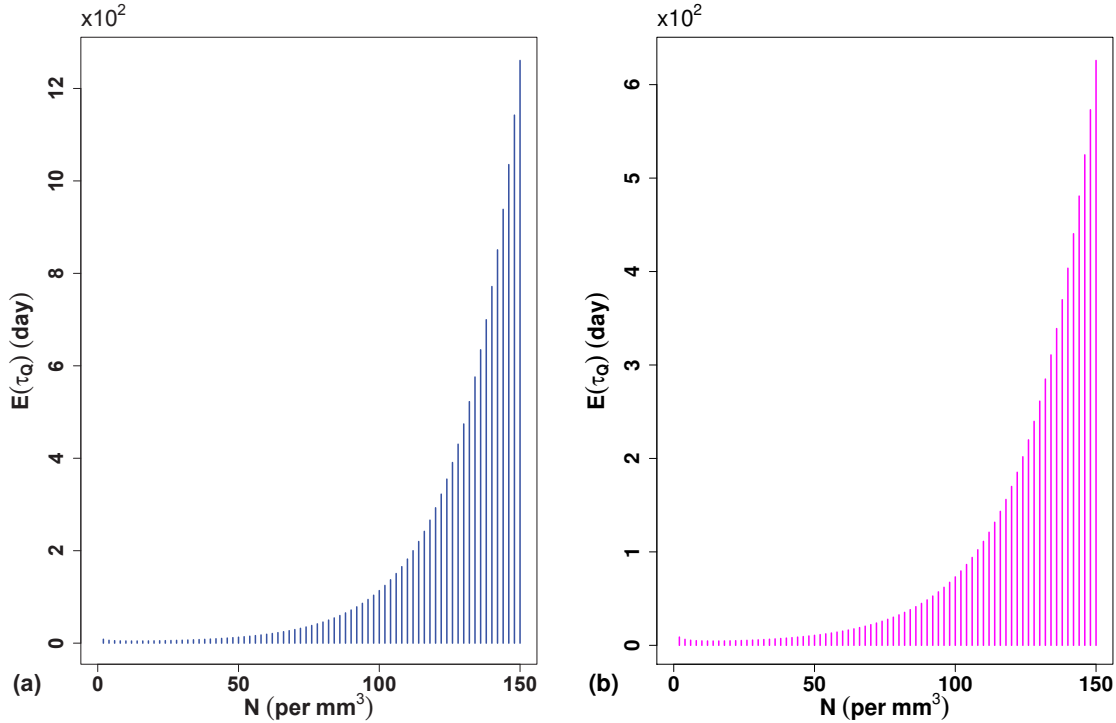


Figure 17.2: Expected time to extinction for the quasi-stationary distribution as a function of N for different ε_{ART} values, when $\varepsilon_{ART} = 0.02$ (Fig. 2(a)) and 0.03 (Fig. 2(b)) respectively. Other parameter values are taken fixed as given in Table 4.3.

17.3.1 Formulation of the Kolmogorov's Forward Equation

The probability of exactly one increment (or one decrement) in an infinitesimally small length Δt of time interval is considered as $\{\text{increment rate (or decrement rate)} \times \Delta t + O(\Delta t)\}$, and that of more than one event is $O(\Delta t)$. Then the probability $p_{m,n}(t + \Delta t)$ is given by,

$$\begin{aligned}
 p_{m,n}(t + \Delta t) = & \lambda_1(m - 1, n)p_{m-1,n}(t)\Delta t + \mu_1(m + 1, n)p_{m+1,n}(t)\Delta t \\
 & + \lambda_2(m + 1, n - 1)p_{m+1,n-1}(t)\Delta t + \mu_2(m, n + 1)p_{m,n+1}(t)\Delta t \\
 & + \{1 - K(m, n)\Delta t\}p_{m,n}(t) + O(\Delta t),
 \end{aligned} \tag{17.3.1}$$

where $K(m, n) = \lambda_1(m, n) + \mu_1(m, n) + \lambda_2(m, n) + \mu_2(m, n)$.

We can write the Kolmogorov forward equations as

$$\begin{aligned}
 p'_{m,n}(t) &= \lim_{\Delta t \rightarrow 0} \frac{p_{m,n}(t + \Delta t) - p_{m,n}(t)}{\Delta t} \\
 &= \lambda_1(m-1, n)p_{m-1,n}(t) + \mu_1(m+1, n)p_{m+1,n}(t) \\
 &\quad + \lambda_2(m+1, n-1)p_{m+1,n-1}(t) + \mu_2(m, n+1)p_{m,n+1}(t) \\
 &\quad - K(m, n)p_{m,n}(t).
 \end{aligned} \tag{17.3.2}$$

17.3.2 The Quasi-Stationary distribution

The marginal distribution of infected CD4⁺T cells at time t is given by,

$$p_{\cdot n}(t) = \sum_{m=0}^{\infty} p_{m,n}(t) = P\{I(t) = n\}. \tag{17.3.3}$$

Putting $n = 0$ in equations (17.3.2), we get

$$\begin{aligned}
 p'_{m,0}(t) &= \lambda_1(m-1, 0)p_{m-1,0}(t) + \mu_1(m+1, 0)p_{m+1,0}(t) \\
 &\quad + \lambda_2(m+1, -1)p_{m+1,-1}(t) + \mu_2(m, 1)p_{m,1}(t) - K(m, 0)p_{m,0}(t). \\
 &= sp_{m-1,0}(t) + \mu_D(m+1)p_{m+1,0}(t) + \mu_I p_{m,1}(t) - (s + \mu_D)p_{m,0}(t).
 \end{aligned}$$

Summing over all m -values, we have

$$\begin{aligned}
 \sum_{m=0}^{\infty} p'_{m,0}(t) &= s \sum_{m=0}^{\infty} p_{m-1,0}(t) + \mu_D \sum_{m=0}^{\infty} (m+1)p_{m+1,0}(t) + \mu_I \sum_{m=0}^{\infty} p_{m,1}(t) \\
 &\quad - s \sum_{m=0}^{\infty} p_{m,0}(t) - \mu_D \sum_{m=0}^{\infty} mp_{m,0}(t). \\
 \text{i.e., } p'_{\cdot 0}(t) &= \mu_I p_{\cdot 1}(t).
 \end{aligned} \tag{17.3.4}$$

The state probabilities $q_{m,n}(t)$ conditioned on not being absorbed are given as follows:

$$\begin{aligned}
 q_{m,n}(t) &= P\{D_C(t) = m, I(t) = n \mid I(t) \neq 0\} \\
 &= \frac{p_{m,n}(t)}{1 - p_{\cdot 0}(t)}, \quad m = 0, 1, 2, \dots, n = 1, 2, 3, \dots
 \end{aligned} \tag{17.3.5}$$

The marginal distribution of infected CD4⁺T-cells at time t is represented by

$$q_{\cdot n}(t) = \sum_{m=0}^{\infty} q_{m,n}(t).$$

Differentiating equation (17.3.5) and using (17.3.4), we have

$$q'_{m,n}(t) = \frac{p'_{m,n}(t)}{1 - p_{\cdot 0}(t)} + \mu_I q_{\cdot 1}(t) \frac{p_{m,n}(t)}{1 - p_{\cdot 0}(t)}. \tag{17.3.6}$$

The differential equations for the conditional state probabilities $q_{m,n}(t)$ can be written as,

$$\begin{aligned}
 q'_{m,n}(t) &= \lambda_1(m-1, n)q_{m-1,n}(t) + \mu_1(m+1, n)q_{m+1,n}(t) \\
 &\quad + \lambda_2(m+1, n-1)q_{m+1,n-1}(t) + \mu_2(m, n+1)q_{m,n+1}(t) \\
 &\quad - K(m, n)q_{m,n}(t) + \mu_I q_{\cdot 1}(t)q_{m,n}(t), \\
 &\quad m = 0, 1, 2, \dots, n = 1, 2, 3, \dots
 \end{aligned} \tag{17.3.7}$$

The quasi-stationary distribution $q_{m,n}$ is the solution of this system of equations.

17.3.3 Distribution of the Time to Extinction

It is possible to find out the distribution of the time to extinction τ with the help of (17.3.2). For the events $\tau > t$ and $\tau \leq t$ we have

$$\begin{aligned} P(\tau > t) &= P\{I(t) > 0\}, \\ P(\tau \leq t) &= P\{I(t) = 0\} = p_{0,0}(t). \end{aligned} \tag{17.3.8}$$

From (17.3.6), by equating $q'_{m,n}(t)$ to 0, we have the following initial value problems

$$p'_{m,n} = -\mu_I q_{1,1} p_{m,n}, \quad p_{m,n}(0) = q_{m,n}, \quad m = 0, 1, 2, \dots, \quad n = 1, 2, 3, \dots \tag{17.3.9}$$

Solutions of (17.3.9) are given by,

$$p_{m,n}(t) = q_{m,n} \exp(-\mu_I q_{1,1} t), \quad m = 0, 1, 2, \dots, \quad n = 1, 2, 3, \dots \tag{17.3.10}$$

Summing the expressions in (17.3.10) over all m -values, we get

$$p_{\cdot,n}(t) = q_{\cdot,n} \exp(-\mu_I q_{1,1} t), \quad n = 1, 2, 3, \dots \tag{17.3.11}$$

Equation (17.3.4) can now be solved with the help of (17.3.11). Using the initial value $p_{0,0}(0) = 0$ we acquire $p_{0,0}(t) = 1 - \exp(-\mu_I q_{1,1} t)$. Let τ_Q be the time to extinction from quasi-stationary. Then τ_Q has an exponential distribution with expected value as given by,

$$E(\tau_Q) = \frac{1}{\mu_I q_{1,1}}. \tag{17.3.12}$$

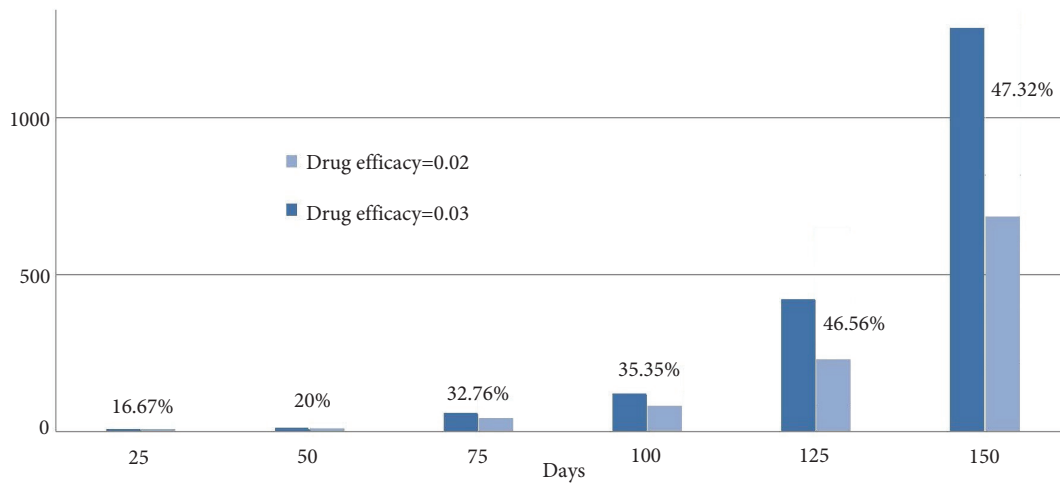


Figure 17.3: Percentage fall in the time to extinction of infected CD4+T cells for different values of ε_{ART} . Height difference between bars at different points indicates the percentage decrease in $E(\tau_Q)$.

Table 17.2: Possible changes in system (17.2.2) with probabilities.

Change	Probability
$\Delta x_1 = [1, 0]^T$	$p_1 = s\Delta t$
$\Delta x_2 = [-1, 0]^T$	$p_2 = \mu_D D_C \Delta t + \beta_2 D_C I \Delta t$
$\Delta x_3 = [0, 1]^T$	$p_3 = \beta_2 D_C I \Delta t + \beta_1 (1 - \varepsilon_{ART}) T_S I \Delta t$
$\Delta x_4 = [0, -1]^T$	$p_4 = \mu_I I \Delta t$

17.3.4 Diffusion approximation and approximation of Quasi-Stationary distribution

The critical point of equation (17.2.2) is $\hat{x} = (\hat{D}_C, \hat{I})$, where $\hat{D}_C = \frac{X}{\beta_2}$, $\hat{I} = \frac{s\beta_2 - \mu_D X}{\beta_2 X}$ and $X = \mu_I - \beta_1(1 - \varepsilon_{ART})T_S$. Possible changes in the two populations of system (17.2.2) are given in Table 17.2.

Let ΔD_C and ΔI denote the changes in the state variables D_C and I respectively during the time interval from t to $t + \Delta t$. Then, with the help of Table 4.2, the mean of the vector $\begin{pmatrix} \Delta D_C \\ \Delta I \end{pmatrix}$ is determined as follows:

$$E \begin{pmatrix} \Delta D_C \\ \Delta I \end{pmatrix} = \sum_{j=1}^4 p_j \Delta x_j = b(x)\Delta t + O(\Delta t), \tag{17.3.13}$$

where

$$b(x) = \begin{pmatrix} s - \mu_D D_C - \beta_2 D_C I \\ \beta_2 D_C I - X I \end{pmatrix}. \tag{17.3.14}$$

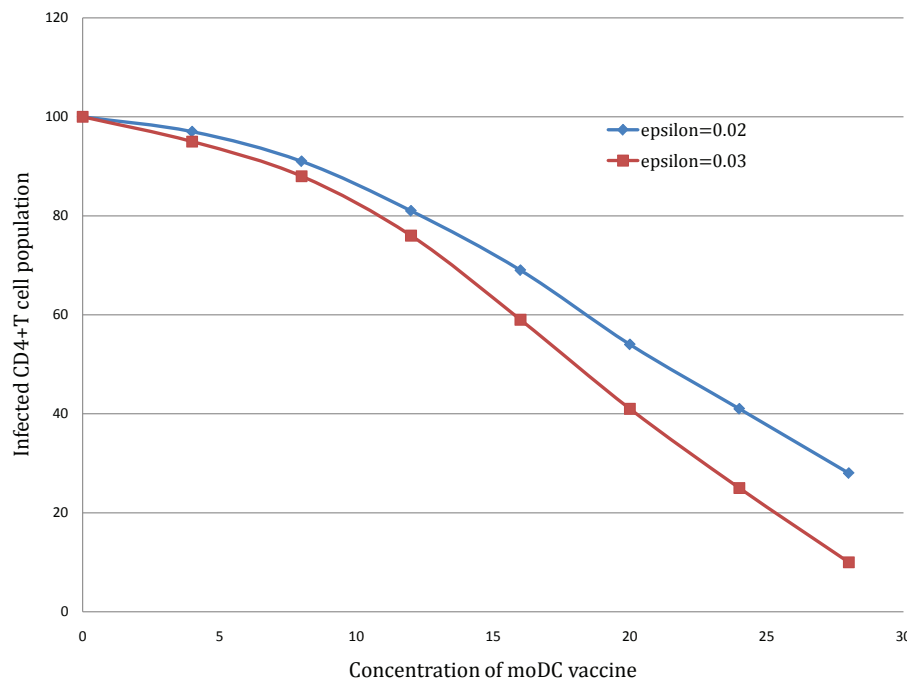


Figure 17.4: Change in infected CD4⁺T cells with DC-vaccine and different drug efficacy.

The Jacobian matrix $B(x)$ of $b(x)$ with respect to x is given by,

$$B(x) = \frac{\partial b(x)}{\partial x} = \begin{pmatrix} -\mu_D - \beta_2 I & -\beta_2 D_C \\ \beta_2 I & \beta_2 D_C - X \end{pmatrix}. \quad (17.3.15)$$

Approximating the matrix $B(x)$ by calculating at \hat{x} , we get

$$B(\hat{x}) = \begin{pmatrix} -\frac{s\beta_2}{X} & -X \\ \frac{s\beta_2}{X} - \mu_D & 0 \end{pmatrix}. \quad (17.3.16)$$

Now, using **Table 4.2**, we find out the covariance of the vector $\begin{pmatrix} \Delta D_C \\ \Delta I \end{pmatrix}$ as given by,

$$\text{Cov} \begin{pmatrix} \Delta D_C \\ \Delta I \end{pmatrix} = \sum_{j=1}^4 p_j \Delta x_j (\Delta x_j)^T = M(x) \Delta t + O(\Delta t), \quad (17.3.17)$$

where

$$M(x) = \begin{pmatrix} 2s & 0 \\ 0 & 2\mu_I I \end{pmatrix}. \quad (17.3.18)$$

$M(x)$ is approximated by evaluating at \hat{x} as follows:

$$M(\hat{x}) = \begin{pmatrix} 2s & 0 \\ 0 & \frac{2\mu_I(s\beta_2 - \mu_D X)}{\beta_2 X} \end{pmatrix}. \quad (17.3.19)$$

We approximate the process $N^{1/2}\{x(t) - \hat{x}\}$ for large values of N , the combined density of DCs and infected CD4⁺T cells, by a bivariate Ornstein-Uhlenbeck process with $B(\hat{x})$ and $M(\hat{x})$. The stationary distribution of this process is approximately bivariate normal with mean 0 and covariance matrix Σ , which can be determined from the following equation,

$$B(\hat{x})\Sigma + \Sigma B^T(\hat{x}) = -M(\hat{x}). \quad (17.3.20)$$

Here $B^T(\hat{x})$ is the transpose of $B(\hat{x})$. Solving relation (17.3.20), we obtain the matrix Σ as $\begin{pmatrix} \sigma_1 & \sigma_2 \\ \sigma_2 & \sigma_3 \end{pmatrix}$, where

$$\begin{aligned} \sigma_1 &= X \left[1 - \frac{\mu_I X}{s\beta_2} \right], \\ \sigma_2 &= \frac{\mu_I}{\beta_2}, \\ \sigma_3 &= \frac{1}{X} \left[(s\beta_2 - \mu_D X) \left(1 - \frac{\mu_I X}{s\beta_2} \right) - \frac{s\mu_I}{X} \right]. \end{aligned}$$

Note that, both of σ_1 and σ_3 are positive. The means of the marginal distributions of the amounts of DCs and infected CD4⁺T cells are \hat{D}_C and \hat{I} respectively and the standard deviations of those are $\sqrt{\sigma_1/N}$ and $\sqrt{\sigma_3/N}$ respectively. We can conclude that, the marginal distribution of infected CD4⁺T cell population in quasi-stationary is approximately normal with mean \hat{I} and standard deviation $\sqrt{\sigma_3/N}$. We approximate the normal distribution by truncated at 0.5 for the consistency of $I \geq 0$. Consequently, the distribution can be approximated by the following:

$$q.n \approx \frac{1}{\sqrt{\sigma_3/N}} \frac{\phi\{(n - \hat{I})/\sqrt{\sigma_3/N}\}}{\Phi\{(\hat{I} - 0.5)/\sqrt{\sigma_3/N}\}}, \quad (17.3.21)$$

where Φ and ϕ are the normal c.d.f. and the normal p.d.f. respectively.

17.3.5 The expected time to extinction

We find the expected time to extinction $E(\tau_Q)$ from the quasi-stationary distribution as given by

$$E(\tau_Q) = \frac{1}{\mu_I q_{1.1}} = \frac{\sqrt{\sigma_3/N} \Phi\{(\hat{I} - 0.5)/\sqrt{\sigma_3/N}\}}{\mu_I \phi\{(1 - \hat{I})/\sqrt{\sigma_3/N}\}}. \quad (17.3.22)$$

17.4 Numerical Illustrations

To illustrate the theoretical results, numerical simulations are performed in this section for approximating quasi-stationary density and expected time to extinction following the Monte Carlo simulations techniques. The values of the parameters are obtained either from several literatures or estimated from different biological sources. Here, the objective is to show how HAART treatment as well as moDC vaccine work on the dynamics of infected CD4⁺T and how it performs on the time to extinction from different scenarios.

First, the marginal distribution profile of the infected CD4⁺T in **Figure** is plotted by varying the combined density of DCs and infected CD4⁺T cells, N , in quasi-stationary state. We consider $N = 150mm^{-3}$, $100mm^{-3}$, $50mm^{-3}$ and plot the graphs. Trajectories in this figure show that the distribution is positively skewed for comparatively lower values and gradually becomes symmetric for higher magnitude of N . Thus, it can be concluded that the density of infected CD4⁺T raises with increasing values of N .

Next, in **Figures 17.2(a)** and **17.2(b)**, the expected time to extinction, $E(\tau_Q)$, as a function of N and vary the values of ε_{ART} (equal to 0.02 and 0.03) from the quasi-stationary distribution is plotted. It is seen from these two figures that the expected time to extinction raises slowly up to $N = 50 mm^{-3}$ and after that it grows rapidly with increasing density of N , which leads to a much longer duration to achieve extinction. Also, application of antiretroviral drugs can slows down the fast generation frequency of infected CD4⁺T, which is evident in the **Figure 17.2(a)**. It can be observed that the expected extinction time of infected CD4⁺T decreases phenomenally with a small increment in efficacy of drug dosage. Increasing drug dosage from $\varepsilon_{ART} = 0.02$ to 0.03 results shortening the period of time to extinction.

In **Figure 17.3**, the results found in **Figures 17.2(a)** and **17.2(b)** is considered again and compared them in bar diagram form. Difference between any two bars here indicates the percentage change in $E(\tau_Q)$. It is clearly seen from this figure that this difference gradually decreases as time passes. To make a clear perception, nextly the graphs in $I - D_C$ plane by varying the value of ε_{ART} is plotted in **Figure 17.4** and trajectories show that the rate of change in infected CD4⁺T cell population decreases when drug efficacy is higher. So, the concentration of infected CD4⁺T cell population starts to decrease, when both HAART treatment and moDC vaccination are carried out in the population.

Finally, in the last **Figure**, a bar diagram is depicted calculating the reduction of infected CD4⁺T cells when two different treatments are being carried out separately (blue and red bars) and together (green bars) in the system. From these figures, we can estimate the growth and death rates of these infected cells at different time interval more narrowly.

It is evident from the numerical analysis that accumulation of infected cell is enhanced when the population size is large. In such a scenario, it is found that instantaneous rate of contact is severely high and contributes

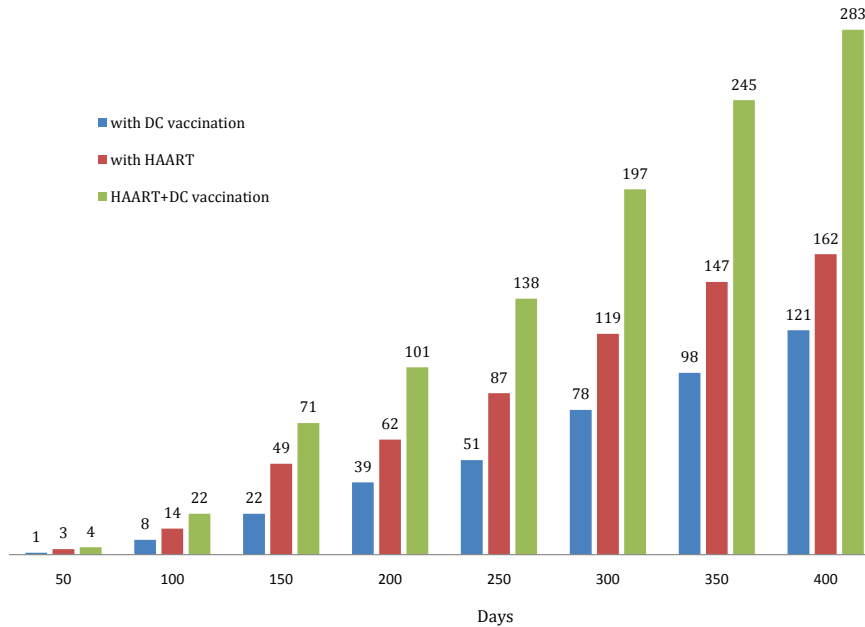


Figure 17.5: Bar diagram calculating the reduction in infected $CD4^+T$ cells when two different treatments are being carried out separately (blue and red bars) and together (green bars) in the system.

higher kurtosis which implies that the instant infection recurring probability is much higher in the population. High contact rate boosts the immunity for larger signal implication which counters balance the negative effect of such alarming contact of infection. Contrastingly, when a low susceptible population is considered, the contact process gets diluted to a large extent and thereby the skewness of the population expands (i.e positively skewed) while the kurtosis gets a little damped implicating a lower contact rate of the infection.

17.5 Summary

A stochastic immunological system of HIV infection in $CD4^+T$ cells is demonstrated considering antiretroviral treatment followed by DC-based vaccine loaded with HIV-1 derived cytotoxic T lymphocytes (CTL). It is obtained that mathematical expressions that are useful to predict the maximum time for complete eradication of the disease. The transition states of the system using Kolmogorovs forward equation to illustrate an approximation for the marginal distribution of infected cells to the expected time to extinction from quasi-stationary transition region is described.

Analytical results are compared with numerical simulations. Numerical results suggest that the quasi-stationary distribution of infected $CD4^+T$ raises with the higher magnitude of combined density, N . Moreover, high efficacy antiretroviral drugs slows down the fast generation frequency of infected $CD4^+T$ and as a result the rate of complete eradication of the disease gets faster. But, it is evident that accumulation of infected cell is enhanced when the population size is large. This is because instantaneous rate of contact is severely high and contributes higher kurtosis in the population.

These findings suggest that a stochastic system gives more realistic way of modelling a immunological

system, while a deterministic model cannot. In particular, as most real world problems are not deterministic, stochastic models helps us in capturing the distribution of state variables from where one can derive an expression for probabilistic extinction and variances which are features that cannot be included in deterministic models. A simple stochastic system is demonstrated that captures some important features and belief that these findings may help students and researchers for future studies.

Unit 18

Course Structure

- Leslie-Gower Predator-prey model with different functional responses
 - Analysis of Different Functional Responses
 - Effect of Nutrients on Autotroph-Herbivore Interaction
 - Phytoplankton-zooplankton System and its Stability Analysis
 - Bio-Control in Plankton Models with Nutrient Recycling
 - Stability of food Chain Models
-

18.1 Leslie-Gower Predator-prey model with different functional responses

The Leslie-Gower predator-prey model is a classic mathematical model used to describe the interactions between predators and prey in ecological systems. It extends the Lotka-Volterra model by incorporating more realistic assumptions about population dynamics. One of the key features of the Leslie-Gower model is the inclusion of different functional responses, which describe how the predation rate of predators varies with changes in prey density. Here's how the model can be formulated with different functional responses:

Let $P(t)$ represent the population of predators at time t , and $N(t)$ represent the population of prey at time t .

The Leslie-Gower predator-prey model with different functional responses can be represented by the following system of differential equations:

$$\frac{dN}{dt} = rN \left(1 - \frac{N}{K}\right) - \sum_i f_i(N)P_i$$
$$\frac{dP_i}{dt} = b_i f_i(N)P_i - d_i P_i$$

where:

- r is the intrinsic growth rate of the prey population.

- K is the carrying capacity of the environment for the prey.
- $f_i(N)$ represents the functional response of predator i , which describes how the predation rate of predator i changes with changes in prey density.
- b_i is the per capita birth rate of predator i .
- d_i is the per capita death rate of predator i .

The functional responses $f_i(N)$ can take various forms, representing different types of predator-prey interactions. Some common functional responses include:

1. **Type I Functional Response (Linear):**

$$f_i(N) = a_i N$$

where a_i represents the attack rate of predator i . In this functional response, the predation rate increases linearly with prey density.

2. **Type II Functional Response (Saturating):**

$$f_i(N) = \frac{a_i N}{1 + h_i N}$$

where h_i represents the handling time of predator i . In this functional response, the predation rate initially increases with prey density but saturates as prey density increases further.

3. **Type III Functional Response (sigmoidal):**

$$f_i(N) = \frac{a_i N^2}{1 + h_i N^2}$$

Similar to the Type II functional response, but with a sigmoidal shape. The predation rate initially increases slowly, accelerates, and then saturates as prey density increases.

These different functional responses capture various aspects of predator-prey interactions and can lead to different dynamics and stability properties of the predator-prey system. Analyzing the model with different functional responses allows researchers to understand how the form of predator-prey interactions influences the long-term behavior of ecological systems.

18.1.1 Characteristics, Classifications and Features

Let's delve deeper into each of the functional responses for the Leslie-Gower predator-prey model and analyze their mathematical characteristics:

1. Type I Functional Response (Linear):

The Type I functional response assumes a linear relationship between the predation rate and prey density. Mathematically, it is represented as:

$$f_i(N) = a_i N$$

where:

- a_i is the attack rate of predator i .

Mathematical Characteristics:

- **Predation Rate:** Increases linearly with prey density.
- **Predator Saturation:** No saturation occurs. Predation rate continues to increase with increasing prey density.
- **Assumptions:** Assumes predators have unlimited handling capacity and encounter prey randomly.

Analysis:

- **Population Dynamics:** The linear functional response implies that predation increases proportionally with prey density, without any limitations due to predator saturation or handling capacity.
- **Stability:** The linear functional response can lead to stable or oscillatory dynamics, depending on other parameters in the model. Stable coexistence of predator and prey populations is possible if the growth rates and other parameters are appropriately balanced.

2. Type II Functional Response (Saturating):

The Type II functional response accounts for predator saturation as prey density increases. It is represented as:

$$f_i(N) = \frac{a_i N}{1 + h_i N}$$

where:

- a_i is the attack rate of predator i .
- h_i is the handling time of predator i .

Mathematical Characteristics:

- **Predation Rate:** Initially increases with prey density but saturates as prey density increases further.
- **Predator Saturation:** As prey density increases, the predator's rate of prey consumption saturates due to handling time constraints.
- **Assumptions:** Assumes predators have limited handling capacity, and their predation rate saturates as prey density increases.

Analysis:

- **Population Dynamics:** The Type II functional response leads to a saturating predation rate, which stabilizes the predator-prey dynamics. As prey density increases, predators consume prey more efficiently, but at a diminishing rate due to handling time constraints.
- **Stability:** This functional response often stabilizes the predator-prey system, promoting coexistence between predators and prey. However, unstable dynamics can occur under certain parameter combinations, leading to limit cycles or predator extinction.

3. Type III Functional Response (Sigmoidal):

The Type III functional response is sigmoidal in shape, capturing a more complex relationship between predation rate and prey density. It is represented as:

$$f_i(N) = \frac{a_i N^2}{1 + h_i N^2}$$

where:

- a_i is the attack rate of predator i .
- h_i is the handling time of predator i .

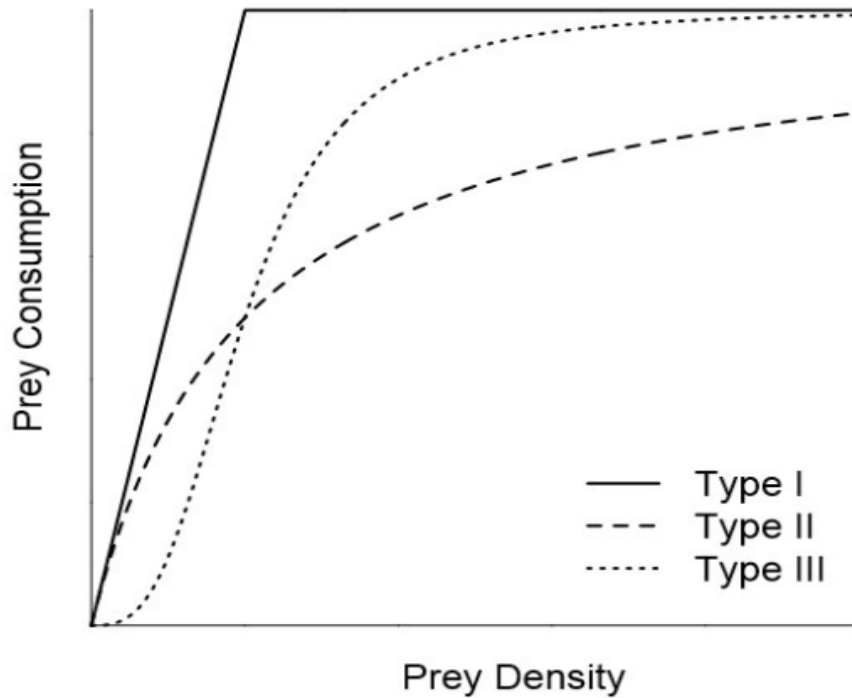


Figure 18.1: Different functional responses.

Mathematical Characteristics:

- **Predation Rate:** Initially increases slowly, accelerates, and then saturates as prey density increases.
- **Predator Saturation:** Similar to Type II, but with a more gradual saturation due to the sigmoidal shape of the response curve.
- **Assumptions:** Assumes predators have limited handling capacity and the predation rate saturates sigmoidally as prey density increases.

Analysis:

- **Population Dynamics:** The Type III functional response introduces a more complex relationship between predation rate and prey density compared to Type II. It allows for a smoother transition from low to high predation rates as prey density increases.
- **Stability:** Similar to Type II, the Type III functional response tends to stabilize the predator-prey system by limiting the predator's ability to overexploit prey at high densities. However, as with Type II, unstable dynamics can occur depending on parameter values.

Summary:

Each functional response captures different aspects of predator-prey interactions, leading to distinct mathematical characteristics and stability properties in the Leslie-Gower predator-prey model. While Type I is the simplest and assumes unlimited predator capacity, Types II and III introduce predator saturation effects, with Type III offering a smoother transition in predation rates. Analyzing the model with these functional responses provides insights into the dynamics and stability of ecological systems under varying conditions.

18.2 Effect of Nutrients on Autotroph-Herbivore Interaction

Effect of Nutrients on Autotroph-Herbivore Interaction:

The interaction between autotrophs (plants or primary producers) and herbivores (animals that consume plants) is a fundamental component of ecological systems. Nutrients play a crucial role in shaping this interaction by influencing the growth and productivity of autotrophs, which in turn affects herbivore populations. Here's an analysis of the effect of nutrients on autotroph-herbivore interactions:

1. Nutrient Availability and Autotroph Productivity:

- **Increased Nutrient Availability:** Higher nutrient availability, particularly nitrogen and phosphorus, can enhance the growth and productivity of autotrophs. Nutrients serve as essential building blocks for plant growth, influencing photosynthesis, biomass accumulation, and reproductive output.
- **Limiting Nutrient Availability:** Conversely, limited availability of nutrients can constrain autotroph growth and productivity. Nutrient limitation can occur in ecosystems with poor soil fertility or in aquatic systems with low nutrient input.

2. Effects on Herbivore Populations:

- **Positive Feedback:** Higher autotroph productivity resulting from increased nutrient availability can lead to larger herbivore populations. More abundant food resources support higher herbivore densities and may lead to increased herbivore reproduction rates.
- **Herbivore Responses to Nutrient Variation:** Herbivores may exhibit complex responses to changes in nutrient availability. Some species may benefit from increased autotroph productivity, while others may experience decreased foraging efficiency or increased competition for food resources.

3. Trophic Cascades and Community Dynamics:

- **Top-Down Regulation:** Changes in herbivore populations due to nutrient availability can cascade through the food web, affecting higher trophic levels. For example, increased herbivore abundance may lead to higher predation pressure on herbivores from predators, thereby influencing community structure and dynamics.
- **Bottom-Up Regulation:** Conversely, changes in autotroph productivity due to nutrient availability can also influence higher trophic levels indirectly. This bottom-up regulation occurs when alterations in autotroph abundance and quality affect herbivore populations, which in turn influence predator populations.

4. Ecosystem Functioning and Stability:

- **Nutrient Enrichment Effects:** Excessive nutrient inputs, such as from agricultural runoff or urban pollution, can lead to eutrophication and alter autotroph-herbivore interactions. Eutrophication can cause algal blooms, shifts in community composition, and disruptions in trophic dynamics.
- **Ecosystem Resilience:** Balanced nutrient cycling is essential for ecosystem resilience and stability. Disruptions in autotroph-herbivore interactions due to nutrient imbalances can lead to ecosystem degradation, loss of biodiversity, and reduced ecosystem services.

5. Management Implications:

- **Nutrient Management:** Sustainable management of nutrient inputs is crucial for maintaining ecosystem health and functioning. Practices such as nutrient cycling, soil conservation, and watershed management can help mitigate the negative effects of nutrient imbalances on autotroph-herbivore interactions.
- **Ecosystem-Based Management:** Integrated approaches that consider the complex interactions between autotrophs, herbivores, and nutrients are essential for effective ecosystem-based management. Adaptive management strategies that account for ecosystem dynamics and feedbacks can promote resilience and sustainability.

In summary, nutrients play a central role in mediating autotroph-herbivore interactions, influencing productivity, population dynamics, trophic cascades, and ecosystem stability. Understanding the complex interplay between nutrients and biotic interactions is essential for ecosystem management and conservation in the face of environmental change.

18.3 Phytoplankton-zooplankton System and its Stability Analysis

Mathematical models of phytoplankton-zooplankton systems are essential for understanding the dynamics of aquatic ecosystems, including nutrient cycling, primary production, and trophic interactions. These models typically describe the population dynamics of phytoplankton (primary producers) and zooplankton (primary consumers) and their interactions with nutrient availability. Here's an overview of such models and their stability analysis:

1. Basic Models:

1. Lotka-Volterra Model:

- The Lotka-Volterra model describes the interaction between two species (e.g., phytoplankton and zooplankton) in terms of population growth and predation.
- Equations describe the rates of change in phytoplankton and zooplankton populations over time, considering growth, mortality, and predation rates.
- Stability analysis involves examining the stability of equilibrium points and the potential for sustained oscillations or population cycles.

2. Resource-Based Models:

- Resource-based models incorporate nutrient dynamics as a driving factor for phytoplankton growth and zooplankton grazing.
- Equations describe the dynamics of nutrient concentrations, phytoplankton biomass, and zooplankton biomass, considering nutrient uptake, phytoplankton growth, grazing, and nutrient recycling.
- Stability analysis involves assessing the stability of nutrient-driven equilibria and the potential for nutrient-driven oscillations or instability.

2. Coupled Phytoplankton-Zooplankton Models:

1. Functional Response Models:

- These models describe the interaction between phytoplankton and zooplankton populations based on functional responses that relate zooplankton grazing rates to phytoplankton biomass.
- Different functional response forms (e.g., linear, Holling type I, II, III) represent different grazing behaviors and prey preferences of zooplankton.
- Stability analysis involves examining the stability of equilibria and the potential for oscillatory behavior or alternative stable states.

2. Size-Structured Models:

- Size-structured models account for size-dependent interactions between phytoplankton and zooplankton populations.
- Equations describe the distribution of individuals across size classes and the rates of growth, mortality, and predation as functions of size.
- Stability analysis considers the stability of size-structured equilibria and the effects of size-dependent processes on population dynamics.

3. Stability Analysis:

1. Equilibrium Stability:

- Linear stability analysis is commonly used to assess the stability of equilibrium points in phytoplankton-zooplankton models.
- Eigenvalue analysis of the Jacobian matrix around equilibrium points helps determine stability properties.
- Stable equilibria indicate coexistence or stable population dynamics, while unstable equilibria may lead to oscillations or regime shifts.

2. Bifurcation Analysis:

- Bifurcation analysis investigates how changes in model parameters lead to qualitative shifts in system behavior.
- Bifurcations such as Hopf bifurcations can result in the emergence of sustained oscillations or alternative stable states.
- Understanding bifurcation phenomena helps identify critical thresholds and tipping points in phytoplankton zooplankton systems.

4. Applications and Management Implications:

- Mathematical models of phytoplankton-zooplankton systems have applications in ecosystem management, fisheries management, and environmental conservation.
- They help assess the effects of environmental changes (e.g., nutrient pollution, climate change) on aquatic ecosystems and inform strategies for sustainable resource use.
- Management strategies informed by these models aim to promote ecosystem resilience, maintain biodiversity, and mitigate the impacts of anthropogenic disturbances.

In summary, mathematical models of phytoplankton-zooplankton systems are valuable tools for understanding the dynamics of aquatic ecosystems and their responses to environmental change. Through rigorous analysis and simulation, these models contribute to our understanding of trophic interactions, nutrient cycling, and ecosystem stability, ultimately guiding management and conservation efforts.

18.4 Bio-Control in Plankton Models with Nutrient Recycling

Bio-control in plankton models with nutrient recycling, we'll consider a simplified model incorporating predator-prey interactions between phytoplankton (P) and zooplankton (Z) populations, along with nutrient cycling dynamics. We'll analyze the stability of the system with and without the introduction of bio-control (i.e., the addition of zooplankton predators).

Let's start with the basic predator-prey model:

$$\frac{dP}{dt} = rP \left(1 - \frac{P}{K} \right) - \alpha PZ$$

$$\frac{dZ}{dt} = \beta \alpha PZ - mZ$$

Where:

- P is the biomass of phytoplankton,
- Z is the biomass of zooplankton,
- r is the intrinsic growth rate of phytoplankton,
- K is the carrying capacity of the environment for phytoplankton,

- α is the encounter rate coefficient between phytoplankton and zooplankton,
- β is the conversion efficiency of consumed phytoplankton biomass into zooplankton biomass,
- m is the mortality rate of zooplankton.

Now, let's introduce the bio-control scenario by modifying the model to incorporate the addition of zooplankton predators. We can represent this by adding a term γZ_{int} , where Z_{int} is the biomass of introduced zooplankton predators, and γ represents the predation rate of introduced predators on phytoplankton:

$$\frac{dP}{dt} = rP \left(1 - \frac{P}{K} \right) - \alpha PZ - \gamma P Z_{\text{int}}$$

$$\frac{dZ}{dt} = \beta \alpha PZ - mZ + \gamma P Z_{\text{int}}$$

To analyze the stability of the system with and without bio-control, we'll:

1. Find the equilibrium points (P^* , Z^*) for both scenarios.
2. Calculate the Jacobian matrix J for each equilibrium point.
3. Compute the eigenvalues of J to determine stability.

By comparing the stability properties of the equilibrium points with and without bio-control, we can mathematically demonstrate the impact of bio-control on the stability of the plankton model with nutrient recycling.

18.5 Stability of food Chain Models

Let's consider a mathematical model of a simple food chain consisting of three trophic levels: primary producers (plants or phytoplankton, denoted by P), primary consumers (herbivores, denoted by H), and secondary consumers (carnivores, denoted by C). The dynamics of this system can be described by a set of ordinary differential equations representing the rates of change of each population over time. Here's an example model and its analysis:

Mathematical Model:

The dynamics of the food chain can be described by the following set of differential equations:

$$\frac{dP}{dt} = rP \left(1 - \frac{P}{K} \right) - \alpha_{PH}PH$$

$$\frac{dH}{dt} = \alpha_{PH}PH - \alpha_{HC}HC - \mu_H H$$

$$\frac{dC}{dt} = \alpha_{HC}HC - \mu_C C$$

Where:

- P is the density of primary producers (e.g., plants or phytoplankton),
- H is the density of primary consumers (herbivores),

- C is the density of secondary consumers (carnivores),
- r is the intrinsic growth rate of primary producers,
- K is the carrying capacity of the environment for primary producers,
- α_{PH} is the consumption rate of primary producers by herbivores,
- α_{HC} is the consumption rate of herbivores by carnivores,
- μ_H is the mortality rate of herbivores,
- μ_C is the mortality rate of carnivores.

Parameters and Variables:

- $r, K, \alpha_{PH}, \alpha_{HC}, \mu_H,$ and μ_C are model parameters representing biological rates and interactions.
- $P, H,$ and C are state variables representing population densities.

let's proceed with the detailed stability analysis of the food chain model

Equilibrium Points:

1. Equation for P :

$$\frac{dP}{dt} = rP \left(1 - \frac{P}{K} \right) - \alpha_{PH}PH = 0$$

Solving for P gives:

$$P^* = 0 \quad \text{or} \quad P^* = K - \frac{\alpha_{PH}H}{r}$$

2. Equation for H :

$$\frac{dH}{dt} = \alpha_{PH}PH - \alpha_{HC}HC - \mu_H H = 0$$

Solving for H gives:

$$H^* = 0 \quad \text{or} \quad H^* = \frac{\alpha_{PH}P}{\alpha_{HC}C + \mu_H}$$

3. Equation for C :

$$\frac{dC}{dt} = \alpha_{HC}HC - \mu_C C = 0$$

Solving for C gives:

$$C^* = 0 \quad (\text{always})$$

Jacobian Matrix:1. **Jacobian Matrix at $P^* = 0$:**

$$J_{P^*=0} = \begin{pmatrix} -r & 0 & 0 \\ 0 & \alpha_{PH} & 0 \\ 0 & 0 & -\mu_C \end{pmatrix}$$

2. **Jacobian Matrix at $H^* = 0$:**

$$J_{H^*=0} = \begin{pmatrix} -r & 0 & 0 \\ 0 & -\mu_H & -\frac{\alpha_{HC}\alpha_{PH}}{\mu_H} \\ 0 & 0 & -\mu_C \end{pmatrix}$$

3. **Jacobian Matrix at $P^* = K - \frac{\alpha_{PH}H}{r}$, $H^* = \frac{\alpha_{PH}P}{\alpha_{HC}C + \mu_H}$, and $C^* = 0$:**

$$J_{P^*,H^*,C^*} = \begin{pmatrix} -r + \frac{rP^*}{K} & -\frac{\alpha_{PH}P^*}{K} & 0 \\ \frac{\alpha_{PH}H^*}{\alpha_{HC}C + \mu_H} & -\alpha_{HC} & -\frac{\alpha_{PH}H^*}{\alpha_{HC}C + \mu_H} \\ 0 & \alpha_{HC} & -\mu_C \end{pmatrix}$$

Eigenvalues:

Finally, we find the eigenvalues of each Jacobian matrix to determine their stability properties. Positive real parts indicate instability, while negative real parts indicate stability.

Unit 19

Course Structure

- Micobacterial Growth with Memory Phenomena
 - Analysis of Fractional Mathematical Systems
 - Extension of Deterministic Model
 - Boundedness, Uniqueness of Solutions and Stability Analysis of Steady States
-

19.1 Preliminaries

Some crucial fundamental definitions from the theory of fractional calculus are presented in this section.

Definition 19.1.1. The Caputo fractional derivative operator of order ζ ($\zeta \geq 0$) & $n \in \mathbb{N} \cup \{0\}$ is defined by

$$D_t^\zeta(u(t)) = \frac{1}{\Gamma(n-\zeta)} \int_0^t (t-\xi)^{n-\zeta-1} \frac{d^n}{dt^n} u(\xi) d\xi \quad (19.1.1)$$

where $n-1 \leq \zeta < n$.

Definition 19.1.2. Let $v \in H'(a, b)$, $b > a$, $0 < \zeta < 1$. Then, the time-fractional Caputo–Fabrizio fractional differential operator is defined as

$${}^{CF}D_t^\zeta(v(t)) = \frac{M(\zeta)}{1-\zeta} \int_0^t \exp\left[-\frac{\zeta(t-\xi)}{1-\zeta}\right] v'(\xi) d\xi, \quad t \geq 0, \quad 0 < \zeta < 1 \quad (19.1.2)$$

where $M(\zeta)$ is a normalization function which depends on ζ and satisfies the condition $M(0) = M(1) = 1$.

Definition 19.1.3. The Caputo–Fabrizio (CF) fractional integral operator of order $0 < \zeta < 1$ is given by

$${}^{CF}\mathcal{I}_t^\zeta(v(t)) = \frac{2(1-\zeta)}{(2-\zeta)M(\zeta)} v(t) + \frac{2\zeta}{(2-\zeta)M(\zeta)} \int_0^t v(\xi) d\xi, \quad t \geq 0. \quad (19.1.3)$$

Here, it is important to note that

$${}^{CF}D_t^\zeta(v(t)) = 0 \text{ if } v(t) \text{ is a constant function.}$$

Furthermore, it is imperative to observe that the previous definitions completely suggest that the fractional integral of a function of order $0 < \zeta < 1$ is actually represented by the average of the respective functions and their integral of order one. Furthermore, the equation

$$\frac{2(1-\zeta)}{(2-\zeta)M(\zeta)} + \frac{2\zeta}{(2-\zeta)M(\zeta)} = 1 \quad (19.1.4)$$

holds true, which provides the following formula:

$$M(\zeta) = \frac{2}{(2-\zeta)}, \quad 0 \leq \zeta < 1. \quad (19.1.5)$$

Here, the specific form of the normalizing function $M(\zeta)$ given in (19.1.5) along with the boundary conditions is used throughout the study and, more specifically, for the purpose of numerical simulations.

Definition 19.1.4. The Laplace transform for the CF fractional operator of order $0 < \zeta \leq 1$ for $k \in \mathbb{N}$ is given as follows:

$$\begin{aligned} \mathcal{L} \left({}^{CF}D_t^{k+\zeta}(v(t)) \right) (p) &= \frac{1}{1-\zeta} \mathcal{L} \left(v^{k+1}(t) \mathcal{L} \left(\exp \left(-\frac{\zeta}{1-\zeta} t \right) \right) \right) \\ &= \frac{p^{k+1} \mathcal{L}(v(t)) - p^k v(0) - p^{k-1} v'(0) \dots - v^k(0)}{p + \zeta(1-p)}. \end{aligned}$$

To be precise, we can say that

$$\begin{aligned} \mathcal{L} \left({}^{CF}D_t^\zeta(v(t)) \right) (p) &= \frac{p \mathcal{L}(v(t))}{p + \zeta(1-p)}, \quad k = 0 \\ \mathcal{L} \left({}^{CF}D_t^{\zeta+1}(v(t)) \right) (p) &= \frac{p^2 \mathcal{L}(v(t)) - p v(0) - v'(0)}{p + \zeta(1-p)}, \quad k = 1. \end{aligned}$$

19.2 The Basic Integer-Order Model and the CF Fractionalized Model

In recent years, fractional-order derivatives have gained huge importance in the field of modeling real-world biological phenomena. The fractional-order derivative is in fact a much generalized version of the integer-order derivative. In this chapter, we now introduce the basic three-dimensional nonlinear ODE-based mathematical model developed that describes the fundamental disease dynamics of leprosy.

$$\begin{aligned} \frac{dS_u}{dt} &= \nu_1 S_u \left(1 - \frac{S_u}{S_{u_{max}}} \right) - \beta_1 S_u B_l, \\ \frac{dS_i}{dt} &= \beta_1 S_u B_l - \mu S_i, \\ \frac{dB_l}{dt} &= \nu_2 B_l \left(1 - \frac{B_l}{B_{l_{max}}} \right) - \beta_2 S_u B_l + \sigma S_i, \end{aligned} \quad (19.2.1)$$

with initial values $S_u(0) = S_{u_0} \geq 0$, $S_i(0) = S_{i_0} \geq 0$ and $B_l(0) = B_0 \geq 0$ at $t = 0$. Here, $S_u(t)$, $S_i(t)$ and $B_l(t)$ denote the concentrations of healthy Schwann cells, infected Schwann cells and *M. leprae* bacteria at any time t . ν_1 and ν_2 describe the intrinsic growth rates of the $S_u(t)$ and $B_l(t)$ populations, where $S_{u_{max}}$ and $B_{l_{max}}$ are the carrying capacity of the same. β_1 is the rate at which healthy cells are infected by *M. leprae* and

μ denotes the natural mortality rate of S_i cells. The bacterial clearance rate results from the infection and the proliferation rates of newly produced free *M. leprae* bacteria, which are indicated by the parameters β_2 and σ , respectively. Modifying the above system in terms of the CF (Caputo–Fabrizio) fractional differential system of equations, we obtain

$$\begin{aligned} {}^{CF}D_t^\zeta S_u(t) &= \nu_1 S_u \left(1 - \frac{S_u}{S_{u_{max}}}\right) - \beta_1 S_u B_l, \\ {}^{CF}D_t^\zeta S_i(t) &= \beta_1 S_u B_l - \mu S_i, \\ {}^{CF}D_t^\zeta B_l(t) &= \nu_2 B_l \left(1 - \frac{B_l}{B_{l_{max}}}\right) - \beta_2 S_u B_l + \sigma S_i \end{aligned} \quad (19.2.2)$$

with initial values $S_u(0) = S_{u_0} \geq 0$, $S_i(0) = S_{i_0} \geq 0$ and $B_l(0) = B_0 \geq 0$ at $t = 0$.

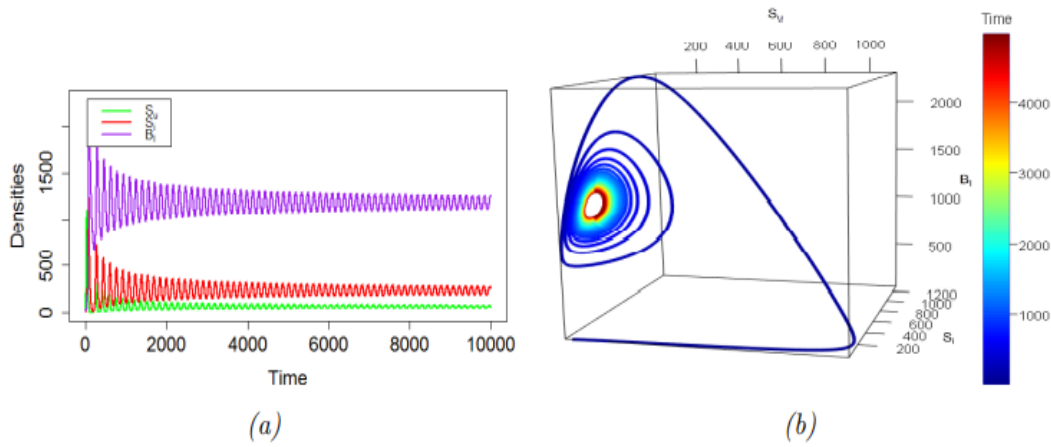


Figure 19.1: Time series and phase portrait diagram of the CF fractionalized system (19.2.2) depicting the unstable oscillatory behavior of the system state populations and appearance of stable limit cycles for $\zeta = 1$. Values of $\nu_2 = 0.03$ and $S_{u_{max}} = 1200$ were used to simulate the subfigures in this figure. (a) Behavior of the trajectories of system (19.2.2); (b) 3-D phase diagram for system (19.2.2) in $S_u - S_i - B_l$ space.

19.2.1 The Iterative Scheme

We now consider system (19.2.2). The term $S_u B_l$ is a nonlinear term and, hence, applying the Laplace transformation operator (\mathcal{L}) on both sides of the system (19.2.2), we obtain that

$$\begin{aligned} \frac{p\mathcal{L}(S_u(t)) - S_u(0)}{p + \zeta(1-p)} &= \mathcal{L} \left(\nu_1 S_u \left(1 - \frac{S_u}{S_{u_{max}}}\right) - \beta_1 S_u B_l \right), \\ \frac{p\mathcal{L}(S_i(t)) - S_i(0)}{p + \zeta(1-p)} &= \mathcal{L} (\beta_1 S_u B_l - \mu S_i), \\ \frac{p\mathcal{L}(B_l(t)) - B_l(0)}{p + \zeta(1-p)} &= \mathcal{L} \left(\nu_2 B_l \left(1 - \frac{B_l}{B_{l_{max}}}\right) - \beta_2 S_u B_l + \sigma S_i \right). \end{aligned} \quad (19.2.3)$$

The set in Equation (19.2.3) can now be rewritten in the following form:

$$\begin{aligned}\mathcal{L}(S_u(t)) &= \frac{S_u(0)}{p} + \left(\frac{p + \zeta(1-p)}{p}\right) \mathcal{L}\left(\nu_1 S_u \left(1 - \frac{S_u}{S_{u_{max}}}\right) - \beta_1 S_u B_l\right), \\ \mathcal{L}(S_i(t)) &= \frac{S_i(0)}{p} + \left(\frac{p + \zeta(1-p)}{p}\right) \mathcal{L}(\beta_1 S_u B_l - \mu S_i), \\ \mathcal{L}(B_l(t)) &= \frac{B_l(0)}{p} + \left(\frac{p + \zeta(1-p)}{p}\right) \mathcal{L}\left(\nu_2 B_l \left(1 - \frac{B_l}{B_{l_{max}}}\right) - \beta_2 S_u B_l + \sigma S_i\right).\end{aligned}\tag{19.2.4}$$

Using the inverse Laplace, we obtain

$$\begin{aligned}S_u(t) &= S_u(0) + \mathcal{L}^{-1}\left[\frac{p + \zeta(1-p)}{p} \mathcal{L}\left(\nu_1 S_u \left(1 - \frac{S_u}{S_{u_{max}}}\right) - \beta_1 S_u B_l\right)\right], \\ S_i(t) &= S_i(0) + \mathcal{L}^{-1}\left[\frac{p + \zeta(1-p)}{p} \mathcal{L}(\beta_1 S_u B_l - \mu S_i)\right], \\ B_l(t) &= B_l(0) + \mathcal{L}^{-1}\left[\frac{p + \zeta(1-p)}{p} \mathcal{L}\left(\nu_2 B_l \left(1 - \frac{B_l}{B_{l_{max}}}\right) - \beta_2 S_u B_l + \sigma S_i\right)\right].\end{aligned}\tag{19.2.5}$$

We now present the series solutions generated by this method as follows:

$$S_u = \sum_{n=0}^{\infty} S_{u_n}, \quad S_i = \sum_{n=0}^{\infty} S_{i_n}, \quad B_l = \sum_{n=0}^{\infty} B_{l_n}.\tag{19.2.6}$$

Furthermore, the series solution representation of the only existing nonlinear term $S_u B_l$ is given as

$$S_u B_l = \sum_{n=0}^{\infty} G_n \quad \text{where} \quad G_n = \sum_{k=0}^n S_{u_k} \sum_{k=0}^n B_{l_k} - \sum_{k=0}^{n-1} S_{u_k} \sum_{k=0}^{n-1} B_{l_k}.\tag{19.2.7}$$

We now use the initial conditions to achieve the following recursive formulas:

$$\begin{aligned}S_{u_{n+1}} &= S_{u_n}(0) + \mathcal{L}^{-1}\left[\frac{p + \zeta(1-p)}{p} \mathcal{L}\left(\nu_1 S_{u_n} \left(1 - \frac{S_{u_n}}{S_{u_{max}}}\right) - \beta_1 S_{u_n} B_{l_n}\right)\right], \\ S_{i_{n+1}} &= S_{i_n}(0) + \mathcal{L}^{-1}\left[\frac{p + \zeta(1-p)}{p} \mathcal{L}(\beta_1 S_{u_n} B_{l_n} - \mu S_{i_n})\right], \\ B_{l_{n+1}} &= B_{l_n}(0) + \mathcal{L}^{-1}\left[\frac{p + \zeta(1-p)}{p} \mathcal{L}\left(\nu_2 B_{l_n} \left(1 - \frac{B_{l_n}}{B_{l_{max}}}\right) - \beta_2 S_{u_n} B_{l_n} + \sigma S_{i_n}\right)\right].\end{aligned}\tag{19.2.8}$$

The approximate solution is assumed to be obtained as a limit when $n \rightarrow \infty$, i.e., $S_u(t) = \lim_{n \rightarrow \infty} S_{u_n}(t)$, $S_i(t) = \lim_{n \rightarrow \infty} S_{i_n}(t)$ and $B_l(t) = \lim_{n \rightarrow \infty} B_{l_n}(t)$.

19.2.2 Stability Analysis

In this section, first, we present the detailed definition of the T-stability of Picard's iteration.

Definition 19.2.1. Suppose T is a self-map on a complete metric space (Y, d) . Consider an iteration $y_{n+1} = g(T, y_n)$. Furthermore, let us assume that $\mathcal{P}(T)$ is the fixed-point set of T with $\mathcal{P}(T) \neq \phi$ and let $\{y_n\}$ converge to some point $y \in \mathcal{P}(T)$. Let $\{z_n\} \subset Y$ and define $\{u_n\} = d(Z_{n+1}, g(T, z_n))$. Now, if $u_n \rightarrow 0$ implies that $z_n \rightarrow y$, then the iteration method $y_{n+1} = g(T, y_n)$ is said to be T-stable. Furthermore, note that the convergence of $\{z_n\}$ guarantees that $\{z_n\}$ must be bounded above. If all these conditions hold true for $y_{n+1} = g(T, y_n)$, then Picard's iteration method is called T-stable.

Let $(\mathbb{X}, \|\cdot\|)$ be a Banach space. As every Banach space is a complete metric space with the metric induced by the associated norm, Definition 19.2.1 holds true for $(\mathbb{X}, \|\cdot\|)$ also.

Theorem 19.2.1. Let T be a self-map on the space $(\mathbb{X}, \|\cdot\|)$, which satisfies the following:

$$\|T_x - T_y\| \leq \Lambda \|x - T_x\| + \varrho \|x - y\| \quad \text{for all } x, y \in \mathbb{X}$$

where $\Lambda \geq 0$ and $\varrho \in [0, 1)$. Suppose T has a fixed point. Then, T is Picard's T-stable.

Now, let us define a self-map T as

$$\begin{aligned} T(S_{u_n}(t)) &= S_{u_{n+1}} = S_{u_n}(0) + \mathcal{L}^{-1} \left[\frac{p + \zeta(1-p)}{p} \mathcal{L} \left(\nu_1 S_{u_n} \left(1 - \frac{S_{u_n}}{S_{u_{max}}} \right) - \beta_1 S_{u_n} B_{l_n} \right) \right], \\ T(S_{i_n}(t)) &= S_{i_{n+1}} = S_{i_n}(0) + \mathcal{L}^{-1} \left[\frac{p + \zeta(1-p)}{p} \mathcal{L} (\beta_1 S_{u_n} B_{l_n} - \mu S_{i_n}) \right], \\ T(B_{l_n}(t)) &= B_{l_{n+1}} = B_{l_n}(0) + \mathcal{L}^{-1} \left[\frac{p + \zeta(1-p)}{p} \mathcal{L} \left(\nu_2 B_{l_n} \left(1 - \frac{B_{l_n}}{B_{l_{max}}} \right) - \beta_2 S_{u_n} B_{l_n} + \sigma S_{i_n} \right) \right] \end{aligned}$$

For all $m, n \in \mathbb{N}$, let us first construct the following differences:

$$\begin{aligned} T(S_{u_n}(t)) - T(S_{u_m}(t)) &= S_{u_n}(t) - S_{u_m}(t) \\ &\quad + \mathcal{L}^{-1} \left[\frac{p + \zeta(1-p)}{p} \mathcal{L} \left(\nu_1 S_{u_n} \left(1 - \frac{S_{u_n}}{S_{u_{max}}} \right) - \beta_1 S_{u_n} B_{l_n} \right) \right] \\ &\quad - \mathcal{L}^{-1} \left[\frac{p + \zeta(1-p)}{p} \mathcal{L} \left(\nu_1 S_{u_m} \left(1 - \frac{S_{u_m}}{S_{u_{max}}} \right) - \beta_1 S_{u_m} B_{l_m} \right) \right], \\ T(S_{i_n}(t)) - T(S_{i_m}(t)) &= S_{i_n}(t) - S_{i_m}(t) + \mathcal{L}^{-1} \left[\frac{p + \zeta(1-p)}{p} \mathcal{L} (\beta_1 S_{u_n} B_{l_n} - \mu S_{i_n}) \right] \\ &\quad - \mathcal{L}^{-1} \left[\frac{p + \zeta(1-p)}{p} \mathcal{L} (\beta_1 S_{u_m} B_{l_m} - \mu S_{i_m}) \right], \\ T(B_{l_n}(t)) - T(B_{l_m}(t)) &= B_{l_n}(t) - B_{l_m}(t) \\ &\quad + \mathcal{L}^{-1} \left[\frac{p + \zeta(1-p)}{p} \mathcal{L} \left(\nu_2 B_{l_n} \left(1 - \frac{B_{l_n}}{B_{l_{max}}} \right) - \beta_2 S_{u_n} B_{l_n} + \sigma S_{i_n} \right) \right] \\ &\quad - \mathcal{L}^{-1} \left[\frac{p + \zeta(1-p)}{p} \mathcal{L} \left(\nu_2 B_{l_m} \left(1 - \frac{B_{l_m}}{B_{l_{max}}} \right) - \beta_2 S_{u_m} B_{l_m} + \sigma S_{i_m} \right) \right] \end{aligned}$$

where $\frac{p+\zeta(1-p)}{p}$ is a Lagrange multiplier in fractional form. As all the solutions S_{u_n} , S_{i_n} , B_{l_n} are Cauchy sequences in the Banach space $(\mathbb{X}, \|\cdot\|)$, it is true that $\|S_{u_n} - S_{u_m}\| \rightarrow 0$, $\|S_{i_n} - S_{i_m}\| \rightarrow 0$ and $\|B_{l_n} - B_{l_m}\| \rightarrow 0$ as $n, m \rightarrow \infty$. Due to this similar behavior of the solutions, i.e., comparative influence of the solutions, we have

$$\begin{aligned} \|S_{u_n}(t) - S_{u_m}(t)\| &\cong \|S_{i_n}(t) - S_{i_m}(t)\|, \\ \|S_{u_n}(t) - S_{u_m}(t)\| &\cong \|B_{l_n}(t) - B_{l_m}(t)\|. \end{aligned} \tag{19.2.9}$$

Now, applying the norm on both sides of the first equation, we obtain

$$\begin{aligned}
\|T(S_{u_n}(t)) - T(S_{u_m}(t))\| &= \|S_{u_n}(t) - S_{u_m}(t) \\
&+ \mathcal{L}^{-1} \left[\frac{p + \zeta(1-p)}{p} \mathcal{L} \left(\nu_1 S_{u_n} \left(1 - \frac{S_{u_n}}{S_{u_{max}}} \right) - \beta_1 S_{u_n} B_{l_n} \right) \right] \\
&- \mathcal{L}^{-1} \left[\frac{p + \zeta(1-p)}{p} \mathcal{L} \left(\nu_1 S_{u_m} \left(1 - \frac{S_{u_m}}{S_{u_{max}}} \right) - \beta_1 S_{u_m} B_{l_m} \right) \right] \| \\
&= \|S_{u_n}(t) - S_{u_m}(t) + \mathcal{L}^{-1} \left[\frac{p + \zeta(1-p)}{p} \mathcal{L} \left[\nu_1 (S_{u_n}(t) - S_{u_m}(t)) \right. \right. \\
&+ \left. \left. \left(-\frac{\nu_1}{S_{u_{max}}} S_{u_n} (S_{u_n} - S_{u_m}) \right) + \left(-\frac{\nu_1}{S_{u_{max}}} S_{u_m} (S_{u_n} - S_{u_m}) \right) \right. \right. \\
&+ \left. \left. \left. (-\beta_1 B_{l_n} (S_{u_n} - S_{u_m})) + (-\beta_1 S_{u_m} (B_{l_n} - B_{l_m})) \right) \right] \right] \|.
\end{aligned}$$

Using triangle inequality, we obtain

$$\begin{aligned}
\|T(S_{u_n}(t)) - T(S_{u_m}(t))\| &\leq \|S_{u_n}(t) - S_{u_m}(t)\| + \mathcal{L}^{-1} \left[\frac{p + \zeta(1-p)}{p} \mathcal{L} \left[\|\nu_1 (S_{u_n}(t) - S_{u_m}(t))\| \right. \right. \\
&+ \left. \left. \left\| -\frac{\nu_1}{S_{u_{max}}} S_{u_n} (S_{u_n} - S_{u_m}) \right\| + \left\| -\frac{\nu_1}{S_{u_{max}}} S_{u_m} (S_{u_n} - S_{u_m}) \right\| \right. \right. \\
&+ \left. \left. \left\| -\beta_1 B_{l_n} (S_{u_n} - S_{u_m}) \right\| + \left\| -\beta_1 S_{u_m} (B_{l_n} - B_{l_m}) \right\| \right] \right].
\end{aligned}$$

Then, using the relations in (19.2.9), we obtain

$$\begin{aligned}
\|T(S_{u_n}(t)) - T(S_{u_m}(t))\| &\leq \|S_{u_n}(t) - S_{u_m}(t)\| + \mathcal{L}^{-1} \left[\frac{p + \zeta(1-p)}{p} \mathcal{L} \left[\|\nu_1 (S_{u_n}(t) - S_{u_m}(t))\| \right. \right. \\
&+ \left. \left. \left\| -\frac{\nu_1}{S_{u_{max}}} S_{u_n} (S_{u_n} - S_{u_m}) \right\| + \left\| -\frac{\nu_1}{S_{u_{max}}} S_{u_m} (S_{u_n} - S_{u_m}) \right\| \right. \right. \\
&+ \left. \left. \left\| -\beta_1 B_{l_n} (S_{u_n} - S_{u_m}) \right\| + \left\| -\beta_1 S_{u_m} (S_{u_n} - S_{u_m}) \right\| \right] \right] \\
&\leq \|S_{u_n}(t) - S_{u_m}(t)\| \left[1 + \nu_1 E_1(\zeta) - 2M_1 \frac{\nu_1}{S_{u_{max}}} E_2(\zeta) \right. \\
&\left. - \beta_1 (M_1 + M_3) E_3(\zeta) \right]
\end{aligned}$$

where $E_1(\zeta)$, $E_2(\zeta)$ and $E_3(\zeta)$ are functions of $\mathcal{L}^{-1} \left[\frac{p+\zeta(1-p)}{p} \mathcal{L}(\cdot) \right]$ and $\|S_{u_n}\| < M_1$, $\|S_{i_n}\| < M_2$ and $\|B_{l_n}\| < M_3$. Proceeding similarly, we obtain from the second and third equations

$$\|T(S_{i_n}(t)) - T(S_{i_m}(t))\| \leq \|S_{i_n}(t) - S_{i_m}(t)\| \left[1 + \beta_1 (M_1 + M_3) E_3(\zeta) - \mu E_4(\zeta) \right]$$

and

$$\begin{aligned}
\|T(B_{l_n}(t)) - T(B_{l_m}(t))\| &\leq \|B_{l_n}(t) - B_{l_m}(t)\| \left[1 + \nu_2 E_5(\zeta) - 2M_3 \frac{\nu_2}{B_{l_{max}}} E_6(\zeta) \right. \\
&\left. - \beta_2 (M_1 + M_3) E_3(\zeta) + \sigma E_7(\zeta) \right]
\end{aligned}$$

where $E_4(\zeta)$, $E_5(\zeta)$, $E_6(\zeta)$ and $E_7(\zeta)$ are functions of $\mathcal{L}^{-1} \left[\frac{p+\zeta(1-p)}{p} \mathcal{L}(\cdot) \right]$ and

$$\begin{aligned} \left[1 + \nu_1 E_1(\zeta) - 2M_1 \frac{\nu_1}{S_{u_{max}}} E_2(\zeta) - \beta_1(M_1 + M_3) E_3(\zeta) \right] &< 1, \\ \left[1 + \beta_1(M_1 + M_3) E_3(\zeta) - \mu E_4(\zeta) \right] &< 1, \\ \left[1 + \nu_2 E_5(\zeta) - 2M_3 \frac{\nu_2}{B_{l_{max}}} E_6(\zeta) - \beta_2(M_1 + M_3) E_3(\zeta) + \sigma E_7(\zeta) \right] &< 1. \end{aligned} \tag{19.2.10}$$

So, we can conclude that the self-map T has a fixed point. In view of (19.2.10) and also choosing $\varrho = (0, 0, 0)$ and

$$\Lambda = \begin{cases} 1 + \nu_1 E_1(\zeta) - 2M_1 \frac{\nu_1}{S_{u_{max}}} E_2(\zeta) - \beta_1(M_1 + M_3) E_3(\zeta), \\ 1 + \beta_1(M_1 + M_3) E_3(\zeta) - \mu E_4(\zeta), \\ 1 + \nu_2 E_5(\zeta) - 2M_3 \frac{\nu_2}{B_{l_{max}}} E_6(\zeta) - \beta_2(M_1 + M_3) E_3(\zeta) + \sigma E_7(\zeta), \end{cases}$$

we can see that all the conditions of Theorem 19.2.1 are satisfied. Thus, the self-mapping T is Picard’s T-stable. Here, it is important to note that Λ is a constant, not a function.

Summarizing the previous discussions, we now present the following theorem.

Theorem 19.2.2. Consider system (19.2.2) with the set of equations denoted above. Let T be a self-map as defined. If the conditions (19.2.10) are satisfied by T , then T has a fixed point and, hence, T is Picard’s T-stable.

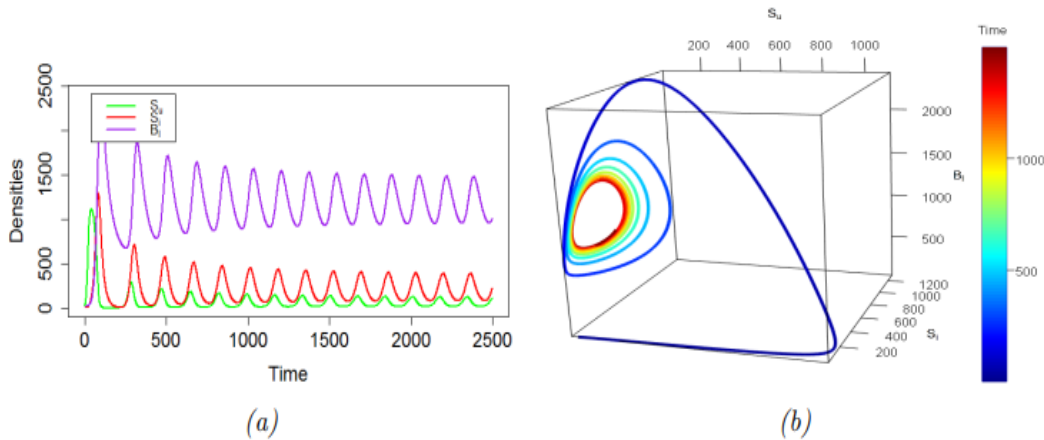


Figure 19.2: Time series and phase portrait diagram of the CF fractionalized system (19.2.2) depicting the unstable oscillatory behavior of the system state populations and appearance of stable limit cycles for $\zeta = 0.8$. Values of $\nu_2 = 0.03$ and $S_{u_{max}} = 1200$ were used to simulate the subfigures in this figure. (a) Behavior of the trajectories of system (19.2.2); (b) 3-D phase diagram for system (19.2.2) in $S_u - S_i - B_l$ space.

19.2.3 Existence of the Solutions

Using fixed-point theory, we now show the existence of the solutions of system (19.2.2) in this subsection. For this, let us first observe that

$$\begin{aligned}
S_u(t) - S_{u_0}(t) &= \frac{2(1-\zeta)}{M(\zeta)(2-\zeta)} \left(\nu_1 S_u(t) \left(1 - \frac{S_u(t)}{S_{u_{max}}} \right) - \beta_1 S_u(t) B_l(t) \right) \\
&\quad + \frac{2\zeta}{M(\zeta)(2-\zeta)} \int_0^t \left(\nu_1 S_u(y) \left(1 - \frac{S_u(y)}{S_{u_{max}}} \right) - \beta_1 S_u(y) B_l(y) \right) dy, \\
S_i(t) - S_{i_0}(t) &= \frac{2(1-\zeta)}{M(\zeta)(2-\zeta)} (\beta_1 S_u B_l - \mu S_i) \\
&\quad + \frac{2\zeta}{M(\zeta)(2-\zeta)} \int_0^t (\beta_1 S_u(y) B_l(y) - \mu S_i(y)) dy, \\
B_l(t) - B_{l_0}(t) &= \frac{2(1-\zeta)}{M(\zeta)(2-\zeta)} \left(\nu_2 B_l(t) \left(1 - \frac{B_l(t)}{B_{l_{max}}} \right) - \beta_2 S_u(t) B_l(t) + \sigma S_i \right) \\
&\quad + \frac{2\zeta}{M(\zeta)(2-\zeta)} \int_0^t \left(\nu_2 B_l(y) \left(1 - \frac{B_l(y)}{B_{l_{max}}} \right) - \beta_2 S_u(y) B_l(y) + \sigma S_i(y) \right) dy.
\end{aligned}$$

Let T_1 be an operator on H to itself, i.e., $T_1 : H \rightarrow H$. Here, T_1 is chosen as an operator for the entire system. Applying it, we obtain that

$$\begin{aligned}
T_1(S_u(t)) &= \frac{2(1-\zeta)}{M(\zeta)(2-\zeta)} K_1(t, S_u(t)) + \frac{2\zeta}{M(\zeta)(2-\zeta)} \int_0^t (K_1(y, S_u(y))) dy, \\
T_1(S_i(t)) &= \frac{2(1-\zeta)}{M(\zeta)(2-\zeta)} (K_2(t, S_i(t))) + \frac{2\zeta}{M(\zeta)(2-\zeta)} \int_0^t (K_2(y, S_i(y))) dy, \quad (19.2.11) \\
T_1(B_l(t)) &= \frac{2(1-\zeta)}{M(\zeta)(2-\zeta)} (K_3(t, B_l(t))) + \frac{2\zeta}{M(\zeta)(2-\zeta)} \int_0^t (K_3(y, B_l(y))) dy
\end{aligned}$$

where

$$\begin{aligned}
K_1(t, S_u(t)) &= \nu_1 S_u(t) \left(1 - \frac{S_u(t)}{S_{u_{max}}} \right) - \beta_1 S_u(t) B_l(t), \\
K_2(t, S_i(t)) &= \beta_1 S_u(t) B_l(t) - \mu S_i(t), \\
K_3(t, B_l(t)) &= \nu_2 B_l(t) \left(1 - \frac{B_l(t)}{B_{l_{max}}} \right) - \beta_2 S_u(t) B_l(t) + \sigma S_i(t).
\end{aligned}$$

Let $P \subset H$ be bounded. We aim to show that $\overline{T_1(P)}$ is compact to ensure the existence and boundedness of the solutions of system (19.2.2), where T_1 is defined as in (19.2.11). We can see that there exist positive reals κ_1 , κ_2 and κ_3 such that $\|S_u\| < \kappa_1$, $\|S_i\| < \kappa_2$ and $\|B_l\| < \kappa_3$. From the first equation of (19.2.11), we can write

$$\begin{aligned}
\|T_1(S_u(t))\| &= \left\| \frac{2(1-\zeta)}{M(\zeta)(2-\zeta)} K_1(t, S_u(t)) + \frac{2\zeta}{M(\zeta)(2-\zeta)} \int_0^t (K_1(y, S_u(y))) dy \right\| \\
&\leq \frac{2(1-\zeta)}{M(\zeta)(2-\zeta)} \|K_1(t, S_u(t))\| + \frac{2\zeta}{M(\zeta)(2-\zeta)} \left\| \int_0^t (K_1(y, S_u(y))) dy \right\| \\
&\leq \left[\frac{2(1-\zeta)}{M(\zeta)(2-\zeta)} + a_1 \frac{2\zeta}{M(\zeta)(2-\zeta)} \right] \|K_1(t, S_u(t))\| \\
&\leq R_1 \left[\frac{2(1-\zeta)}{M(\zeta)(2-\zeta)} + a_1 \frac{2\zeta}{M(\zeta)(2-\zeta)} \right]
\end{aligned}$$

which implies

$$\|T_1(S_u(t))\| \leq \frac{2R_1}{M(\zeta)(2-\zeta)}(1 + \zeta a_1 - \zeta)$$

and also proceeding similarly, we can obtain

$$\begin{aligned} \|T_1(S_i(t))\| &\leq \frac{2R_2}{M(\zeta)(2-\zeta)}(1 + \zeta a_2 - \zeta), \\ \|T_1(B_l(t))\| &\leq \frac{2R_3}{M(\zeta)(2-\zeta)}(1 + \zeta a_3 - \zeta) \end{aligned}$$

where

$$\begin{aligned} R_1 &= \max_{\substack{t \in [0,1] \\ S_u \in [0, \kappa_1]}} K_1(t, S_u(t)), \\ R_2 &= \max_{\substack{t \in [0,1] \\ S_i \in [0, \kappa_2]}} K_2(t, S_i(t)), \\ R_3 &= \max_{\substack{t \in [0,1] \\ B_l \in [0, \kappa_3]}} K_3(t, B_l(t)). \end{aligned}$$

Hence, we have proved that $T_1(P)$ is bounded. Let, $t_2 > t_1$ and $S_u, S_i, B_l \in P$. So, for a given $\epsilon > 0$, there exists η satisfying that $\|(t_2 - t_1)\| < \eta$, and we can write the following:

$$\begin{aligned} \|K_1(t_2, S_u(t_2)) - K_1(t_1, S_u(t_1))\| &\leq \nu_1 \|S_u(t_2) - S_u(t_1)\| \\ &\quad + \frac{\nu_1}{S_{u_{max}}} \|S_u(t_2) + S_u(t_1)\| \|S_u(t_2) - S_u(t_1)\| \\ &\quad + \beta_1 \|B_l\| \|S_u(t_2) - S_u(t_1)\| \\ &\leq \nu_1 \|S_u(t_2) - S_u(t_1)\| + 2\kappa_1 \frac{\nu_1}{S_{u_{max}}} \|S_u(t_2) - S_u(t_1)\| \quad (19.2.12) \\ &\quad + \beta_1 \kappa_3 \|S_u(t_2) - S_u(t_1)\| \\ &\leq \left[\nu_1 + \frac{2\kappa_1 \nu_1}{S_{u_{max}}} + \beta_1 \kappa_3 \right] \|S_u(t_2) - S_u(t_1)\|. \end{aligned}$$

Assuming that if the function $S_u(t)$ is Lipschitz-continuous, i.e., for some real number $L_1 \geq 0$ and for all t_1, t_2 , the inequality $\|S_u(t_2) - S_u(t_1)\| \leq L_1 \|t_2 - t_1\|$ holds, we can rewrite (19.2.12) as

$$\|K_1(t_2, S_u(t_2)) - K_1(t_1, S_u(t_1))\| \leq G_1 \|t_2 - t_1\| \quad (19.2.13)$$

where $G_1 = L_1 \left[\nu_1 + \frac{2\kappa_1 \nu_1}{S_{u_{max}}} + \beta_1 \kappa_3 \right]$. Similarly, we have

$$\|K_2(t_2, S_i(t_2)) - K_2(t_1, S_i(t_1))\| \leq G_2 \|t_2 - t_1\|, \quad (19.2.14)$$

$$\|K_3(t_2, B_l(t_2)) - K_3(t_1, B_l(t_1))\| \leq G_3 \|t_2 - t_1\| \quad (19.2.15)$$

if $S_i(t)$ and $B_l(t)$ are also Lipschitz-continuous, i.e., for some real numbers $L_2, L_3 \geq 0$, the conditions

$$\begin{aligned} \|S_i(t_2) - S_i(t_1)\| &\leq L_2 \|t_2 - t_1\|, \\ \|B_l(t_2) - B_l(t_1)\| &\leq L_3 \|t_2 - t_1\| \quad \text{hold, respectively, for all } t_1, t_2. \end{aligned}$$

Furthermore,

$$\begin{aligned} \|T_1(S_u(t_2)) - T_1(S_u(t_1))\| &\leq \frac{2(1-\zeta)}{M(\zeta)(2-\zeta)} \|K_1(t_2, S_u(t_2)) - K_1(t_1, S_u(t_1))\| \\ &\quad + \frac{2\zeta}{M(\zeta)(2-\zeta)} R_1 \|K_1(t_2, S_u(t_2)) - K_1(t_1, S_u(t_1))\| \\ &\leq \frac{2(1-\zeta)}{M(\zeta)(2-\zeta)} G_1 \|t_2 - t_1\| + \frac{2\zeta}{M(\zeta)(2-\zeta)} R_1 G_1 \|t_2 - t_1\| \\ &\quad \text{(using inequality (19.2.13)).} \end{aligned}$$

Finally, choosing

$$\eta = \frac{\epsilon}{\frac{2(1-\zeta)}{M(\zeta)(2-\zeta)} G_1 + \frac{2\zeta}{M(\zeta)(2-\zeta)} R_1 G_1},$$

we can see that $\|T_1(S_u(t_2)) - T_1(S_u(t_1))\| \leq \epsilon$ holds.

Similarly proceeding and using inequalities (19.2.14) and (19.2.15), we can also easily show that $\|T_1(S_i(t_2)) - T_1(S_i(t_1))\| \leq \epsilon$ and $\|T_1(B_l(t_2)) - T_1(B_l(t_1))\| \leq \epsilon$ hold, which guarantees the equicontinuity of T_1 . Hence, according to the well-known Arzela–Ascoli theorem, we can say that $\overline{T_1(P)}$ is compact. Next, we present the following theorem by summarising the previous discussions on the existence of the solutions of system (19.2.2), and then we move forward to show the uniqueness of the solutions of system (19.2.2).

Theorem 19.2.3. Let $P \subset H$ be bounded and T_1 be defined as in (19.2.11). Then, there exist κ_1 , κ_2 and κ_3 such that if the functions $S_u(t)$, $S_i(t)$ and $B_l(t)$ are Lipschitz-continuous, i.e., if for some real numbers, L_1 , L_2 and $L_3 \geq 0$, the following conditions hold

$$\begin{aligned} \|S_u(t_2) - S_u(t_1)\| &\leq L_1 \|t_2 - t_1\|, \\ \|S_i(t_2) - S_i(t_1)\| &\leq L_2 \|t_2 - t_1\|, \\ \|B_l(t_2) - B_l(t_1)\| &\leq L_3 \|t_2 - t_1\|, \end{aligned}$$

for all t_1, t_2 , then $\overline{T_1(P)}$ is compact. Thus, all the solutions of system (19.2.2) exist and are bounded.

19.2.4 Uniqueness of the Solutions

To prove the uniqueness of the solutions of system (19.2.2), let us consider the mapping T_1 again which was defined previously. Now,

$$\begin{aligned} \|T_1(S_u(t)) - T_1(\tilde{S}_u(t))\| &= \left\| \frac{2(1-\zeta)}{M(\zeta)(2-\zeta)} (K_1(t, S_u(t)) - K_1(t, \tilde{S}_u(t))) \right. \\ &\quad \left. + \frac{2\zeta}{M(\zeta)(2-\zeta)} \int_0^t (K_1(y, S_u(y)) - K_1(y, \tilde{S}_u(y))) \right\| \\ &\leq \left[\frac{2D_1}{M(\zeta)(2-\zeta)} \right] \|S_u(t) - \tilde{S}_u(t)\|. \end{aligned}$$

Similarly, we can obtain

$$\begin{aligned} \|T_1(S_i(t)) - T_1(\tilde{S}_i(t))\| &\leq \left[\frac{2D_2}{M(\zeta)(2-\zeta)} \right] \|S_i(t) - \tilde{S}_i(t)\|, \\ \|T_1(B_l(t)) - T_1(\tilde{B}_l(t))\| &\leq \left[\frac{2D_3}{M(\zeta)(2-\zeta)} \right] \|B_l(t) - \tilde{B}_l(t)\| \end{aligned}$$

where $D_1, D_2, D_3 \in \mathbb{R}$. Hence, the operator T_1 is a contraction if the following conditions hold:

$$\begin{aligned} \frac{2D_1}{M(\zeta)(2-\zeta)} \|S_u(t) - \tilde{S}_u(t)\| &< 1, \\ \frac{2D_2}{M(\zeta)(2-\zeta)} \|S_i(t) - \tilde{S}_i(t)\| &< 1, \\ \frac{2D_3}{M(\zeta)(2-\zeta)} \|B_l(t) - \tilde{B}_l(t)\| &< 1 \end{aligned}$$

which ensures the existence of unique positive solutions of system (19.2.2) using fixed-point theorem.

19.3 Equilibria and Stability

Our CF fractionalized mathematical model (19.2.2) has two equilibria, namely the disease-free equilibrium E_0 and the endemic equilibrium E^* . Here, E_0 is given as $E_0 = (S_{u_{max}}, 0, 0)$. The value of the basic reproduction number R_0 is given as $R_0 = \frac{\beta_1 \sigma S_{u_{max}}}{\mu(\beta_2 S_{u_{max}} - \nu_2)}$. R_0 is actually interpreted as the secondary number of new infections in a completely susceptible healthy Schwann cell population and, based on the above, we now present the following theorem on the stability of E_0 for our system (19.2.2) as follows:

Theorem 19.3.1. The disease-free equilibrium E_0 of system (19.2.2) is locally asymptotically stable if $R_0 < 1$.

To obtain the coordinates of the endemic equilibrium E^* , we now set the right-hand sides of system (19.2.2) to zero. Hence, we obtain the values of S_u^* , S_i^* and B_l^* . In this context, we now present the following theorem, which describes the required criterion about the stability of E^* .

Theorem 19.3.2. If the matrix $(I - (1 - \zeta)\mathcal{J})$ is invertible, then the endemic equilibrium E^* of the CF fractionalized system (19.2.2) is locally asymptotically stable if all the roots of the characteristic equation $\det(x(I - (1 - \zeta)\mathcal{J}) - \zeta\mathcal{J}) = 0$ of system (19.2.2) evaluated at E^* are negative real or have negative real parts where \mathcal{J} denotes the Jacobian matrix of system (19.2.2) at $E^* = (S_u^*, S_i^*, B_l^*)$.

Unit 20

Course Structure

- Predator prey model in presence of infection
 - Jacobian, Characteristic Polynomial and Stability Analysis of Steady States
 - Mathematical Model on Viral Infection of phytoplankton-zooplankton system
-

20.1 Predator Prey Model in Presence of Infection

Some key points explaining why studying the predator-prey model in the presence of infection is important in ecology:

1. **Population Dynamics:** It helps understand how the dynamics of predator and prey populations are influenced by the presence of infectious diseases.
2. **Ecosystem Stability:** Provides insights into how diseases affect the stability and resilience of ecosystems by altering predator-prey interactions.
3. **Disease Spread:** Helps predict the spread of diseases within ecological communities through interactions between predators, prey, and pathogens.
4. **Biodiversity Conservation:** Aids in the development of strategies for biodiversity conservation by considering the impact of diseases on predator and prey populations.
5. **Community Structure:** Examines how infectious diseases shape the structure and composition of ecological communities by altering predator-prey dynamics.
6. **Species Interactions:** Illustrates the complex interplay between species interactions and disease dynamics, leading to cascading effects throughout ecosystems.
7. **Human Health:** Provides insights into zoonotic diseases, which can spread from wildlife to humans through predator-prey interactions.
8. **Climate Change:** Helps assess the impact of climate change on disease dynamics within predator and prey populations, influencing ecosystem health.

9. **Resource Management:** Guides resource management and conservation efforts by considering the role of diseases in shaping predator-prey relationships.
10. **Modeling Complexity:** Challenges researchers to develop and refine mathematical models that incorporate the complexities of both ecological and epidemiological processes.

20.1.1 Jacobian, Characteristic Polynomial and Stability Analysis of Steady States

The predator-prey model in the presence of infection combines elements of the classic Lotka-Volterra predator-prey equations with the spread of an infectious disease among one or both populations. Here's a simplified mathematical representation of such a model:

Let's denote:

- $P(t)$: The population of prey (e.g., rabbits).
- $P'(t)$: The rate of change of the prey population.
- P_{birth} : The birth rate of the prey.
- P_{death} : The natural death rate of the prey.
- α : The infection rate of prey by the predator.
- $I(t)$: The population of infected prey.
- β : The recovery rate of infected prey.

For the predator:

- $Q(t)$: The population of predators (e.g., foxes).
- $Q'(t)$: The rate of change of the predator population.
- Q_{birth} : The birth rate of the predator (possibly influenced by the number of infected prey).
- Q_{death} : The natural death rate of the predator (possibly influenced by the number of infected prey).
- δ : The rate at which predators acquire infection from prey.
- γ : The recovery rate of infected predators.

The basic equations for such a model could be:

1. For the prey population:

$$\frac{dP}{dt} = P_{\text{birth}} \cdot P - P_{\text{death}} \cdot P - \alpha \cdot P \cdot Q - \beta \cdot P \cdot I$$

2. For the infected prey population:

$$\frac{dI}{dt} = \alpha \cdot P \cdot Q - \beta \cdot P \cdot I$$

3. For the predator population:

$$\frac{dQ}{dt} = Q_{\text{birth}} \cdot Q - Q_{\text{death}} \cdot Q + \delta \cdot P \cdot Q - \gamma \cdot Q \cdot I$$

4. For the infected predator population:

$$\frac{dR}{dt} = \delta \cdot P \cdot Q - \gamma \cdot Q \cdot R$$

These equations capture the interactions between prey, predators, and the infection dynamics between them.

Let's solve the system of equations to find the equilibrium points (P^*, Q^*, I^*, R^*) :

Given the equations:

- For the prey population: $P' = P_{\text{birth}} \cdot P - P_{\text{death}} \cdot P - \alpha \cdot P \cdot Q - \beta \cdot P \cdot I = 0$,
- For the infected prey population: $I' = \alpha \cdot P \cdot Q - \beta \cdot P \cdot I = 0$,
- For the predator population: $Q' = Q_{\text{birth}} \cdot Q - Q_{\text{death}} \cdot Q + \delta \cdot P \cdot Q - \gamma \cdot Q \cdot I = 0$,
- For the infected predator population: $R' = \delta \cdot P \cdot Q - \gamma \cdot Q \cdot R = 0$.

Setting each equation equal to zero, we can solve for the equilibrium points. However, it's important to note that the system of equations is nonlinear and might not have simple analytical solutions.

To find the Jacobian matrix, we first need to express the system of equations in a vector form. Let's define the vector of variables as $\mathbf{X} = (P, Q, I, R)$, and the vector of equations as $\mathbf{F} = (P', Q', I', R')$. Then, the system of equations becomes:

$$\mathbf{F}(\mathbf{X}) = \begin{pmatrix} P' \\ Q' \\ I' \\ R' \end{pmatrix} = \begin{pmatrix} P_{\text{birth}} \cdot P - P_{\text{death}} \cdot P - \alpha \cdot P \cdot Q - \beta \cdot P \cdot I \\ Q_{\text{birth}} \cdot Q - Q_{\text{death}} \cdot Q + \delta \cdot P \cdot Q - \gamma \cdot Q \cdot I \\ \alpha \cdot P \cdot Q - \beta \cdot P \cdot I \\ \delta \cdot P \cdot Q - \gamma \cdot Q \cdot R \end{pmatrix}$$

Now, we can find the Jacobian matrix \mathbf{J} by taking the partial derivatives of \mathbf{F} with respect to each variable:

$$\mathbf{J} = \begin{pmatrix} \frac{\partial P'}{\partial P} & \frac{\partial P'}{\partial Q} & \frac{\partial P'}{\partial I} & \frac{\partial P'}{\partial R} \\ \frac{\partial Q'}{\partial P} & \frac{\partial Q'}{\partial Q} & \frac{\partial Q'}{\partial I} & \frac{\partial Q'}{\partial R} \\ \frac{\partial I'}{\partial P} & \frac{\partial I'}{\partial Q} & \frac{\partial I'}{\partial I} & \frac{\partial I'}{\partial R} \\ \frac{\partial R'}{\partial P} & \frac{\partial R'}{\partial Q} & \frac{\partial R'}{\partial I} & \frac{\partial R'}{\partial R} \end{pmatrix}$$

Let's compute these partial derivatives explicitly:

$$\begin{aligned} \frac{\partial P'}{\partial P} &= P_{\text{birth}} - P_{\text{death}} - \alpha \cdot Q - \beta \cdot I \\ \frac{\partial P'}{\partial Q} &= -\alpha \cdot P \\ \frac{\partial P'}{\partial I} &= -\beta \cdot P \end{aligned}$$

$$\frac{\partial P'}{\partial R} = 0$$

$$\frac{\partial Q'}{\partial P} = \delta \cdot Q$$

$$\frac{\partial Q'}{\partial Q} = Q_{\text{birth}} - Q_{\text{death}} - \alpha \cdot P - \gamma \cdot I$$

$$\frac{\partial Q'}{\partial I} = -\gamma \cdot Q$$

$$\frac{\partial Q'}{\partial R} = 0$$

$$\frac{\partial I'}{\partial P} = \alpha \cdot Q - \beta \cdot I$$

$$\frac{\partial I'}{\partial Q} = \alpha \cdot P$$

$$\frac{\partial I'}{\partial I} = -\beta \cdot P$$

$$\frac{\partial I'}{\partial R} = 0$$

$$\frac{\partial R'}{\partial P} = \delta \cdot Q$$

$$\frac{\partial R'}{\partial Q} = -\gamma \cdot R$$

$$\frac{\partial R'}{\partial I} = 0$$

$$\frac{\partial R'}{\partial R} = -\gamma \cdot Q$$

Now, we can assemble these partial derivatives into the Jacobian matrix \mathbf{J} .

To find the characteristic equation related to the Jacobian matrix \mathbf{J} , we first need to compute the determinant of the matrix $\mathbf{J} - \lambda \mathbf{I}$, where λ is the eigenvalue we're solving for and \mathbf{I} is the identity matrix. Then, we set the determinant equal to zero to find the characteristic equation.

Let's denote $\mathbf{J} - \lambda \mathbf{I}$ as $\mathbf{J}(\lambda)$. The characteristic equation is given by:

$$\det(\mathbf{J}(\lambda)) = 0$$

where $\det(\cdot)$ denotes the determinant.

Let's denote the elements of $\mathbf{J}(\lambda)$ as j_{ij} , where i and j are the row and column indices, respectively.

So, the characteristic equation will be of the form:

$$a_4 \lambda^4 + a_3 \lambda^3 + a_2 \lambda^2 + a_1 \lambda + a_0 = 0$$

where a_4, a_3, a_2, a_1 , and a_0 are coefficients determined from the determinant expansion of $\mathbf{J}(\lambda)$.

20.2 Viral Infections on Phytoplankton and Zooplankton System

- **Biotic Interactions:** Viral infections influence the interactions between phytoplankton and zooplankton, impacting community structure and dynamics.
- **Nutrient Cycling:** Viral lysis of phytoplankton releases nutrients that can be utilized by zooplankton, affecting nutrient cycling and ecosystem productivity.
- **Top-Down Control:** Viruses act as top-down regulators of phytoplankton populations by infecting and reducing their abundance, which can cascade through the food web.
- **Genetic Diversity:** Viral infections drive genetic diversity in phytoplankton populations through selective pressures, influencing evolutionary processes.
- **Carbon Sequestration:** Viral lysis of phytoplankton affects carbon sequestration in the ocean by altering the fate of organic carbon in the water column.
- **Ecosystem Resilience:** Understanding viral infections enhances our ability to predict and mitigate the impacts of environmental stressors on ecosystem resilience.
- **Biogeochemical Cycling:** Viral infections play a significant role in biogeochemical cycling by mediating the fluxes of carbon, nitrogen, and other essential elements.
- **Climate Feedbacks:** Viral infections within phytoplankton-zooplankton systems contribute to climate feedback loops by influencing oceanic carbon dioxide uptake and release.
- **Microbial Loop:** Viruses are integral components of the microbial loop, regulating the flow of energy and nutrients between phytoplankton, zooplankton, and bacteria.
- **Ecological Modeling:** Incorporating viral infections into ecological models improves our ability to accurately predict the dynamics and functioning of aquatic ecosystems under changing environmental conditions.

20.2.1 Mathematical Model on Viral Infection of phytoplankton-zooplankton system

A mathematical model describing viral infection within a phytoplankton-zooplankton system:

Let's denote:

- $P(t)$: The population of phytoplankton at time t .
- $Z(t)$: The population of zooplankton at time t .
- $V(t)$: The population of viruses infecting phytoplankton at time t .

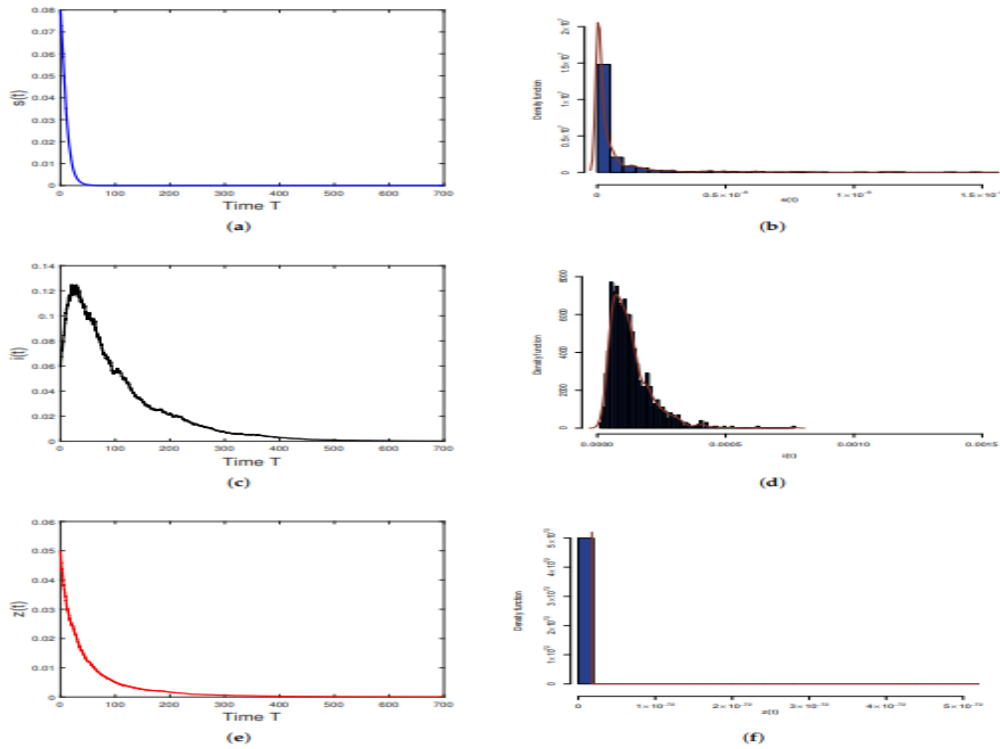


Figure 20.1: Susceptible phytoplankton ($s(t)$), infected phytoplankton ($i(t)$), and zooplankton ($z(t)$) exponentially tend to zero with probability one.

The model can be represented by the following set of differential equations:

1. **Phytoplankton Growth and Viral Infection**:

$$\frac{dP}{dt} = r_P P - g_P P Z - \beta P V$$

This equation describes the growth of phytoplankton P with a logistic growth rate r_P , and its consumption by zooplankton Z at a rate g_P . Additionally, the phytoplankton population is reduced due to viral infection at a rate β .

2. **Zooplankton Growth**:

$$\frac{dZ}{dt} = r_Z Z \left(1 - \frac{Z}{K} \right) - g_Z P Z$$

This equation describes the growth of zooplankton Z with a logistic growth rate r_Z and a carrying capacity K . Zooplankton feed on phytoplankton at a rate g_Z .

3. **Viral Reproduction and Decay**:

$$\frac{dV}{dt} = p V P - d_V V$$

This equation represents the reproduction of viruses V at a rate p proportional to the abundance of phytoplankton P , and the decay of viruses at a rate d_V .

In this model, r_P , g_P , r_Z , K , g_Z , β , p , and d_V are parameters representing growth rates, carrying capacity, consumption rates, infection rates, and decay rates, respectively.

This model captures the interactions between phytoplankton, zooplankton, and viruses in an aquatic ecosystem affected by viral infection. Adjustments and refinements can be made based on specific ecological characteristics and experimental data.

References

1. K. E. Watt : Ecology and Resource Management-A Quantitative Approach.
2. R. M. May : Stability and Complexity in Model Ecosystem.
3. Y. M. Svirzhev and D. O. Logofet : Stability of Biological Communities.
4. A. Segel : Modelling Dynamic Phenomena in Molecular Biology.
5. J. D. Murray : Mathematical Biology. Springer and Verlag.
6. N. T. J. Bailey : The Mathematical Approach to Biology and Medicine.
7. L. Perko (1991): Differential Equations and Dynamical Systems, Springer Verlag.
8. F. Verhulst (1996): Nonlinear Differential Equations and Dynamical Systems, Springer Verlag.
9. H. I. Freedman - Deterministic Mathematical Models in Population Ecology.
10. Mark Kot (2001): Elements of Mathematical Ecology, Cambridge Univ. Press